The impacts of silver nanoparticles on planktonic and biofilm bacteria

by

JÚLIA FÀBREGA CLIMENT

A thesis submitted to the University of Birmingham

for the degree of

DOCTOR OF PHILOSOPHY

School of Geography, Earth and Environmental Sciences

University of Birmingham

July 2009

The impacts of silver nanoparticles on planktonic and biofilm bacteria

Júlia Fàbrega Climent

ABSTRACT

Nanoscale silver particles represent a new generation of cost-effective antibacterial technologies. Due to the increased manufacturing and use of silver nanoparticles (Ag NPs) in consumer goods their release and accumulation into the environment is highly likely but their fate, behaviour and toxicity to organisms is still very much unknown. The present study has investigated the effect that different environmental conditions have on the behaviour and fate of Ag NPs in waters by determining aggregation state, stability and solubility. This work has also determined their interaction and uptake to laboratory grown planktonic and biofilm bacteria, as well as to natural marine biofilms using analytical, electron microscopy and molecular tools.

The outcomes of this work describe the effects that environmental factors such as pH, ionic strength and presence of humic substances (HS) have on the stability, behaviour and ultimately fate of Ag NPs in water, with direct implications on bioavailability of NPs to organisms. Higher pH values as well as the presence of organic of matter in the media increased stability and with this the residence time of the particles in suspension. On the other hand, pH values of 6 and also absence of organic matter increased the precipitation of NPs in suspension.

Planktonic *Pseudomonas fluorescens* was highly susceptible to Ag NPs when grown and exposed at pH 9 only. However, toxicity was also mitigated when natural organic matter (HS) was present. Due to the low solubility of the Ag NPs in the media a NP-mediated toxic mechanism is suggested as the mode of toxicity of Ag NPs to planktonic *P. fluorescens* cells.

Environmental parameters were also crucial for the uptake and interaction of Ag NPs to 3-d old *Pseudomonas putida* biofilms. Ag NPs were uptaken by the cells under all conditions, and decreased biofilm biovolume per surface area when HS were not present. With HS, Ag NPs did not significantly affect biomass; however uptake of Ag NPs doubled under this condition.

Ag NPs in suspension had an effect on a natural marine biofilm community. A dose-dependent decrease on biomass was recorded, but more importantly Ag NPs stopped biofilm succession and development and/or settling of new taxa on the resident biofilm community.

Critical characterisation of Ag NP behaviour under different conditions is crucial for determining which organisms are more likely to interact with Ag NPs in different environmental compartments, and assess the possibility of longer term exposures.

This work provides relevant information on the fate and toxicological effects of a short term exposure of Ag NPs to bacterial cells in an aqueous environment, with possible implications on their bioaccumulation and food web transfer.

To Nick

To my family

& To the triplets

ACKNOWLEDGEMENTS

I would like to start by thanking my supervisors Prof. Jamie Lead and Dr. Jo Renshaw for their guidance and support for the last three years. Thank you Jamie for giving me the opportunity to do this PhD in your group, even knowing the very poor chemical background I arrived with! And thank you very much Jo for your great help in the lab and at any time, really!

A great thanks goes to Universitas 21 for giving me the opportunity to travel to Singapore and to spend 5 exotic months in Asia. Thank you to Prof. Wen-Tso Liu for hosting me in you lab during my stay and teaching me about DNA. And thanks Rui for translating me the meaning of genomics, and of course for your enormous helping during field sampling under extreme weather conditions! Thanks to the Tropical Marine Science Institute of the University of Singapore for letting me use their field site. And a big big thanks to all my colleagues during my visit: Pei Ying, Johnson, Ee Ling, Christy, Rui, Jill, Stanley, Olivier, Chia Lung and Chee Ming .

Special thanks to Paul Stanley from the Electron Microscopy Centre for his constant help in finding bugs and nanoparticles under the scope, and for the entertaining chicken talks we had during all the hours I ended up spending in the centre.

Thanks Shona for your help. Chapter 4 would not have been presented in this thesis if it wasn't for your hard work.

My time at the University of Birmingham would not have been the same without the presence of all the people working there. I wish to thank all past and present members of the Jamie's group and office especially Bożena, Emilia, Montse, Adriana and Maria for making work more entertaining.

And for the human part of this thesis I would like to thank Svetlana, Moni, Andreu, Susi, Santi, Yasmine and Hania. I don't know what I would have done without you all these years in Birmingham!

To David and Carole, and Roy and Fran for making of Birmingham a sweeter home.

To those from the beginning, thanks to Jessica, Janhavi, Idoia, Inna and Aruni for your friendship all these years; and many warm thanks to my undergraduate friends Anna, Laura, Salva, Albert, Helena and Vanessa at the University of Barcelona for all the welcoming meals and sarcastic comments over the last few years: - yes, I finally finished a PhD!

Thanks to my dad. The most optimistic person I will probably ever meet. Thank you for all your support all these years at anything I have decided to embrace. For your interest despite the distance. To my mom and to my sister Andrea. Thanks for your visits (even if they were mostly focused on eating fruit cakes!). To my brothers Joan and Valentí, to my grandma and to Nancy for keeping me posted about life in Manresa and at home. I have really missed you all these years.

Thanks to '*the girls'* for getting me out of bed too early even in winter and for keeping me happy, sane and entertained during my writing up stage at Chadders.

The biggest thanks to Nick. Not only for your constant help fixing my leaky flow cells during most of your spare time but thanks for your endless support, love and care at each and every stage of this project.

LIST OF CONTENTS

LIST OF TABLES

CHAPTER 1

CHAPTER 2

CHAPTER 3

CHAPTER 5

CHAPTER 6

LIST OF FIGURES

CHAPTER 1

CHAPTER 4

CHAPTER 5

LIST OF COMMON ABBREVIATIONS

AAS	Atomic absorption spectroscopy
Ag NP	Silver nanoparticle
BLM	Biotic ligand model
BVSA	Biovolume to surface area ratio
C60	Fullerene
CNT	Carbon nanotubes
CSLM	Confocal scanning laser microscopy
DLS	Dynamic light scattering
EPS	Extracellular polymeric substances
HA	Humic acids
HS	Humic substances
ICPMS	Inductively coupled plasma mass spectroscopy
ID	Inner diameter
LC50	Lethal concentration 50 (concentration of a compound that kills 50% of a sample population
MDM	Minimum Davis media
MWCNT	Multiwall carbon nanotubes
NP	Nanoparticle
OD	Optical density
OM	Organic matter
PBS	Phosphate buffer saline
PPB	Parts per billion
PPM	Parts per million
QD	Quantum dot
ROS	Reactive oxygen species
SDS	Sodium Dodecyl sulphate
SRFA	Suwannee river fulvic acids
SRHA	Suwannee river humic acids
SWCNT	Single walled carbon nanotubes
TEM	Transmission electron microscope
THF	Tetrahydrofuran
TOC	Total organic carbon
T-RF	Terminal restriction fragment
UF	Ultrafiltration
UPW	Ultra pure water
UV-VIS	Ultraviolet-Visible
XRD	X-ray diffraction
ZVI	Zero valent iron

1 Introduction

1.1. What is nanotechnology?

Nanotechnology has been called the next industrial revolution and is based on the manufacturing of nanomaterials (or particles with at least one dimension between 1 and 100 nm (ASTM 2006; Moore 2006)). The aim of nanosciences and nanotechnology is to create new products and materials at a nano-scale, by the careful manipulation of matter at the atomic and molecular level to produce particles with novel physico-chemical properties that improve conductivity, strength, durability, reactivity or other properties of products and applications (Neal 2008; Powell *et al.* 2008; Tiede *et al.* 2009). These novel properties can be exploited in a wide range of applications, including renewable clean energy, clean water, medical advances, cosmetics, food and food packaging, paints, coatings, information, technologies and aerospace developments, to name a few. Nanotechnology will potentially lead to great impacts in terms of energy saving and minimal harm to the environment.

Currently, there are an estimated 807 consumer products on the market utilising nanotechnology in one way or another (Woodrow Wilson Database, 2009; http://www.nanotechproject.org/inventories/consumer/, April 23rd 2009). The nanotechnology sector already has a market worth many billions of US dollars, and it has been projected that this will grow to 1 trillion US dollars by 2015 (Aitken *et al.* 2006), and 3 trillion US dollars by 2018 (Global Industry Analysts 2008; Nanotechnologies 2009; WoodrowWilson 2009). Currently, millions of tonnes of nanomaterials are produced annually worldwide (Powell *et al.* 2008), and the production will probably increase sharply in the near future. The development and application of new technologies tend to carry uncertainties and public concern due to the lack of research on health and environmental risks prior to commercialisation. The

manufacturing and use of nanomaterials is still a controversial technology, although most research suggests a low health and environmental impact for most nanomaterials used. While governmental investments still prioritise medical and industrial research, a very small fraction of it goes to investigate the potential risks and effects to organisms and to the environment (Lead & Wilkinson 2006b; Neal 2008).

1.2. Types of nanomaterials

To date there are no internationally agreed formal definitions of nanomaterials (NMs) and nanoparticles (NPs) (Handy *et al.* 2008). However, NMs are usually described as a material with at least one dimension between about 1 nm and 100 nm (SCENIHR 2005; Moore 2006) and can be nanofilms (1 dimension in this size range, Fig 1.1.A), nanowires and nanotubes (2 dimensions, Fig 1.1 B) or nanoparticles (three dimensions, Fig.1.1 C) (Handy *et al.* 2008).

Nanomaterials are usually categorised based on the core material they are made from. However, this categorisation does not necessarily reflect their physico-chemistry. Indeed, size and shape (i.e. rod-shapes, prisms, tubes, and spheres), as well as crystal structure are all factors that influence their physical and chemical properties. NMs can also be manipulated and differentiated by adding coatings or capping agents and functionalising their surface. Thus two particles of the same material but of different size and shape may have different physical and chemical properties and uses (Ju-Nam & Lead 2008; Tiede *et al.* 2009).

Nanomaterials can be made of *carbon* (fullerenes, nanotubes, etc.) or *inorganic based* materials. The latter including metal oxides (zinc oxide, iron oxide, titanium dioxide, cerium oxide, etc), metals (silver, gold, iron, etc) and quantum dots (cadmium sulphide and cadmium

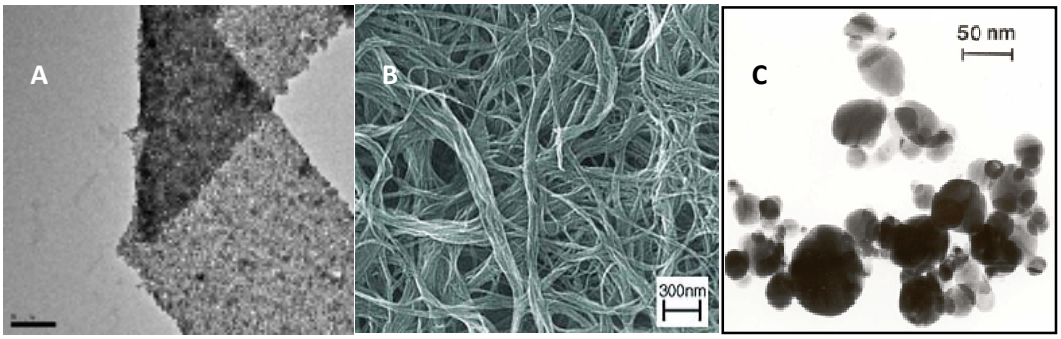

Figure 1.1. A) Carbon nanofilm (from http://www.nanolitic.com/images/2.jpg) ; B) Carbon nanotubes (from http://www.antnanousa.com/dev/news/news141048611.html) & C) silver nanoparticles (from http://www.tms.org/pubs/journals/jom/0607/murr-0607.html).

selenide) (Ju-Nam & Lead 2008). Some of the most commercially used nanomaterials are briefly described below.

1.2.1. Carbon based nanomaterials

Carbon based nanomaterials are used in a variety of applications including optics, electronics and biomedicine.

- **Fullerenes**

Fullerenes are molecules of 60 atoms of carbon (C_{60}). Fullerenes and derivates are very insoluble in biofluids (Ros *et al.* 2001), which limits their application in the medical field. However, they have attracted the attention of many scientists for the variety of interesting applications in this field, and preliminary studies have investigated their role on HIV-Protease inhibition, DNA photocleavage, neuro-protection, apoptosis, among others biological effects (Wilson 2000) (Fig. 1.2).

- **Carbon nanotubes**

Carbon nanotubes (CNTs) are single-walled (SWCNT) or multi-walled (MWCNT) cylindrical-shaped carbon particles with a diameter of 1 - 10 nm and length of a few micrometers (Ju-Nam & Lead 2008). They are robust but flexible and have been used not only in the manufacturing industry (i.e. aircrafts, sports equipment, etc.), but also as electron

field emitters, nanoprobes in atomic force microscopy, supports for heterogenic catalysis, microelectrodes in electrochemical reactions, and they are currently being investigated as potential hydrogen storage devices (Dresselhaus *et al.* 2001). However, further modification and optimisation is still required for their success in many of the aforementioned applications (Ajayan & Zhou 2001) (Fig. 1.2).

1.2.2. Metal oxide nanoparticles:

- **Iron oxide NPs:**

Iron oxides NPs (FeO_x) are naturally present in high concentrations in the environment (Ju-Nam & Lead 2008). Some of their supermagnetic properties and generally low toxicity, makes them ideal for nanobiotechnological applications (Duguet *et al.* 2006), and they have been already used as contrast agents for magnetic resonance imaging (Gupta & Gupta 2005; Veiseh *et al.* 2005), drug delivery (Barnett *et al.* 2007), gene therapy (efficient delivery of the desired gene and release inside the cell) (Medarova *et al.* 2007), clinical diagnosis (Chen 2008) to name a few. (Fig. 1.2)

- **Zinc oxide NPs:**

Zinc oxide (ZnO) NPs are conventional band gap semiconductors (an energy range in a solid where no electron states exist), and their properties have been investigated due to their potential applications in electronic devices (Kachynski *et al.* 2008; Laiho *et al.* 2008), chemical sensors, solar cells (Zhang *et al.* 2009b), antimicrobials (Li *et al.* 2008c; Padmavathy & Vijayaraghavan 2008; Spencer *et al.* 2009), water remediation technologies (Eslami *et al.* 2008) and because of their ability to block UV-A and UV-B rays while being optically transparent, also as sunscreens and cosmetics (Ju-Nam & Lead 2008) (Fig. 1.2).

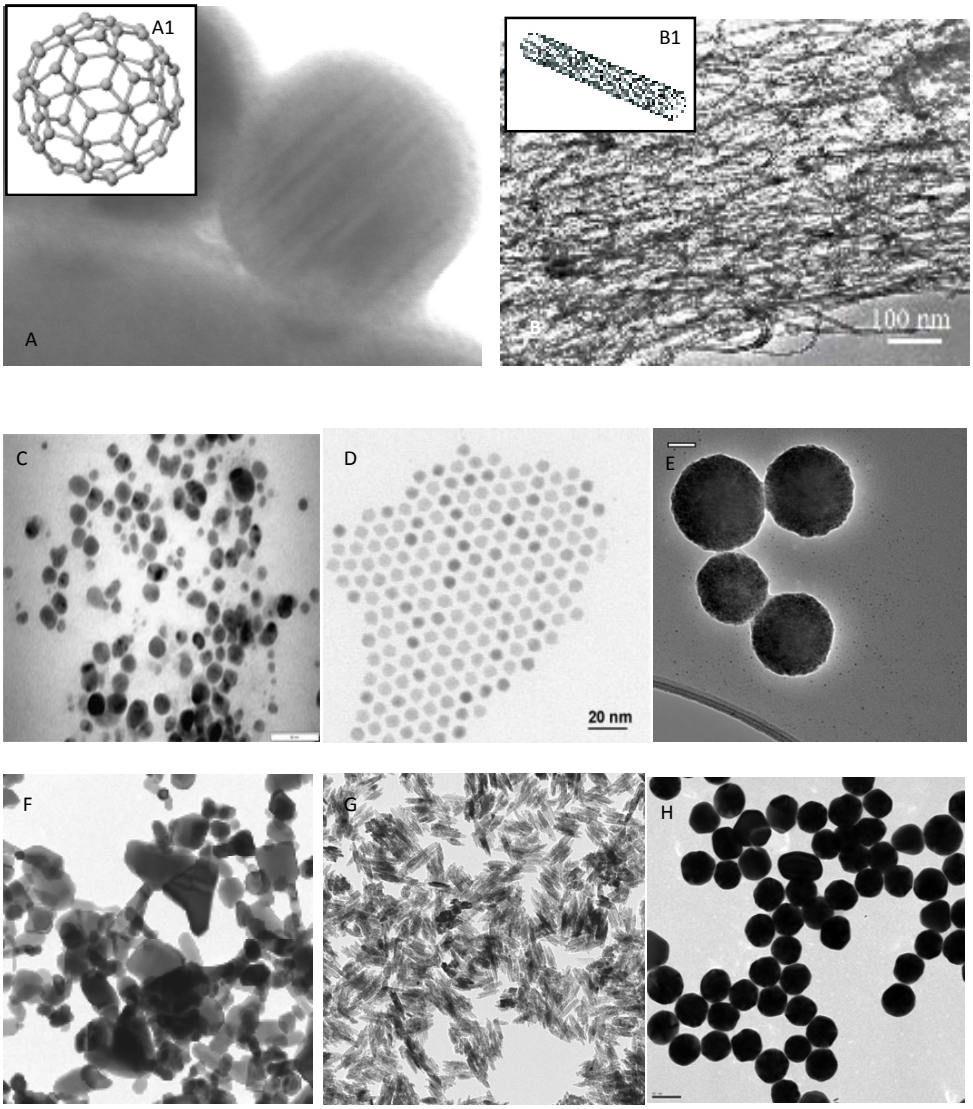

Figure 1.2. TEM imaging of different types of NMs. A) Fullerene (A1 diagram of fullerene); B) SWCNT (B2 diagram of SWCNT); C) silver NP; D) Quantum dots; E) Iron oxide NP; F) Zinc oxide NP; G) titanium dioxide NP and H) gold NP. Images are taken from: A) http://www.ceo.msu.edu/images/news/Fullerene_STEM_BF_11_full.png A1) http://www.ch.ic.ac.uk/local/projects/unwin/Full erenes.html; B) http://coewww.rutgers.edu/~sdytse/pictures/TEM-CNTs.jpg B1) www.ewels.info/img/science/nano.html C) http://www.nanowerk.com/spotlight/id465_1.jpg D) http://library.thinkquest.org/05aug/01179/quantum-dot-tem-PbSe.jpg E) http://www.seas.upenn.edu/~atsourk/Home_Pics/Iron_Oxide.jpg F) Wiench et al. 2009; G) Wiench et al. 2009 and H) http://www.polysciences.com/. Accessed on May 2009.

- **Titania NPs:**

Titanium dioxide (TiO_2) has received much attention for the application in the fields of photocatalytic activity (Hattori & Fujino 2006) and photocells (Ogura & Uchida 1987) due to its stability and low cost. TiO_2 particles can also be used as energy storage devices (Wang et al 2007), and in paints and coatings (Vargas *et al.* 2006; Wildeson *et al.* 2008), sunscreens, etc (Huang *et al.* 2006). TiO_2 can be synthesized in three crystalline phases: rutile, brookite and anatase. The latter being the most studied materials for photocatalysis and each of them presenting different properties and therefore different applications (Boccaccini *et al.* 2004). As ZnO NPs, TiO_2 NPs are also considered an excellent band-gap semiconductor (Ju-Nam & Lead 2008). However, TiO_2 nanoparticles tend to aggregate rapidly (Fig. 1.2).

- **Ceria NPs:**

Cerium (IV) oxide is used as catalysts, high dielectric capacitors, and components of solid oxide fuel cells and sensors. Cerium oxide also has high oxygen ion conductivity at intermediate temperatures (500-800 ˚C). Its catalytic effects are due to the partial Ce^{4+} to Ce^{3+} reduction since at elevated temperatures and in reducing atmospheres a large amount of oxygen vacancies within the ceria electrolyte can be formed. Some cerium (IV) oxide is reduced to cerium (III) oxide under these conditions with an increase on the electronic conductivity of the material (Yao & Yao 1984; Wang *et al.* 2007) (Fig. 1.2).

1.2.3. Other types of NPs

- **Quantum dots:**

Quantum dots (QDs) are semiconductor nanocrystals which show great potential as a new type of labelling and imaging material in biological and biomedical applications because of their unique optical properties, such as tuneable fluorescence and narrow and symmetric

emission profile with a broad excitation range (Yang & Gao 2005; Hardman 2006; Yang *et al.* 2007). However their medical use is still restricted due to the cytotoxicity exerted by the metals that the quantum dots are made of, and also due to their instability in aqueous media (Fig. 1.2).

1.2.4. Metal nanoparticles

- **Zero-valent Iron NPs:**

The major application of zero-valent iron (ZVI) NPs is in bioremediation technologies due to their size, and primarily due to their ability to degrade and adsorb to pollutants, which is partly size dependent (Zhang 2003; Huang *et al.* 2008; Lee *et al.* 2008a). ZVI successively reduces chlorine substitutes or chlorinated organic solvents to chlorides, eliminating chlorine atoms and yielding to a final non toxic product (Zhang 2003). The large volume to surface area enhances their effectiveness and increases the electron transfer required to eliminate toxic atoms (Huang *et al.* 2008; Lee *et al.* 2008a).

- **Gold NPs:**

Au NPs are quite stable, inert and their electronic, magnetic and optical properties can be adjusted (Ju-Nam & Lead 2008). Au NPs have been utilised coupled to biomolecules for medical applications. For example they can detect DNA with high sensitivity and selectivity (Sun *et al.* 2009) and have potential applications as contrast agents in cancer diagnosis and therapy, as well as mutations, single nucleotide polymorphisms (SNPs), chromosomal translocations, gene expression, and pathogens from clinical samples (Patra *et al.* 2007) (Fig. 1.2).

- **Silver NPs:**

The work in this thesis has been conducted with Ag NPs and they will be reviewed in greater detail.

Ag NPs have been intensely investigated due to their excellent unique properties associated to novel metals such as conductivity, chemical stability, catalytic activity, non-linear optical behaviour, and bactericidal activity (Capek 2004). These properties makes them suitable for a variety of applications including inks, microelectronics (Frattini *et al.* 2005), and bacterial disinfectant in medical equipment such as catheters (Roe *et al.* 2008), infusion systems and medical textiles (Silver 2003). Yet special social interest is aroused when applied to consumer goods, such as cosmetics, toothpaste, containers, clothing, electrodomestic, soaps, keyboards, baby pacifiers, to name a few. The manufacturing of Ag NPs is relatively cheap (Capek 2004), and the addition of these particles into goods (i.e. plastics, clothing, creams and soaps) increases their market value due to the consumer valued antimicrobial property (Frattini *et al.* 2005). Despite silver being classified as a toxic element under Section 313 of the Emergency Planning and Community Right-to-Know Act of 1987 (USEPA 1987) there are more than 260 products in the market containing Ag NPs (Woodrow Wilson Database, March 2009; http://www.nanotechproject.org/inventories/consumer/), and it was in 2008 when a coalition among consumer, health and environmental groups filed the first legal petition to the U.S. Environmental Protection Agency, asking the latter to regulate the sales and consider pesticides all those products using Ag NPs (http://www.ens-newswire.com/ens/may2008/2008-05-02-093.asp, Accessed April 4th 2009).

1.3. Silver nanoparticles: synthesis and physico-chemistry

Electronic, optical and catalytic properties differ from the bulk metals when the particle size decreases, especially at sizes between 1 and 100 nm (Niemeyer 2001; Moore 2006), and these novel properties have made NPs attractive for research in many fields. Overall, all different types of nanomaterials can be generated by either top *down* synthesis, where they are created by the formation of atoms from the bulk material, starting with a bulk

solid and decomposing it, i.e. lithography, etching, milling, etc, or by a *bottom up* synthesis, in which NPs are formed by the reaction and nucleation of smaller molecular components (Ju-Nam & Lead 2008). Nanomaterials are produced using a physical or a chemical approach. A physical method involves the manufacturing of NPs by different distribution techniques, while chemical methods generate NPs mainly by reducing metal salts to a zero valent state. All techniques always aim for a reproducible batch of identical size range, shape, morphology and chemical composition (Ju-Nam & Lead 2008). One of the problems of chemical synthesis is that the lifetime of the atoms in the dispersion is short and NPs tend to come together into large aggregates. This problem is often overcome by the use of capping agents, which coat the particles in order to reduce high surface energies (i.e. citrate, polymers, organic molecules) (Ju-Nam & Lead 2008). However, capping agents can then alter the desired physicochemical properties of the NP.

In the case of Ag NPs some of the most used methods for producing them are listed in Table 1.1.

Green synthesis or biosynthesis of Ag NPs aims for an environmentally friendly manufacturing and uses extracts from organisms (i.e. biomolecules), non toxic reductants and benign substances for particle stability (Sharma *et al.* 2009). Although efforts towards a greener synthesis are being developed, the chemical reduction method has been extensively used and studied for stable colloidal suspensions in water or organic solvents (Ju-Nam & Lead 2008), and it is also the most frequently applied method for manufacturing Ag NPs (Sharma *et al.* 2009). For Ag NPs the chemical reduction method works by reducing Ag ions in an aqueous solution using borohydride, citrate, ascorbate, or elemental hydrogen. When Ag ions are reduced they form silver atoms (Ag^{o}) that will eventually agglomerate into oligomeric clusters and finally lead to colloidal Ag particles (Sharma *et al.* 2009). Different

Table 1.1. Commonly used physical and chemical techniques for Ag NP production.

Methods	Chemical	Physical	References
Solution-Phase	√		(Mallin & Murphy 2002; Ju *et al.* 2005)
UV photolysis		√	(Isaeva et al. 2006; Tan et al. 2006; Balan et al. 2007)
Metal vapour deposition	√		(Hozumi *et al.* 2006; Palgrave & Parkin 2006)
Thermal decomposition		√	(Lee *et al.* 2008b)
Sonochemical decomposition	√	√	(Salkar *et al.* 1999; Yang & Li 2008)
Electrochemical techniques	√		(Richmonds & Sankaran 2008)
Laser ablation		√	(Murray & Shin 2008; Tsuji *et al.* 2008)
Microwave plasma synthesis	√		(Chau *et al.* 2005)
Biosynthesis/Green synthesis	√		(Ahmad *et al.* 2003; Duran *et al.* 2005; Sharma *et al.* 2009)

reductants will yield different colloidal particle sizes (Zhang *et al.*). So for example, borohydride tend to produce monodispersed small particles, but generation of larger particles are difficult to control with this reductant. The use of weaker reductants such as citrate (also a capping agent) results in a slower reduction rate (and larger particles) and leads to larger size distributions (Sharma *et al.* 2009). To overcome the problem of large size distributions, a two step controlled synthesis is used, by firstly utilising a strong reducing agent for the production of small NPs, and secondly narrowing the size distribution with a weaker agent.

1.4. Manufactured and Natural Nanoparticles in the environment

1.4.1. Natural Nanoparticles

Colloids (defined as between 1-1000 nm) (Lead and Wilkinson 2006), are more recently defined as natural nanoparticles and have been in the Earth for millions of years as a key component in our ecosystem. They are produced by microbial processes, sedimentation,

natural combustion (in atmosphere), and other natural processes (Dunphy Guzman *et al.* 2006; Sengul *et al.* 2008) (Table 1.2).

Table 1.2 Classification of environmental aquatic colloids according to their origin and composition. From Christian *et al.* 2008

Natural Colloids		Anthropogenic colloids	Engineered nanomaterials
Inorganic colloids	Organic colloids	Wear & Corrossion products	Standard industrial products
* **silicates**	***Macromolecules**	***from tire and brakes**	***polymers**
smectites	humic acids	***from cartalysis (e.g. Pt, Pd)**	***surfactants**
chlorites	fulvic acids	***metals (wear in bearings)**	***dyes & pigments**
Mica	Polysaccharides	***metal oxides**	***metal oxides**
kaolinite	Proteins	***additives to lubricants**	NP metals & metal oxides
***oxides/hydroxides**	Peptides		***metals (Au, Ag, Fe)**
Fe-oxohydroxides	exo-polymers	Waste & combustion products	***metal oxided (of Ti, Zn, Zr, Ce, etc)**
Mn-oxides	***bio-colloids**	***soot**	***metal tubes and wires**
***carbonates**	Bacteria	***tar leachate in plumes**	carbon based
***phosphates**	Viruses	***fly ash**	***fullerenes**
***metal sulfides**	Fungi	***fine dust (organic & inorganic)**	***single and multiwalled nanotubes**
	***coal/soot/black carbon**		Hybride structures
	***cellular debris**		***quantum dots**
			***functionalised materials**
			***core-shell structures**

Origin

Composition

1.4.2 Anthropogenic nanoparticles

Anthropogenic (incidental or adventitious) nanoparticles have existed since the earliest days of civilisation. However, anthropogenic emissions of inorganic NMs have more than doubled the mass of natural nanoparticles into the atmosphere (Farre *et al.* 2009). Until recently NMs were referred as ultrafine particles in the air (i.e. NMs resulting from diesel- and gasoline-fuelled vehicles and stationary combustion sources), colloids in soil (i.e. clays, organic matter, iron oxides and other minerals important for biogeochemical processes) and also colloids in water (comprising macromolecules, humic and fulvic acids, proteins and peptides, and hydrous iron and manganese oxide (Klaine *et al.* 2008)) (Table 1.2). .

1.4.2.1 Manufactured nanoparticles

The global impact of manufactured nanomaterials is yet unknown, but previous knowledge of environmental and health effects of ultrafine particles give an indication of the potential effects the manufactured of NMs could cause on ecosystems. For example, ultrafine particles in the atmosphere have been linked to health effects (Ferin *et al.* 1990; Oberdorster *et al.* 1990; Oberdorster *et al.* 1992; Oberdorster *et al.* 1995; Oberdorster 2001) and other environmental processes such as the modification of cloud properties that can affect the nature of a whole ecosystem (Lee *et al.* 2003; Pierce & Adams 2007). The uncertainty and the increasing concerns about the safety of nanomaterials in the environment is in part due to the media (Feder 2006) and to the calls by many environmental based NGOs for a ban, stringent regulations and safety testing of NMs before commercialisation. Although many reports (RS/RAE 2004; RCEP 2008) have rejected calls for a blanket ban since the development and implementation of strict policy and regulation are not simple given the many factors such as composition, shape, size, capping agent, to name a few, that will modify the nature of the N and affect its fate and toxicity.

1.5 How much is already in the environment?

To predict toxicity and bioavailability of any type of particle it is necessary to have information about its concentration in the environment. However, detection of NMs in natural systems is not easy, and to date there has been no direct quantification that can tell us how much of it has already been released (Shi *et al.* 2001; Aitken *et al.* 2006; Luoma 2008; Nowack 2009). The reason that detection of NMs in the environment is complex it is (1) because of their low concentrations (estimated to be in the range of ng l^{-1} or lower (Boxall *et al.* 2007; Mueller & Nowack 2008; Boxall *et al.* 2008 ; Tiede *et al.* 2009)(Table 1.3), (2) the relative high concentrations (mg l^{-1}) of natural NMs (i.e. iron oxides, and carbon based

molecules), and (3) lack of reliable detection methods able to separate dissolved and background levels of trace metals from metal NMs (Handy *et al.* 2008).

To date, predictions have been made by estimating the predicted environmental concentrations (PEC) using a modelling approach based on the manufacturing and life cycling of the nanoproduct (Benn & Westerhoff 2008; Blaser *et al.* 2008; Mueller & Nowack 2008; Tiede *et al.* 2009). Table 1.3 defines the PECs for different nanomaterials. The discrepancies on the values obtained from different researches arise from the differences on modelling approaches. Mueller and Nowack 2008 use a life cycle perspective to model the quantities of engineered NMs released into the environment. Yet, the risk assessment was carried out with data from Switzerland only, and when sufficiently detailed data was missing assessments based on worse-case scenarios were accepted. On the other hand, Boxall *et al.* 2009 carried out a more comprehensive study with algorithms and simplistic models applied to estimate the likely concentrations of NMs in the UK environment. These models used a 10% market penetration scenario, which is likely to overestimate the current exposure of certain NMs. Also, the models used by the latter researchers provide conservative estimates since they do not consider degradation and interactions with soil, sediment and others.

Fig. 1.3 shows a schematic overview of potential entries of Ag NPs into the environment from Ag-containing plastics and textiles. Modelling analyses have suggested that up to 15 % of the total Ag emitted to water in Europe may be released from biocidal plastics and textiles in 2010 (Blaser *et al.* 2008). Leaching of Ag NPs and Ag ions from Ag containing products will end up with its accumulation into wastewater (Benn & Westerhoff 2008). Wastewater will either be treated in a sewage plant (STP, 90% in EU) or will end up in the environment without further management. Sewage sludge will then be either applied to agricultural soil, end up in a landfill or incinerated by thermal wastewater treatment (TWT).

Table 1.3 Predicted concentrations of NMs in the environment released from consumer products. Data pooled from Mueller and Nowack 2008 and Boxall *et al.* 2008 (in bold).

	Air	Water	Soil
	$\mu g\ m^{-3}$	$\mu g\ l^{-1}$	$\mu g\ Kg^{-1}$
Ag	1.7×10^{-3}	0.03/**0.01**	0.02/**0.43**
TiO_2	1.5×10^{-3}	0.7/**24.5**	0.4/**1030**
CNT	1.5×10^{-3}	0.0005	0.01
AlO_3		**0.0002**	**0.01**
Au		**0.14**	**5.99**
CeO_2		**<0.0001**	**<0.01**
Fullerenes		**0.31**	**13.1**
Hydroxyapatite		**10.1**	**422**
Latex		**103**	**4307**
Organo-silica		**0.0005**	**0.02**
SiO_2		**0.0007**	**0.03**
ZnO		**76**	**3194**

If sludge ends up in a field it is quite likely Ag will leach to groundwater. In addition, if biocidal products are disposable, they will directly end up in landfill (Blaser *et al.* 2008). Thus regardless of the path, once Ag NPs are manufactured and used in goods, they will inevitably accumulate in the environment. High concentration of Ag in the biosolids could prevent or limit their use as agricultural fertilisers (Benn & Westerhoff 2008).

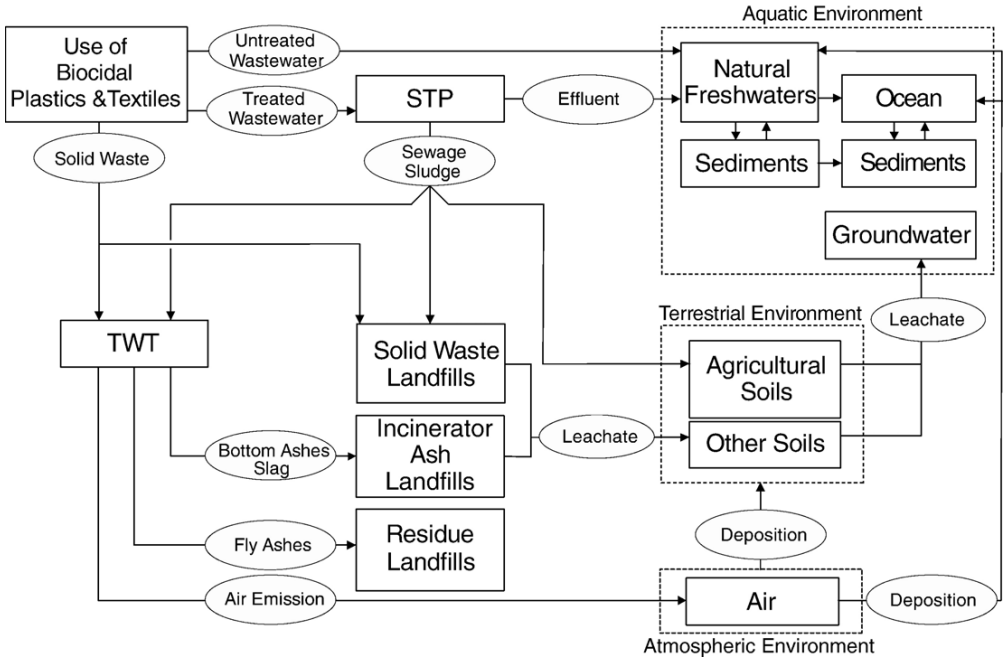

Figure. 1.3 Scheme of Ag flow triggered by biocidal goods. Arrows represent silver flows; dashed lines indicate different environmental compartments. TWT: Thermal waste treatment; and STP: sewage treatment plant. From Blaser *et al.* 2008.

While in 2006 the global market worth of nanotechnology was US$ 10.5 billion. THis is expected to have more than doubled by 2011 (McWilliams 2006). In 2011 the annual worldwide production of SWCNT is also estimated to exceed 1,000 tones (Lekas 2005). In the case of Ag NPs and due to the significant growth on the market for Ag containing products, its current production is estimated to be ca. 30 tonnes/annum (Mueller & Nowack 2008) and projected to reach 110-230 tonnes by 2010 (Blaise *et al.* 2008). The release of particles into the environment can occur involuntarily during the manufacturing process (i.e. spillages) (Moore 2006), or leaching from paints (i.e. TiO_2, ZnO), clothing (i.e. Ag), sunscreen and cosmetics (TiO2, ZnO) (Klaine *et al.* 2008), but their release can also be voluntarily, i.e. used in soils as tools for remediation of contaminated soils (i.e. zero valent iron NPs). Nevertheless, regardless of their use, these particles will ultimately end up in water and land, and interact with the organisms living there (Klaine *et al.* 2008).

1.6 Techniques used for the characterisation of nanoparticles

Understanding the behaviour (transport, persistence, fate) of NMs in natural systems is fundamental to the accurate prediction of exposure, and thus bioaccumulation, depuration and biological effects to biota (Moore 2006). However, there are multiple parameters which need to be analysed in order to have a clear understanding of their physico-chemical properties of NMs in an aqueous suspension and predict their fate and behaviour under relevant environmental conditions and in different environmental compartments. Table 1.4 describes some of the most commonly used techniques for the characterisation of NMs.

For optimising their analyses, often nanoparticles have to be separated from complex samples containing other particles. Fractionation is commonly done by centrifugation, ultrafiltration, cross-flow ultrafiltration (CFF) or field flow fractionation (FFF) (Wigginton *et al.* 2007). These methods are sensitive and allow samples to be used for further physico-chemical analysis (Farre *et al.* 2009). Physical parameters such as size distribution, specific surface area and volume can be quantified in either fractionated or unfractionated samples. Size distribution can be analysed by laser or diffuse light scattering: LLS (Funfer *et al.* 1963; Woodward 1963) or dynamic light scattering (DLS) (Chakraborty *et al.* 2003; Bootz *et al.* 2004; Ito *et al.* 2004), laser-induced breakdown detection (LIBD) (Loree & Radziemski 1981), X-ray diffraction (XRD) (Cannas *et al.* 1999; Chen *et al.* 2008), atomic force microscopy (AFM) (Arcoleo & Liveri 1996; Gu *et al.* 2005), and transmission electron microscopy (TEM). Surface area can be determined indirectly by using the diameter of particles obtained with AFM or TEM measurements or by the Brunauer–Emmett–Teller (BET method) (Madden & Hochella 2005; Madden *et al.* 2006). Suitable chemical analysis include atomic adsorption spectroscopy (AAS) (Amos & Willis 1966), inductively coupled plasma (mass or atomic emission) spectroscopy (ICPMS/ICPAES) (Bouby *et al.* 2008; Ge *et al.*

2008), X-ray energy dispersive spectroscopy (EDS), electron energy loss spectroscopy (EELS). Often it is crucial to be able to directly visualize the particles of interest. Two common visualization methods are AFM and electron microscopy (Wigginton *et al.* 2007).

1.7 Nanoparticle behaviour in the environment

When determining the fate of a NM in the environment there are a series of questions we must address, such as 'how will NMs behave in an aqueous system and which variations on parameters will lead to a change on the predicted behaviour? Do manmade NMs associate with other nanoparticles, colloids and larger particles? Will they bind to pollutants and affect their fate/toxicity/biodegradability? How do NMs partition in various environmental phases and how does this affect their mobility and biodegradation? Are surface properties sufficient to predict toxicity and behaviour?

Natural colloids and nanoparticles in the environment can interact with one another and also with other larger particles (Simonet & Valcárcel 2009). The physical properties of a particle (e.g. conductivity, reactivity, etc) vary dramatically as a function of size, composition and coatings (Handy *et al.* 2008) and can be very different from bulk material (Madden & Hochella 2005; Madden *et al.* 2006). Most importantly, the surrounding environment of the particles defines crucial ecological parameters, such as solubility, stability, biodegradability that will affect their toxicity and impact on ecosystems.

Very little information is yet available on the fate and ecological role of manufactured nanoparticles in the environment. Nevertheless, due to their similar size to colloidal particles, any previous work done on this topic certainly helps understanding the fate of their manmade counterparts (Lead & Wilkinson 2006b).

Table 1.4 Methods for analysis and classification of NMs (Modified from Hasselov et al 2008 and Wigginton et al 2007).

	Instrument and method	Limit of detection	Limitations	Advantages
Sample fractionation	TFF	ppm/ppb	Concentrated samples (<5-10 times)	Low sample perturbation
	FFF	ppm/ppb	Carrier liquid may affect results/ wall interactions	Fast/low sample volume/no sample prep
	Ultrafiltration	ppm/ppb	Binding with UF membrane	Low sample perturbation/no sample preparation
	Centrifugation	detection dependent	Low accuracy	Low sample perturbation/mass separation
Physical properties				
Diameter	EM	ppb-ppm	Sample preparation may affect results	High resolution
	AFM	ppb-ppm		High resolution
	Flow-FFF	ppb/ppm	wall interactions	wide size range separation/fast/non-destructive
	DLS	ppm	Sample dispersability not polydispersed	Fast/accurate
Volume	Sed-FFF	ppb/ppm	Dilution required and adsorption to walls	Good recovery of sample/non-destructive
Area	EM	ppb/ppm	High resolution and visualisation of large areas	Destructive
	AFM	ppb/ppm	image distortion	3D images/High resolution
	BET	dry powder	Powdered samples	High precision
Mass	LC-ESMS	ppb/ppm		
Surface charge	z-potential, electrophoretic mobility	ppm	Background noise if sample is not filtered	Low concentrations
Crystal structure	XRD	dry powder	Powdered samples	Low concentrations
	TEM-EDX	ppm in single particle	Sample staining not needed	Accurate and very fast
Chemical composition	ICP-MS	ppt/ppb	Sample preparation may limit detection	Multiple metal analysis
	ICP-OES	ppt/ppb	Sample preparation may limit detection	Multiple metals- limit of detection is low
	AAS	ppt/ppb	Single metal , sample preparation	
	TEM-EDX	ppm in single particle		
Other properties				
Aggregation state	DLS	ppm	Sample dispersability not polydispersed	fast and accurate
	AFM	ppb/ppm		
	ESEM	ppb/ppm		
Hydrophobicity	Liquid-liquid extraction chromatography			Use of complex solvent mixtures
Dissolution rate	Dialysis or voltammetry or spectrometry			low concentrations
Surface chemistry	X-ray spectroscopy, acid base titrations		Powdered samples	low concentrations

The high surface/volume ratio of nanoparticles due to their small size results in a high reactivity of the particles, which tend to aggregate. To prevent aggregation and settling particles can be stabilized sterically and electrostatically. Steric stabilisation is a mechanism by which hydrophilic compounds that are capping or surrounding the particles inhibit their coagulation in suspension. This type of stabilisation is very effective even at high salt concentrations due to the hydrophilic nature of the coating compounds that strongly interact with water rather than other surfaces. Electrostatic stabilisation comes from the combined effect of attractive (van der Waals) and repulsive (electric double layer, EDL) forces between the particles, and Van der Waals forces are the ones responsible for particle aggregation.

The DLVO theory was developed by Derjaguin & Sidorenkov (Derjaguin & Sidorenkov 1941) and independently by Verwey and Overbeek (Verwey & Overbeek 1948), and describes the force between charged surfaces interacting through a liquid medium and helps predict the stability of particles in suspension. However, this theory does not take into consideration steric effects the effects of particle shape, charge heterogeneity or surface roughness which may also influence aggregation (Bhattacharjee *et al.* 1998). The EDL is a layer of charge surrounding the surface of the particle and electric field generated by the charged surface, which can be positive or negatively charged depending on the surface ligands of the particle. The repulsive forces generated by the EDL layer, if strong enough, can stabilise a colloidal suspension. However, if this layer of charge is compressed, the suspension becomes unstable due to the aggregation of particles and ultimately precipitation. Salt ions (NaCl), act by accumulating onto the EDL layer and compressing it. They generate forces of attraction between the Na^+ and Cl^- ions that set onto the EDL layers among NMs. Thus, salt ions in a medium allow particles to approach each other more closely and become affected by attractive forces acting at shorter distances (Brant *et al.* 2005). In natural waters, when moving from a freshwater environment to seawater, stable colloids precipitate out of

suspension induced by seawater salts (Stolpe & Hassellov 2007), and this behaviour has also been described by other authors on several NMs. TiO2 (Domingos *et al.* 2009; French *et al.* 2009; Jiang *et al.* 2009), fullerenes (Brant *et al.* 2005; Fortner *et al.* 2005b), gold (Viudez *et al.* 2006), silica (Singh & Song 2007), carbon nanotubes (Liu *et al.* 2006), etc., have been shown to aggregate and precipitate at higher rates when the solution ionic strength increases.

In addition to ionic strength, other factors influence the stability of particles in suspension since they will affect the charge of the particles in suspension. Humic and fulvic acids (highly negatively charged) bind and form a film onto the surface of colloids (Lead *et al.* 2005; Baalousha & Lead 2007) and nanoparticles (Giasuddin *et al.* 2007; Hyung *et al.* 2007; Christian *et al.* 2008; Baalousha *et al.* Submitted) and depending on the surface charge of the particle, HS can sterically stabilise or destabilise NMs. Overall, for negatively charged NMs, HS tend to stabilise particles in suspension at circumneutral pH values, as it is the case of CNTs (Hyung *et al.* 2007) and TiO_2 (Domingos *et al.* 2009), fullerenes (Chen & Elimelech 2008) and gold (Diegoli *et al.* 2008), but they can also help destabilise particles as it is in the case of positively charged FeO NPs (Baalousha et al 2008).

An important factor in determining the stability of colloidal dispersions is often pH (Ishikawa *et al.* 2005; Guzman *et al.* 2006; Lead & Wilkinson 2006b; Jiang *et al.* 2009). Many NMs are net negatively charged over a large range of pH values, and others, such as oxides and carbonates show a positive charge at low circumneutral pH values. Overall, if the pH values are far from the point of zero charge (PZC; or condition when the electrical charge density on a surface is zero) the suspensions are more stable (Guzman *et al.* 2006; Pettibone *et al.* 2008).

The behaviour of NMs in the environment can be predicted to a limited extent based on the previous knowledge of colloidal dispersion and also initial studies of NM suspensions.

As with colloids, the surrounding environmental conditions must be taken into consideration to understand and predict their fate.

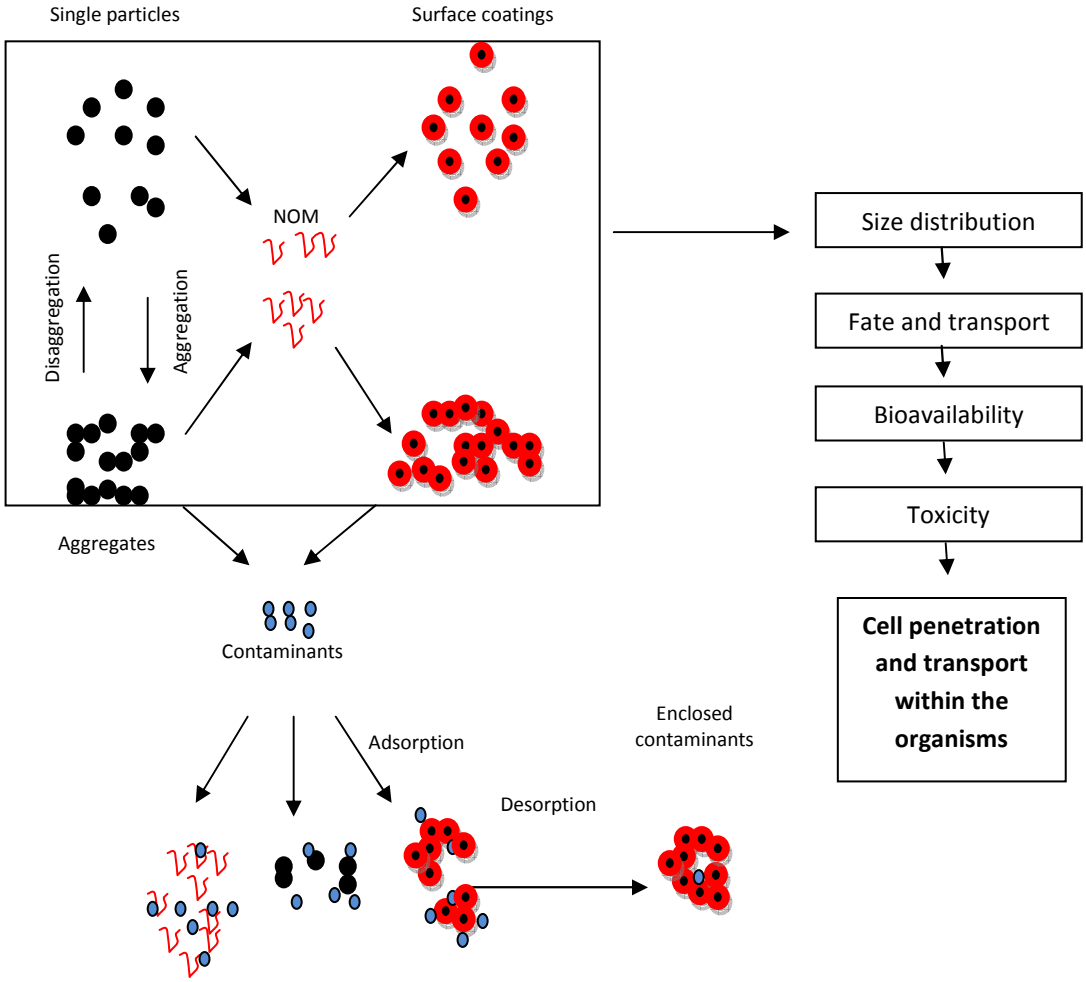

Figure 1.4 Interaction of NPs with natural water components (From Christian *et al.* 2008).

A well studied property of manmade NMs is their role on the partitioning of contaminants in a polluted site. As well as colloids (Tronczynski 1992; Honeyman & Mackay 1993; Lead *et al.* 1999; Flury & Qiu 2008; Persson *et al.* 2008), NMs can play a crucial role in the segregation of contaminants by strongly binding to them and helping their dispersion or precipitation (Zhang 2003; Giasuddin *et al.* 2007; Hu *et al.* 2008; Pan & Xing 2008; Samonin *et al.* 2008; Schierz & Zanker 2009) (Figure 1.4). Sorption onto NM surfaces depends on both, the physico-chemical properties of the particles (i.e. size, purity, structure) as well as the solution properties (pH and ionic strength) (Christian *et al.* 2008). Thus, the stability of

nanoparticles in suspension can predict the residence time of metals in suspension and predict dispersion. The more stable the particles are in suspension the further they can be transported together to any metal or pollutant bound to them (Brant *et al.* 2005). On the other hand, coagulation and flocculation will facilitate the aggregation and precipitation of those large enough to sediment (Mylon *et al.* 2004). Therefore, particle stability in aqueous suspension is crucial for determining targeted environmental compartments for NP accumulation as well as those organisms that are more likely to be exposed to them (Figure 1.5)

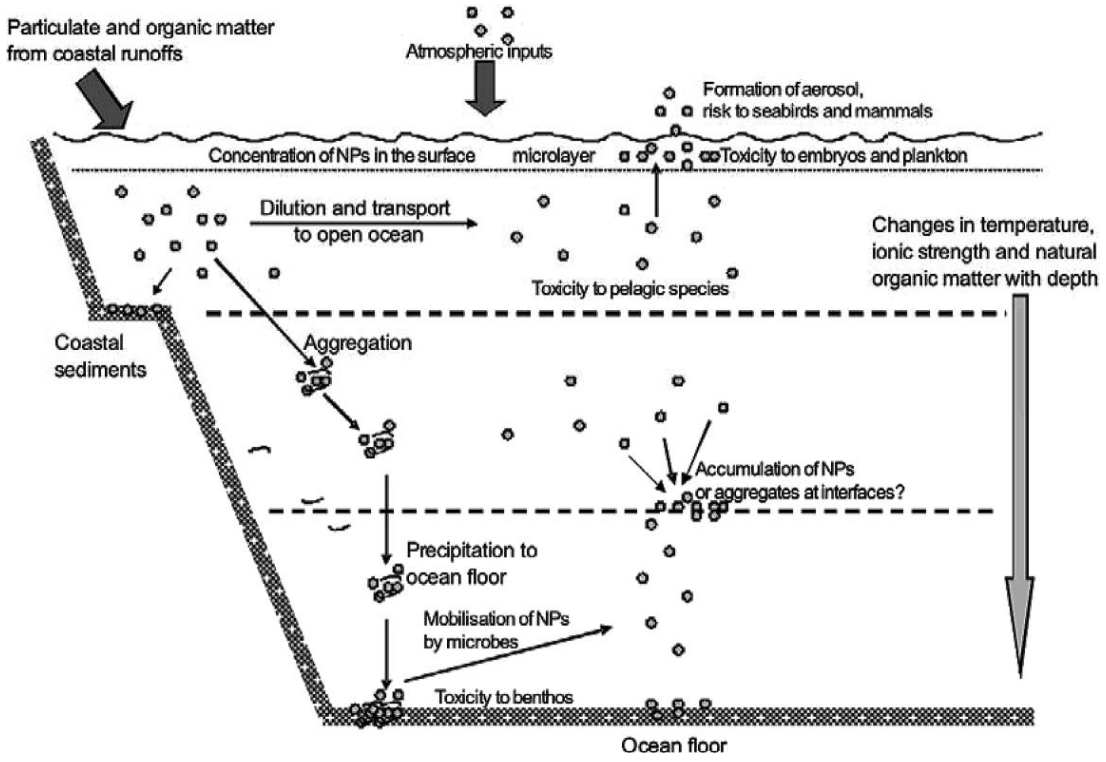

Figure 1.5 Schematic diagram outlining the possible fate of NPs in the marine environment as well as organisms at risk of exposure (From Klaine *et al.* 2008).

1.8 Silver ions in the environment

Silver is a rare chemical element (67th in abundance among the elements) with an atomic weight of 47. Silver has long been used by humans in many forms and for many applications: ranging from silverware and jewellery, to storage vessel for water and wine in ancient civilisations, to furniture, etc. The ability to interfere with bacterial reproduction and

growth is one of the most remarkable properties of silver, and in the medical field it was in 1884 when the obstetrician C. S. F. Crede developed and employed for the first time a silver solution used for the prevention of eye infections. In World War I silver compounds were used extensively to prevent wound infection. However with the introduction of more selective antibiotics like penicillin and cephalosporin the use of silver in medical applications and devices declined (Luoma 2008), and the use of silver preparations in medicine was restricted to burn treatments (Silver 2003).

Silver can be introduced into the environment by natural geological sources, as well as through anthropogenic activities such as the photographic industry, electroplating materials, conductors, dental alloys (Herrera *et al.* 2001), solder and brazing alloys, paints, jewellery, silverware, coinage, and mirror production.

Although concentrations of dissolved silver are very low in natural waters (0.1-0.3 ng 1^{-1}) and in oxidised sediments (0.1 μg g^{-1} dry weight), its anthropogenic input can increase 100-300 times this amount (Sanudo-Willhelmy & Flegal 1992). Nevertheless, as with all metals, the cationic nature of silver and association with various ligands make its speciation, and thus toxicity, dependent on the chemistry of the surrounding environment (Luoma *et al.* 1995; Erickson *et al.* 1998). Factors such as pH, complexing agents (i.e. organic matter) and alkalinity (i.e. concentration of competing ions) are likely to have a very strong effect on its toxicity and bioavailability.

In freshwater environments, the monovalent Ag ion is the dominant silver species (Luoma *et al.* 1995). Humic acids can bind to Ag due to their high proportion of S- and N-containing groups (Sikora & Stevenson 1988). The stability constants for Ag complexes with ligands containing oxygen and nitrogen donor atoms (i.e. humic substances) are quite small and complexes will occur if competing ions are not present. For example, Ag forms stable

complexes with chloride, iodide and sulphur in aqueous solutions (Nieboer & Richardson 1980). Colloidal partitioning of Ag has been found to decrease with increasing salinity (Sanudo-Willhelmy & Flegal 1992; Luoma *et al.* 1995; Wen *et al.* 1997; Reinfelder & Chang 1999).

On the other hand, in seawater Ag does not form strong complexes with natural organic matter since chloride and other stronger ligands are present in a higher amount (Miller & Bruland 1995; Herrin *et al.* 2001; Ward *et al.* 2006). Thermodynamic models show that strong chloro complexes ($AgCl°$, $AgCl_2$, $AgCl_3^{2-}$, $AgC1_4^{3-}$) dominate speciation (Cowan *et al.* 1993; Ferguson & Hogstrand 1998; Reinfelder & Chang 1999), and this complexation favours the retention of Ag in a dissolved form enhancing dispersal. Thus, organic complexation is less important for silver in estuarine and marine environments (Miller & Bruland 1995; Ward *et al.* 2006), and instead of ionized Ag^+ uncharged $AgCl^\circ$ is the dominant Ag species in saline waters (Nieboer & Richardson 1980).

1.9 Silver ion toxicity and the biotic ligand model

1.9.1 Toxicity to fish and invertebrates

Aquatic organisms are able to accumulate dissolved and particulate silver (Reinfelder & Chang 1999) hence the chemical species and uptake mechanisms should be understood in order to predict the fate and effects of Ag in ecosystems. Most of the research on silver toxicity has been done in freshwater organisms (Ratte 1999), while marine life has received little attention.

Understanding metal speciation and monitoring water quality parameters has been a topic of interest for many years, and recently the biotic ligand model (BLM) has been developed as a predictive tool to evaluate quantitatively the way in which water chemistry

affects the speciation and bioavailability of metals in aquatic systems (Paquin *et al.* 2002). This model uses the gill as a negatively charged ligand (Janes & Playle 1995) since it is the primary site of metal interaction in freshwater fish and crustaceans (Bianchini *et al.* 2005) to which Ag can bind. There has been much research done on the toxicity and toxicity mechanisms of Ag in fish (Janes 1995; Wood *et al.* 1996; Galvez & Wood 1997; Morgan *et al.* 1997; Hogstrand & Wood 1998; Wood *et al.* 1999; Wood *et al.* 2002; Wood *et al.* 2004; Nichols *et al.* 2006; Bielmyer *et al.* 2008). Ag affects the gill functions in freshwater fish by primarily inhibiting the carbonic anhydrase activity followed by the inhibition of the Na^+/K^+ ATPase, which leads to a net loss of Na^+ and Cl^- in fish (Zhou *et al.* 2005; Nichols *et al.* 2006) and in some invertebrates (Bianchini & Wood 2008). Mechanisms of toxicity in freshwater and in seawater fish differ. However the exact mechanisms of Ag toxicity have not been fully elucidated. In freshwater Ag toxicity is reduced when complexing with humic or fulvic acids (Ward *et al.* 2006). This reduced toxicity due to presence of organic matter is negligible in seawater. In seawater, chloride concentration plays a fundamental role. For example, in a study performed by Hogstrand *et al.* (1996) on Ag exposures the LC50 value for juvenile rainbow trout in freshwater was 111 nM, while in brackish water (50 mM NaCl) no acute toxicity was observed over 168 h under a similar concentration. A similar study done by Ferguson *et al.* (1998), also suggested different Ag toxicities, being with Ag ions in freshwater and AgCl*n* complexes in seawater the toxic chemical species affecting rainbow trout. In the latter, Ag toxicity showed a clear salinity dependence in the salinity range of 15 to 30‰, with increasing mortality rates as salinity increases.

The BLM can be successfully applied to freshwater systems, although recent research suggested that species-specific testing is required due to the physiological differences among freshwater fish (Bianchini & Wood 2008). In addition, in marine fish the gill is not the only site of interaction with silver. Seawater fish also tend to drink water to replace water loss by

osmosis across the gills, so the gut is also an important target for Ag interactions and accumulation (Grosell *et al.* 1999; Hogstrand *et al.* 1999; Webb & Wood 2000; Bianchini *et al.* 2005).

The BLM constants have been copiously calculated for fish, although it is still uncertain if the same BLM constants can be used between species and how laboratory established parameters can be used under field conditions (Slaveykova & Wilkinson 2005).

1.9.2 Toxicity to microorganisms

Ag ions are one of the most toxic forms of heavy metals to organisms and especially to bacteria (Cornfield 1977; Ratte 1999; Silver 2003). The antimicrobial activity of silver ions has been studied by many authors (Trevors 1987; Tsezos *et al.* 1997; Efrima & Bronk 1998; Klaus *et al.* 1999; Feng *et al.* 2000; Ibrahim *et al.* 2001; Zeiri *et al.* 2002; Silver 2003; Chou *et al.* 2005; Hwang *et al.* 2007; Throback *et al.* 2007; Yoon *et al.* 2008), and exploited for preventing infections by means of silver ion release from either solid silver or silver solutions (i.e. silver nitrate). The addition of silver in medical products (i.e. dental fillings (Herrera *et al.* 2001), catheters (Roe *et al.* 2008), bandages and inserts (Silver *et al.* 2003)) decreases the chance of bacterial infections. By the same principle, adding silver into consumer goods has increased the market value of many products by advertising them as able to kill noxious bacteria and decrease bacterial growth that otherwise lead to bad odours and food spoilage (i.e. soaps, washing machines, clothing, Tupperware, etc...).

Ag occurs under several oxidation states, including elemental silver (Ag°), monovalent silver ion (Ag^{+} ,the most common oxidation state), and higher oxidation states (Ag^{2+} and Ag^{3+}). Ag^{+} causes toxicity to bacterial cells by the binding to DNA and to thiol groups inactivating vital enzymes affecting bacterial replication and respiration (Bragg & Rainnie 1974; Trevors 1987; Slawson *et al.* 1992b; Feng *et al.* 2000; Holt & Bard 2005; Landsdown

& Williams 2007). Ag granules can be easily detected attached to cell membranes in cells exposed to silver solutions (Trevors 1987; Tsezos *et al.* 1997; Feng *et al.* 2000). Ag toxicity to microorganisms also depends on the concentration of halide ions in the surrounding environment. For instance, chloride affects the bioavailability of Ag (Silver 2003) by strongly binding to Ag^+ and precipitating out of solution as AgCl. Thus, when Cl^- ions are low, soluble Ag^+ binds tightly to bacterial cells surfaces, moderate concentration of Cl^- ions remove Ag as precipitates AgCl. However, higher concentrations of Cl^- bring the silver back into solution as a bioavailable $AgCl_2$ (Silver 2003). Many bacterial strains can show resistance to Ag and the mechanisms of resistance to heavy metals that are encoded by various plasmid-based genes have been well studied and characterised (Gupta *et al.* 1999; Silver 2003; Silver *et al.* 2005).

Toxicity of Ag NPs has often been suggested to be the result of the release of Ag ions in solution. Thus, previous knowledge on silver speciation and behaviour in natural waters can help investigate the mode of action of Ag NPs and discriminate the potential toxic mechanisms of silver ions from Ag NPs (see Section 1.11).

1.10 Ecotoxicology of engineered nanomaterials

Recently there has been an increased focus on the potential environmental and health impact arising from the use and release of nanomaterials (Engineering 2004; Feder 2006; Maynard *et al.* 2006; Moore 2006; Nowack & Bucheli 2007; Handy *et al.* 2008; Feder May 17 2006). When implementing a new technology it is important to consider the safety aspects at early stages of their development (Baun *et al.* 2008). Currently (April 2009) there are more than 600 studies that have investigated the risks of nanomaterials to organisms. However, just a few are environmentally relevant to species (Baun *et al.* 2008) and few, if any, have been performed at environmentally relevant conditions.

The lack of knowledge about the novel properties of manmade nanomaterials and limited published research raises concerns on their potential harm to ecosystems (Moore 2006; Tiede *et al.* 2009). The fate and bioavailability of such manmade particles in the environment and their impact is still very much unknown. To date there is insufficient data to predict the effects of NPs which have already been released into the environment (Neal 2008), and safety testing and regulations do not exist anywhere in the world (Tiede *et al.* 2009).

The fate and toxicity of NPs may be influenced by many factors, including particle size and shape, distribution, solubility, state of aggregation, crystal structure, surface area, charge and chemistry. The properties that make nanomaterials useful may also make them more likely to react with tissues in the body and cause cellular and tissue damage (Powell *et al.* 2008). Although the number of ecotoxicology tests and organisms being investigated is increasing sharply, data on the effects of NPs to whole organisms are still scarce (Klaine *et al.* 2008) and *in vitro* and studies on microorganisms have been more prevalent until now. The toxicity mechanisms of NPs are not fully clear, and seem to be highly dependent on particle-specific properties. Multiple mechanisms of toxicity have also been suggested for certain type of NPs, such as Ag and ZnO, where the soluble fraction of the particle may be the cause of the effects detected. Nevertheless, from most research a variety of effects have been described, including: disruption of cellular membrane or membrane potential, oxidation of proteins, genotoxicity, interruption of energy transduction, formation of ROS, release of toxic constituents, among others (Klaine *et al.* 2008) (Fig 1.6). However, it is important to take into consideration that recent research has suggested that the most common methods for reactive oxygen species (ROS) detection in cells (colorimetric methods) can lead to false positives (Lyon & Alvarez 2008; Shinohara *et al.* 2009), and sample handling and preparation are crucial for non-biased and meaningful results.

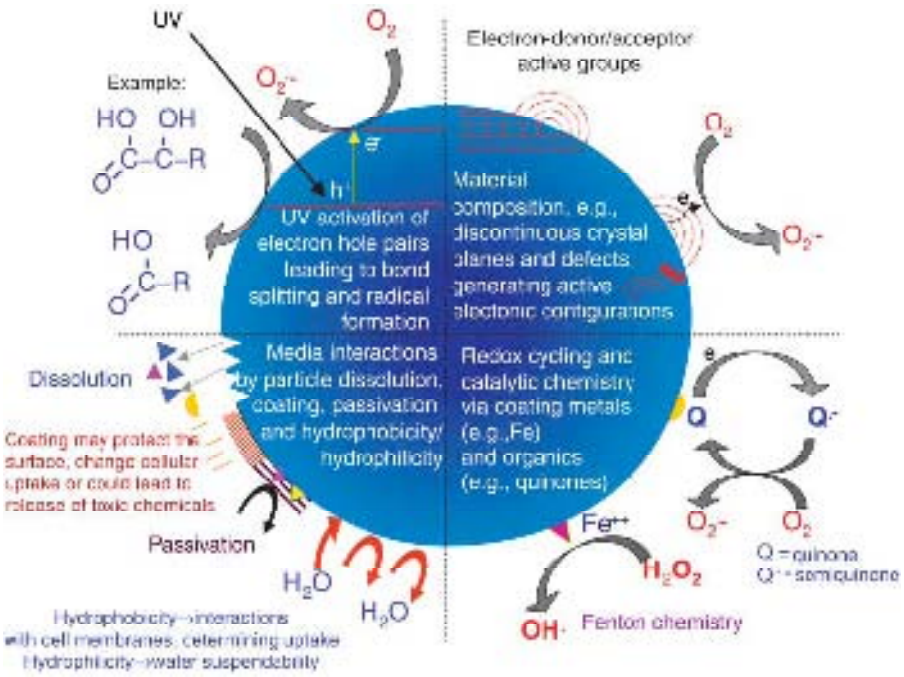

Figure 1.6 Potential mechanisms of interaction of NPs with cells. Examples illustrate the importance of material composition, electronic structure, coatings, bonded structures, solubility and interaction with other biotic and abiotic factors (e.g. UV activation). From Nel *et al.* 2006

- **Ecotoxicology of carbon based nanomaterials**

Toxicity of fullerenes and CNTs is poorly understood. Unfunctionalised CNTs are highly hydrophobic and are poorly dispersible in aqueous media. This makes it difficult to study their toxicity and bioavailability to planktonic organisms, since in nature their contact with the hazardous substance may be unlikely, and research should concentrate on benthic organisms, for which exposure may be higher. In order to overcome the problem of particle solubility and determine their toxicity, NPs have been dispersed and stabilised with the aim of obtaining single-particle suspensions which organisms are more likely to interact with, and thus their toxicological effects determined. A variety of dispersants have been used including Tween 80 (Warheit *et al.* 2005; Rastogi *et al.* 2008), sodium dodecyl sulphate (SDS) (Jeevananda *et al.* 2008; Hermant *et al.* 2009), and the most common tetrahydrofuran (THF)

(Bauer *et al.* 2007; Hsu *et al.* 2008). Manipulation of nanomaterial suspensions raises questions of (1) how realistic is an approach that modifies the potential hazardous substance to a point that if the NP is untouched it is not likely to ever interact with organisms, and (2) how toxic is the surfactant being used to solubilise the particles and make them more bioavailable?. The use of surfactants as dispersants has raised many questions. For instance recent work suggests that cytotoxic effects to aquatic invertebrates are most likely due to the degradation products resulting from the stabilisers used than from the NP *per se* (Zhu *et al.* 2005; Spohn *et al.* 2009).

Fullerenes have high antioxidant properties (Tikhomirov *et al.* 2008; Lucente-Schultz *et al.* 2009; Misirkic *et al.* 2009), and are a promising material for cancer treatment (Wang *et al.* 2006; Harhaji *et al.* 2008; Jou 2008), AIDS treatment as well as efficient bactericidals (Li *et al.* 2008a; Lyon & Alvarez 2008; Lyon *et al.* 2008a; Lyon *et al.* 2008b) (Table 1.5 & Table 1.6). A few authors have concluded that fullerenes and carbon nanotubes are not cytotoxic (Nyberg *et al.* 2008; Lucente-Schultz *et al.* 2009; Misirkic *et al.* 2009; Spohn *et al.* 2009) and that the effects observed are the result of the more toxic dispersants used for the manufacturing that stay trapped within the NP aggregate (Fortner *et al.* 2005a) or remaining in the media during exposures (Zhu *et al.* 2006). For instance, the acute toxicity of fullerenes to fish has been investigated by several authors with slightly contradictory results. Due to the lipophilic nature of fullerenes, it has been hypothesised that they can selectively translocate into the brain via the olfactory bulb in mammals and fish. In vitro studies by Sinohara *et al.* (2009) on the lipid peroxidation in brain cells of *Cyprinus carpio* concluded there was a significant lack of effect from the NP to the cells as well as a lack of uptake. The researchers suggested that due to lipid peroxidation under light conditions, false positives can arise due to sample manipulation and preparation and may have been the cause of toxicity detected by other researchers. For instance, Oberdoster (2004) investigated the effects of THF-stabilised

uncoated fullerenes to largemouth bass with results indicating high levels of lipid peroxidation in the gills, as well as protein damage. Zhu *et al*. (2008b) exposed a water – stirred suspension of fullerenes to *Carassius auratus*, a freshwater fish, and demonstrated that lipid peroxidation levels decreased in most cases, especially in the gills and brain, but increase in liver, suggesting that the latter might be the targeted organ for lipophilic NPs. An effect of the dispersant was also noted by Zhu *et al.* (2006). Daphnia and fathead minnow fish were exposed to both, THF-fullerenes and water stirred fullerenes. In the fish, the results were conclusive: 100% of the organisms exposed to THF stabilised solutions were dead at the end of the assay. In daphnids the increased mortality was also significantly higher compared to the control, and again was possibly due to the toxic nature of the dispersant.

Carbon nanotubes have fibrous structures similar to that of asbestos and research has shown their asbestos-like cytotoxic properties (Brunner *et al.* 2006; Sealy 2008). CNTs have been associated with oxidative stress (Yang *et al.* 2009), cytotoxicity, inflammation, granuloma formation, and fibrogenesis in *in vitro* and *in vivo* studies (Poland *et al.* 2008). The problems associated to CNT are the same as with fullerenes: they are lipophilic and have a strong tendency to precipitate out of suspension. SWCNTs delay early developmental stages of zebrafish embryos, including hatching (Cheng *et al.* 2007). Rainbow trout exposed to 0.1-0.5 mg l^{-1} SDS/sonicated-dispersed SWCNTs showed an increase in the rate of ventilation as well as several gill pathologies and enhanced mucus secretion, however a few of these effects were attributed to the solvent used. In addition, aggressive behaviour among treated populations was common, including fin nipping and ultimately death. Other researchers have described alternative behavioural patterns of organisms when exposed to CNT. For instance, starved Daphnia is able to ingest lipid coated CNTs (Roberts *et al.* 2007) and use the coating a source of carbon. However, normal behavioural patterns were altered, and impeded

movement was often detected, with implications in reproductive behaviour and enhanced vulnerability to predators (Table 1.5 & Table 1.6).

Overall, toxicological *in vitro* and *in vivo* studies are still not conclusive. Stringent guidelines should be developed for NP characterisation, sample preparation, and exposures for relating physico-chemistry with toxicity.

- **Quantum dots**

Quantum dots (QDs) have received a large amount of interest due to their relevance in biomedical research. Structurally QDs consist of a metalloid crystalline core and a "cap" or "shell" that shields the core (Hardman 2006). Cores are typically made of cadmium or lead, highly toxic metals to cells and organisms (Hardman 2006). Oxidative stress and DNA damage have been detected on mussel exposed to CdTe QDs (Gagne *et al.* 2008), as well as the ability to bind to bacterial cells and impair the cell's antioxidative system (Lu *et al.* 2008). Most toxicological research has indicated the potential harm QDs may cause since in oxidative and light conditions their protective coating can degrade liberating free metals (e.g. Cd^{2+} ions due to deterioration of the CdSe lattice) (Derfus *et al.* 2004). When coated QDs were nontoxic, since coating prevented solubilised cadmium to leach from particle. Also, coated CdTe QDs were 10 times less toxic than uncoated ones to tumour cells (Lovric *et al.* 2005). Exposure of coated and uncoated QDs to *Ceriodaphnia dubia* and *Pseudokirchneriella subcapitata* also showed a decreased toxicity with coated ones (Bouldin *et al.* 2008). Nevertheless, recent research has suggested that the type of coating and charge are the cause of toxicity of most QDs, independently of the core material (Hoshino *et al.* 2004).This finding was also corroborated by Geys *et al.* (2008) who injected carboxyl-coated and amino-coated QDs to mice. Both QDs caused vascular thrombosis in the pulmonary circulation, but carboxyl-coated QDs were more toxic than the latter ones (Geys *et al.* 2008) (Table 1.5).

Table 1. 5 Effects of nanomaterials to bacteria (Modified from Kleine et al. 2008)

Nanomaterial	Toxic effects	References
Carbon containing fullerenes		
C60 water suspension	Antibacterial to broad range of bacteria	(Lyon *et al.* 2005; Lyon *et al.* 2006; Lyon & Alvarez 2008)
C60 capped with polyvinylpyrrolidone	Antibacterial to broad range of bacteria	(Kai *et al.* 2003)
Hydroxilated fullerene	Biocidal for Gram +	(Rozhkov *et al.* 2003)
Carboxyfullerene	Biocidal for Gram +	(Mashino *et al.* 1999b; Tsao *et al.* 1999; Tsao *et al.* 2001)
Fullerene derivate	Inhibited E. coli growth	(Mashino *et al.* 1999a; Mashino *et al.* 1999b; Mashino *et al.* 2003)
Other derivates of C60	Inhibit Mycobacteria growth	(Bagrii & Karaulove 2001)
Carbon nanotubes		
Single walled	Antibacterial-cell damage	(Kang *et al.* 2007; Wei *et al.* 2007)
Multi walled	Cytotoxic	(Biswas & Wu 2005)
Metallic		
Quantum dots	Production of ROS-uncoated toxic	(Kloepfer *et al.* 2005)
Silver	bactericidal and viricidal	(Sondi & Salopek-Sondi 2004; Elechiguerra *et al.* 2005; Morones *et al.* 2005; Lok *et al.* 2007; Pal *et al.* 2007)
Gold	Low toxicity to bacteria	(Hernandez-Sierra *et al.* 2008; Simon-Deckers *et al.* 2008)
Metal oxides		
TiO2	Antibacterial by ROS production	(Rincon & Pulgarin 2004b, a)
MgO	Antibacterial	(Huang *et al.* 2005)
CeO2	Antimicrobial	(Thill *et al.* 2006)
ZnO	Antibacterial	(Huang *et al.* 2008b)
Others		
SiO2	Toxicity due to ROS production	(Adams *et al.* 2006)

Again, toxicological results suggest that QDs toxicity depends on multiple factors derived from both the inherent physicochemical properties of QDs (size, concentration, charge, outer coating and oxidative, photolytic and mechanical stability) as well as their environmental conditions (Farre *et al.* 2009).

- **Metal oxides**

There are many metal and metal oxide NPs, but most of the toxicological studies have investigated titanium dioxide (TiO_2), zinc oxide (ZnO), and iron oxides (FeOx) NPs.

Most research have also focused on freshwater species (Farre *et al.* 2009), more specifically fish and daphnids. Metal oxide NPs have been found to cause oxidative stress in brain cells and interference with mitochondrial activity (Long *et al.* 2006), movement impediment on daphnids and further effects on behavioural patterns (Lovern *et al.* 2007), oxidative stress on gills of rainbow trout (Federici *et al.* 2007; Handy *et al.* 2008)*, in vitro* uptake into mammalian ovary cells (Suzuki *et al.* 2007), as well as bactericidal properties due to the photoactivity exerted by some of the particles by being redox active (Adams *et al.* 2006; Tsuang *et al.* 2008) (Table 1.5). Some researchers classify oxide particles as highly toxic and preliminary work suggests they can also be the cause of transient health problems in humans (Warheit *et al.* 2007; Powell *et al.* 2008). Some metal oxides are highly soluble in aqueous solutions. Many authors have not found a significant difference on the toxic effects from nanomaterials compared to the effects shown when organisms were exposed to the bulk form of it. For instance, both bulk and nano-ZnO show detrimental effects during early developmental stages of zebrafish embryos, decreasing their survival and hatching rates. The LC50 of nano-ZnO and ZnO/bulk aqueous suspensions on the zebrafish embryo after 96 h exposure are quite similar, being 1.793 mg l^{-1} and 1.550 mg l^{-1} respectively (Zhu *et al.* 2006). Few researchers have considered the effects of particle solubility on the toxicity of metal

oxides and metal particle. In a study done with the freshwater algae *Pseudokirchneriella subcapitata* exposed to ZnO NPs the soluble fraction of the particle was close to 20 % (mg l^{-1} range), and the observed toxicity was related to solubility (Franklin *et al.* 2007). However, zebrafish exposed to copper NPs show morphological changes in gills and gene expression patterns which differ from those of zebrafish exposed to soluble cooper, indicating a direct effect from the NP and not only from the soluble fraction of it (Griffitt *et al.* 2007).

Often knowing the size of the NP has been considered essential for predicting toxicity, since the smaller the particle the easier it is to be taken up or translocated into cells. However, Li *et al.* (2007) did not find any significant difference on pulmonary toxicity among 3 nm and 20 nm TiO_2 particles, and supported the pH of the medium rather than the nanoparticle size played an important role on pulmonary toxicity.

- **Gold nanoparticles**

Due to the scientific interest and use of Au NPs in biomedical research most of the cytotoxicity studies done with Au NPs have been on different lines of carcinogenic human cells. As with most NPs, recent literature contains conflicting data regarding the cytotoxicity of Au NPs (Pan *et al.* 2007). Although most gold complexes are known to be cytotoxic (Denko & Anderson 1944; Swanson *et al.* 1947) and have been found to cause DNA damage, zero valent Au NPs are biocompatible due to their relative inertness of gold in their bulk form, their stability, size-controlled synthesis and easy surface modifications with amine and thiol groups for conjugation with DNA and proteins (Shukla *et al.* 2005). DNA damage and downregulation of DNA repair genes have been detected at low concentrations of 1 nM of 20 nm particles in human fetal lung fibroblasts (Li *et al.* 2008b), and also apoptosis in carcinoma type II epithelial cancer cells when exposed to 33 nm particles (Patra *et al.* 2007). However, most research have not detected cytotoxic effects such as production of ROS, secretion of

inflammatory cytokines and cytoskeleton malformations in cells (Shukla *et al.* 2005; Khan *et al.* 2007; Mao *et al.* 2007; Pan *et al.* 2007), but Au NPs have always been detected being taken up into the cytoplasm (Shukla *et al.* 2005; Pan *et al.* 2007; Patra *et al.* 2007; Li *et al.* 2008b), and nucleus (Khan *et al.* 2007). Uptake is thought to be via pinocytosis and lysosome mediated (Shukla *et al.* 2005; Mao *et al.* 2007). A recent study done by Pan *et al.* (2008) on water-soluble Au NPs ranging from 0.8 to 15 nm and stabilised with triphenylphosphine derivatives showed that particle cytotoxicity was size dependent, with only the smallest particles (< 1.2 nm) causing apoptosis and cytoskeleton abnormalities.

The studies investigating the effect of Au NPs onto bacteria have shown a low bactericidal activity of these particles when compared to Ag or ZnO NPs (Hernandez-Sierra *et al.* 2008; Simon-Deckers *et al.* 2008) (Table 1.5).

It is still difficult to extract conclusions from most research done on toxicology since most particles have been manufactured differently and there are many physico-chemical properties besides their metal composition that are also likely to be important. As happens in carbon NPs, addition of surfactants can cause a much higher toxic effect (Lovern & Klaper 2006; Zhu *et al.* 2006).

The toxicity of Ag NPs is discussed in further detail in the next section.

1.11 Ecotoxicology of silver nanoparticles

1.11.1 Toxicity to vertebrates

Very little work has focused on investigating the effects Ag NPs may have to invertebrates and vertebrates, and only a handful of studies have used other organisms rather than bacteria to investigate their toxicity (Table 1.7).

A few studies have investigated the effects of Ag NPs on the model freshwater fish zebrafish. Using this freshwater model Griffitt *et al.* (2007) discriminated the effects from Ag NPs from the effects of the soluble metal fraction of it. NPs were found attached to the gills, although they did not cause any morphological alterations. However, transcriptional studies showed how different organs were affected differently depending on the source of silver zebrafish were exposed to, indicating different mechanisms or pathways of toxicity. Yeo & Pak (2008) investigated the effects 10-20 nm Ag NPs had on zebrafish during caudal fin regeneration. The highest concentrations of 4 ppm was found to inhibit caudal fin regeneration, with a suggested mechanism due to ROS formation (although not measured by the authors) and ultimately causing DNA damage. In this study, the lowest concentration of 0.4 ppm showed a slower fin regeneration rate at the end of the 36 d exposure. Ag NPs were detected accumulating in blood vessels, and genomic studies showed how the p53 gene pathway was highly altered. The p53 protein is a 'master guardian' of the cell and responsible for activating cycle checkpoints, DNA repair and apoptosis. Another study (AshaRani *et al.* 2009) demonstrated that albumin and bovine stabilised Ag NPs were also able to increase cell apoptosis in zebrafish embryos and the NPs were detected in the brain, heart, as well as in the yolk. Finally, Lee *et al*. (2007) used the model of zebrafish to investigate the use of Ag NPs in *in vivo* imaging as a potential tool for the visualisation of transport mechanisms on developing embryos. Ag NPs passively diffused via chorion pore channels, and although the aim of the research did not aim to determine toxicity, dose response phenotypic aberrations were detected.

In mammals, the effects of Ag NPs have been specifically investigated in rats, and the research has focused on respiratory health. Inhalation toxicity of Ag NPs has been investigated by a few authors (Ji *et al.* 2007; Sung *et al.* 2008). Prolonged (90 days and 28 days exposures) at aerosol concentrations ranging from 0.7×10^6 particles/cm^3 to 2.9×10^6

Table 1.6. Effects of nanoparticles to organisms (Modified from Handy et al. 2008 and Klaine et al. 2008)

Nanomaterial	**Organisms**	**Toxic effects**	**References**
SWCNT coated with lysophosphatidylcholine	*Daphnia magna*	Increased ventilation rates, gill pathology and mucus. Effects brain, gill and liver	(Roberts *et al.* 2007)
SWCNT 1.1 nm particles-Dispersed in SDS	*Rainbow trout*	Ingestion and use as food source	(Smith *et al.* 2007)
C60- Dispersed in THF	Largemouth bass	Reduced lipid peroxidation in liver and gill tissue	(Oberdorster 2004)
C60-Dispersed by stirring	Fathead minnow	Downregulation in expression of peroxisomal lipid	(Oberdorster *et al.* 2006)
C60-Dispersed by stirring	Fathead minnow	Elevated lipid peroxidation in gill and possibly in brain	(Zhu *et al.* 2006)
C60-Dispersed by THF	*Daphnia magna*	Possitive correlation between mortality and concentration	(Lovern & Klaper 2006)
C60-Sonicated	*Daphnia magna*	Highest mortality rates at 9 mg/l	(Lovern & Klaper 2006)
C60- Dispersed by stirring	*Daphnia magna*	Decrease offspring production. Mortality	(Oberdorster *et al.* 2006)
C60- Dispersed by stirring	*Hyalella azteca*	No behavioural effects detected	(Oberdorster *et al.* 2006)
C60- Dispersed by stirring	Marine copepod	No effects detected	(Oberdorster *et al.* 2006)
C60- Dispersed by stirring	*Daphnia magna*	Changes in heart rate and locomotion	(Kashiwada 2006)
C60	Zebrafish	Delayed embryonic development. Low hatching success	(Zhu *et al.* 2008)
TiO_2-*Dispersed by THF*	*Daphnia magna*	Positive correlation between mortality and concentration	(Lovern & Klaper 2006)
TiO_2-Dispersed by sonication	*Daphnia magna*	No mortality reported	(Lovern & Klaper 2006)
TiO_2-Dispersed by sonication	Rainbow trout	Oxidative stress and pathologies in gills and other organs	(Federici *et al.* 2007)

particles/cm^3 chronically affected the lung function as well as causing inflammatory reactions after 90 days (Sung *et al.* 2008),but no significant physiological changes were detected after 28 days exposures (Ji *et al.* 2007). Arora *et al.* (2008) investigated the *in vitro* toxicity of Ag NPs to human cells with results suggesting that cell morphology was not altered up to 6.25 µg ml^{-1}, but cellular alteration and apoptosis were detected at higher doses, and increase in oxidative stress and impeded mitochondrial function affected in a dose-dependent manner from 3.12-50 µg ml^{-1}. *In vitro* studies on embryonic stem and fibroblast mouse cells showed how the effects of 25 nm polysaccharide coated and uncoated Ag NPs caused different cell damaged but both types affected the expression of p53 protein, caused DNA breakage, and apoptosis (Ahamed *et al.* 2008).

To my knowledge, only a couple of studies have been done on Ag NPs and invertebrates and algae: the ciliate, *Paramecium caudatum,* the crustacean *Daphnia* and the green algae *Chlamydomonas reinhardtii* have been investigated. The concentrations of Ag NPs required to cause toxicity to those are significantly higher than for other organisms and bacteria. The LC50 of *P. caudatum* exposed to a stable aqueous dispersion of Ag NPs for 1 h was 39 mg l^{-1}, a concentration almost 63 times higher than the one required of ionic silver to cause the same effects (Kvitek *et al.* 2009). The authors also describe the effects the surfactants used to stabilise the Ag NPs (Tween 80 and SDS) have on increasing toxicity of Ag NPs (Kvitek *et al.* 2008; Kvitek *et al.* 2009). Navarro *et al*. (2008) investigated the effects of Ag NPs on *Chlamydomonas reinhardtii* and took into consideration the potential NP effect and compared it to the soluble fraction of Ag ions released from the particles during exposure. Ag NP solubility was close to 1%, however they appeared to be more toxic than $AgNO_3$, which suggested a particle effect. Nevertheless when cysteine, a strong ligand and complexing agent for Ag ions was present, Ag NP toxicity was neglected due to formation of less bioavailable Ag-cysteine complexes, indicating Ag NP toxicity was mediated by Ag ions

release, which could be further oxidised in the presence of algae (by the production of H_2O_2). The effects of Ag NPs on *Daphnia pulex* were investigated in adults and juveniles with similar values of 48h LC50 of less than 1 mg/L. However, Ag ions were more toxic than Ag NPs but since dissolution of the NP was low during exposures the observed mortality was partially attributable to the intrinsic properties of the Ag NP (Griffitt *et al.* 2008).

1.11.2 Toxicity to microorganisms

Bacteria are vital to life on Earth and are involved in a variety of process from nutrient cycling to waste decomposition (Klaine *et al.* 2008; Neal 2008). Nevertheless they are also the cause of infections and lethal diseases. The increase on the number of bacterial strains resistant to antibiotics has called for the formulation of novel bactericides to use in addition to antibiotics and provide efficient sterilisation when required. The bactericidal effectiveness of silver has lead to a new generation of products and disinfectants that use its chemical and physical properties to reduce bacterial growth (Woodrow Wilson database, 2009). Currently, the mechanism of toxicity is not known. Several studies suggest the key role NP size and shape have determining toxicity (Sondi & Salopek-Sondi 2004; Morones *et al.* 2005; Pal *et al.* 2007; Griffitt *et al.* 2009) while others have suggested that it is the dissolution of ionic Ag from the NP which is responsible for toxicity (Lok *et al.* 2007; Navarro *et al.* 2008b) (Table 1.7).

The mode of toxic action of Ag NPs is not yet fully characterised but both the release of silver ions and the NP characteristics may play a key role to its highly bactericidal properties and have already been investigated by several authors (Jain & Pradeep 2005; Morones *et al.* 2005; Lok *et al.* 2006; Duran *et al.* 2007; Lok *et al.* 2007; Pal *et al.* 2007; Shahverdi *et al.* 2007; Shrivastava *et al.* 2007; Choi *et al.* 2008; Choi & Hu 2008b; Raffi *et al.* 2008). Besides the intrinsic toxicity of the NP, they have also been suggested to enhance

antibiotic effectiveness when mixed together to combat *S. aureus*, *P.aeruginosa*, and *E.coli* infections (Shahverdi *et al.* 2007; Birla *et al.* 2009), and have also shown to bind *in vitro* to HIV virus preventing replication and spread by disabling their binding to host cells (Elechiguerra *et al.* 2005) (Fig 1.7), as well as to the respiratory syncytial virus reducing the number of infections by 44% (Sun *et al.* 2008).

Although the catalytic oxidation of Ag NPs and reaction with dissolved monovalent silver ion is likely to contribute to its bactericidal effect, the large surface area to volume ratio of NPs leads to high particle reactivity and increase contact with cells; which have made particle size (Morones *et al.* 2005; Choi & Hu 2008b) and shape (Pal *et al.* 2007) parameters to be taken into consideration when investigating toxicity and NP effects. For instance, direct interaction of particles with cell membranes affects regulation and transport though the membrane and has been suggested as the cause of membrane 'pit' formation (Sondi & Salopek-Sondi 2004; Cho *et al.* 2005) (Fig 1.8) and accumulation of intracellular ROS (Choi & Hu 2008b).

Nevertheless, other studies indicate that "pit" formation is not the result of particle interaction with bacterial cells but related to the free radical formation, a process reported as a result of metal depletion which subsequently induced membrane damage affecting permeability and function (Kim *et al.* 2007).

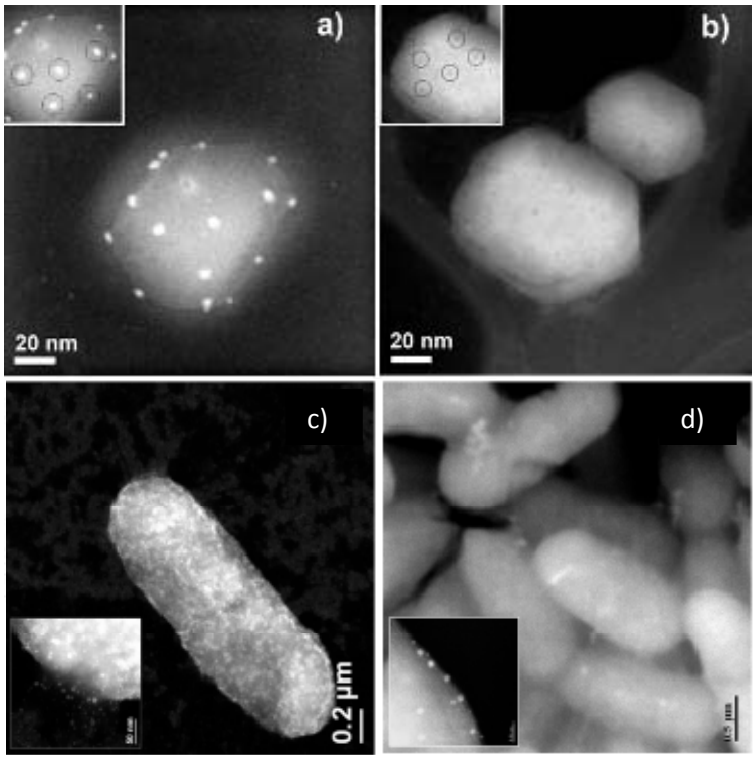

Fig 1.7 a) Ag NPs (bright dots) bound to HIV virus; b) HIV virus not exposed to Ag NPs; c) Pseudomonas aeruginosa bound to Ag NPs and d) E.coli bound to Ag NPs (From Elechiguerra *et al.* 2005 and Morones *et al*. 2005).

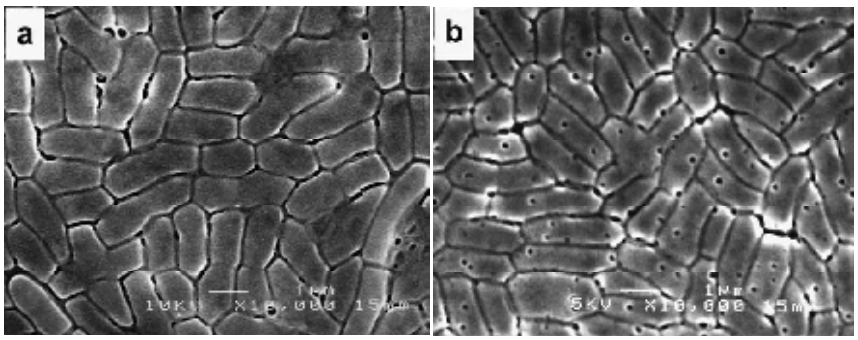

Figure 1.8. Left panel TEM image of *E. coli* cells. A) TEM image of *E. coli* untreated cells. B) TEM image of *E. coli* cells after exposure to Ag NPs. Notice pitting onto cell surface. From Sondi and Solopek-Sondi (2004).

Research has shown particles of less than 10 nm are most likely to be incorporated into cells (Morones *et al.* 2005; Choi & Hu 2008b). However, particle shape has also been suggested as a factor affecting toxicity, and truncated triangular Ag NPs with a {111} lattice

plane as the basal plane displays the strongest bactericidal effect (Morones *et al.* 2005; Pal *et al.* 2007).

In order to investigate the mode of action of Ag NPs and discriminate it from Ag^{+} ions a proteomic approach investigating E. coli was used (Lok *et al.* 2006). Short exposures of Ag NPs induced stress, by altering expression of envelope and heat shock proteins. Ag NPs reduced the proton motive force by inducing massive loss of intracellular potassium and decreased cellular ATP levels, affecting membrane potential and culminating in the loss of cell viability. The mechanism of toxicity of Ag NPs and of Ag ions was suggested to be similar, but Ag NPs were much more efficient as antimicrobials with similar bactericidal effectiveness in the nM range compared to the μM range for Ag ions. Nevertheless, another study indicated that the partial oxidation of Ag NPs was required for their bactericidal properties, indicating Ag ion release as a prerequisite for NP toxicity, and implying a synergistic mode of action from both: particle size and shape and release of Ag ions (Lok *et al.* 2007). Hwang et al. (2008) also investigated the mode of action of Ag NPs with end points looking at promoter activities instead of cellular viability. The strong induction of *sodA* promoter after exposure of *E. coli* to Ag NPs suggested the production of superoxide radicals, ultimately showing an effect via membrane and oxidative stress damage, but not affecting the DNA.

An increase on silver nanotechnologies is not expected to produce pollutant concentrations in excess of the ng/L range (Luoma 2008). Models taking into consideration the behaviour of Ag in natural freshwater systems and applying a mass balance model for calculating predicted environmental concentrations (PEC) also conclude that the expected concentrations of Ag NPs ending up in nature is of the range of 0.01 $\mu g\ l^{-1}$ in water and 0.43 $\mu g\ Kg^{-1}$ in soil (Mueller & Nowack 2008), and from 2 to 28 $\mu g\ Kg^{-1}$ of Ag NPs are expected in sewage treatment plants (Blaser *et al.* 2008).

Very few studies have investigated the effects Ag NPs may cause to natural communities of microorganisms. Ag ions have been shown to affect a natural bacterial community of sewage sludge, showing an overall reduction on its denitrifying activity, but selecting and increasing the diversity of organisms able to denitrify (Throback *et al.* 2007). To my knowledge only two studies (Choi *et al.* 2008; Choi & Hu 2008b) have investigated the effects of Ag NPs to a natural bacterial community of microorganisms. Choi *et al.* (2008) investigated the effects of Ag NP and silver ions to nitrifying organisms. On one hand Ag NPs inhibited autotrophic nitrifying organisms the most, while silver ions appeared to be most toxic to heterotrophic organisms. The authors did not investigate different mechanisms of toxicity of Ag and Ag NPs, but cellular viability was not compromised, which was suggested to be the results of the larger size of particles used (>10 nm). Results from Throback et al. (2007) and Choi and Hu (2008) indicate that stringent regulations of Ag NPs entering waterways are required. Nitrifying and denitrifying microorganisms are crucial in current wastewater treatments and nutrient cycling. Inactivation of them would impede treatment plant efficiency (Choi *et al.* 2008). However, a recent modelling study done by Blaser *et al.* (2008) concluded that the predicted concentrations of Ag NPs from nanotechnologies ending up in sewage sludge would still be below the highest observed non-effect concentration, and thus Ag accumulation in sewage plants would not affect the performance of the water treatment process.

In summary, Ag NPs are bactericidal and bind to bacterial cells. However, the variation among effective bactericidal concentrations of different species, cell types (gram positive vs. gram negative), and even among bacterial strains makes it difficult to investigate

Table 1.7. Effects of silver nanoparticles to organisms

	Ag NP								
Organism	**Size (nm)**	**Surface Coating**	**Shape**	**Synthesis**	**Concentration or LC50s**	**Exposure Time**	**Sample preparation**	**Major NP effects**	**Reference**
Zebrafish embryo	20-30	ND	Spherical	Electrolysis in tap water	10-20 ppt	72 h	Dilution with tap water	Penetration of Ag NP aggregates into skin and circulatory system	Yeo and Yoon 2009
Zebrafish	10-20	ND	Spherical	Electrolysis in tap water	0.4-4 ppm	2-36 days	Dilution with tap water	Aleration of p53 gene pathway. Defects in fin regeneration & penetration into organelles & cell nucleous	Yeo and Pak 2009
Zebrafish	26.6+8.8	Metal Oxide	Spherical	Gas phase Condensation	1000 mg L	48 h	Sonication in MIlliQ water	High binding of Ag NP with gills. Distinct gene expression profile between Ag and Ag NP.	Griffitt et al. 2009
Zebrafish	20-30	Sodium Citrate	Spherical	Gas phase Condensation	LC50 7.07 mg L	48 h	Sonication in MIlliQ water	Differential toxicity of Ag NPs at different developmental stages overall Ag is more toxic than Ag NPs, except in fish fry stage.	Griffitt et al. 2008
Zebrafish embryo	5-20	BSA or potato starch	Spherical	Chemical reduction with borohydrate	5-100 mg L	72 h	ND	Deposition in cell nucleus, brain, nervous system and in blood	Asharani et al 2008
Zebrafish embryo	11.6+3.5	ND	Spherical	Chemical reduction with borohydrate	0.19 nM	0-2h	Washed by centrifugation & incubated in egg water for 120 h	Transport of Ag NPs though chrion channels	Lee et al. 2008

Table 1.7 Effects of Ag NPs to organisms (continues)

	Ag NP								
Organism	**Size (nm)**	**Surface Coating**	**Shape**	**Synthesis**	**Concentration or LC50s**	**Exposure time**	**Sample preparation**	**Major NP effects**	**Reference**
Japanese medaka	49.6	ND	Cuboctahedral & decahedral	Purchased Powder	1-25 ug L	96h	1 h sonication in 2 min interval. Stirring for 2 weeks and filtration (100 nm filter size).	Ag Np cause cellular and DNA damage Differential mode of action between Ag and Ag NPs. Increas gene expression of oxidative stress biomarkers.	Chae et al 2009
Daphnia pulex	20-30	Sodium citrate	Spherical	Gas phase condensation	LC50 0.04 mg L	48h	Sonication in MIlliQ water	Low toxicity of Ag NPs compared to Ag ions.	Griffitt et al. 2009
Cerodaphnia	20-30	Sodium citrate	Spherical	Gas phase condensation	LC50 0.067 mg L	48h	Sonication in MIlliQ water	higher toxicity of Ag NPs comapred to Ag ions.	Griffitt et al. 2009
Cerodaphnia dubia	20-30	Metal oxide	Spherical	Gas phase condensation	LC50 0.46 mg L $LC50_{OM}$ 6.18 mg L	48h	Addition of NPs in media, shake horizontally and filtered to use filtrate to remove large aggregates.	Increase in organic matter decreases Ag NP toxicity	Gao et al 2009
Pseudokirchneriella subcapitata	20-30	Sodium citrate	Spherical	Gas phase condensation	LC50 0.19 mg L	96h	Sonication in MIlliQ water	Low toxicity of Ag NPs compared to Ag ions.	Griffitt et al. 2009
Chlamydomonas reinhardtii	25+13	Carbonate coated	Spherical	ND	$EC50_{1h}$: 3300 nM $EC50_{5h}$ 829 nM	1-5h	Aqueous suspension	Toxicity of Ag NPs mediated by Ag ions released form Ag NP in contact with cell	Navarro et al. 2008
Paramecium caudatum	30-40	Tween 80, PEG35000 or PVP 360	Spherical	Modified Tollens process. Chemcial reduction of $[Ag(NH3)2]+$ with D-maltose.	$LC50_{NP}$ 39 mg L $LC\ 50_{TweenNP}$ 16 mg L	1h	Suspended in Milli Q water	Ag NP toxicity was enhanced when Tween 80 capped	Kvitek et al. 2009

Table 1.7. Effects of silver nanoparticles to organisms (continues).

	Ag NP								
Organism	**Size (nm)**	**Surface coating**	**Shape**	**Synthesis**	**Concentration or LC50s**	**Exposure Time**	**Sample preparation**	**Major NP effects**	**Reference**
Caenorhabditis elegans	14-20	ND	ND	Powder Sigma aldrich-	0.05-0.5 mg L	24-72h	Dispersed in MilliQ water & sonication for 13 h, stirring for 7 days & filtered 100nm	reduced reproductive success. Increase in oxidative stress Ag NPs accumulated around uterine area.	Roh et al 2009
MetPlate-Bacterial bioassay	20-30	Metal oxide	Spherical	Gas phase condensation	LC50 47 ug L LC50OM 112ug L	1.5 h	Shake in aqueous media Filtration to remove aggregates	An increase in organic decreases Ag NP toxicity.	Gao et al 2008
Bacteria spp	26	PVPs, PEGs, Tweens, non-ionic surfactants from Brij group	Spherical	Modified Tollens process. Chemcial reduction of [Ag(NH3)2]+ with D-maltose.	MIC range of 1.69 to 6.75 ug ml	24h	Aqueous dispersions	SDS, Tween 80 and PVP360 increased particle stabilisation as well as antibacterial activity of Ag NPs	Kvitek et al. 2009
Bacteria spp	16+8	ND	Cuboctahedral, multiple twinned icosahedral and decahedral	Purchased NPs powder in a carbon matrix.	0-100 ug ml	30 min	Aqueous dispersion a nd homogenation with ultrasonic cleaner.	Ag Nps < 10 nm attached to bacterial cells. NPs with a high reactivity facet {111} were the most toxic.	Morones et al. 2008
Bacteria spp	10-15	ND	ND	Chemical reduction by D-glucose and hydrazine	5-35 ug/ml	24h		Ag NPs are more effective in gram negative than in gram postive bacteria	Shrivastava et al. 2007
E. coli	10	ND	Spherical & truncated	Chemical reduction with formaldehyde, hydrazing and sodium formal-dehydesulfoxylate	0.1-1 mg/l	24h	Dispersed in culture media	Cell membrane/protein damage. No DNA damage	Hwang et al.2008

Table 1.7 Effects of Ag NPs to organisms (continues)

Organism	Size (nm)	Surface Coating	Shape	Synthesis	Concentration or LC50s	Exposure Time	Sample preparation	Major NP effects	Reference
E. coli	From 39	Citrate	Rod truncated, triangular and spherical	*Spherical:* Chemical synth. by borohydrate Reduction *Trunc. triang NPs:* Solution phase synteh.	0.1-10ug/ml	0-26h	Aqueous suspension	Truncated triangluar NPs have a higher biocidal capacity than others.	Pal et al 2007
E. coli	9.3+2.8	Citrate	Spherical	Chemical synthesis by borohydride reduction	0.4-0.8 nM	30 min	Dilution in biological media (Hepes buffer and M9 medium).	Ag NPs are more toxic than Ag ions. Destabilisation of outer membrane, collapse of plasma memb. Potential.	Lok et al. 2006
E. coli	9.3+2.8	Citrate	Spherical	Chemical synthesis by borohydride reduction	0-100 ug/ml	24 h		Ag NP toxicity mediated by chemisorbed Ag ions from the NP. Thus, smaller NPs are more toxic than larger ones due to volume of oxidised surfaces and release of Ag ions.	Lok et al. 2006
E. coli	12 nm	Daxad 19	ND	Chemical synthesis] with ascorbic acid	0-100 ug/ml	10h	Sonication in aqueous dispersion	Ag NP created 'pits' in the bacterial cell wall	Sondi & Salopek Sondi 2004
Nitrifying bacetria	21-21	PVA	ND	Chemical reduction with borohydrate	0.05-1 mg/l	180 days	Freshly synthtised suspensions	Growth inhibition correlated with Ag NPs < 5 nm due to generation of intracellular ROS	Choi et al 2008
Autotrophic nitrifying bacteria	14+6	PVA	ND	Chemical reduction with borohydrate	1 mg/l	>24 h	from synthesis batch	Ag NPs inhibit respiration by ca. 87%, almost twice as much as Ag+ and $AgCl_2$ Ag NPs bound to bacreria But did not affect Viability	Choi et al 2008

Table 1.7 Effects of Ag NPs to organisms (continues)

	Ag NP								
Organism	**Size (nm)**	**Surface coating**	**Shape**	**Synthesis**	**Concentration or LC50s**	**Exposure time**	**Sample preparation**	**Major NP effects**	**Reference**
Nitrifying bacetria	15+9	PVA	Elipsoidal and spherical	Chemical reduction with borohydrate	1 mg/l	18 h	from synthesis batch	The ligand sulfide forms AgxSy complexes or precipitates and reduced Ag NP toxicity by 80%.	Choi et al. 2009
Soil bacterial Community	56+18.6	ND	ND	Purchased Powder	0-1000 ug L	30 days	In MilliQ water and sonicated for 5 h for a stock suspenion 100 ug L stock was sonicated for 30 min prior exposure	Ag NPs accumulated in the top 3 mm but did not affect the bacterial diversity either in the sediment nor water column.	Bradford et al. 2009

the proper mode of action of the particle. For instance, Kim *et al*. (2007) found that gram positive bacteria was considerably more resistant than gram negative to 12 nm Ag NPs, while Yoon found the exact opposite for 40 nm Ag NPs. They both investigated the effects in bacteria growing on agar plates and supplemented with NPs, although the differences could have been the result of the particle size used. Furthermore, a later study by Rupariella *et al.* (2008) on *E. coli* and *S. aureus* species of 3 nm Ag NPs but with a variety of strains show how toxicity was different for each strain tested, without a clear pattern relating the type of membrane.

The different types of NPs (metal, metal oxides, QDs and carbon base), different manufacturing processes, in addition to the high number of possible surface modifications, makes their toxicological characterisation a very difficult task, as seen with the vast number of results obtained from same Ag NPs, and many of them contradictory. Still, the mode of action of most NPs is not yet understood and controversial. Moreover the lack of standardised testing procedures increases the difficulty of interpreting results and predicting fate and toxicity of groups of particles.

The next section describes the fundamental aspects of biofilm formation and their environmental relevance.

1.12 Structure and Behaviour of Biofilms

In the natural environment, the majority of bacteria exist as surface-attached communities known as biofilms (Teitzel 2003) (Fig.1.9). Biofilms are aggregations of microorganisms embedded in a matrix of extracellular polymeric substances (EPS), responsible for the cohesion and adhesion of cells (Wingender *et al.* 1999). The physiological (Beveridge *et al.* 1997; Davies 2000.; Stoodley 2002), genetic (Decho 1999; Wolfaardt *et al.*

1999; Ehlers 2000), and ecological (Davey & O'Toole 2000; Marsh & Bowden 2000) distinctiveness between biofilms (sessile) and planktonic (freely moving) bacterial cells is well documented. Biofilm is the predominant form of bacteria in the environment. In a biofilm state, a bacterial cell has a higher protective value against predators (Beveridge *et al.* 1997) as well as an increased gene transfer due to its proximity to neighbouring cells. The overproduction of extrapolymeric substances by biofilm cells in comparison to planktonic cells allow for a better protection to toxins, potential for synergistic consortia and an increase in nutrient uptake, especially favourable in oligotrophic environments (Wingender *et al.* 1999).

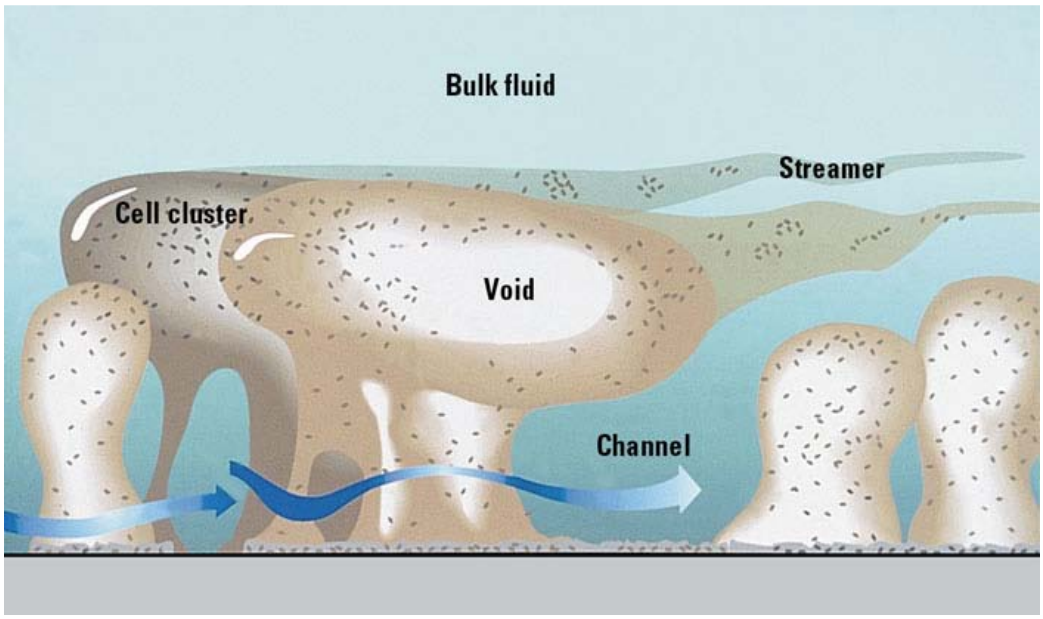

Figure 1.9. Conceptual model of a mature biofilm architecture (from Center for Biofilm Engineering at MSU Bozeman, USA).

1.12.1 Stages in the Formation of Biofilms

Biofilm formation can be portrayed as a sequence of linear events: development of a conditioning film, microbial mass transport, adhesion of microorganisms, microcolony and biofilm formation, surface growth and detachment (Percival *et al.* 2000) (Fig.1.10).

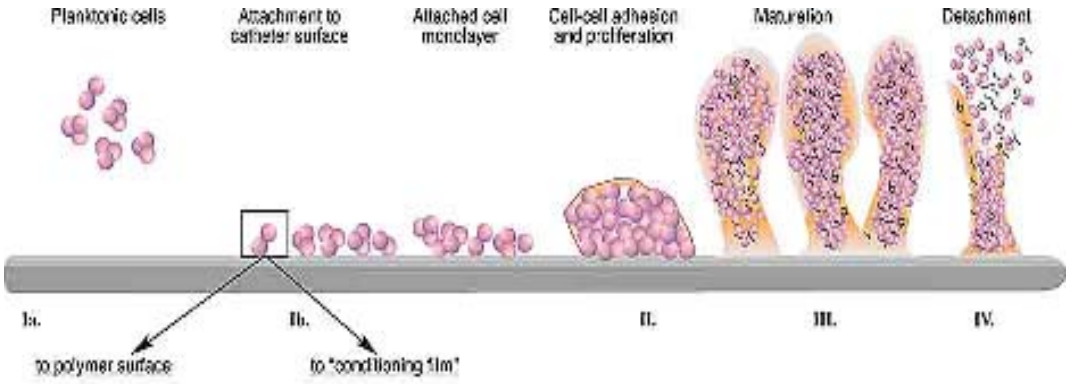

Figure 1.10 Scheme of biofilm formation shown as a four-step process involving initial attachment, accumulation, maturation, and detachment. Factors involved in the attachment and accumulation phases have been described and are noted on the bottom of the figure. Initial attachment can occur as direct adhesion to the surface or depend on the interaction of dedicated bacterial binding proteins with host matrix proteins that cover the surface as a "conditioning film". Modified from Michael Otto, Rocky Mountains Laboratories (Available at www.bioscience.org/2004/v9/af/1295/figures.htm, May 2nd 2009).

- **Formation of a conditioning film**

When a bare surface is exposed to an environmental fluid, organic molecules and colloids will bind to it (van Hoogmoed *et al.* 2000). The type and composition of absorbed molecules is dependent on the surface characteristics (Busscher and van der Mei 2000), nature of the molecules and environmental factors. Molecules will bind in a different way between positively and negatively charged substrate materials and these prepare the substrate for microbial colonisation (Fig 1.10).

- **Microbial Mass Transport**

The success of biofilm to develop on a substrate depends on the concentration of microbial cells in the water and the nutrients in the substrate. Planktonic bacteria can be randomly propelled towards the surface or can have a directed movement though chemotaxis (Dunne 2002). Pereira *et al.* (2002) studied the effects of both laminar and turbulent flow on the morphology of a *Pseudomonas fluorescens* biofilm with confocal scanning laser microscopy and scanning electron microscopy. The results show how under laminar flow conditions biofilms grow thicker but are less dense. In contrast, the turbulent flow yields denser and more established biofilms since it allows bacteria and nutrients to get closer to a substrate.

- **Adhesion**

Bacterial attachment to a surface can be divided into two main phases: *primary* or *reversible adhesion*, and *secondary* or *irreversible adhesion.* Reversible adhesion of bacterial cells to a substrate is the result of physicochemical forces while irreversible adhesion is the result of a chemical step followed by the secretion of EPS by the bacteria (Terada *et al.* 2005). The reversible adhesion is due to electrostatic interactions from the overlapping diffuse layer and van der Waals forces (DLVO forces) (Busscher *et al.* 2000; Terada *et al.* 2005).

Electrostatic interactions are influenced by the surface potential of cells, substratum or the ionic strength of the solution, and will tend to favour repulsion, because most bacteria and inert surfaces are negatively charged (Dunne 2002). Other short range forces (steric interactions or forces of hydrophobic nature) are also important (Terada *et al.* 2005). Hydrophobic interactions probably have a larger influence on the outcome of primary adhesion than electrostatic ones (Dunne 2002) (Fig. 1.10). The second stage of adhesion is the anchoring phase. At this stage microorganisms will bind tightly to a substrate by binding cell surface adhesins with components of the substratum. Bacterial cells will then secrete exopolysaccharides which will complex with substratum components in order to consolidate this irreversible adhesion process (Dunne 2002).

- **Microcolony and biofilm formation**

The attachment of microbial cells onto a substrate is followed by growth and recruitment, as well as by the colonization of other organisms (Percival *et al.* 2000). Microcolonies are round-shaped aggregates of microorganisms and extrapolymeric substances, separated from each other through water-filled voids (Lewandowski 2000). The co-aggregation and co-adhesion among biofilm cells is influenced by temperature, pH, and ionic strength (Busscher and van der Mei 2000). Microcolonies bring functional and structural complexity to the community, and allows for interspecific, synergistic and mutualistic interactions. (Fig. 1.10)

- **Detachment**

Cells can detach from a biofilm by erosion, sloughing, human intervention, grazing, and abrasion (Percival *et al.* 2000). Detachment is a poorly understood phenomenon, which seems to depend on shear and microbial growth rates, although in general, it is considered to be due to internal stress (Picioreanu *et al.* 2001). Oxygen depletion, activation of specific enzymes, pH, temperature, presence of organic molecules, *etc*. are factors that can lead to

biofilm detachment (Percival *et al.* 2000). From an evolutionary point of view, biofilm detachment is beneficial in order to increase genetic diversity, and the colonization of new niches.

1.12.2 The role of extracellular polymeric substances (EPS) in the formation of a biofilm

Biofilm architecture is very variable depending on the type of community as well as environmental conditions. However, more than 90% of a biofilm biovolume corresponds to EPS (Percival *et al.* 2000). EPS are mainly responsible for the integrity of the biofilm, and are implicated in determining the structure, charge, flocculation and dewatering properties (Flemming *et al.* 2000). The most frequent components of EPS are polysaccharides, proteins, and nucleic acids (Wingender *et al.* 1999; Lattner *et al.* 2003). Thus, the extracellular matrix is composed of a variety of functional groups such as carboxylic, hydroxyl, amino and phosphate sites (Fein *et al.* 1997), which at physiological pH values are negatively charged (Langley & Beveridge 1999). EPS components form a highly hydrated gel-like structure which confers stability and allows for cellular communication by quorum sensing. During initial biofilm formation, the production of EPS facilitates the anchoring of bacteria to a substratum. In mature biofilms EPS play a key role in holding cells together (attachment, coaggregation, and floc formation) (Flemming *et al.* 2000; Busscher and van der Mei 2000). EPS production may be used as a long term store of carbon and energy, but it has been suggested that under oligotrophic conditions EPS may help to concentrate nutrients and therefore allowing cells to grow under these conditions (Wolfaardt *et al.* 1997). It has also been suggested that the production of EPS may protect the cells from extreme pH values, extreme temperatures, dehydration, detergents (Wolfaardt et al. 1999), biocides and heavy metal ions (Hentzer *et al.* 2001; Surdeau *et al.* 2006). EPS may also enhance intracellular

transfer of genetic material (Percival *et al.* 2000). Both gram-positive and gram-negative bacteria communicate through quorum-sensing signals to coordinate population behaviour, and recently, DNA has been described as a major structural component of the EPS in biofilms, and DNA binding-uptake system is involved in biofilm formation and growth (Petersen *et al.* 2005).

1. 12.3 Factors influencing biofilm structure and its heterogeneity

Several environmental signals may trigger the development of a biofilm. These signals can include: ambient temperature, hydrodynamic conditions (type of flow and velocity), nutrient availability, electrochemical characteristics of the surface, pH, presence of particulate matter, *etc* (Percival *et al.* 2000). The heterogeneity of biofilms has been confirmed by several researchers. For instance, de Beer *et al*.1994 injected fluorescent latex spheres and tracked their behaviour by using confocal microscopy. By doing so they found out the way water moves through the voids and cell clusters. Neu and Lawrence (Neu & Lawrence 1997) studied the development of stream biofilms employing molecular techniques (such as LIVE/DEAD fluorescent probes for determining cellular viability, and lectin binding assays). They combined such techniques with CSLM and the results revealed the heterogeneity of biofilms in terms of biomass and cellular architecture. Another important technique is the use of microelectrodes which measure concentration profiles with high resolution. These measurements give an insight of the biochemistry within the biofilm, and prove that as heterogeneity increases, chemical and physical microgradients develop. Hunter & Liss (1979) described pH heterogeneity by using a fluorescent radiometric probe and CSLM for analyzing 3D microgradients in a biofilm of *Pseudomonas aeruginosa*. The results showed how the community organization of bacterial biofilms causes a differential diffusion of nutrients, metabolic products, and oxygen; which also result on the development of localized

microenvironments (i.e. pH, redox potentials).

In summary, biofilm are the predominant physiological state of bacterial cells. Biofilms are dynamic systems that are formed by the recruitment and growth of planktonic cells, and can be worn down producing flocs (planktonic biofilms) and planktonic bacteria by physical, chemical, and biological processes (Moore 2006). On the other hand, the evolution of a biofilm community depends on a range of intrinsic (cell to cell communication) and extrinsic (environmental and substrate type) factors. The type and abundance of different taxa will also determine the morphology and functionality of the biofilm community.

Progress in new microscopic and molecular techniques has revolutionized our understanding on biofilm communities at their molecular, cellular, and structural level. Such knowledge has lead to important advances on new technologies for the prevention or treatment of biofilms (especially important in the medical field), as well as in exposing their potential use as bioremediation appliances in water treatment facilities. Understanding the physiological states and ecological role of biofilm bacteria in marine and freshwater communities, as well as their key role in the speciation of metals and artificial compounds is important for improving our knowledge on the geochemistry and fate of organic and inorganic compounds in such systems and in food webs.

1.13 Aims & objectives

The antibacterial property of Ag^+ is well documented (Trevors 1987; Silver 2003), and Ag^+ toxicity to aquatic organisms varies with environmental parameters such as solution ionic strength and presence of organic material (e.g. Nichols et al. 2006; Ward et al. 2006).
The growing production and use of Ag NPs will inevitably lead to their release into the environment. Yet, the potential environmental risk and the mode of action of Ag NPs to

bacterial communities once these are discharged into water bodies is still very much unknown.

The objective of this work was to investigate if changes in environmental conditions, including variations in the ionic strength of the media, changes of pH, and presence of organic matter would affect the physico-chemical properties of Ag NPs; and the implications these would have on toxicity to planktonic and biofilm bacterial cells.

Aim 1: The initial aim of this project was to determine if the behaviour of Ag NPs in different aqueous suspensions would differ with varying environmental parameters such as pH and the presence of organic matter.

In order to address this matter, the following hypotheses were tested:

Ho: If Ag NP behaviour does not vary with changes of pH values of 6, 7.5 and 9, and presence or absence of 10 mg l^{-1} humic substances, then no variations on aggregate formation, residence time in suspension and solubility will be observed across conditions.

H1: If Ag NP behaviour does vary with changes of pH values of 6, 7.5 and 9, and presence or absence of 10 mg l^{-1} humic substances, then variations on aggregate formation, residence time in suspension and solubility will be observed across conditions

Aim 2: Secondly, this work aims to determine if the toxicity of Ag NPs to *Pseudomonas fluorescens* planktonic bacteria would be affected by variations on the pH of the exposure media, as well as by the presence of organic matter.

In order to address this matter the following hypothesis were tested:

Ho: If the toxicity of Ag NPs to planktonic Pseudomonas fluorescens does not vary with changes of pH values of 6, 7.5 and 9, and presence or absence of 10 mg l^{-1} humic substances, then no variations on the population density of the exposed bacteria will be observed across conditions.

H1:If the toxicity of Ag NPs to planktonic Pseudomonas fluorescens does vary with changes of pH values of 6, 7.5 and 9, and presence or absence of 10 mg l^{-1} humic substances, then variations on the population density of the exposed bacteria will be observed across conditions.

Aim 3: Thirdly, in order to address the effects different environmental conditions may

have on the uptake and effects of Ag NPs by *Pseudomonas putida* biofilm the following hypotheses were addressed:

Ho: If the effects of Ag NPs to biofilm Pseudomonas putida do not vary with changes of pH values of 6 and 7.5, and presence or absence of 10 mg l^{-1}humic substances, then no effect on the biofilm biovolume, cellular viability and silver uptake of the exposed bacteria will be observed across conditions.

H1: If the effects of Ag NPs to biofilm Pseudomonas putida do not vary with changes of pH values of 6 and 7.5, and presence or absence of 10 mg l^{-1}humic substances, then an effect on the biofilm biovolume, cellular viability and silver uptake of the exposed bacteria will be observed across conditions.

Aim 4: Finally, when Ag NPs are release into natural waters they are likely to appear and accumulate in coastal waters. In order to address the potential effects Ag NPs may have on a natural bacterial biofilm community the following hypothesis were formulated:

Ho: If exposure of Ag NPs does not affect marine biofilms, then a change on biofilm biovolume and variations on the species composition of the community will not be observed.

H1: If exposure of Ag NPs does affect marine biofilms, then a change on biofilm biovolume and variations on the species composition of the community will be observed.

The outcomes of this work will provide a clearer understanding of the potential role environmental parameters may have on the toxicity of Ag NPs to bacterial cells.

2 Materials & Methods

2.1 Introduction

This chapter describes the methods used to study the effects and interaction of Ag NPs to planktonic and biofilm bacteria.

For laboratory assays, two different species of pseudomonids were selected. Pseudomonids can be found in many different environments including soil (Funnell-Harris *et al.* 2008), water, (Ivanova *et al.* 2002; van de Mortel & Halverson 2004), plants (Van Wees *et al.* 2008), and animals (Rivas *et al.* 2001). The species chosen for this work were *Pseudomonas fluorescens* and *Pseudomonas putida.* Both are representative of microorganisms found in natural waters (Vanderkooij 1977; van de Mortel & Halverson 2004). *P. fluorescens* was used in the planktonic assays, and *P. putida* in biofilm assays. Both organisms grow well under low nutrient conditions (Vanderkooij *et al.* 1982) and they have been widely used as a model organisms in laboratories (Delaquis *et al.* 1989; Korber *et al.* 1994; Allison *et al.* 1998; O'Toole & Kolter 1998). Different pseudomonid species were used for both planktonic and biofilm studies. Initially *P. fluorescens* SBW25 was the chosen species for planktonic studies. *P. fluorescens* has been the model organisms chosen for many medical (Zhang *et al.* 2009a) and environmental (Browne *et al.* 2009; Vanitha *et al.* 2009) research and its genome has been sequenced (Silby *et al.* 2009). Also, due to its ubiquity and versatile metabolism it can be found in soil and water. The biofilm work was done with *Pseudomonas putida* OUS 82. This strain was a gift from Professor Wen-Tso Liu from the National University of Singapore and was chosen since part of the biofilm work was started at Prof. Wen-Tso Liu's laboratory, where this strain was the preferred pseudomonid strain due to their extensive work done on biofilms using this species (Pang *et al.* 2005; Pang & Liu 2007).

Natural bacterial biofilms were grown in western Singapore waters (Andaman Sea). The site was coastal and close to an oil refinery centre, constantly frequented by commercial ships. The harbour was chosen since it represents a typical industrial port, and if Ag NPs end up in natural waters, they are likely to emerge in coastal environments of high human activity.

To understand the behaviour of Ag NPs in the environment and the impact of these NPs on bacterial populations and communities, three main experiments were performed:

- **Aim 1*:*** to determine the toxicity of Ag NPs to planktonic *Pseudomonas fluorescens.* This study aimed to discriminate between the toxic effect of a Ag NP from the well known toxicity of ionic Ag (Slawson *et al.* 1992b; Silver 2003), and also from the potential toxicity of NPs of the same size but manufactured with a material considered non-toxic (in this case latex NPs). This study also investigates the effect of environmental parameters such as variation of the pH values in the surrounding media and presence or absence of organic matter on toxicity of Ag NPs.
- **Aim 2:** to determine the uptake and toxicity of Ag NPs by *P. putida* biofilms. This study investigated the effects of Ag NPs on biofilms under different environmental conditions (variations of pH and presence/absence of organic matter) by determining biofilm viability, changes in biofilm biomass, as well as defining the interaction of Ag NPs with the bacterial cells.
- **Aim 3:** to determine the toxicity of Ag NPs to a natural marine biofilm community. This study investigated the uptake of Ag NPs by a complex community of biofilms, its biocidal effect as well as changes on species composition after a short exposure to Ag NPs.

2.2 Organisms and Media

Both media compositions are described in Appendix1.

Pseudomonas fluorescens SBW 25 was obtained from Prof. C. M Thomas (University of Birmingham) in a Petri dish (9 cm diam.) containing 1.5 % agar-1X M9 salts enriched with 1 mM $MgSO_4$, 1mM thiamine, 0.1 M $CaCl_2$, and 0.2 % glucose. P. fluorescens was subsequently inoculated and grown on Pseudomonas agar plates. Pseudomonas agar was used for short term storage of *P. fluorescens*. This medium is a modification of Kings medium A, which uses magnesium chloride and potassium sulphate to enhance production of the pigments pyocyanin and fluorescein secreted by pseudomonids.

Pseudomonas putida OUS 18 was obtained from Prof. Wen-Tso Liu (National University of Singapore) in a 15 % glycerol stock stored at -80 °C. P. putida was revived into sterile Luria Bertani (LB) broth and subsequently grown onto Pseudomonas agar Petri dishes.

2.2.1 Storage and maintenance

For short term storage (4-5 weeks) both pseudomonids were maintained in Petri dishes in Pseudomonas agar solidified isolation medium at 4 °C. For long term storage (>5 weeks) single colonies were individually inoculated into 15 % (v/v) glycerol in 1.5 ml Eppendorf tubes and stored frozen at -80 °C. The revival of frozen stocks was performed by dipping a sterile plastic loop into the glycerol stock and inoculating the bacteria into 2 ml of sterile LB. LB is a rich medium and very efficient at stimulating growth. The culture was then incubated at 25 ºC and shaken at 120 rpm until growth was detected**.**

2.2.2 Assay media

Minimal Davis medium (MDM, Appendix 1) was used for the nanoparticle toxicity assays. MDM made by reducing the potassium phosphate concentration of Davis media by

90% (Atlas 1993; Lyon *et al.* 2005). This media has been previously used for nanoparticle toxicity assays, since previous research indicates that high phosphate medium provokes the precipitation of certain nanoparticles out of suspension (Lyon *et al.* 2006). MDM was prepared at pH 6, 7.5 and 9. MDM still contains enough phosphates to affect particles stability.

Artificial seawater (Appendix 1) was used for the characterisation of Ag NPs for the marine biofilm assay (Section 2.7.5).

2.2.3 pH measurements

The pH of the solutions was measured using a Fisherbrand Hydrus 300 pH meter. Buffers 4, 7 and 9 were used for calibrations of the electrode before each measurement. The pH was calibrated over the appropriate range using the standard buffers. For measurements and adjustments the pH meter was dipped into the liquid medium while being stirred. NaOH (0.1 M) and H_2SO_4 (0.1M) were used to adjust the pH.

2.3 Humic and fulvic substances

Suwannee river humic substances (SRHA, Standard II, 100 mg) and Suwannee river fulvic substances (SRFA, Standard II, 100 mg) were obtained from The International Humic Substances Society (St Paul, MN, USA). Solutions of 100 mg l^{-1} were prepared in sterile 50 ml Falcon™ tube in sterile and filtered (Millipore, 0.22 µm pore size) MDM (Section 2.2.2) or artificial seawater (Section 2.2.2). Solutions were mixed for 24 h before use by shaking them (240 rpm, IKA® KS 130 Basic shaker). Solutions were made fresh 1 or 2 days before use and stored at 4 ˚C.

2.4 Latex nanoparticles

Nanosphere™ Latex nanoparticles (latex NPs, APS 21±1.5 nm dia; 10 ppm stock solution) were obtained from Duke scientific Corporation. Solutions of 100 mg l^{-1} were prepared in sterile 50 ml Falcon™ tube in sterile and filtered (Millipore, 0.22 µm pore size) MDM (Section 2.2.2). Solutions were made fresh every month and stored at room temperature.

2.5 Preparation of assay materials

Ultrapure water (UPW, MilliQ 18.2 MΩ cm^{-1}) was the only source of water used for preparing solutions, media as well as for cleaning and rinsing all material.

2.5.1 Cleaning

All glass- and plasticware were acid washed by soaking them in a solution of 10 % HNO_3 for a minimum of 24 h. Thereafter, the material was rinsed thoroughly 4-5 times with UPW and air dried.

2.5.2 Sterilising

Material was sterilised by autoclaving (Boxer Series 200, Sterilization at 121 ºC, 15 min). If autoclaving was not an option due to the low melting points of the tools to be sterilised, they were immersed for a period of 5-7 h into a solution of 20 % hydrochloric acid. Thereafter, the material was rinsed thoroughly 4-5 times with sterile UPW and air dried in a class II safety cabinet.

2.6 Silver Nanoparticles

Silver nanoparticles (Ag NPs) were used for this work. Silver nanopowder was purchased from Stanford Materials Corp. (Aliso Viejo, CA, USA). The reported average particle size (APS) was 30-50 nm diameter, the standardized surface area (SSA) was 5-10 m^2g^{-1} and the purity 99.9%.

2.6.1 Ag NPs stock suspension

A suspension of Ag NPs was prepared by dispersing 5 g of silver nanopowder into 1 L sterile UPW and 0.25 mM sodium citrate for stabilization. The resultant suspension was sonicated (Ultrasonic bath Fisherbrand unheated, 230V 50Hz) for 30 min/day for 4 consecutive days. After the last sonication, the suspension was left to stand for 96 h. Thereafter, the supernatant was carefully removed and the final Ag NP concentration was quantified by Inductively Coupled Plasma Mass Spectrometry (ICP-MS, Agilent 7500ce Octopole Reaction System with a Shield Torch System, Section 0). The stock suspensions were stored at 4 ºC. Before each experiment stock suspensions were stirred for a ~ 2 h.

2.6.2 Characterization of Ag NPs

The stability, agglomerate size and changes in surface properties of Ag NP solutions were investigated in MDM (Section 2.2.2) under different environmental conditions (Section 2.7.1) and in artificial seawater (Section 2.2.2) under the same water parameters natural biofilms were exposed to NPs (Section 2.7.5.2). MDM and artificial seawater were filtered (Millipore, 0.22 μm pore size) before adding 10 % v/v SRHA/SRFA 100 mg l^{-1}, when needed, (Section 2.3) and at the appropriate volume of Ag NPs suspension of the concentrated stock (Section 2.6.1) to attain the final Ag NP concentration. The mixtures were shaken for 24 h and analyzed by transmission electron microscopy and energy dispersive X-

ray spectrometry, zeta potential/electrophoretic mobility, dynamic light scattering, ultrafiltration, BET surface area analysis, and X-Ray diffraction analysis. These techniques were used as described below.

2.6.2.1 Transmission electron microscopy & and energy dispersive X- ray spectrometry

The morphology of the aggregates and size of primary Ag NPs were studied by transmission electron microscopy (TEM, Section 2.9.1). To identify the metal composition of particles detected by TEM-energy dispersive X-ray spectrometry (EDX) was used on selected samples. A frequency distribution was obtained from measurements of individual Ag NPs under all conditions with the software package SPSS (SPSS Inc., Chicago IL). The total number of particles in each concentration of Ag NPs used (Section 2.7.1.3) was estimated by adding a known volume of the sample onto a Formvar coated copper grid and counting the number of particles in 10 out of the 300 mesh squares composing a grid. Three grids were analysed per concentration and only the concentrations of 2000 and 20 ppb were counted. The amount of particles in the other 2 concentrations used (2 and 200 ppb) were estimated from the samples of 20 and 2000 ppb.

The TEM uses a high voltage electron beam emitted by an electron gun which fits with a tungsten filaments cathode as an electron source. The acceleration of the electron beam (from 40 to 100 kV) is focused by electrostatic and electromagnetic lenses and directed towards the specimen in observation (Fig 2.1). When the electron beam hit the specimen a fraction of them will be scattered, and relative to the density of the sample. The electrons that go through the specimen (unscattered electrons) will hit a fluorescent viewing screen, coated

with either phosphor or zinc sulphide. An image is produced and the different darkness relates to the sample density and scattered electrons.

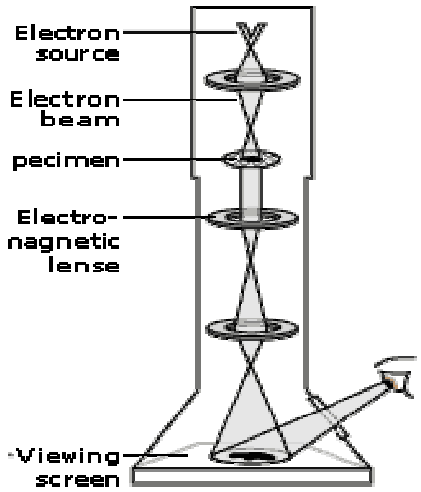

Figure 2.1.Schemtic representation of TEM

Spherical aberration limits the resolution of TEM, which has lately been overcome by the use of special corrector lenses.

2.6.2.2 Dynamic light scattering

Dynamic light scattering (DLS, Fig 2.2) works based on the principle that when particles are hit by a monochromatic beam of laser light, the intensity of the scattered light varies at a rate that is dependent upon the diffusion coefficient (hydrodynamic radius) of the particles. DLS is suitable for determining small changes in mean diameter such as those due to adsorbed layers on the particle surface or variations in manufacturing processes (Malvern Instruments, 2008).

The particle/aggregate size distribution of Ag NPs was studied by DLS (He-Ne laser Malvern High Performance Particle Seizer HPPS 5001). A 1 ml sample of Ag 2000 ppb NPs suspension was placed into disposable plastic low volume cuvettes and the hydrodynamic diameter of the particles/aggregates was measured. Measurements were done at 25 °C and

each suspension was measured in triplicate. Only solutions of 2000 ppb were measured. Due to air dust contamination low particle concentrated samples can generate results skewed toward larger size of particles since light scattered from dust in the sample will broaden the apparent size distribution and limit reproducibility (Filella *et al.* 1997). A limitation of this technique relates to the mode of data acquisition. Particle size distribution is based on the intensity of reflected light, which relates to the size of the particle and not the number of particles. Thus, polydispersed solutions cannot be accurately measured with this technique.

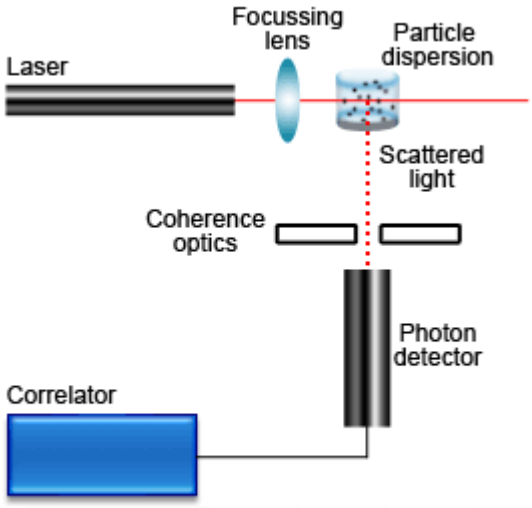

Figure 2.2. Diagram of a DLS. A monochromatic coherent He-Ne laser with a fixed wavelength of 633 nm is used as the light source. Ag NP size distribution in MDM and in artificial seawater (Section 3.2.2) under different environmental parameters (Section 2.7.1) was investigated. A 1 ml sample of the suspension was placed into plastic cuvettes and the hydrodynamic diameter of the particles/aggregates was measured. Measurements were done at 25 °C and each suspension was measured in triplicate. From Malvern Instruments (3).

2.6.2.3 Zeta (ζ) potential and electrophoretic mobility

When particles are suspended in an aqueous fluid, they acquire a surface charge due to ionization of surface groups, adsorption of charged particles or substitution of lattice ions with other ion e.g Ca^{2+} and Al^{3+}. This results in a charged layer surrounding the particle. If the particle moves, this layer moves with the particle. The ζ potential measures the potential at the point of this layer where it moves past the bulk suspension (slipping plane) (Fig 2.3). The charge at the slipping plane is highly dependent on the ionic strength and type of ions in suspension and size and shape of particle. ζ potential measures the magnitude of the repulsion between particles. Particles with a high ζ potential (either positive or negative, i.e < -30mV and > +30 mV) will repel each other. Hence, a high ζ potential will stabilize small particles and thus remain in suspension. For low ζ potential (> -30mV and < +30 mV) attraction due to van der Waals and other forces exceeds repulsion and will tend to flocculate (Malvern Instruments 2, 2008). Other effects e.g. steric interactions may play a role but this was not the case using citrate stabiliser.

The electrophoretic mobility (μ) is the velocity of a particle in an electric field, and it is dependent on the strength of the electric field, the dielectric constant of the medium, the viscosity of the medium and the ζ potential. This value is the one directly measured by laser Doppler velocimetry, and it is further converted to ζ potential value by applying Henry's equation:

$$U_E = 2\varepsilon \zeta f(ka)/3\eta^{-1}$$

Where;

ζ : zeta potential.

U_E : Electrophoretic mobility.

ε : Dielectric constant.

η: Viscosity.

f(*k*a): Henry's function.

In this study the electrophoretic mobility/ ζ potential of Ag NPs was measured by Malvern Instruments Zetasizer 1000. Five ml of Ag NP solutions (Section 2.6.2) were injected using a 10 ml syringe into the inlet of the instrument. Ten measurements were done per sample and a minimum of three replicates were done per treatment.

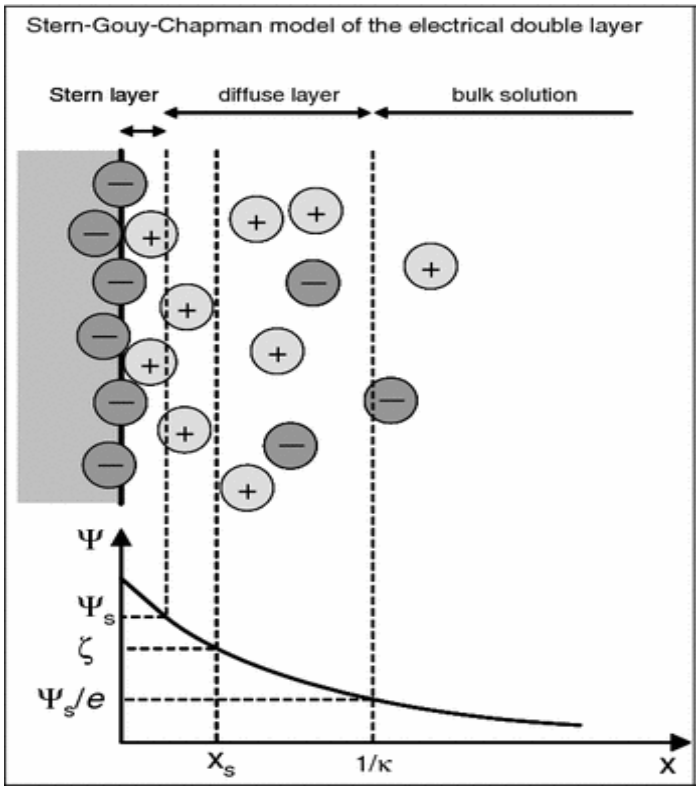

Figure 2.3. Schematic representation of the electrical double layer (EDL). Abbreviations: zeta potential (ζ), electrostatic potential (ψ), electrostatic potential at the stern layer (ψ_S), Euler's number (*e*), Boltzmann constant (*k*). X is a distance from the surface, X_s is the distance where ions and molecules are mobile and can be sheared off (shear plane), and potential here is measured as the zeta potential. The diffusion layer is an unstirred layer of water adjacent to the surface, and the bulk suspension is the free moving water. From Handy *et al.* 2008.

2.6.2.4 Ultrafiltration

Ultrafiltration was the technique selected to determine the solubility of Ag NPs in solution. If a system is in dynamic equilibrium, a constant ratio of concentrations for that equilibrium can be described. Therefore, assuming:

$$\text{Ag NP} \longleftrightarrow \text{Ag}^{+}$$

Then,

$$K_C = \frac{[\text{Ag}^{+}]}{[\text{Ag NP}]}$$

Thus, after 24 h we assume that the concentration of Ag^{+} released by the Ag NPs has reached an equilibrium (or at least steady state) for the specific conditions. The equilibrium constant K_c varies with ionic strength, temperature and pressure.

All suspensions were shaken at 25 ºC for 24 h (expected time for a solution to reach a equilibrium or steady state. Thereafter, they were ultrafiltered (Ultrafiltration system Amicon Stirred Cells, Models 8400, Millipore; membranes of regenerated cellulose: 76 mm diam, NMWL: 1,000). 25 psi of nitrogen gas pressure was applied to the ultrafiltration device to allow separation of particulates from soluble fraction. Only the soluble fraction of the Ag NP suspension is collected in the ultrafiltrate. Total Ag of both, ultrafiltrated and non-ultrafiltered samples were measured by GFAAS 600 (Section 2.8) and the percentage solubility calculated for each condition.

Solubility was studied with those solutions containing Ag NPs only, and not containing also SRFA/SRHA (section 2.3) due to the possibility of loss of SRFA/SRHA attached Ag through the ultrafiltration membrane. In Chapter 6 due to problems of

interference of chloride with atomic absorbance spectrometry/inductive coupled mass spectrometry analysis (Section 2.8, Byrne et al. 1992), undiluted artificial seawater could not be used. Thus, to avoid this analytical problem but still determine the Ag NP solubility in a high ionic strength medium, a sodium nitrate solution at the same salt concentration of the seawater used for natural biofilm assays (Section 2.7.5) was prepared. A dilution series of 0, 5, 10, 20, 30 and 35 ‰ sodium nitrate solutions with 200 ppb Ag NPs and pH 8 was prepared to correlate changes on solubility with increased salt concentration. For MDM (Section 2.2.2), solutions of Ag NPs ranging from 0-2000, and pH values of 6, 7.5 and 9 (Section 2.7.1.3 and Section 2.7.1.4) were prepared.

2.6.2.5 X-Ray diffraction analysis

X- ray diffraction analysis (XRD) is a technique for studying the structure and size of crystals. XRD analysis using a Siemens D5000 diffractometer was done by Dr. Colin Greaves from the Department of Chemistry at The University of Birmingham, UK. XRD analysis gave further information about particle size and crystal structure.

2.7 Nanoparticle exposure assays

2.7.1 Selection of culture conditions

All experiments were performed at selected environmentally relevant conditions.

2.7.1.1 Temperature

The temperature chosen for all planktonic and biofilm laboratory assays was of 25 ºC. This temperature was chosen since it allowed for an appropriate growth of both pseudomonids used. Temperatures of 25 ºC are found in many freshwater ecosystems. Major freshwater bodies such as the lake Eire, USA-Canada, lake Victoria, Tanzania-Uganda, lake

Titicaca, Peru or the Aral sea, Kazakhstan-Uzbekistan, have water temperatures of ca. 25 ºC for part of the year. For seawater, temperatures of 25 ºC are found in subtropical and tropical regions (Australia Government, Bureau of Meteorology 2008).

2.7.1.2 Organic matter

The amount of dissolved organic carbon in natural waters varies with the source and type of water. For instance, in groundwater and seawater concentrations are as low as 0.5 mg l^{-1}, but in eutrophic swamps, marshes and bogs organic matter can be present in amounts of up to 60 mg l^{-1}. Rivers and lakes average from 2 to 10 mg l^{-1} (Thurman 1985). Humic substances are a group of weak organic acids which can be isolated from waters or soils. Aquatic humic substances constitute about 40-50% of total dissolved carbon. Aquatic humic substances can be divided into humics and fulvic acids. The former is the fraction that precipitates at pH 2, while the latter remains soluble at this pH and lower. The elemental composition of humic substances is 50 % carbon, 4-5 % oxygen, 1-2 % nitrogen and less than 1 % sulphur and phosphorus. Their major functional groups include carboxylic acid, phenolic hydroxyl, carbonyl, and hydroxyl groups (Thurman 1985). The concentration of organic matter used for the assays was in the form of SRHA and SRFA (Section 2.3), and it was of 10 mg l^{-1}, except for laboratory seawater assays, where the concentration used was of 4 mg l^{-1} since this was the value of organic carbon obtained from the field site (Section 2.7.5.1).

2.7.1.3 Ag NPs

The range of concentrations of Ag NPs chosen were selected taking into consideration the values stipulated as the minimum Ag allowed in drinking water and the concentrations of silver complexes found in natural environments. The Drinking Water Inspectorate, DEFRA 2002 and the Food Standards Agency 2001, stipulate that the maximum amount of Ag allowed in drinking water is 10 ppb. Although, The Food Standards Agency

states that if Ag is used for water treatment processes the maximum allowed in drinking water can then be of 80 ppb. Higher concentrations of Ag have been also found in industry discharges and sediments (IPCS 2002).

Table 2.1 Silver concentrations reported during 1970-1980. (Int'l programme on Chemical Safety, IPCS, Concise International Chemical Assessment Document 44, 2002, published online) http://www.inchem.org/documents/cicads/cicads/cicad44.htm

Source	*Concentration (ppb)*
Pristine and unpolluted water	0.01
Urban and industrialized water	0.01-0.1
Photographic manufacturing waste discharges	250
Steam wells	300
Soils	31000
Certain hot springs (from US)	43000
Crude oils	100000
River sediments (from US river)	150000

Due to the lack of data on concentrations of Ag NPs in natural waters, in this study the concentrations of Ag NPs chosen were within the range of concentrations of Ag complexes found in the natural environment: 2, 20, 200 and 2000 ppb (Table 2.1).

2.7.1.4 pH

The pH values used in this study were 6, 7.5 and 9. As well and being environmentally relevant pH values, the strains chosen were able to grow well (*Pseudomonas*

putida and *Pseudomonas fluorescens*) and these were considered suitable values for investigating the effects of different water chemistries on NP toxicity and behaviour.

2.7.2 Bacterial growth

2.7.2.1 Quantification

Three different assays were used to quantify the amount of bacteria/biofilm in the samples. The assay chosen for each experiment depended on the type of sample. For aqueous samples (e.g. bacteria in MDM), bacterial density was quantified by measuring the optical density of the cell suspension (Section 2.7.2.1.1), while for biofilm samples two different methods were used: a Crystal Violet Assay (Section 2.7.2.1.2) and cell dyes coupled to confocal scanning laser microscopy image analysis (Section 2.7.2.1.3).

2.7.2.1.1 UV-VIS Absorbance

For aqueous samples containing bacteria its density was measured by UV-VIS absorbance at a wavelength of 595 nm (OD_{595}) using a Lightwave Spectrophotometer, WPA diode array. Samples were diluted when needed to ensure that the readings were within their linear range of calibration. Disposable low volume and sterile plastic cuvettes were used.

2.7.2.1.2 Crystal violet assay

This assay was used to quantify marine biofilm biomass. Due to the size of marine biofilms, as well as the large number of samples this technique was quick and non-destructive.

Glass slides containing biofilm were rinsed three times by dipping them into filtered sterilized PBS solution. Thereafter slides were fixed by immersing them into methanol for 15 min. Thereafter, slides were air dried at room temperature. Once dried 3 ml of crystal violet

was added and incubated at room temperature for 5 min. Slides were rinsed 3 to 4 times with abundant UPW and air dried. A 1 ml drop of 33% glacial acetic acid was added to each slide to bleach the dye. Dye concentration was quantified by UV-VIS OD_{570} (Henriques *et al.* 2006). Samples were diluted when needed to ensure that the reading were within their linear range.

2.7.2.1.3 Exopolysaccharide staining and viability assays

Staining the biofilm exopolysaccharides (EPS staining) with fluorescent dyes coupled to CSLM imaging give us information about the architecture as well as the abundance of biofilm per surface area ($\mu m^3 \mu m^{-2}$). A viability assay such as the LIVE/DEAD staining techniques gives information on cellular viability and also total biomass per surface area ($\mu m^3 \mu m^{-2}$). Both techniques were used for marine and laboratory grown biofilms, respectively and are explained in detailed in section 2.9.2.2 and section 2.9.2.3, respectively.

2.7.2.2 Inoculation and growth on shake flask cultures

P. fluorescens and *P. putida* were grown in 500 ml flasks containing 250 ml MDM (Section 2.2.2) adjusted to the experimental pH value. A single bacterial colony from an agar plate (Section 2.2.1) was selected and picked with a sterile plastic loop and inoculated into the MDM. Cultures were incubated at 25 ºC and shaken at 120 rpm to its exponential phase using a Jeio Tech, Model SI-900R incubator. Cells were collected by centrifugation at 4,000 rpm for 10 min, the supernatant was discarded and the pellet was washed and resuspended into sterile MDM of the same pH value. This procedure was repeated three times. The final concentration of the bacterial suspension was measured with UV-VIS at OD_{595}. The bacterial concentration was adjusted to OD_{595} of 0.1 by addition of sterile MDM.

A concentration of OD_{595} of 0.1 was used as the initial concentration for planktonic (Section 2.7.3) and flow cell reactor (Section 2.7.4) experiments. At this optical density (OD_{595} of 0.1) the concentration of bacteria at the start of the experiment was low, and after 24 h (exposure time) its growth would still be exponential (see Ch. 4). The population would have not reached a stationary phase for the growth conditions selected, which could mask potential detrimental effects if exposure to NPs/silver nitrate would have delayed or slowed (but not impeded) growth.

2.7.3 Planktonic assay

All the material was acid washed (Section 2.5.1) and sterilized (Section 2.5.2) before use. The purpose of this project was to determine the effects of Ag NPs to planktonic bacteria and to discriminate between the toxic effect of a Ag NP from the well known toxicity of ionic Ag (Slawson *et al.* 1992b; Silver 2003), and also from the potential toxicity of NPs of the same size but manufactured with a material considered non-toxic (in this case latex NPs). This study also takes into account the possible alterations on the strength of toxicity of Ag NPs and correlates them with changes of pH values, and presence or absence of organic matter.

2.7.3.1 Experimental set up

Conical flasks (50 ml) were used containing bacterial suspension in MDM (Section 2.7.2.2) at the experimental pH value (section 2.7.1.4). Subsequently a 10 % v/v concentrated Ag NPs, Ag nitrate or latex NP suspension was added to each of the flasks to obtain the final desirable concentration. A 10 % v/v 100 mg L^{-1} SRHA suspension was also added to those treatments requiring 10 mg L^{-1} humic substances. The final volume was of 25 ml and the initial bacterial concentration was OD_{595} 0.1.

2.7.3.2 Experimental conditions

Pseudomonas fluorescens (Section 2.2) was used.

Flasks were incubated (Jeio Tech, Model SI-900R incubator) and shaken at 120 rpm. The temperature was maintained at 25 ºC for the duration of the assay.

A total of six different conditions were tested:

- Condition 1: pH 6 without SRHA
- Condition 2: pH 6 with SRHA
- Condition 3: pH 7.5 without SRHA
- Condition 4: pH 7.5 with SRHA
- Condition 5: pH 9 with SRHA
- Condition 6: pH 9 without SRHA

The concentrations of Ag NPs chosen were 2, 20, 200 and 2000 ppb (Section 2.7.1.3). Controls contained only bacteria at the same conditions without Ag NPs, as well as only Ag NPs, latex NPs or Ag nitrate with and without SRHA. The latter controls would determine potential background readings from test solutions.

2.7.3.3 Sample collection

Aliquots of 1 ml were sampled from all flasks 3 and 24 h after exposure to Ag NPs, Ag nitrate or latex NPs. The concentration of bacterial cells in each flask was measured by UV-VIS spectroscopy (Section 2.7.2.1.1).

2.7.3.4 Metal loss

The percentage of Ag NPs lost over 24 h (Ag NPs + dissolved Ag) was quantified by AAS (Section 2.8). 50 ml flaks containing only Ag NPs under all conditions (Section 2.7.3.2) were sampled at t = 0 and t = 24 h and the percentage loss (%) estimated by:

$$[Ag]_{t=24} * 100 / [Ag]_{t=0}$$

Where:

$[Ag]_{t=0}$ is the concentration of Ag in the flasks at the beginning of the experiment.

$[Ag]_{t=24}$ is the concentration of Ag in the flasks at the end of the experiment.

2.7.3.5 Biomass quantification

To determine the effects of Ag NPs, Ag nitrate and latex NPs to bacterial cells the change on bacterial density in the culture was measured using the following equation:

$$G_t = A_{test}/A_{control} \times 100$$

Where:

G_t = Percentage (%) of bacterial growth at the sampling time t

A_{test} = Absorbance OD_{595} of the test culture, and

$A_{control}$ = Absorbance OD_{595} of the control.

A one-way ANOVA and a Tukey test (Section 2.10.3) were used to determine which treatments and concentrations caused an effect to planktonic *P. fluorescens*.

2.7.4 Flow cell reactor

2.7.4.1 Experimental set up

All the material was acid washed (Section 2.5.1) and sterilized (Section 2.5.2) before use. Biofilms were grown into Perspex flow cell (Fig.2.7.4.1). The flow cell dimensions are described in detailed in Figure 2.4 and in Figure 2.5. The volume capacity of the flow cell chamber where biofilms were grown was of 3.7 cm^3. The complete flow cell reactor system consisted of a total of 8 flow cells independently connected to a 2 L conical flask containing MDM (Section 2.2.2). The conical flask was capped with a rubber bung (5 cm diam. by 4 cm length) containing 5 holes (4 mm diam.). One hole was connected to an air vent. Glass rods (~ 30 cm diam. OD 4 mm, ID 2 mm) were inserted through 4 of the holes and connected to ~ 30-35 cm of silicone tubing (OD 4 mm ID 2 mm). The silicon tubing was connected to a peristaltic pump (ISMATEC) though peristaltic tubing (Cole Palmer, 2- stop silicone tubing ID 0.89 mm), and to the inlet of the flow cells by an addition of ~10 cm of silicon tubing attached to the peristaltic pump tubing . The outlet of the flow cell connected with a 5 L waste container with a 1.1 m silicone tubing (Fig. 2.6).

2.7.4.2 Experimental conditions

Pseudomonas putida (section 2.2) was used to grow the biofilms.

The complete reactor (apart from the waste container) was placed inside a static incubator (Jeio Tech, Model SI-900R) and the temperature was maintained at 25 ºC for the duration of the assay.

A total of four different conditions were tested:

- 1: pH 6 without SRFA
- 2: pH 6 with SRFA
- 3: pH 7.5 without SRFA
- 4: pH 7.5 with SRFA

The concentrations of Ag NPs chosen were 20, 200 and 2000 ppb (section 2.7.1.3).

The flow rate of the reactor was adjusted and maintained at 0.1 ml min^{-1} at all times. This flow velocity was chosen since it was adequate for managing the total volume of media required daily for the whole reactor as well as of waste produced and collected.

Due to time constrains the selection of conditions used for the biofilm study did not include pH 9, as it did the planktonic study.

2.7.4.3 Suspension of Ag NPs

500 ml of Ag NPs solutions were prepared as described in section 2.6.2 with the only modification that the MDM was not filtered beforehand. Ag NPs electrophoretic mobility of all suspensions was measured as described in Section 2.6.2.3 before passing over the biofilm and after to determine changes in electrophoretic mobility of the particles, once they have been in contact with the biofilm.

2.7.4.4 Operation

For those biofilms to be analyzed for metal uptake, three sterile round plastic coverslips (13 mm diam.) were attached to the bottom of each flow cell with Fomblin (perfluorinated grease, Rocol YVAC-3). These coverslips were easy to sample, manipulate, and acid digest for metal analysis at the end of each experiment (Section 2.9.1.2). Biofilms used for biomass/cellular viability quantification were grown directly on the bottom coverslip of the flow cell (Fig.2.3), and the 13 mm coverslips were not required.

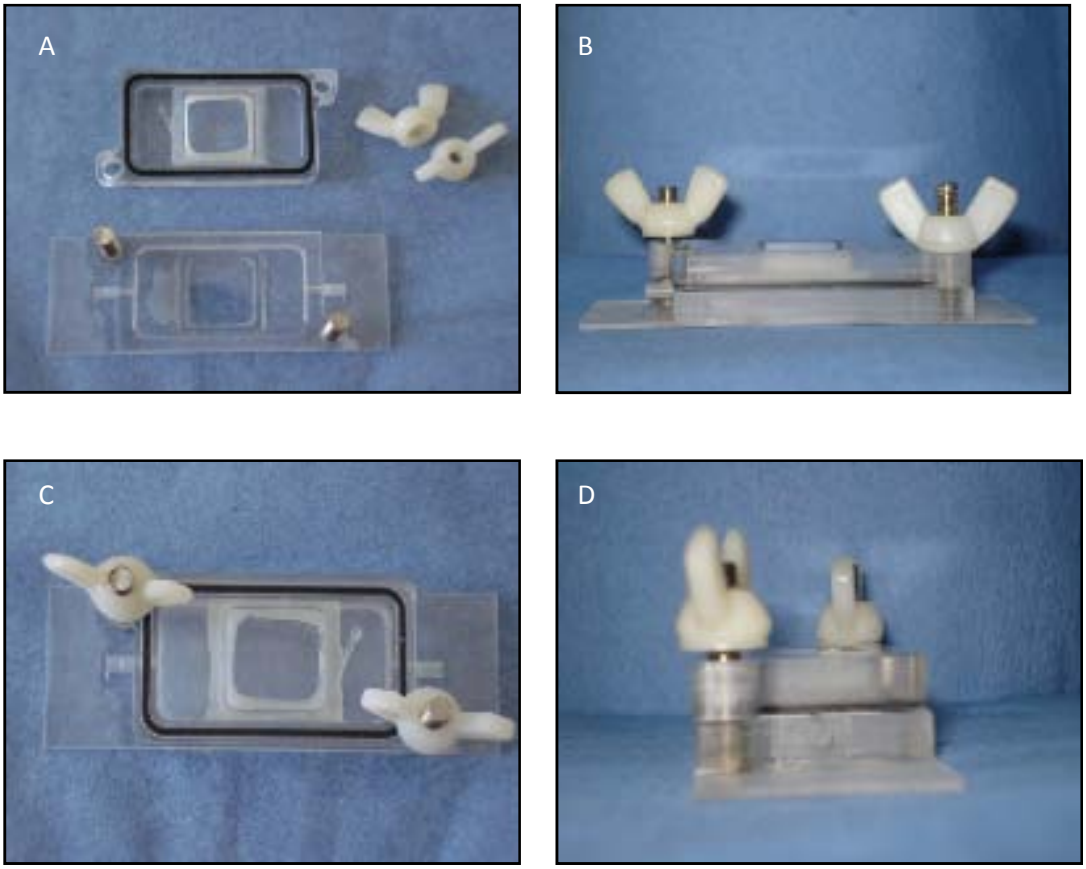

Figure 2.4. Pictures of a flow cell. A) Complete open flow cell; B) flow cell side view; C) flow cell upper view; D) flow cell end view.

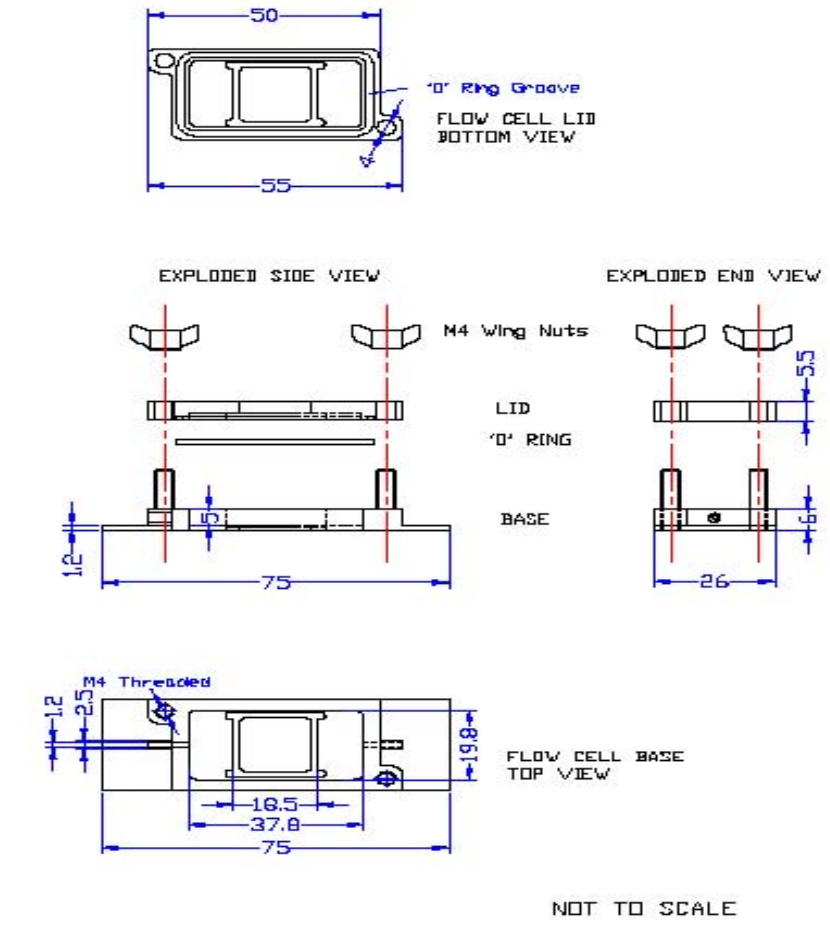

Figure 2.5. Diagram of Perspex flow cell used for the laboratory biofilm assay. Biofilms were grown inside each flow cells for 3 days (flow rate 0.1 ml min^{-1}, temp 25 °C, *I*=0.05 M) at different pH values. After 3 days biofilm were exposed to different concentrations of Ag NPs, or no Ag NPs with or without SRFA (flow rate 0.1 ml min^{-1}, temp 25 °C, *I*=0.05 M).

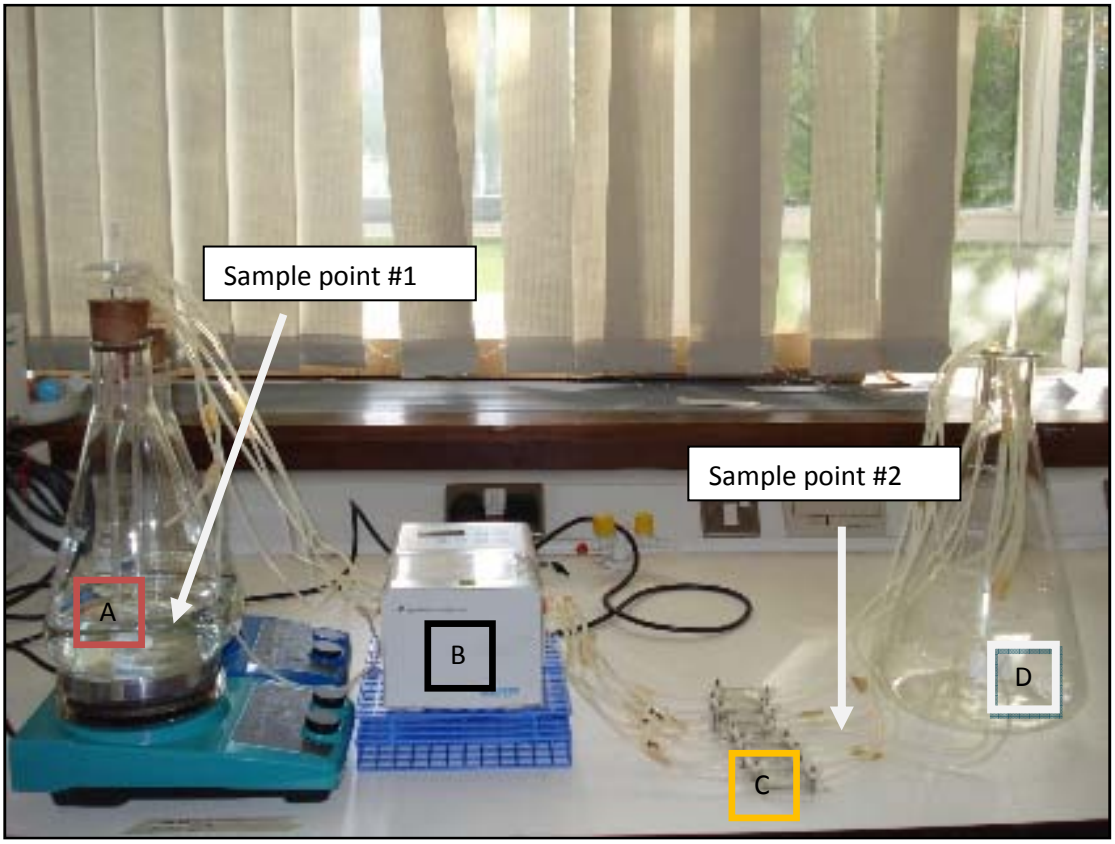

Figure 2.6 Complete biofilm flow cell reactor consisting of: (A) 2x2-L conical flasks containing MDM, capped with a rubber bung with 5 holes. One whole connected an air vent, and glass rods were inserted though the other 4 holes, and connected the MDM with the flow cells (C) though a peristaltic pump (B). The outlet of the flow cell connected to a 5 L waste container (D). Sample point # 1 is where the initial concentration of Ag NPs was measured, and Sample point # 2 is where the outflow from the biofilm containing material sloughing off and Ag NPs was collected.

An aliquot of 3 ml of bacterial suspension (Section 2.7.2.2) was injected in the flow cell and the flow cell was untouched for 2 h. This time is sufficient to allow adhesion of a small number of bacterial cells to the surface (Dunne 2002). Thereafter, MDM was passed over the biofilms at 0.1 ml min^{-1}. Biofilms were allowed to grow undisturbed for 3 days. Flasks were restocked with fresh and sterile MDM daily.

On day 3, suspensions of Ag NPs (Section 2.7.4.3) were passed though the experimental flow cells for 24 h. Control flow cells continued receiving MDM only, and SRFA were added if required (Section 2.3).

Six flow cells were used per each different concentration and treatment (3 flow cells for metal and three flow cells for biomass/cellular viability quantification). Two control flow cells were used for metal analysis, while 3 were used for biomass and cellular viability quantification.

2.7.4.5 Sample collection

2.7.4.5.1 Metals

In order to study the uptake by biofilms and behaviour of Ag NPs in the flow cell reactor several samples, liquid and from the biofilm, were taken at different points along the reactor (Fig 2.5). All handling was done under sterile conditions.

2.7.4.5.1.1 Initial Ag NPs concentration- Sampling point 1

Samples of 20 ml from the initial Ag NPs solutions and the MDM that run though the system were taken to verify the initial concentrations of Ag NPs being used ([Ag $NP_{initial}$]). Fig 2.5.

2.7.4.5.1.2 Biofilm outflow- Sampling point 2

Samples of 20 ml were taken from the outflow coming off the flow cell though the outlet (Fig 2.5). The outflow contained the material (bacterial cells and Ag NPs) being detached from the biofilm as well as those Ag NPs not being taken up by it. The outflow was collected into 200 ml acid washed (Section 2.5.1) and sterile (Section 2.5.2) glass bottles during the exposure time 8 -24 h. The tubing was inserted into the top of the bottle and the bottle was capped with sterile foam during the length of the sampling. All bottles were kept on ice in a polystyrene container during the duration of the sampling to prevent bacterial growth once in the collecting bottle. This results are an indication of the amount of Ag NPs flowing through and not being uptake by the biofilm ([Ag $NP_{outflow}$].

2.7.4.5.1.3 Filtration

Samples of 25 ml of the outflow collected (Section 2.7.4.5.1.2) were filtered using a Nalgene polysulfone 500 ml filter unit equipped with a 0.22 μm pore size nitrocellulose disk (Millipore, diam. 25 mm). The results would give an indication of the amount of free-Ag NPs (which would pass through the 0.22 μm pore size filter) and of the amount of Ag NPs bound to the biomass being slough off by assuming:

- If total concentration of Ag NPs exiting the biofilm (free Ag NPs + Ag NPs bound to bacterial biomass) is quantified in the outflow ([Ag $NP_{outflow}$], Section 2.7.4.5.1.2), and then the total Ag NPs not bound to biomass is quantified in the filtrate ([Ag NP_{free}]),

Then:

$$[\text{biomass-Ag NP}] = [\text{Ag } NP_{outflow}] - [\text{ Ag } NP_{free}]$$

Where:

[Ag $NP_{biomass}$] = amount (ppb) of Ag NPs attach to bacteria/biomass.

[Ag $NP_{outflow}$]= total amount (ppb) of Ag NPs

[Ag NP_{free}]= amount (ppb) of Ag NPs not attached to bacteria

2.7.4.5.1.4 Ultrafiltration

A sample of 10 ml of the filtered outflow (Section 2.7.4.5.1.3) was ultrafiltered as previously described (Section 2.6.2.4). The results would give an indication of the percentage (%) of Ag that is dissolved from the Ag NPs under each condition (Section 2.7.4.2).

$$Ag^{+}_{UF} * 100 / [Ag\ NP_{free}]$$

Ag_{UF} = Total amount (ppb) of ionized (dissolved) Ag.

[Ag NP_{free}] = Total amount (ppb) of Ag NPs in the filtrate.

2.7.4.5.1.5 Biofilms

At the end of the assay, 2 or 3 13 mm coverslips were recovered from each flow cell. Coverslips were rinsed by dipping them three times into sterile and fresh MDM and gently dried to remove loss bacteria and Ag NPs of the surface of the biofilm.

All samples for metal analysis were processed and analyzed as described in section 2.8

2.7.4.5.2 Biofilm and bacterial biomass quantification

2.7.4.5.2.1 *Shedding biofilm biomass*

The biomass of biofilm being slough off due to Ag NPs exposure was collected in the outflow as described in Section 2.4.6, also including a sampling time from 0-4 h after exposure of the biofilm to Ag NPs. A 1 ml aliquot from each flow cell was measured by UV-

VIS spectrometry (OD_{595}) (Section 2.7.2.1.1). Each flow cell outflow was measured three times at each sampling time.

2.7.4.5.2.2 *Biofilm biomass*

The biomass of biofilms was quantified by confocal scanning laser microscopy (CSLM) as described in Section 2.9.2.

2.7.4.5.3 Microscopy

TEM and TEM-EDX (Section 2.6.2.1) were used to study the interaction of Ag NPs with *P. putida* biofilms. Two 13 mm coverslips from each treatment (Section 2.7.4.2) and controls were sampled at the end of each assay, washed three times by gently dipping them into sterile and fresh MDM media and fixed with a suspension of 2.5 % glutaraldehyde in PBS. Samples preparation for TEM analysis were processed as described in section 2.9.1.1.

2.7.5 Marine biofilm cultures

2.7.5.1 Site selection

Biofilms were grown at the western marina of Singapore (Andaman Sea) (Fig.2.7). This marina is very developed and subjected to a large volume of vessel traffic though the strait of Jurong, with high concentrations of organochlorinated (Monirith *et al.* 2003) and persistent heavy metals (Orlic & Tang 1998) in the seawater. This location was chosen for growing biofilms since if Ag NPs are released and end up in natural waters, they are likely to be present in locations with a high input of human activities, as it is the case of this site (Orlic & Tang 1998). Thus, the biofilm species composition grown in this site can be taken as a representative community of microorganisms, able to survive and grow in a contaminated marine environment.

2.7.5.2 Field set-up

Approximately 240-250 glass slides were acid washed and sterilized before immersion in seawater. Slides were placed parallel to each other into rectangular plastic frame holders (Fig 2.8 A). Each glass slide was separated from the following one by about 1 cm. Holders containing the slides where submerged at about 1 m depth for 3 days (3-d) to allow biofilm colonization (Fig 2.8 B). After 3-d biofilms were transported to the laboratory. To lower biofilm disturbance during collection and transport, plastic frame holders were placed into a ~ 5 L cooler filled with fresh seawater from the same site. The time between field sampling and treatment exposure in the laboratory was less than 30 min. Biofilms were grown in the field under water conditions of: temperature 30.1 ± 1.45 ºC, dissolved oxygen 87.18 ± 12.03 %, pH of 7.96 ± 0.12, and salinity of 29.08 ± 2.13 ‰. These seawater parameters were recorded every 3 days by the Tropical Marine Science Institute (TMSI) for the months biofilms were grown (months of September to November), and averaged. The total organic and inorganic carbon (TOC) of the seawater was measured once. Water from the site was collected in acid washed 1 l glass bottles previously cleaned with 10 % HCl and rinsed thoroughly with UPW (Section 2.5.1). In the field, bottles were rinsed three times in with fresh seawater before collection. Seawater was kept at 4 ºC protected from sunlight and atmospheric oxygen and the total organic carbon was measured before 5 h. TOC was measured with a Shimadzu TOC analyser. Total carbon was determined by high temperature combustion incorporating a platinised alumina catalyst. Inorganic carbon was determined by phosphoric acid digestion. Organic carbon was determined by substracting the inorganic fraction from the total carbon of the sample. Calibrations were done with organic and inorganic carbon standards. Glass vials were previouly washed with Decon 90 and 10 % HCl, pre-rinsed with UPW and the sample to be analysed. The average of five injections was used as the mean value of the sample.

2.7.5.3 Laboratory set up

Once it the laboratory biofilms were split into treatments, each containing 60-65 slides. Biofilms would grow under laboratory conditions (25 ± 0.6 ˚C) for a further 24 h (until d-4), with or without Ag NPs (Section 2.7.1.3). Two samples of also 60-65 slides each were processed as "3-d biofilm samples", thus they were not subjected to any further treatment or growth in the lab. Slides were removed from the holders they were grown in the field and suspended vertically into 3-4 l fresh seawater containers (Fig 2.9). The seawater used for the assays was collected in sterile Nalgene bottles (Section 2.5.2) from the same depth and site the day of the sampling. Each container sat on the top of a magnetic plate which allowed the seawater in the containers to be slowly and continuously stirred. Subsequently, the containers were spiked with a concentrated suspension of Ag NPs (Section 2.6.1), to give the appropriate concentration of NPs needed for the exposure assay. To determine the impact of Ag NPs on the total biomass of marine biofilms the concentrations used were 20, 200 and 2000 ppb (Section 2.7.1.3). However, to determine the impact of Ag NPs on biofilm species richness by TRFLP analysis (Section 2.7.5.10) only a concentration of 2000 ppb was used, due to the length of time required for this type of analysis. Each experiment and condition was repeated three times.

In the lab, biofilms were incubated with Ag NPs at a constant temperature of 25°C ± 0.6 for 24 h. The pH of all treatments was measured at the beginning and at end of the incubation period to confirm that the pH remained constant during the exposure.

2. 7. 5. 4. Metal analysis

2.7.5.4.1 Water

2.7.5.4.1.1. Background silver

To determine any background level of Ag in seawater, samples were collected in acid wash (Section 2.5.1) plastic bottles from the field site each time an experiment was carried out. Samples were acidified to pH ~ 1.6 and stored at 4 ºC until processed for AAS analysis (Section 2.8).

2.7.5.4.1.2 Silver loss over time

To estimate the loss of Ag NPs over the time of the exposure (24 h) in the absence of biofilms due to aggregation and sedimentation and, possibly, to sorption to container walls, seawater samples were taken at the exposure times of t=0 h and t=24 h, from containers containing seawater with Ag NPs only (no biofilms). Samples were acidified to pH ~ 1.6 and stored at 4 ºC until processed for AAS analysis (Section 2.8).

2.7.5.4.1.3 Biofilm

Five glass slides from 3-d (controls) and 4-d old (control and treatment) marine biofilms were gently rinsed by dipping the slide 3 times in filtered sterilized PBS solution to remove loose nanoparticles from the surface of the biofilm, scraped with a sterile glass

Figure 2.7 A) Map of Singapore. Red circle demarks the geographic location where marine biofilms were grown during the months of September-November of 2007 (Section 2.7.5.1). B) Picture of the site A.

Figure 2.8. A) Holder containing ~30 glass slides (76x26x1mm) (Section 2.7.5.1). Each glass slide was separated from the following one by ~ 1 cm. B) Holders containing the slides where submerged at about 1 m depth for 3-d to allow biofilm colonization. After 3-d biofilms were transported to the laboratory.

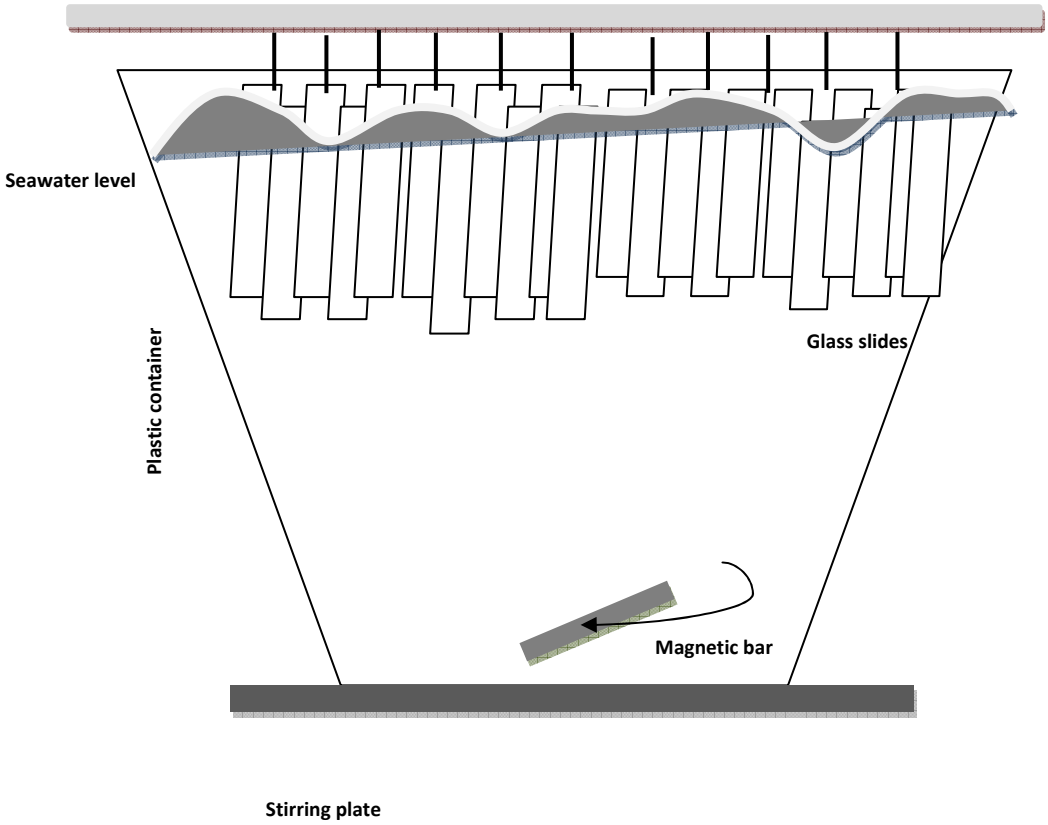

Figure 2.9. Scheme of the laboratory set up for the marine biofilm exposure to Ag NPs. Slides were removed from the holders they were grown in the field (Fig 4) and suspended vertically into 3-4 l fresh seawater containers. Each container sat on the top of a magnetic plate which allowed the seawater in the containers to be stirred continuously. The seawater in the containers was spiked with a concentrated suspension of Ag NPs, to give the appropriate concentration of NPs needed for the exposure assay. Incubations were done for 24 h at 25 ± 0.6 ºC.

coverslip and pooled (5 glass slides from the same treatment were pooled). Four replicates were done per treatment. Pooled biofilms were put into sterile 2 ml Eppendorf tube and digested (Section 2.8.1.2) with concentrated HNO_3 right away and stored at 4 ºC until processed for AAS analysis (Section 2.8).

2.7.5.5 Biomass quantification

Two different assays were performed to estimate the changes on biomas/biovolume per surface area after exposure to Ag NPs: the Crystal Violet assay and the Exopolysaccharides quantification by CSLM. Both are described in detailed in Sections 2.7.2.1.2 and 2.7.2.1.3, respectively.

2.7.5.6 Biomass for DNA extraction

All 3-d (controls) and 4-d old (d4-0 ppb, and d4-2000 ppb) marine biofilms grown on glass slides were rinsed by dipping the slide 3 times in filtered sterilized PBS solution, scraped with a sterile glass coverslip and pooled (25-30 biofilms on glass slides from the same treatment were pooled). Two replicates where done per treatment. Pooled biofilms were put into sterile 2 ml Eppendorf tube and the biofilm was pellet by centrifuging the tubes at 10,000 rpm for 5 min in a KUBOTA 3700. Samples were not stored and DNA extraction proceeded immediately (Section 2.7.5.6.1). The experiment was done three times over the months of September to November 2007.

2.7.5.6.1 Environmental DNA extraction

DNA was extracted by a phenol-chloroform protocol following lyzozyme and proteinase K treatment as describer in Zhou *et al*. 1996, with some modifications. In brief, 588 ml DNA extraction buffer (10 ml 1 M Na_2SO_3; 14 ml 5 M NaCl; 10 ml 1 M pH 7.5 Tris/HCl; 10 ml 0.5 M EDTA; 10 ml 10 % v/v SDS. Solution adjusted to a final volume of 100 ml by addition of NPW and sterilized), 6 µl of lyzozyme (100 mg ml^{-1}) and 6 µl achromopeptidase were added to each tube, mixed by inversion and incubated at 37 ºC for 30 min. Thereafter, 3 µl of proteinase K (20 mg ml^{-1} in TE buffer) and 60 µl of SDS (10 %) were added to each tube. Samples were vortexed and incubated at 37 ºC for 2 h, and mixed gently

every 30 min. After the incubation time 60 µl of CTAB (10 %) and 84 µl of NaCl (5 M) were added to each tube, vortexed and incubated at 60 ºC for 30 min. After incubation, an equal to the incubated mixture volume of chloroform-isoamylalcohol (24:1 v/v) was added, mixed by inversion, and then centrifuged at 10,000 g for 5 min. The aqueous phase was carefully collected and placed into new tubes and purified again with the chloroform-isoamylalcohol mixture and centrifuged. The upper phase was transferred into a new tube and an equal volume of isopropanol at -20 ºC was added and mixed gently. The mixture was incubated for 15 min at room temperature, and then centrifuged at 10,000 g for 15 min. The supernatant was discarded, the DNA pellet was washed with 70 % ethanol, air dried, and dissolved in 100 µl of sterile UPW. Due to the high organic contamination in crude DNA, and additional purification procedure was applied with DEAE-Sephacel column (Sigma, I6505) in a Bio-Rad spin-column tube (Bio-Rad, 732-6008), as recommended previously (Lovell & Piceno 1994; Dang & Lovell 2000). The column was equilibrated by adding 4 ml of 0.3 M NaCl in TE buffer (10 mM Tris, 1 mM EDTA, adjusted to pH 7.5 with HCl). Thereafter 1 M NaCl in TE buffer was added to the sample and the mixture was brought to 0.3 M NaCl. The sample was added into the column and the column washed with 1 ml aliquots of 0.3 M NaCl in TE buffer. The DNA was eluted using 0.5M NaCl in TE and the DNA fraction was collected into 2 ml tubes. 1 ml isopropanol was added to the tube, mixed well and incubated for 2 h at -20 C. Thereafter the sample was centrifuged at 10,000 g for 30 min. The DNA pellet was washed with 70 % ethanol, air dried, and dissolved in 100 µl of sterile UPW. The suspension was stored at -20 ºC until needed

2.7.5.7 Oligonucleotide primers

Oligonucleotide primers were obtained from 1st Base company. Stock solutions were made with sterile UPW to 2.5 µM and stored at -20 ºC. The amplification of bacterial 16S rRNA genes was performed with universal primers:

- 27F (5'- AGA GTT TGA TCC TGG CTC AG-3'), fluorescently labeled with Cy5
- 907R (5'- CCG TCA ATT CMT TTG AGT TT-3').

2.7.5.8 Agarose gel electrophoresis

Agarose gel electrophoresis was used to determine size, purity and quantify of DNA extracted and PCR products. Agarose gels of 1.5 % (v/v) were prepared in Tris-acetate-EDTA (TAE; 50 mM Tris base (2-amino-2-hydroxymethyl-propane-1,3-diol); 20 mM glacial acetic acid,1 mM EDTA pH 8). Ethidium bromide stock (10 mg ml^{-1}) was added to the gel for a final concentration of 0.5 ug ml^{-1}. DNA sample buffer (1 µl; 0.1 % (v/w) bromophenol blue, 0.1% (w/v) xylene cyanol, 30% (v/v) glycerol, 5 mM EDTA and 10 mM Tris/HCl, pH 7) was added to the DNA sample, prior to loading it in the gel wells. 5 µl of 1 kB DNA ladder was applied to the agarose gel as a reference to estimate the size of the unknown DNA. Ethidium bromide at the same concentration was added to the buffer. Agarose gel (1.5 %) electrophoresis was conducted at 0.7-1 V ml^{-1}. The size and purity of the DNA and PCR products was visualised using a Vilber Lourmat imaging system and size of the DNA bands was estimated by comparison to the DNA ladder. Images of the gels were obtained.

2.7.5.9 PCR amplification of 16S rRNA gene

PCR reaction mixture (50 µl) contained 5 µl PCR buffer (10 x), 3 µl of $MgCl_{2\,(aq)}$ (25 mM), 200 µM of each deoxynucleoside triphosphate (1 µl of dNTP mix, 10 mM dATP, dTTP, dTCP, dGTP), each primer at a concentration of 0.1µM, and 0.5 U of Ex-Taq DNA

polymerase (TAKARA), and ~10 ng of template DNA. The PCR reaction was performed using a BioRad iCycler. The PCR cycling was as follows: 95°C for 3 min; 30 cycles of 95°C for 1 min, 55°C for 1 min, 72°C for 1 min; and 72°C for 10 min. PCR products purified with the QIAquick PCR Purification Kit (Qiagen) according to the manufacturer's protocol. Mung bean nuclease (NEB M0250) digestion was used to remove possible pseudo-TRFs produced during PCR. In this case, DNA (0.1 µg µl) was suspended in 1X Mung Bean Nuclease buffer. 1.0 U of the enzyme Mung Bean Nuclease was added per µg of DNA in the sample. The mixture was incubated at 30 °C for 30 min, and thereafter the enzyme was inactivated by addition of SDS to 0.01%. The DNA was recovered by ethanol precipitation, air dried and resuspended in 50 µl of MilliQ sterile water.

2.7.5.10 Terminal Restriction Fragment Length Polymorphisms

Products of three PCR products (about 50 ng) were pooled and digested with three restriction enzymes *Alu* I, *Hha* I and *Rsa* I (NEB) at their optimal temperature for 6 h according to the manufacturer's protocol. Digested products were precipitated by two volumes of cold absolute ethanol, centrifuged at 16, 000 g at 4°C for 15 min, and washed with 100 µl of 70 % of cold ethanol. After centrifugation and removal of the supernatant, the DNA pellets were dissolved in 20 µl of double-distilled water. Purified products (10 µl) were mixed with 0.125 µl of the internal size standard (MapMarker1000, BioVentures). This mixture was denatured for 2 min at 95°C, immediately chilled on ice, and subjected to electrophoresis on a CEQ 8000 Genetic Analysis System (Beckman Coulter).

2.7.5.11 Analysis of T-RFs

All T-RFs analyses were performed using Fragment Analysis in the Genetic Analysis System software package (Beckman Coulter). For each sample, peaks over a threshold of 50

fluorescence units were used and T-RFs <30 bp and >1,000 bp were excluded from the analysis to avoid detection of primers and uncertainties of size determination, respectively. To normalize this variation of sample loading, T-RFs with peak area less than 1% of total peak area of each sample were removed. The presence/absence and area of T-RFs were exported to Excel (Microsoft 2003). Because the amount of DNA loaded on the capillary could not be accurately controlled, the sum of all T-RF peak areas in a pattern (total peak area) varied among samples. To normalize this variation, the percentages of each T-RF peak area over the total peak area of each sample were calculated. The peak area analysis thresholds were set at 0.1%, 0.5%, and 1.0% of total peak area. T-RFs with areas less than the threshold value for a sample were removed from the data set. The percentage values of the remaining T-RFs were used to set up new data matrixes. The remaining T-RFs data were analyzed using Primer 5 software (Clarke & Warwick 1994). The presence/absence and area of peaks in T-RFLP patterns were analyzed by multidimensional scaling (MDS). For data of the presence or absence of peaks, the Bray-Curtis measures of similarity were used to examine the matrices (Clarke and Warwick, 1994). MDS analyses for matrices of peak areas with the threshold as 0.5% of the total area were based on Log (x+1) transformation of percentage values and Euclidean distance.

2.7.5.12 Clone library analysis

PCR products with same primers above, without Cy5 labelling, were used for clone library analysis. About 900bp bacterial 16S rRNA gene fragment was cloned into the vector with a TOPO TA Cloning Kit (Invitrogen) according to the manufacturer's instructions. The insertion of DNA fragments of the appropriate sizes was confirmed by PCR amplification with M13F and M13R primers, which corresponded to both sides of the cloning site on the vector. The 16S rRNA genes were sequenced from both ends using the primers M13F and

M13R with ABI DNA autosequencer. Phylogenetic affiliation of sequenced was determined by BLASTN program on the NCBI website (http://www.ncbi.nlm.nih.gov) and RDP. The DNA sequences obtained in this study are available from the Genbank under the accession numbers GU066397-GU066500.

The possible assignment of T-RFs revealed by T-RFLP analysis for environmental samples was performed with *in silico* digestion of clones and experimentally verified with T-RFLP analysis for each clone. A variation of 1bp was applied for the comparison between T-RF positions of community-based and clone-based T-RFLP analysis.

2.8 Metal analysis

Graphite furnace atomic absorbance spectroscopy (GF-AAS, AAnalyst™ 600 Perkin Elmer) and inductive couple plasma mass spectrometry (ICP-MS Agilent 7500ce Octopole Reaction System with a Shield Torch System) have proven to be convenient techniques for determining the total amount of metal in a sample in a rapid and precise way, with low detection limits (Tuncel *et al.* 2004). The main differences among both spectrometers is that the ICPMS is capable of detecting concentrations of many concentrations of different metals simultaneously, with a detection limit of 1 ppt, while the GF-AAS can only detect the concentration of one metal at a time with a lower detection limit (usually low 0.5-1 ppb). The GF-AAS uses absorption spectrometry to quantify the concentration of an analyte in a sample. In order to analyze a sample for its constituents it must be atomized. By adsorbing energy, the electrons in the atomizer are promoted to higher orbitals for a short amount of time, and this amount of energy is specific to a particular electron transition in a particular element, therefore the concentration of the metal in the sample can be quantified. On the other hand, the ICP-MS combines a high temperature inductive coupled plasma (argon) and a mass

spectrometry to quantify the concentration of an analyte in a sample. After the sample is introduced into the ICP torch and ionized, the ions enter the mass spectrometer and are separated by their mass-to-charge ratio determining the analyte concentration in the sample.

2.8.1 Sample preparation for metal analysis

All samples were prepared as described by Anthemidis *et al.* (2002) with minor modifications.

2.8.1.1 Liquid samples

Liquid samples of MDM or seawater (Section 2.2.2) were acidified with concentrated nitric acid (HNO_3, 70%) to a final pH value of ~1.5-1.8.

2.8.1.2 Bacterial and biofilm samples

Liquid samples containing bacteria (Section 2.7.3 & Section 2.7.4.5.1.) were acidified with concentrated HNO_3 to a final concentration of 20 % HNO_3. Non-aqueous samples, such as those containing biofilms (Section 2.7.4.5.1.5), were processed by adding 1 ml of concentrated HNO_3 (enough volume to cover the sample). Samples containing bacteria were digested under pressure in a waterbath 60 ºC in a sealed vial for a period of 7 h. Thereafter, samples were diluted with 0.25 mM citrate solution to a final pH ~ 1.6. All samples were stored at 4 ºC for less than a week before analyzing their Ag content (Section 2.9).

An AA 600 Analyst Perkin Elmer graphite furnace atomic absorption spectrometer was used to quantify total Ag content in the samples. The multi step temperature programme is summarized in table 2.2.

Table 2.2 AAS parameters used for the quantification of Ag NPs.

Step	Temp ^{o}C	Ramp Time (s)	Hold Time (s)	Internal flow
Drying Temp	800	10	20	250
Ashing Temp	1500	0	3	0
Atom. Temp	2400	1	3	250

Ag wavelength = 328.1 slit width 0.7 L.

THGA Graphitew furnace Perkin Elmer AAnalyst 600

Hollow Cathode ray tube (5UA Ag –A) B51 539

The matrix modifiers and concentrations used were: 0.005 mg Pd, 0.003 mg $Mg(NO_3)_2$

A standard curve was prepared using a silver nitrate solution (Pure AAS calibration standard Perkin Elmer 10,000 ppm, 2% HNO_3). Blanks and standard calibration solutions were also placed randomly in the AAS sampling tray during the measurements to ensure readings were accurate for the duration of the analysis. Three readings were taken for each replicate.

An inductively coupled mass spectrometer Agilent 7500ce Octopole Reaction System with a Shield Torch System was used to quantify the stock of Ag NPs (Section 2.6.1).

2.9 Microscopy

2.9.1 Transmission electron microscope

Grids were visualized using transmission electron microscopy (TEM) JEOL 1200 EX at 80 kV laser intensity. For EDX analysis of biofilms and Ag NPs, selected samples were visualized and analyzed using a TEM JEOL 7000 FEGSEM coupled to and Inca EDS at 20 kV laser intensity.

2.9.1.1 Sample preparation

2.9.1.1.1 Liquid samples

Morphology of primary particles and aggregate of Ag NPs was studied with TEM. Samples of 20 ml were ultracentrifuged into 35 ml Beckman centrifuge tubes at 20,000 rpm for 30 min at 25 °C using a Beckman Coulter Avanti J-25 (Rotor Beckman JA-20). A Formvar coated cooper grid was placed at the bottom of each centrifuge tube. After ultracentrifugation the grid was removed from the tube and carefully dried by touching its edge with a Whatman filter paper grade No. 1.

2.9.1.1.2 Biofilm

Biofilms grown on 13 mm coverslips were primarily fixed with 2.5 % glutaraldehyde in PBS solution for 3 to 24 h. A detailed protocol is described in table 2.3. In brief, thereafter the primary fixative was discarded and the coverslip was rinsed three times with PBS and stored in the same buffer at 4 ºC. A secondary fixation of the coverslips was performed with 1 % osmium tetroxide in the same buffer for 1 h. The coverslip was rinsed 3-5 times with UPW and dehydrated with a series of graded ethanol. A mixture of ethanol and resin was used to

pre-condition the biofilm for resin fixation. Biofilms were then placed in 100 % resin and later polymerized with fresh new resin. Ultrathin (60-70 nm, for good resolution) sections were cut with a diamond knife and stained with uranyl acetate and lead citrate prior visualization by TEM. Due to problems encountered with dye precipitation in the samples, a few of the samples were not stained with uranyl acetate and lead citrate for EDX samples. Also, thicker samples (>100 nm) were used for a few EDX analysis since the strength of the laser damaged thin samples.

2.9.2 Confocal Scanning Laser Microscope

Marine biofilm samples were examined with a LSM 5 PASCAL confocal laser scanning microscope (CLSM, Carl Zeiss, Jena, Germany), equipped with 543 nm helium/neon and 488 nm argon-ion lasers, and laboratory grown biofilms were examined with a Leica DMIRE2 inverted CLSM microscope equipped with the same lasers, as well as with a constant temperature chamber. Images were obtained with a 63x/1.4 N.A. Plan-Apochromat oil immersion DIC lens. The potential of CSLM for investigating microbial biofilms was first demonstrated by Lawrence *et al.* (1991). CSLM allows examination of thick biological samples in 4 dimensions (x, y, z and time) with the assessment of multiple parameters. Advantages of this technique include: visualization and quantification of fully hydrated living microbial communities of up to 100 μm thickness; noninvasive optical sectioning; visualization of section in horizontal (xy), vertical (x,z) and temporal (x,t) dimensions; application of fluorescent and non fluorescent probes; quantitative static and dynamic analysis; as well as 3-D organization of polymeric aggregates, single cells, and colonies (Bitton 2002).

2.9.2.1 Marine Biofilms - Lectin staining of extracellular polymeric substances (EPS)

EPS represents a major structural component of biofilms and they can be used to determine the biovolume of complex communities (Neu & Lawrence 1997; Neu & Lawrence 1999). To observe the changes on biofilm architecture across Ag NPs treatments (Section 2.7.5.3) tetramethyl rhodamine isothiocyanate (TRITC) labeled lectin Concanavalin A was used to stain the EPS of the biofilms developed on glass slides. It was necessary to embed the biofilm in a polyacrylamide matrix due to: 1) large amounts of organic matter deposited on the slides (organic matter is autofluorescent and contributes to a high background noise during imaging acquisition (Karl 1986); 2) the irregular thickness of the biofilm due to debris and occasional macrofouling colonisation, which if untreated would caused tilting of coverslips, and thus uneven focusing in the oil immersion. Polyacrylamide maintains the natural 3D hydrated structure of the biofilm and allows its easy manipulation. Also, the gel enabled homogenisation of the thickness of the sample to be visualized (Christensen *et al.* 1999), as well as reducing the background created by the autofluorescence from organic matter deposited in the sample. This procedure involved fixing the biofilms with a 4 % paraformaldehyde solution (200 µl l^{-1} 10 M NaOH, 40 g l^{-1} paraformaldehyde, 330 ml l^{-1} 3x PBS pH 7.2) for 1-3 h. Thereafter, biofilm were washed three times with 1 x PBS (pH 7.2), and embedded with a mixture of 20% (w/v) acrylamide monomer (200:1, acrylamide-bisacrylamide), 8 µl ml^{-1} *N,N,N',N'*- tetramethylethylenediamide (TEMED), and 20 µl ml^{-1} 1% (w/v) freshly prepared ammonium persulfate. After the gel polymerized, squared sections of 5x5 mm were cut and stained with lectin (final concentration 100 µg ml^{-1}) and also with SYTO®9, a green fluorescent nucleic acid stain. The former allowed for the EPS visualization while the latter bound to the cell DNA. Dyes were kept in the freezer at -20 ºC and were

Table 2.3 Procedure used for fixing biofilm samples for TEM visualization.

	Chemical	Temperature	Time	Repetitions
Primary fixation	2.5% glutaraldehyde in PBS buffer	4°C	3h to overnight	1
Wash	PBS buffer (pH 7.2)	4°C	10-20 minutes	3-5
Secondary fixation	1% osmium tetroxide in PBS	room temp.	1-2 hours	1
Wash	UPW	room temp.	10-20 minutes	3-5
en bloc staining	0.5% uranyl acetate	0-4°C	overnight	1
Wash after en bloc staining	distilled water	4°C	10-15 minutes	2
Dehydration	25% ethanol	Room temp.	10 minutes	1
	50% ethanol		10 minutes	1
	70-75% ethanol		10 minutes	1
	90-95% ethanol		10 minutes	1
	100% ethanol		10 minutes	2
	Transition solvent if embedding resin is not miscible with ethanol		10 minutes	2
Infiltration	1 part resin/2 parts solvent	room	15 minutes-overnight	1
	1 part resin/1 part solvent (optional)	room	15 minutes-overnight	1
	2 parts resin/1 part solvent	room	15 minutes-overnight	1
	100% resin	room	15 minutes-1 hour	1
Embedding	Place in 100% resin in suitable container			1
Degassing (optional)	Place in vacuum oven	60° C	3-30 minutes	
Polymerization		60-70° C	Overnight	

thawed before use. A volume of 3 µl of each dye was use to stain each sample. Biofilms were incubated at 25 ºC for 15-20 min in the dark (Pang *et al.* 2005) before CSLM visualization.

2.9.2.2 Bacterial viability and total biomass of laboratory grown biofilms

A LIVE/DEAD® *Bac*Light™ Bacterial Viability Kit (Invitrogen, Molecular probes) was used for monitoring the viability of the biofilm population, as well as to estimate total bacterial counts. *Bac*Light™ is composed of two nucleic acid-binding stains: SYTO®9 and propidium iodide. SYTO®9 is a membrane permeate dye that penetrates all bacterial membranes and stains the cells green. Propidium iodide can only penetrate cells with compromised cell membranes (dead cells), and the combination of both stains into these types of cells produce a red fluorescing cell (Boulos *et al.* 1999). The dyes are supplied dry and pre-measured into pairs of polyethylene transfer pipettes. Each dye was diluted with 5 ml UPW water and aliquot into 1.5 ml microtubes. Dyes were kept in the freezer at -20 ºC and thawed before use. A volume of 3 µl of each dye was use and the biofilms were incubated at 25 ºC for 15-20 min in the dark. After this time, a drop of *Bac*Light mounting oil (refractive index $_{25\,^{\circ}C}$= 1.517 ± 0.003) was added to the biofilm and a coverslip was placed on the top of it. Viable (green) and dead (red) cells were imaged simultaneously (the excitation/emission maxima for these dyes are about 480/500 nm for SYTO 9 stain and 490/635 nm for propidium iodide).

The LIVE/DEAD® *Bac*Light™ Bacterial Viability assay did not give successful results with natural marine biofilms. Marine biofilms accumulated a large amount of organic and inorganic material in their matrix, which was difficult to eliminate without affecting the structure and cellular viability of cells. Organic matter on the samples bound non-specifically

and strongly to the dyes, especially to propidium iodide, which interfere with the imaging analysis of the samples. Since for viability assays embedding into acrylamide gels was not an option due to the vulnerability of cellular viability, this assay was not applied in marine biofilms.

2.9.2.3 Image analysis

A minimum of 30 microscopic images were taken for each treatment (n=3) and controls (n=3) (Section 2.7.5.2) and were analyzed by the software Image Structure Analyzer-2 (ISA-2) developed by (Beyenal *et al.* 2004). The software was used to calculate biovolume to surface area (BVSA, $\mu m^3 \mu m^{-2}$) of live (green) and dead (red) biomass in each treatment, and thus differentiate the impact on biofilm viability of Ag NPs independently of the remaining biomass. The addition of both, live and dead BVSA gave an estimate of the total biofilm volume to surface area, thus indicating in which conditions Ag NPs were more toxic and provoked a decrease on biofilm biomass. For EPS a change on BVSA was considered to give a direct indication of the toxic effects of Ag nanoparticles. The effects of Ag nanoparticles to biofilms were analyzed using a one-way analysis of variance (ANOVA) followed by a Tukey test (SPSS Inc., Chicago IL) (Section 2.10.3 & 2.10.4) . *P* values less than 0.05 were considered statistically significant.

2.10 Statistical analysis

Data was initially analysed for the parametric assumptions of normality and equality of variances prior selection of statistical tests for sample comparisons. All data complied with the aforementioned assumptions and the following statistical test were selected for multisample hypothesis:

2.10.3 Analysis of variance (ANOVA)

A one way ANOVA was performed with the SPSS statistical software (SPSS Inc., Chicago IL). A $p<0.05$ was considered significant in all occasions.

However, and due to the large number of samples compared, if *Ho* was rejected it did not imply that all means were different from one another. Thus, in order to allocate significant differences among treatments the Tukey test was used (Zar 1999).

2.10.4 Tukey test

A Tukey test with equal sample sizes was used for multiple comparison procedure (SPSS Inc., Chicago IL). With this test different pairwise comparisons can be made to determine which treatments are significantly different from controls when *Ho* has been rejected using a one way ANOVA (Zar 1999).

3 Results & Discussion 1: Characterisation of Silver Nanoparticles

3.1 Summary

This chapter reports the physico-chemical properties of Ag NPs under different environmental conditions (Section 2.7.1): different ionic strength, pH values and presence or absence of SRHA or SRFA. The particle size, electrophoretic mobility, solubility, and aggregate morphology and size in MDM were studied (Section 2.2.2.) and compared between pH 6, 7.5 and 9 with and without the presence of 10 mg l^{-1} SRHA at 25 ºC. To determine the same parameters in a high ionic strength medium Ag NPs were dispersed in artificial seawater (Section2.2.2, Appendix 1), at a pH of 8, 4 mg l^{-1} SRFA, and 25 ºC, and salinity of 30 ‰ (conditions natural marine biofilms were exposed to Ag NPs, see Section 2.7.5.2). Results demonstrate that Ag NPs tend to aggregate in all media; however addition of HS decreases the average size of the aggregates and allows individual and dispersed particles to be present. The aqueous stability improved in MDM with increasing pH and with the presence of HS, although this stabilisation by HS did not occur with Ag NPs in seawater. Ag NPs in the latter medium remain unstable with HS although a decrease in mean aggregate size due to the presence of HS was also observed.

Ag NP solubility was minimal (< 2 %) under all pH values and in both media. This results will help understand the interaction and toxicity of Ag NPs to planktonic and biofilm bacteria, investigated in Chapters 4, 5 and 6.

3.2 X-Ray Diffraction analysis (XRD)

X-ray diffraction (XRD) (Section 2.6.2.5) performed on powder sample revealed information about the chemical composition of the nanoparticles, confirming they were made of silver, as well as their detailed crystallographic structure (Fig. 3.1). The X-ray diffraction finds the geometry of a molecule from the elastic scattering of X-rays from the inner electronic structures (Azároff *et al.* 1974), and characterises the crystallographic structure and grain size. This method is based on projecting a monochromatic X-ray beam onto the material at an angle theta. The angular positions and intensities of the resultant diffracted peaks as a result of varying the angle (*theta*) of the projected monochromatic beam (theta) result on a pattern characteristic of the samples. The peak assigned in the Ag NP sample were [111] [200] [220] [311] and [222]. Based on the principle of X-ray diffraction structural, physical and chemical information about the material investigated can be obtained. For instance, according to the Scherrer equation (this relates the peak breadth of a specific phase of a material to the mean crystallite size of that material), based on the calculation using the width of [111] the Ag NPs are about 100 ± 20 nm. According to the manufacturer's data (Section 2.6) the particle sizes were 30-50 nm.

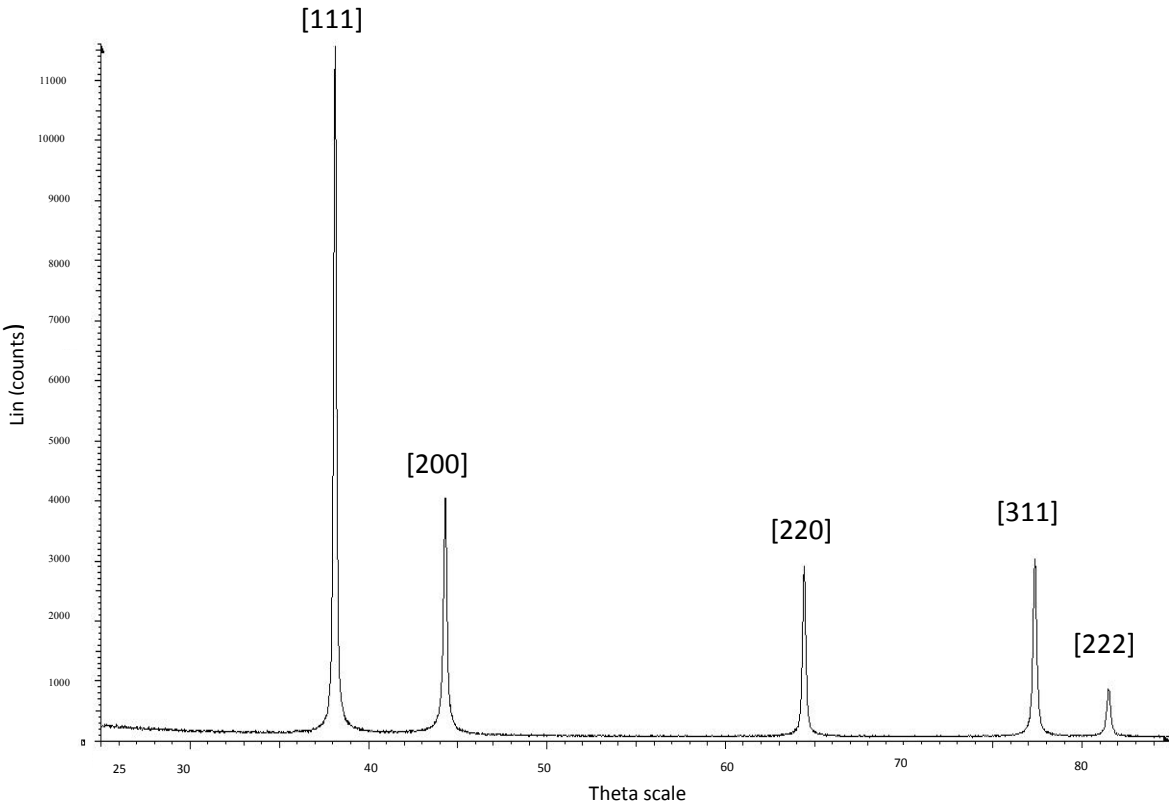

Figure 3.1 XRD pattern of the Ag NPs. The peaks are assigned to [111] [200] [220] [311] and [222]. The analysis were done by Scherrer method using a Siemens D5000 diffractometer. The results determined Ag NPs are about 100 ± 20 nm.

3.3 BET surface analysis

The average surface of the particles was 2.40 ± 0.18 $m^2 g^{-1}$. According to the manufacturer's data (Section 2.6) standardised surface area was 5-10 $m^2 g^{-1}$.

3.4 Total particle count

The total number of Ag NPs in the concentrations used for the assays was calculated by counting the number of particles in samples of 20 and 2000 ppb by TEM (Section 2.6.2.1) and they are summarised in Table 3.1. From the 20 and 2000

ppb counts, the particle concentration in 2 and 200 ppb was estimated.

Table 3.1 Total number of Ag NPs in the concentrations used in Ag NP exposure assays (average ± 1 standard deviation) (Section 2.7.1.3). Particles were counted by imaging them by TEM (Section 2.6.2.1).

Ag NP Concentration	Total number of particles	Estimated number of particles
2		6×10^7
20	$5.83 \times 10^8 \pm 3.23 \times 10^6$ ($\sim 6 \times 10^8$)	
200		6×10^9
2000	$6.35 \times 10^{10} \pm 6.91 \times 10^9$ ($\sim 6 \times 10^{10}$)	

3.5 Transmission electron microscopy

The morphology of Ag NPs primary particles and aggregates was investigated by TEM using a JEOL 1200 EX at 80 kV of laser intensity (Section 2.9). For EDX analysis selected samples were visualized and analyzed using a TEM JEOL 7000 FEGSEM coupled to and Inca EDS at 20 kV laser intensity (Section 2.6.2.1 & 2.9.1).

3.5.1 Characterisation in MDM

TEM images showed that the dominant form of Ag NPs in MDM (Section 2.6.2) is small aggregates of several hundred nanometers (Fig 3.2). The size of the aggregates did not vary significantly across pH values, although the number of aggregates observed per treatment was not sufficient to acquire enough information for statistical comparisons. The size of primary particles comprising the aggregates did not differ among pH values or presence/absence of SRHA (n=100, ANOVA, p >

0.05) and it was ca. 65 ± 30 nm diam. (mean ± std dev.). In the presence of SRHA two effects were observed by TEM. Firstly, the small Ag NP aggregates were coated and surrounded by what appeared to be SRHA, as the film was only present when HS were added (Figure 3.2). Secondly, in the presence of SRHA, the size of the aggregates was smaller, indicating that disaggregation of Ag NPs had occurred, and fully dispersed primary particles (verified by EDX analysis) were observed in the presence of SRHA only (Figure 3.3). Qualitatively, TEM images revealed that these single NPs in the presence of SRHA were large in terms of particle number, although their mass concentrations were low. Mass appeared to be dominated by small aggregates even in the presence of SRHA. The size distribution of Ag NPs in MDM is represented in Figure 3.4.

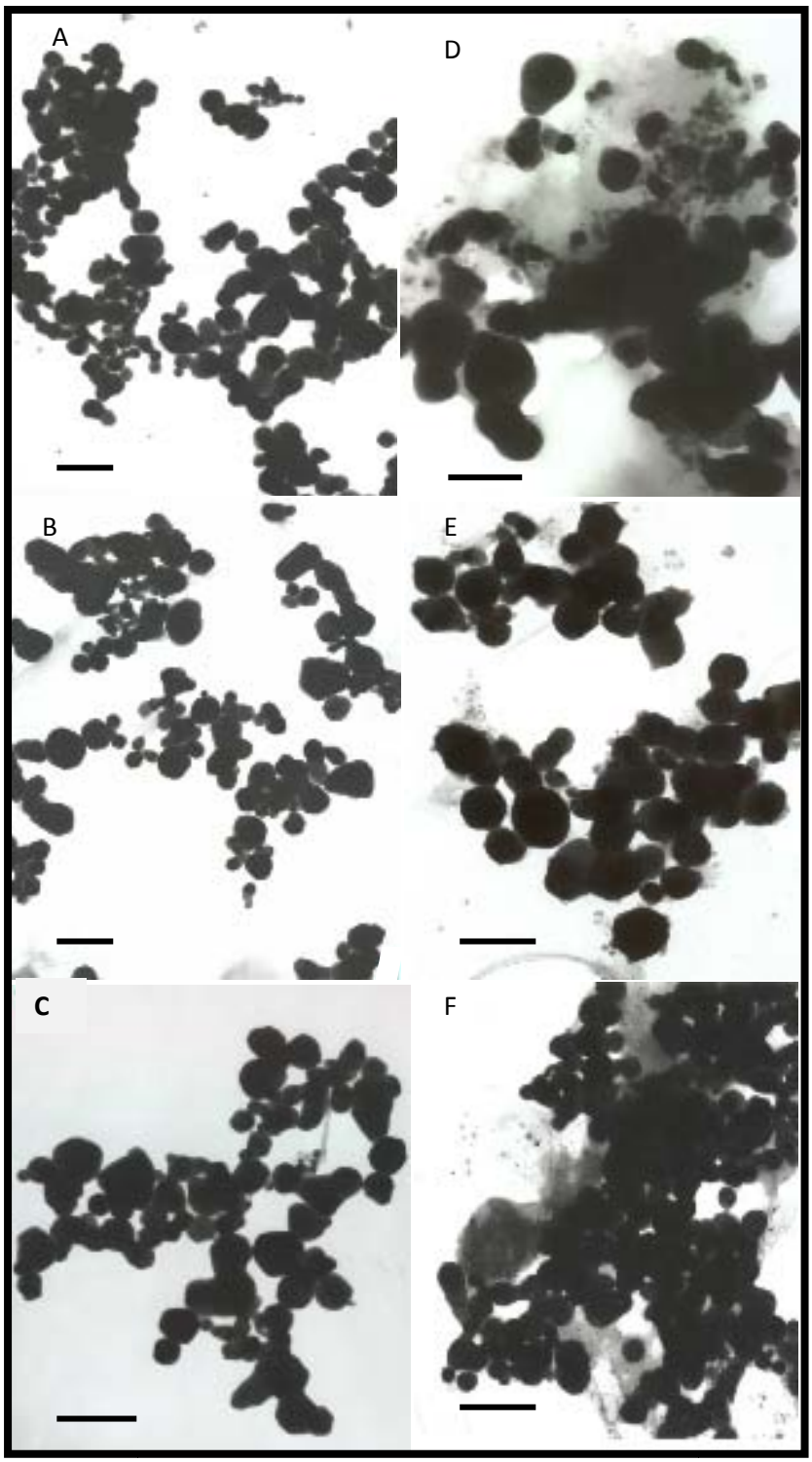

Figure 3.2. Transmission electron micrographs of Ag NPs at A) pH 6 B) pH 7.5, C) pH 9 D) pH 6 & 10 mg L^{-1} SRHA, E) pH 7.5 & 10 mg L^{-1} SRHA and F) pH 9 & 10 mg L^{-1} SRHA. Bars represent 100 nm.

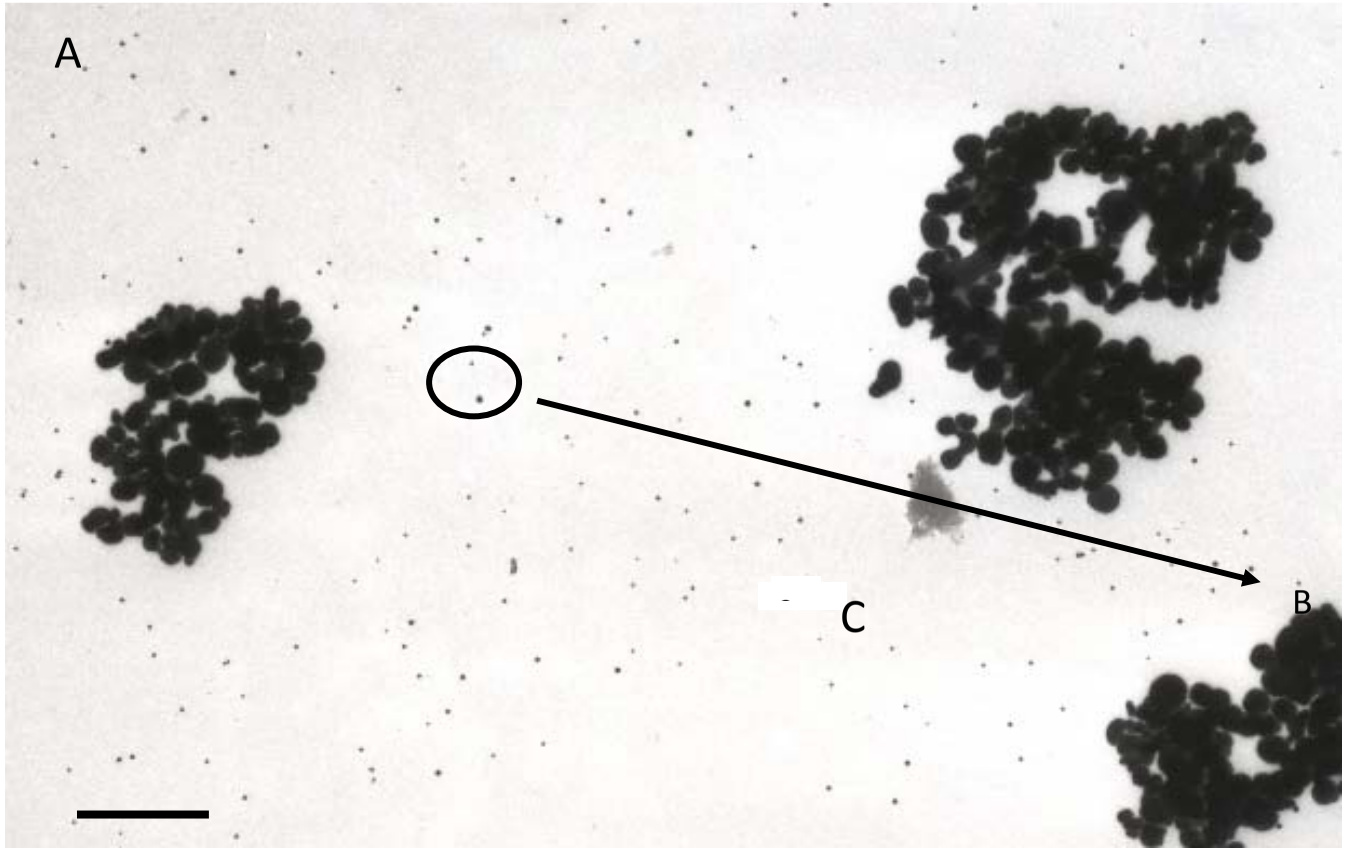

Figure 3.3. Transmission electron micrographs of Ag NPs at A) pH 7.5 with 10 mg L^{-1} SRHA. Line represents 500 nm B) Selected (circle) area for EDX analysis. Line represents 50 nm C) EDX profile of dispersed nanoparticles.

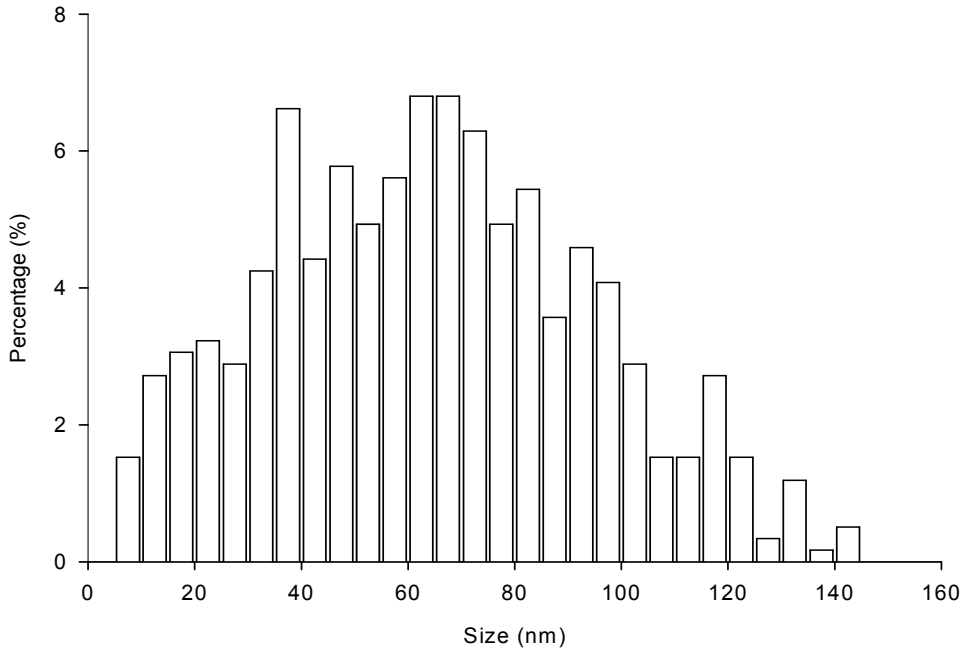

Figure 3.4. Histogram of Ag NPs size (nm) distribution (%) in MDM (Section 2.2.2).

3.5.2 Characterisation in artificial seawater

TEM imaging showed that the dominant form of Ag NPs in MDM is of aggregates of several hundred nanometers. As in MDM, addition of HS in the media increased disaggregation of NP, reducing the average aggregate size (Figure 3.5).

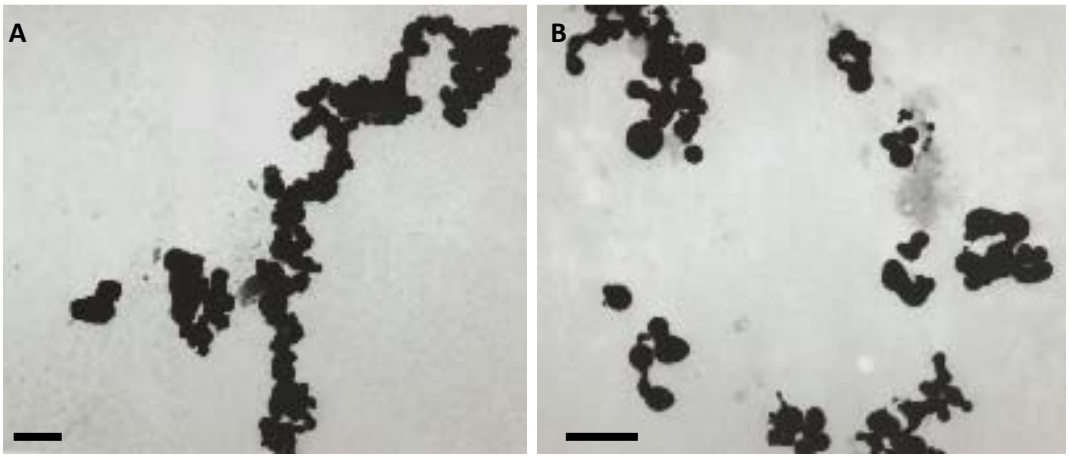

Figure 3.5. TEM images of Ag nanoparticles in seawater without (A) and with (B) 4 mg l^{-1} SRFA. Bar represents 500 nm.

3.6 Dynamic light scattering

DLS measurements (Section 2.6.2.2) are based on the percentage intensity of light scattered by particles of different sizes, and are plotted in graphs 3.6, 3.7, 3.8 and 3.9 and described in Table 3.5. Thus, the amplitude of the intensity peaks do not correlate with the number of nanoparticles at that size range since smaller particles scatter less light than larger ones. Nevertheless, the results give an indication of the overall effects pH and presence of HS has on NP aggregates.

3.6.1 Characterisation in MDM

Multimodal size distributions of Ag NPs in MDM show that the dominant form of Ag NPs is of small aggregates of a few hundred nanometers (Fig. 3.6, 3.7 and 3.8, Table 3.5), and these results are consistent with those obtained with TEM analysis. Addition of SRHA (Section 2.3) decreased the average size of the aggregates across all pH values. A summary of descriptive statistics for the Ag NP size distributions can be found in Table 3.2, however these results should be interpreted with caution, since statistics such as the mean and median and standard deviation may not be as descriptive when used on a multimodal distribution.

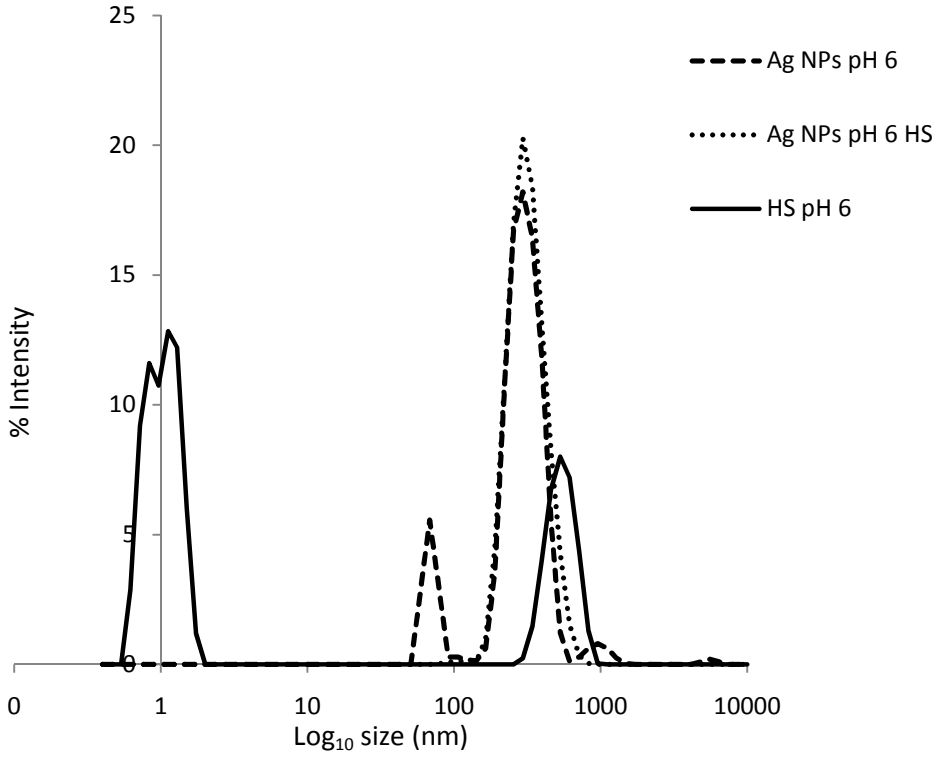

Figure 3.6 Intensity (%) distributions (n=3) of humic substances (SRHA), Ag NPs at pH 6 and at pH 6 with SRHS (pH 6 HS).

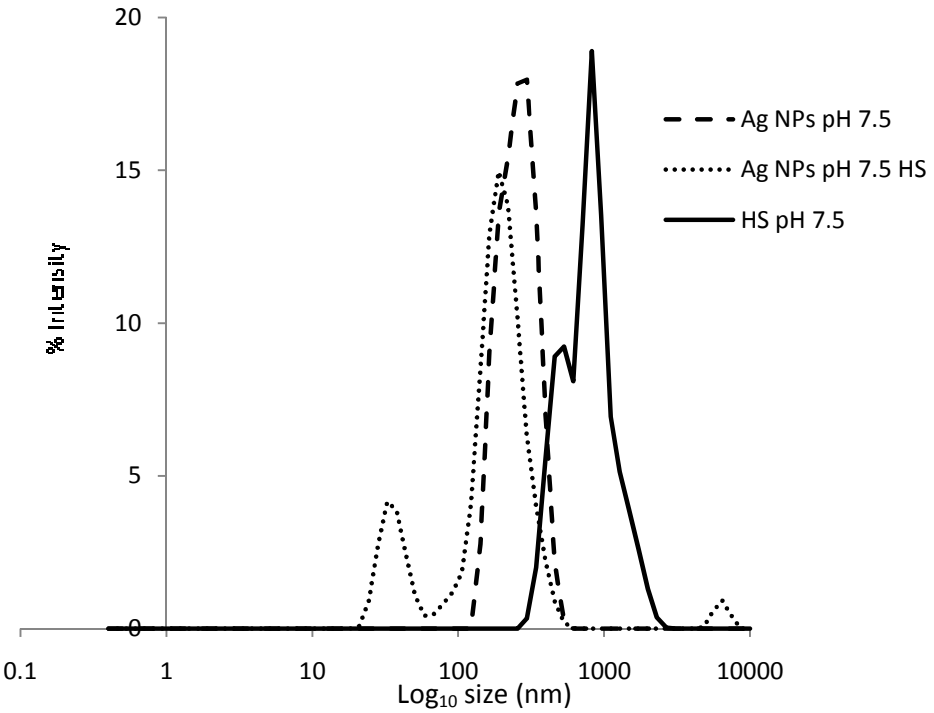

Figure 3.7 Intensity (%) distributions (n=3) of humic substances (SRHA), Ag NPs at pH 7.5 and at pH 7.5 with SRHS (pH 7.5 HS).

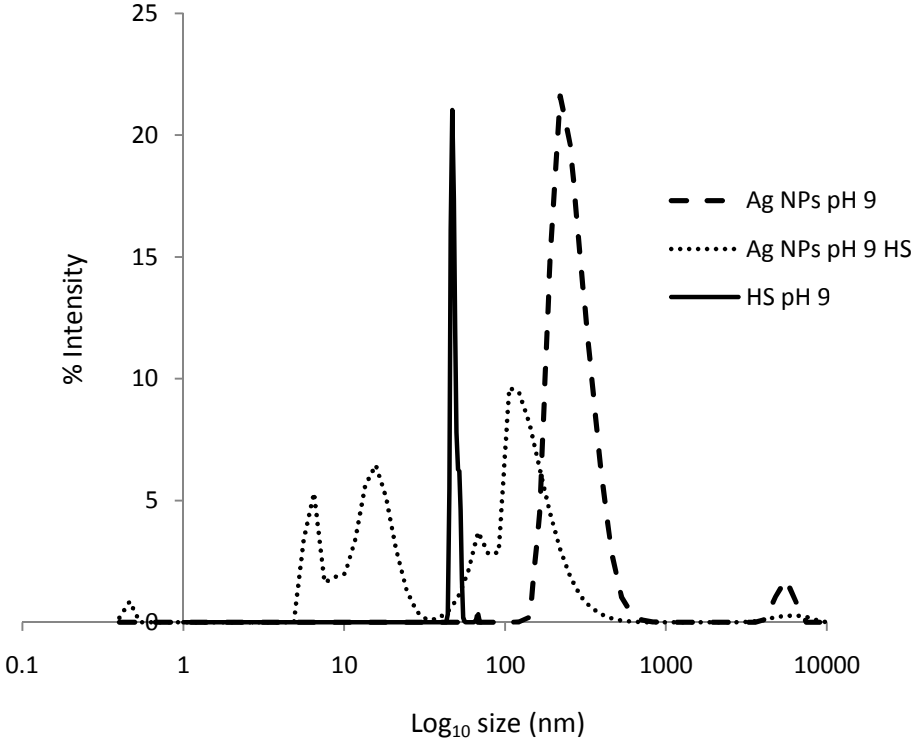

Figure 3.8 Intensity (%) distributions (n=3) of humic substances (SRHA), Ag NPs at pH 9 and at pH 9 with SRHS (pH 9 HS).

Table 3.2. Summary of descriptive statistics from DLS analysis of Ag NPs in different artificial media.

Condition	Mean±stdev (nm)		Mode (nm)		Median (nm)		Range (nm)	
	Without HS	With HS	Without HS	With HS	Without HS	With HS	Without HS	With HS
MDM pH 6	319.4±17.6	325.47±23.4	295	295	275	275	59-1480	79-825
MDM pH 7.5	263.4±18.49	262.78±12.5	295	164	237.5	153	142-531	18-6440
MDM pH9	464.17±27.11	158.9±10.1	255	106	237.5	79	122-6440	0.4-8630
Seawater	248±17.9	178.9±21.6	295	190	400	259	164-712	122-342

3.6.2 Characterisation in seawater

As is the case in MDM, DLS results showed that the dominant form of Ag NPs in artificial seawater is also small aggregates of 248±179.24 nm nanometers, and the addition of SRFA decreases the mean aggregate size to 178.9±215.9 nm (Fig.3.9, Table 3.2).

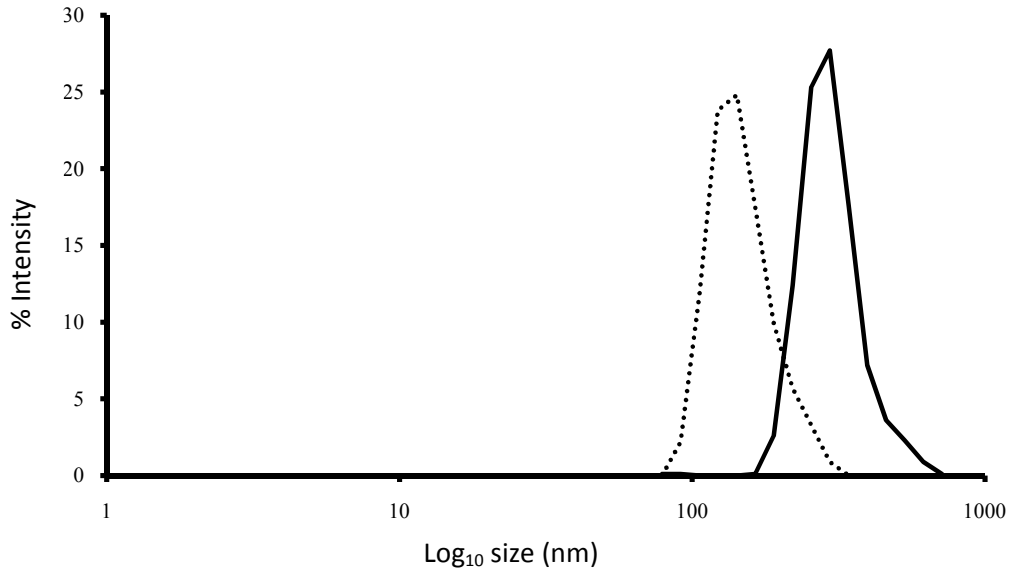

Figure 3.9 Intensity distributions (n=3) of Ag NPs at pH 8 (solid line) and at pH 8 with SRFA (dotted line). Samples were prepared in artificial seawater (Section 2.2.2) and stirred for 24 h at 25 ºC (Section 2.6.2) before analysis.

3.7 Electrophoretic mobility

3.7.1 Characterisation in MDM

Ag NPs were clearly negatively charged with electrophoretic mobilities (ζ) of ca -2 at pH 6 and ca -3.5 $cm^2 V^{-1}s^{-1}$ at pH 7.5 and 9 (Figure 3.10). In the presence of humic acids ζ was more negative and greater than -4.0 for all pH values, improving nanoparticle stability. ζ potential was in most cases > 30 mV: -23.94 ± 2.89, -53.13 ± 6.68 and -46.30 ± 4.45 mV at pH values of 6, 7.5 and 9, respectively; and -52.00 ± 1.6, -54.03 ± 4.55 and -63.96 ± 5.53 mV at pH 6, 7.5 and 9 with SRHA, respectively. This also indicates that the suspension was stable.

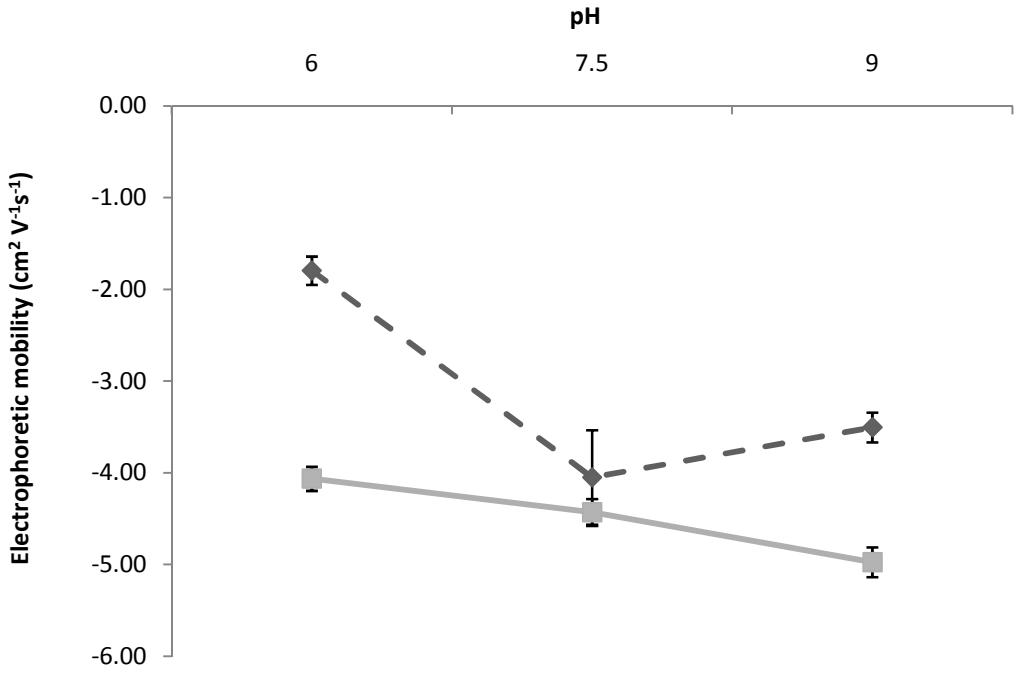

Figure 3.10 Electrophoretic mobility of Ag NPs at pH values of 6, 7.5 and 9 with (■) and without (◆) SRHA (n=3). Samples were prepared in MDM (Section 2.2.2) and stirred for 24 h at 25 ºC (Sections 2.6.2).

3.7.2 Artificial Seawater

Ag NPs were negatively charged with electrophoretic mobilities (μ) of -1.02 ± 0.67 $cm^2 V^{-1}s^{-1}$ without SRFA and -1.32 ± 0.27 $cm^2 V^{-1}s^{-1}$ with 4 mg l^{-1} of SRFA at pH 8 (Figure 3.11) In high ionic strength media particles tend to aggregate and precipitate out of solution at a higher rate than at low ionic strength solutions (Gunnars *et al.* 2002). The stability of Ag NPs did not improve when 4 mg l^{-1} SRFA were present. The ζ potential of the solutions was -13.18 ± 8.8 mV without SRFA and -18.7 ± 3.07 mV with SRFA.

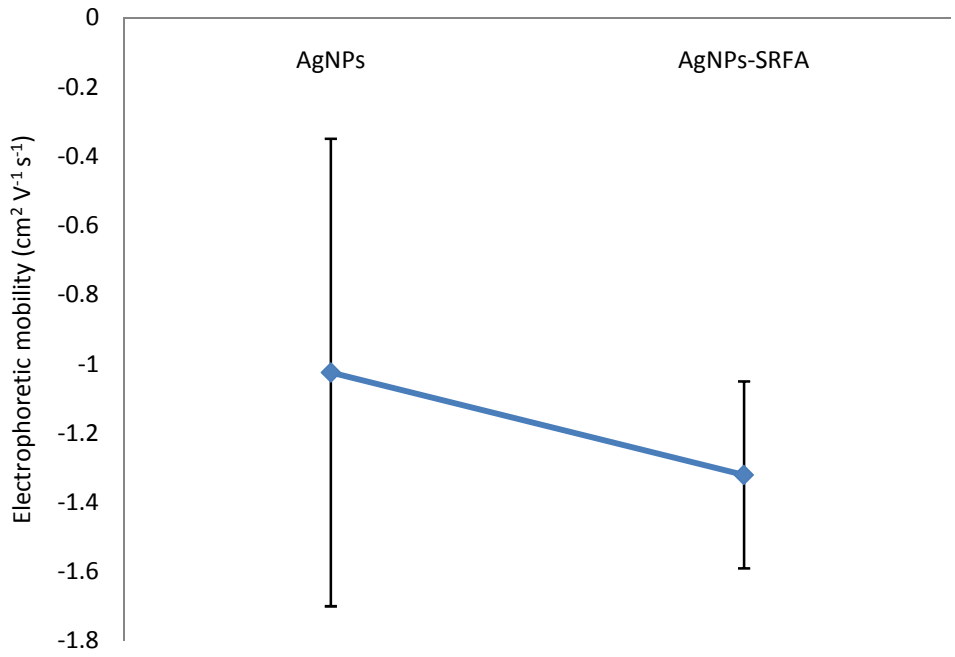

Figure 3.11 Electrophoretic mobility of Ag NPs in artificial seawater at pH 8 without SRFA (Ag NPs) and with 4 mg l^{-1} SRFA (Ag NPs-SRFA) (n=3). Samples were prepared in filtered artificial seawater (Section 3.2.2) and stirred for 24 h at 25 ºC.

3.8 Solubility

3.8.1 Solubility in MDM

The concentration of dissolved silver from Ag NPs in MDM (Section 2.2.2) without SRHA (Ag NP concentrations 20-2000 ppb) after 24 h was measured at pH 1, 6, 7.5 and 9 (Section 2.6.2.4). The results (Table 3.3) show the amount of Ag^{+} being released into solution phase was minimal (1-2 %) for all concentrations for pH values 6, 7.5 and 9; solubility increased with increasing pH at the highest NP concentration (2000 ppb from 6 ± 0.04 ppb at pH 6 to 43.2 ± 0.06 ppb at pH 9). At lower Ag NP concentrations no trends were found as measurements were close to the limits of detection. At pH 1, over 20 % of the total Ag was in the dissolved form.

TABLE 3.3. Amount (ppb) of dissolved silver (Ag^{+}_{aq}) released by silver nanoparticles in MDM, 25 °C (Section 2.6.2). At lower Ag NP concentrations no trends were found as measurement was close to the limits of detection (N/D).

	Total Ag^{+}_{aq} released (ppb)			
Ag NPs conc. (ppb)	**pH 1**	**pH 6**	**pH 7.5**	**pH 9**
2000	503.65 ±4.35 (4695nM)	6±0.04 (56nM)	18.8±2.6 (175.7±24.3nM)	43.2±0.06 (403.7±0.56nM)
200	46.11±5.80 (430nM)	3.08±0.36 (28.8nM)	N/D	3.66±0.1 (34.2±0.93nM)
20	14.31±0.2 (134nM)	0.02±0.03 (0.2nM)	N/D	N/D

3.8.2 Solubility in high ionic strength media

The concentration of dissolved silver from a suspension of 200 ppb Ag NPs in sodium nitrate solution (0-35 ‰, pH 8; Section 2.6.2.4) without SRFA was measured to estimate the amount of Ag dissolved from the Ag NPs while increasing the ionic strength of the media. The results (Table 3.4) showed that the amount of Ag^+ being released into solution phase was minimal (0.2-1.8 %) for all conditions and was not correlated to changes on ionic strength.

Table 3.4 Amount (ppb) of dissolved silver (Ag^+_{aq}) released by 200 ppb Ag NPs in a solution of varying ionic strength at pH 8 and 25 ºC (Section 3.2.2) without SRFA.

	Total Ag^+_{aq} released (ppb)
Salinity ($NaNO_3$) (‰)	**pH 8**
0	3.60±0.82 (33.64±7.66 nM)
5	0.52±0.61 (4.85±5.70nM)
10	0.45±0.33 (4.20±3.08 nM)
20	2.88±1.91 (26.91±17.85nM)
30	1.70±0.95 (15.88±8.87nM)
35	0.66±0.79 (6.16±7.38nM)

3.9 Discussion

3.9.1 Size and stability of Ag NPs

The bioavailability and further uptake of NMs by cells is strongly influenced by the size, stability, solubility and aggregation of NMs (Franklin *et al.* 2007), and these aforementioned properties depend on the media the particles are suspended in. A summary of these physico-chemical parameters is given in Table 3.5.The average

size of discrete, individual Ag NPs was reported by the manufacturers to be 30-50 nm and this was broadly in agreement with the results from TEM analysis showing primary particle size to be ca. 65 ± 30 nm (TEM, mean ± standard deviation). However, the results form XRD analysis showed primary Ag NP sizes of 100 ± 20 nm (XRD, mean ± 2 standard deviation) (Table 3.5). XRD data will measure the crystallite size rather than particle size, and since it is unknown if the Ag NPs used for this work are all made of single crystals, this could be the source of the discrepancy among results. However, the discrepancy is not statistically unreasonable taking into consideration that the mean is represented with 2 standard deviations.

Table 3.5 Summary of physico-chemical parameters of Ag NPs measured when suspended in MDM and in artificial seawater.

Measurement	Technique	Value	
Size	TEM/XRD	60±30/100±20 nm (mean ± stdev)	
Surface area	BET	2.40 ± 0.18 m^2 g^{-1} (mean ± stdev)	
Crystal structure	XRD	Peaks [100], [200], [220], [310], [222]	
Composition	EDS	Silver	
Type of media		***MDM***	***Seawater***
Stability in solution	Electrophoretic mobility	< -2 cm2 $V^{-1}s^{-1}$	ca. -1 cm2 $V^{-1}s^{-1}$
Aggregate size distribution	DLS	ca. 250 to 450 nm w/o HA and ca. 150-320 nm w/SRHA	248±17.9 nm and 178.9±21.6 nm w/HA
Solubility	Ultrafiltration	≤ 2%	≤ 2%

The primary particle sizes measured by TEM ranged from 5 to 145 nm (Fig. 3.2). No significant differences in primary particle size were found among pH values and presence of SRHA (ANOVA, $P>0.05$, $n=600$). Thus, there is a good agreement between the manufacturer's data, TEM, and XRD data, although slight discrepancies may have been due to sample polydispersity and different biases of the measurements involved. DLS size distribution results obtained in MDM showed that

pH did not significantly affect the average aggregate size of Ag NPs but the addition of 10 mg l^{-1} of SRHA in the media did lower considerably the aggregate sizes and also increased polydispersity, mostly noticeable at pH 7.5 and 9 (Fig 3.7 and 3.8). TEM micrographs also showed how HS seemed to adsorb to Ag NP surface (Fig 3.3) creating a layer surrounding the particles. However, this phenomenon was only observational and was neither measured nor quantified. Micrographs also showed that the dominant form of Ag NPs in MDM is as small aggregates of several hundred nanometers (Fig. 3.2). Only when SRHA were present disaggregation of the Ag NPs occurred and fully dispersed primary particles (verified by EDX analysis) were observed (Fig 3.3). Individual primary particles were not detected by TEM imaging without SRHA. Qualitatively, TEM images revealed that these single NPs in the presence of SRHA were large in terms of particle number, although their mass concentrations were low. Mass was dominated by small aggregates even in the presence of SRHA. The attraction/repulsion between particles is affected by the surface and so will be altered by the amount of coverage of the particle by HS and degree of charge neutralisation (Wilkinson 2005), and so it is likely that higher concentrations of HS than the ones used in this work may increase Ag NP disaggregation. However, in certain cases the presence of HS helps to destabilise NM instead, as it is in the case of FeO NPs (Baalousha *et al.* 2008).

The electrophoretic mobility (μ) is usually reported as zeta potential (ζ), but is presented here as electrophoretic mobility data because of the questionable physical meaningfulness of ζ for soft colloids such as SRHA; in soft colloids it is difficult to define the slipping plane of the particle (Duval *et al.* 2005; Diegoli *et al.* 2008). The electrophoretic mobility provides information on the electrical and hydrodynamic properties of particles (Duval *et al.* 2005), determining stability,

rheological behaviour and sedimentation (Alarcon-Waess & Mendez-Alcaraz 2008). The results show that in MDM Ag NPs were clearly negatively charged and in the presence of HS they were more negative and close or greater than -4.0 cm^2 V^{-1} s^{-1} for all pH values. The decrease in μ reported here indicates humic acid absorption on the Ag NPs and consequent NP dispersion, as has been shown for other NPs (Baalousha *et al.* Submitted) and for colloids and macroscopic surfaces since the 1970s (Lead *et al.* 2005).

The results from TEM, DLS and ζ potentials data indicate that in freshwater systems SRHA are major components changing Ag NP stability, size of aggregates, and charge when present in the media. Similar results were observed in a higher ionic strength media. In the artificial seawater Ag NPs were also negatively charged, although the solution was not stable, and the addition of SRFA did not increase significantly the stability of the particles in solution due the higher salinity. Hence, although HS decreased aggregate size of Ag NPs in seawater, the polydispersity and high tendency of aggregation are clear from the ζ potential results. Neihof and Loeb (1972) demonstrated that most particles in natural seawater carry an electronegative surface charge. Any material (even positively charged material) in contact with seawater becomes negatively charged by adsorption of organic matter. This organic matter creates a film surrounding the particles, masking the intrinsic properties of the underlying particles and dominating their surface properties (Wilkinson 2006) affecting behaviour and fate. Dispersed HS aggregate at high $CaCl_2$ concentrations by intermolecular bridging via Ca^{2+} complexation to form humic substances aggregates. These aggregates then bridge to NPs which accelerate the growth of the aggregates (Wilkinson 2005; Chen & Elimelech 2007).

Studies done with ferric oxides and HS in brackish water and seawater show

that when aggregation occurs it happens within minutes (Gunnars *et al.* 2002). Van der Waals forces of attraction exceed repulsive forces among HS coated particles and results with the contraction of the electrical double layer as well as a decrease in the net surface charge by seawater cations binding to functional HS groups (Boyle *et al.* 1977; Stolpe & Hassellov 2007). Since aggregation of NMs in seawater is a rapid phenomenon, the sample preparation time here of 24 h should have been appropriate to detect total aggregate formation. Certain nanoparticles are stabilized when HS are present (CNTs, Hyung *et al.* 2007), but also high concentrations of $CaCl_2$ are known to destabilize fullerenes (Chen & Elimelech 2007) and FeO NPs (Tipping & Higgins 1982).

Nevertheless, more recent studies have shown that salt induces aggregation of colloids and particles larger than 3 nm diam., but does not affect colloids and particles of 0.5-3 nm diameter (Stolpe & Hassellov 2007). This could be the reason HS (<3 nm) in seawater increased Ag NP disaggregation. HS may have remained in suspension and helped the disaggregation of large Ag NPs aggregates, as observed in Fig 3.9. However, this phenomenon was not further investigated.

3.9.2 Solubility of Ag NPs

The concentration of dissolved Ag from Ag NPs in MDM without SRHA after 24 h was low (< 2 %) for pH values 6 to 9 (Table 3.3). At pH 1, more than 20 % of the Ag NP dissolved but this pH is not relevant to the bacterial exposures. With an increasing ionic strength solution (sodium nitrate series dilutions, Table 3.4), the amount of Ag dissolved from the NPs was almost negligible and lower than 2 % in all cases. Overall, the results suggest that Ag NPs are not very soluble in the media (MDM and seawater) used in the assays. However, the solution did not reach an equilibrium state and longer sample preparation times (~ 50 h) should be considered

in the future. Franklin et al (2007) studied the solubility of ZnO nanoparticles by dialysis and the equilibrium was reached at ~ 45-50 h. For insoluble nanoparticles, such as Ag, dissolution experiments over the time frame of weeks and months are more suitable for determining persistence in waters and toxicity to natural communities (Franklin *et al.* 2007). Other authors also suggest that the interaction of particles with NOM and organisms can also increase particle solubility (Navarro *et al.* 2008a), which should be taken into consideration when investigating the effects of NMs to organisms, due to the well documented toxicity of Ag ions. This work did not quantify the solubility in the presence of SRHA, since the technique chosen to estimate solubility could bias the results due to the possibility of loss of SRHA attached Ag through the membrane.

Investigating solubility of Ag NPs is crucial since dissolved silver ions are highly toxic to a broad range of microorganisms. Ag ions bind to cell walls causing the production of reactive oxygen species that deactivate vital enzymes, and eventually lead to cell death (Choi & Hu 2008a). When identifying the toxicity of Ag NPs it is necessary to differentiate between the toxicity exerted by the particle itself (surface, charge and/or shape) from the toxicity of the soluble fraction of the particle (due to release of Ag ions). Derfus *et al*. (2004) showed how the release of free Cd from CdSe quantum dots, rather than the particle itself was responsible for the observed cytotoxicity to eukaryote cells; and Brunner et al. (2004) compared the cytotoxic effects of soluble and insoluble metal oxide nanoparticles, with results suggesting that the harmful effect of soluble oxide nanoparticles (ZnO and FeO) could be attributed purely to the release of toxic ions, whereas the toxicity observed from insoluble metal oxide nanoparticles (CeO_2 and TiO_2) could not only be explained solely by the release of ions, hence indicating a nanoparticle specific

cytotoxicity mechanism.

From the results obtained in this study, the presence of HS and ionic strength appear to be the parameters that mainly influenced the physico-chemical properties of the Ag NPs in the media used. The size and properties of the NMs establishes their residence time in suspension. As with colloids, small and stable nanoparticles will be suspended in the water column and can be transported long distances. However, coagulation and flocculation will facilitate the aggregation and precipitation of those large enough to sediment (Lead & Wilkinson 2006a; Klaine *et al.* 2008).

4 Results and Discussion 2 : Impact of silver nanoparticles on planktonic *Pseudomonas fluorescens*: effect of pH, concentration and organic matter

The bacterial growth data in this chapter were collected by the MSc student Shona R. Fawcett under my direct supervision. This work is included here for completeness and because of my extensive involvement in supervision and data collection. Results from Chapters 3 and 4 have been accepted for publication by Environmental Science and Technology (Appendix 2).

4.1 Summary

The effect of well characterised Ag NPs (see Chapter 3) on planktonic *Pseudomonas fluorescens SBW 25* was studied (Section 2.7.3) after a 3h and 24h exposure, under different conditions involving a range of Ag NP concentrations (0, 2, 20, 200 and 2000 ppb, Section 2.7.1.3), pH values of 6, 7.5 and 9 (Section 2.7.1.4), and presence or absence of 10 mg l^{-1} of SRHA (Section 2.7.1.2). To discriminate between the effects of Ag NPs from their soluble metal form and from the potential particle-size specific toxicity, silver nitrate (positive control) and latex NPs (negative control, Section 2.4) were used to determine their effects on growth under the same experimental conditions and sampling times. The growth of biomass was quantified by measuring optical density (Section 2.7.2.1.1).

The bactericidal effects of Ag nitrate were evident after 3 h of exposure in all samples at concentrations as low as 200 ppb, and only at the highest dose of 2000 ppb after 24 h. At both sampling times the presence of SRHA did not affect the bactericidal properties of Ag nitrate. However, Ag NPs were toxic only at the highest dose in the absence of SRHA and at pH 9 only. Under these conditions Ag NPs are

quite insoluble, and the soluble fraction of (<2 %, ca. 45 ppb, Chapter 3) was not sufficient to cause a toxic effect to the planktonic *P. fluorescens*, as determined by the exposure to Ag nitrate. Therefore the observed toxic effect of the Ag NPs could not be caused only by the dissolved Ag fraction from the Ag NPs, indicating that the cause of toxicity is related to the NP itself and its interactions with the bacteria. Also, the difference in response with and without humics suggests a particle specific effect and indicates the protective effect of HS on Ag NP toxicity

4.2 Growth of *Pseudomonas fluorescens* at different pH values

Preliminary studies of *P. fluorescens* growth in MDM (Section 2.2.2) under different pH values (Section 2.7.1.4) and SRHA (Section 2.3) showed that the conditions chosen were suitable for bacterial growth, suggesting this microorganisms to be a good laboratory model for studying the effects of Ag NPs over a 24 h exposure. Figure 4.1 and Figure 4.2 show the growth curves of *P. fluorescens* over time without and with 10 mg l^{-1} SRHA, respectively. At a pH of 6 and 7.5 optimal bacterial growth was achieved compared to pH 9. The lag phase, or period of acclimation to the media before exponential growth, was also longer for pH 9.

Buffers could not be added to the media because high phosphate concentrations have proven to increase particle aggregation and precipitation (Lyon *et al.* 2005). However, with the low buffering capacity of the MDM, variation in pH can occur. For this reason the pH variation of the cultures was also investigated.

4.2.1 SRHA

Presence of SRHA increased the growth of the microorganisms by 20-30 % in MDM independently of the pH value (Fig 4.1 and Fig 4.2). This indicates that *P. fluorescens* is able to utilise HS as a source of carbon when added in the media.

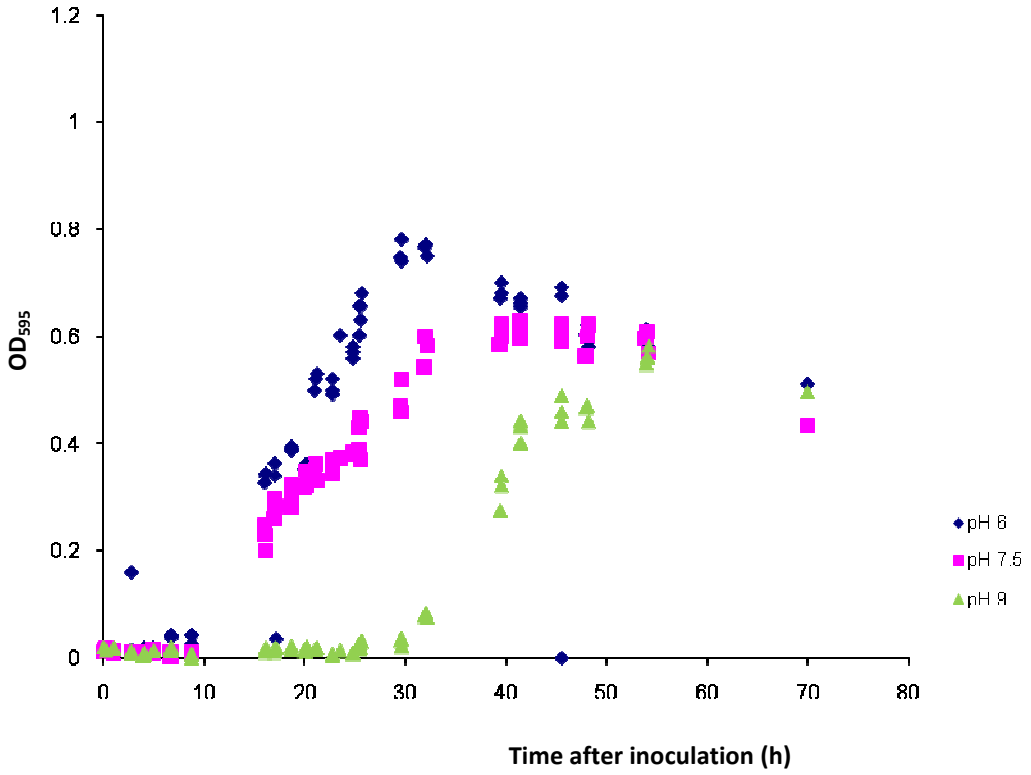

Figure 4.1. Growth curve of *Pseudomonas fluorescens* SBW 25 (Section 2.2) in sterile MDM (Section 2.2.2) under different pH values at 25 °C (N=3). Growth was monitored by measuring optical density at 595 nm (OD_{595}). Samples were diluted as required to ensure that measurements were within the linear range of calibration.

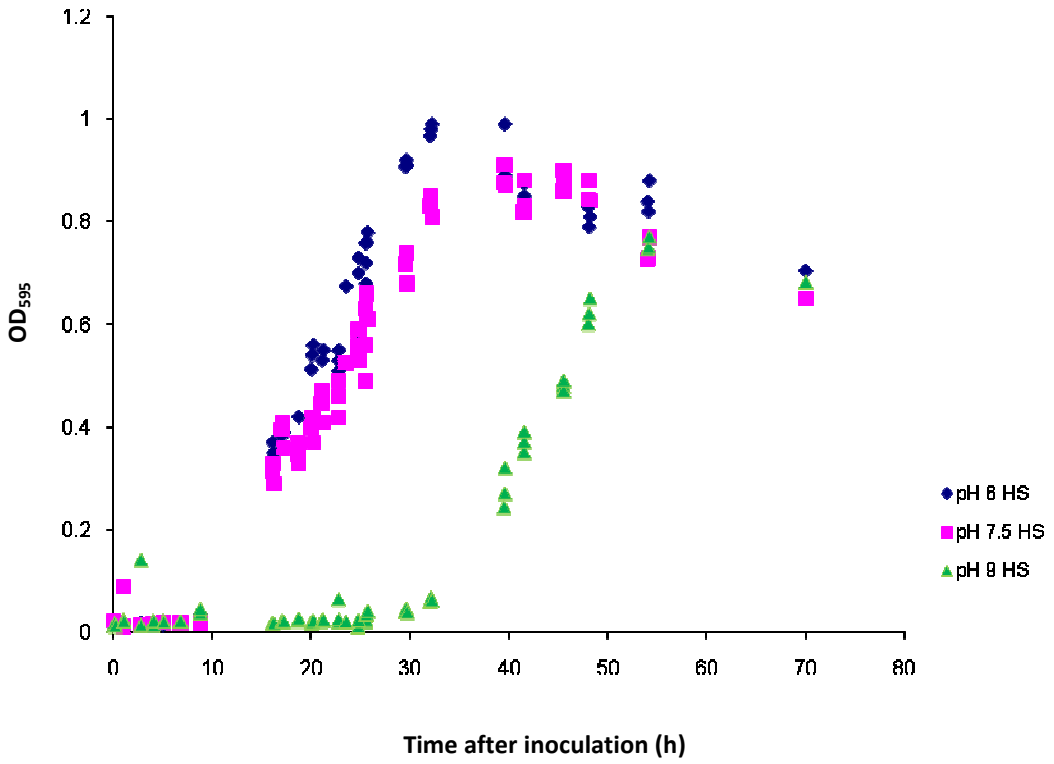

Figure 4.2. Growth curve of *Pseudomonas fluorescens* SBW 25 (Section 2.2) in sterile MDM (Section 2.2.2) and with 10 mg l^{-1}SRHA (Section 2.3) under different pH values and 25 °C (N=3). Growth was monitored by measuring optical density at 595 nm (OD_{595}). Samples were diluted as required to ensure that measurements were within the linear range of calibration.

4.2.2 pH

Figure 4.3 shows the variation in pH (Section 2.2.3) from bacterial cultures with a low initial bacterial density (OD_{595}=0.1; same initial concentration of cells as used for planktonic assays with Ag NPs) for over a week (180h). Results show that the changes in pH over 24 h of an initial bacterial culture of a density of OD_{595}=0.1 were minimal; the low initial concentrations of bacterial solution (Section 2.7.3.1) decreased the chance of sharp pH variations due to production of bacterial exudates

and waste. Therefore, MDM is a suitable medium for the exposure assays when the initial concentration of bacteria used is low.

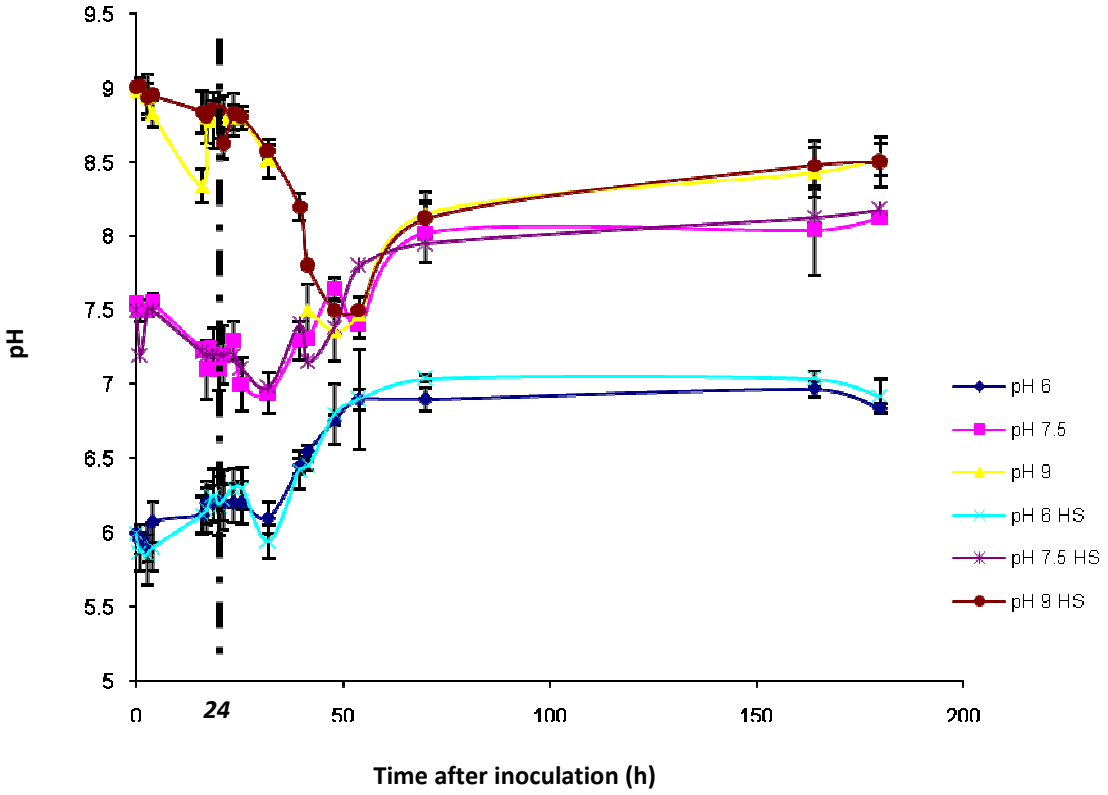

Figure 4.3. pH variation of a *Pseudomonas fluorescens* SBW 25 (Section 2.2) culture grown in sterile MDM (Section 2.2.2) with and without 10 mg l^{-1}SRHA (Section 2.3) under different pH values and at 25 °C (N=3). The initial concentration of the bacterial solution was OD_{595}=0.1. Bars are 1 standard deviation.

4.3 Bactericidal effect of Ag NPs

P. fluorescens was grown in MDM with Ag NPs, Ag nitrate (positive control) or latex nanoparticles (negative control) added at varying concentrations (2, 20, 200,and 2000 ppb in all cases), and in MDM media alone, with and without

SHRA at pH values of 6, 7.5 and 9 for 24 h at 25 ^{o}C. MDM not inoculated with bacteria, but amended with Ag NPs, Ag nitrate or latex particles were also incubated. Cultures were sampled at 3 h and 24 h.

The potential background absorbances at 595nm of Ag NPs, latex NPs and Ag nitrate MDM solutions with and without SRHA were quantified and were negligible (OD_{595} < 0.002) (Section 2.7.2.1.1). These absorbances remained unchanged under all conditions and sampling times.

4.3.1 3 hour exposure

4.3.1.1 Silver nitrate

The bactericidal effects of Ag nitrate were evident at concentrations as low as 200 ppb at pH 6 (ANOVA, $p<0.01$), 7.5 and 9 (ANOVA, $p<0.05$) decreasing the population density by 60 ± 2.1 % at pH 6, 19.1 ± 2.5 % at pH 7.5 and 29.9 ± 4.9 % at pH 9, independently of the presence of SRHA (Fig 4.4). At 2000 ppb the toxic effect was higher in most conditions, decreasing the population density by 48.2 ± 3.2 %, 44.2 ± 0.81 % and 64.15 ± 1.04 % at pH 6, 7.5 and 9 respectively, and by 61.2 ± 1.88 %, 64.9 ± 1.1 % and 49.0 ± 3.1 % at the same pH values and with SRHA. Concentrations of 2 and 20 ppb did not show a significant toxic effect under any treatment condition (ANOVA, $p>0.05$).

4.3.1.2 Silver nanoparticles

Ag NPs were only toxic at pH 9 without SRHA (ANOVA, $p<0.01$) at the highest concentration of 2000 ppb. Under this condition Ag NPs caused a 49.7 ± 3.4

% decrease in the population density (Fig 4.4). There was no significant effect on growth at any other concentration and/or pH value (ANOVA, $p>0.05$).

4.3.1.3 Latex nanoparticles

A significant detrimental effect on growth from latex NPs was not observed under any pH or concentration (ANOVA, $p>0.05$). In fact, a slight increase in growth at high concentrations of latex NPs was observed at pH 7.5 and 9 (ANOVA, $p<0.5$); this was more pronounced with SRHA (ANOVA, $p<0.5$) (Fig 4.4).

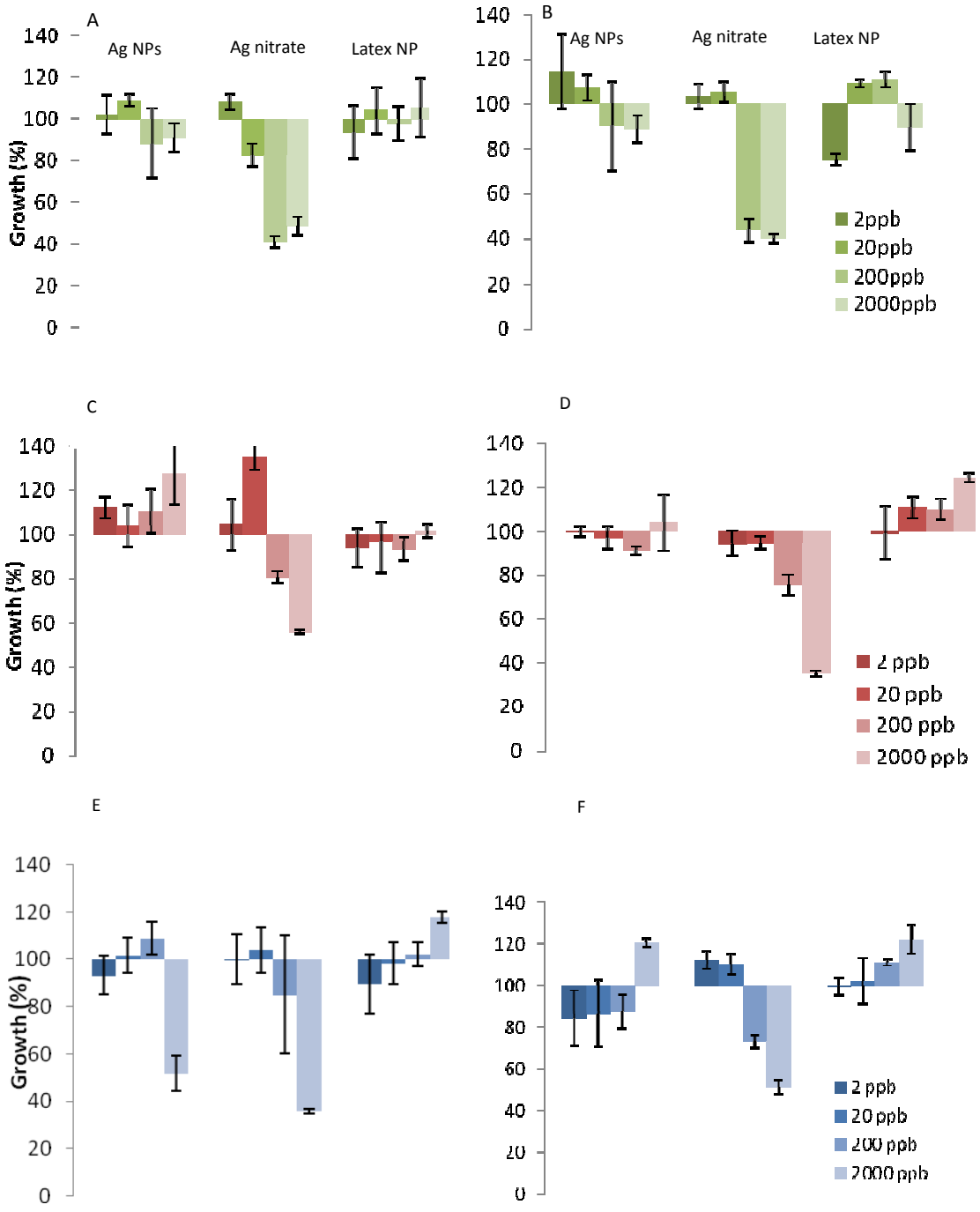

Figure 4.4. Percentage decrease on growth from control treatments of planktonic *P. fluorescens* cultures 3 h after exposure to silver nitrate (Ag nitrate), Ag NPs and latex NP at A) pH 6, B) pH 6 with 10 mg l^{-1} SRHA, C) pH 7.5 D) pH 7.5 with 10 mg l^{-1} SRHA, E) pH 9, F) pH 9 with 10 mg l^{-1} SRHA. N=3. Bars are 1 standard deviation.

4.3.2 24 hours after exposure

4.3.2.1 Silver nitrate

Only a concentration of 2000 ppb was harmful for *P. fluorescens* causing a significant reduction in biomass. Exposure resulted in a decrease in biomass of ~ 90% under all pH values, with and without SRHA (ANOVA, $p<0.01$) (Fig. 4.5). Contrary to the results obtained for exposure after 3 hours (Section 4.3.1), lower concentrations of 200 ppb did not have a significant toxic effect (Fig. 4.5, ANOVA, $p>0.05$).

4.3.2.2 Silver nanoparticles

Ag NPs affected the bacterial population only at pH 9 without SRHA at the highest concentration of 2000 ppb, causing a decrease in biomass of 89.9 ± 2.2 % (ANOVA, $p<0.01$; Fig 4.5). All other conditions did not result in any significant detrimental effect on growth (ANOVA, $p>0.05$). TEM images show the Ag NPs interaction with bacterial cells (Fig. 4.6).

4.3.2.2 Latex nanoparticles

Latex NPs showed a significant toxic effect at pH 6 and 7.5 without SRHA (ANOVA, $p<0.05$), decreasing the population density by 12-19 % and by 25-30 %, respectively. The effect was not concentration specific since the lowest concentration of 2 ppb already show a toxic effect similar to the one of quantified in bacteria exposed to 2000 ppb of latex NPs (Fig 4.5).

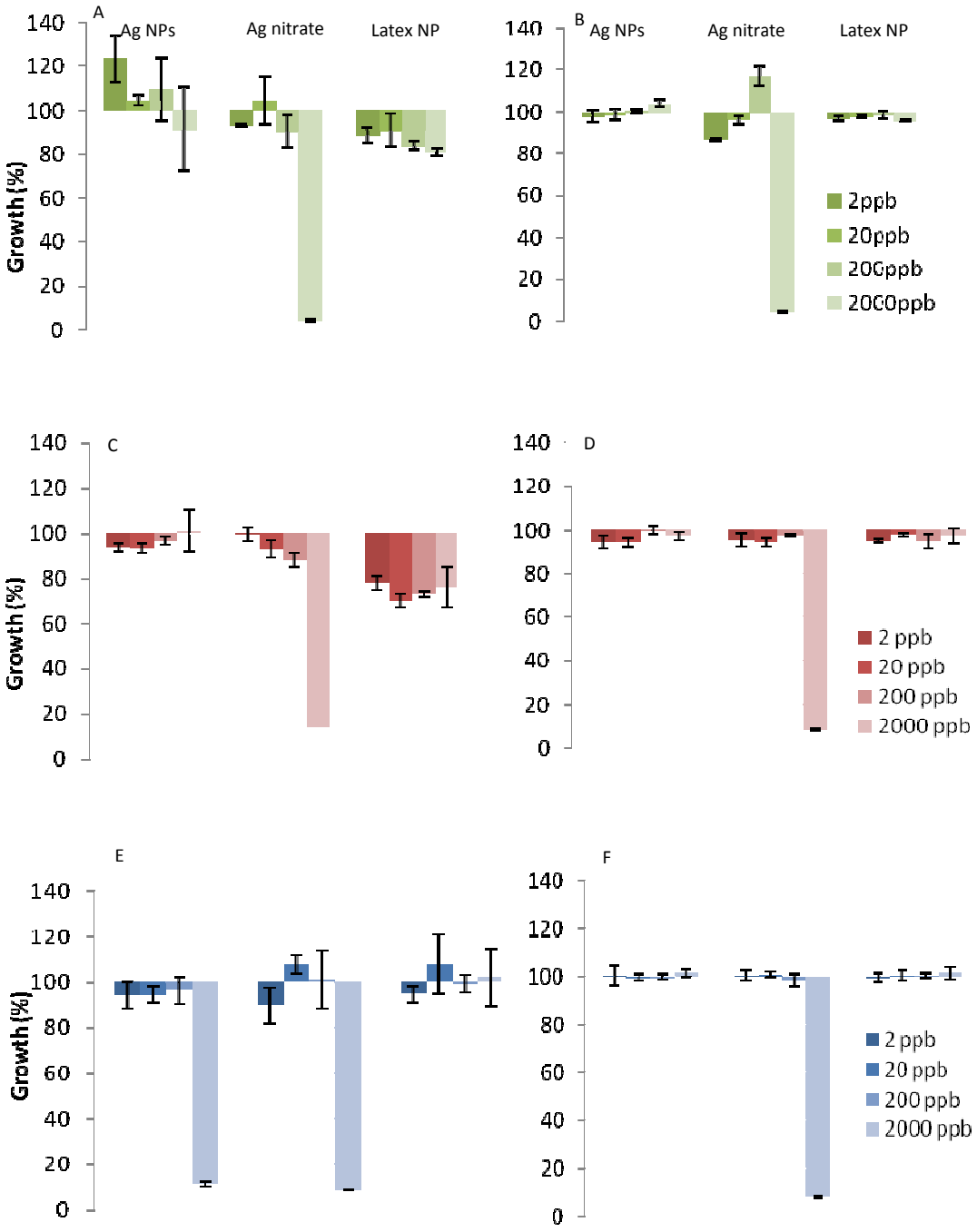

Figure 4.5. Percentage decrease on growth from control treatments of planktonic *P. fluorescens* cultures 24 h after exposure to silver nitrate (Ag nitrate), Ag NPs and latex NP at A) pH 6, B) pH 6 with 10 mg l^{-1} SRHA, C) pH 7.5 D) pH 7.5 with 10 mg l^{-1} SRHA, E) pH 9, F) pH 9 with 10 mg l^{-1} SRHA. N=3. Bars are 1 standard deviation.

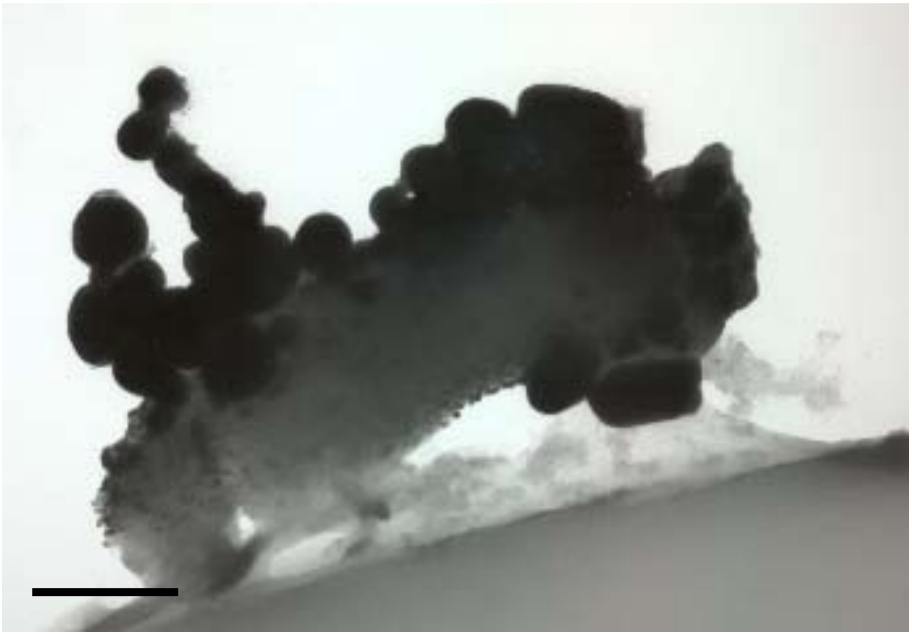

Figure 4.6. TEM micrograph of *Pseudomonas fluorescens* interaction with Ag NPs. Bar represents 200 nm.

4.4 Discussion

4.4.1 Bacterial growth and pH variations in MDM

The growth of *P. fluorescens* in MDM at different pH values was investigated. *P. fluorescens* showed a comparable growth curve at pH values of 6, 7.5 and 9, with slightly different lag phases and biomass concentrations (Fig 4.1). Also, the biomass concentration in MDM increased when SRHA were present, indicating that the bacterium can use HS as a carbon source. During the toxicity assays, when cultures were exposed to Ag NPs, Ag nitrate or latex NP, the maximum bacterial concentration detected was found to be comparable with the concentrations observed here at the late logarithmic phase and never reached the biomass concentrations of the stationary phase of the media.

The compromise between using a culture media with appropriate buffering capacity and a media that due to the high concentrations in salts would increase the aggregation and precipitation rates of Ag NPs was attained using MDM (Section 2.2.2). Previous studies assessing at the toxicity of nanotubes have also used MDM as bacterial media due to the benefits of its lower phosphate content reducing NP precipitation (Lyon *et al.* 2005; Lyon *et al.* 2006; Lyon *et al.* 2008c). The changes in the pH of the MDM during incubations were monitored (Fig. 4.3) and were found to be minimal. Therefore, this confirmed that MDM is a suitable medium for 24 h exposure assays of Ag NPs using the model organism *P. fluorescens* when the initial concentration of bacteria used is low.

4.4.2 Toxicity of Ag nitrate

Ag nitrate, the positive control used in the exposure assays, is a known bactericide (Schreurs & Rosenberg 1982; Gupta & Silver 1998; Ratte 1999; Silver 2003; Hwang *et al.* 2007), and a decrease in the population density of *P. fluorescens* was expected after exposure to low concentrations.

The bactericidal effect of Ag nitrate was evident after 3 h of exposure at all pH values at concentrations as low as 200 ppb (ANOVA, $p<0.05$). In addition, the presence of SRHA did not modify the bactericidal effect of Ag in this case, unlike in other NM studies (e.g. fullerenes *Li et al.* 2008 a). SRHA and $AgNO_3$ were added to the bacterial media at the same time, and Ag ions and SRHA were not mixed beforehand and were not at equilibrium prior to addition to the cultures. If $AgNO_3$ and SRHA would have been equilibrated in advance, a decrease in toxicity may have been observed (Glover *et al.* 2005). Although this procedure may not be ideal for metal speciation studies this was adequate in order to discriminate between NP and

metal ion toxicity. In effect, we exploited but did not measure the differences between ratios of the kinetics of SRHA and Ag NP interaction and biological interactions compared to the same ratios for the dissolved ions.

After 24 h of exposure, only 2000 ppb of Ag nitrate caused a significant toxic effect, for all pH values and conditions. This shows that at this concentration, dissolved Ag is highly toxic; although some of the concentrations used are high, the exposure was also short (24 h) and this resulted in an almost complete cell death. At 2000 ppb the *P. fluorescens* population did not recover from the early exposure, whilst at the lower concentration of 200 ppb, the population could recover. The presence of SRHA did not affect the bactericidal properties of Ag nitrate at 2000 ppb consistent with the 3 h exposure; suggesting that any binding of Ag by the SHRA had no effect on toxicity.

Prior to research on Ag NPs, toxicity of silver was thought to occur mainly on aqueous phase and depend on the concentration of free Ag^+ ions (Hogstrand *et al.* 1996, Wood *et al.* 2002). Ionic silver disrupts enzymes by interacting with their thiol groups, affects DNA replication, and modifies membrane structure and the electron transport chain (Trevors 1987; Morones *et al.* 2005). The behaviour, availability, and toxicity of dissolved metals is also strongly influenced by particulate organic, and inorganic material (Mittelman M.W. 1985; Ferris *et al.* 1989; Kaschl *et al.* 2002; Kola *et al.* 2004; Plaza *et al.* 2006), as well as for the chemical form the metal species is present. Thus binding to organic molecules and other reactants reduces the concentration of the ionized Ag, and therefore its bioavailability and toxicity (Ratte 1999). Sparse data are available on dissolved Ag binding to SRHA and in many previous studies silver has been reported to bind to HS sites and decrease the Ag bioavailability. These and other binding characteristics of silver and HS have been

previously studied by Sikora *et al*. (1988), VanGenderen *et al.*(2003), and Kramer *et al.* (2007).

In this work the presence of HS did not affect the toxicity of silver under any condition and sampling time (due to non-equilibration of Ag-SRHA prior to bacterial exposure and this helped us to discriminate between the toxicity of different Ag forms). The limited binding by HS under these conditions, or that the HS-Ag complex is still sufficiently labile to be taken up by the bacteria are possible reasons for the observed lack of reduce toxicity when HS are present.

Production of EPS and cell exudates by *P. fluorescens* could also lower silver ion toxicity; however the implications of exudates production was not investigated in this work. EPS plays an important role in the biosorption of heavy metals through chelation by EPS functional groups such as carboxyl, phosphoric, amine, and hydroxyl groups. EPS formation is highly affected by environmental parameters such as pH and presence of heavy metals; and as a response mechanism the production increases as metal content in the surrounding media also increases (Kocberber Kilic & Donmez 2008). For the above reasons, EPS production and binding with Ag ions could also have been the cause of reduced silver bioavailability and negligible effect on growth in all treatments, except at the highest concentration.

4.4.3 Toxicity of silver nanoparticles

Ag NPs were toxic only at a concentration of 2000 ppb, at pH 9 without SRHA. Under these conditions, (pH 9, without SRHA, 2000 ppb) the soluble fraction of the Ag NPs was only ~ 2% (43.3 ± 0.06 ppb; Chapter 4, Section 3.8.1) in the absence of bacteria and SRHA. This amount of soluble Ag is considerably lower

than the concentration of Ag nitrate (200 or 2000 ppb, depending on exposure time) required to causing a similar decrease in bacterial cell density. Therefore the observed toxic effect of the Ag NPs could not be caused by the dissolved Ag from the Ag NPs. The cause of toxicity is related to the NP itself and its interactions with the bacteria. The toxicity of Ag NPs under any condition and sampling time was negligible when SRHA were present in the media, and the growth of the population was unaffected.

TEM images (Chapter 3, Section 3.5.1) suggest that Ag NPs tend to disaggregate with SRHA present, and give a high concentration of very small NPs. Therefore, presence of SRHA would be expected to increase toxicity, since many authors have previously suggested that NP toxicity relates to able to penetrate the cell and disrupt the cellular machinery (Sondi & Salopek-Sondi 2004; Morones *et al.* 2005; Pal *et al.* 2007; Choi *et al.* 2008). However, the results in this study (Fig 4.4 C and Fig 4.6 C) indicate that although the presence of SRHA decreased the size of the NP aggregates, leading to smaller aggregates and even single NPs, they also decreased their toxicity. Most likely, toxicity was mitigated due to the sorption of SRHA onto the NP surface and consequent changes in surface properties of the particle, as described in detailed in Chapter 3 and consistent with other work (Li et al 2008a, Mahendra *et al.* 2008). Previous studies suggest that the toxic effects of Ag NPs are caused by their interaction and uptake by bacteria (Sondi & Salopek-Sondi 2004; Morones *et al.* 2005; Shrivastava *et al.* 2007). Ag NPs can create 'pits' on cell membranes that lead to cell disruption and death (Sondi & Salopek-Sondi 2004). This study shows that the intrinsic properties of the Ag NPs are responsible for toxicity. The HS may simply be providing a physical barrier between the cell and NP. In addition, the change on the surface charge of the Ag NPs once coated will

also affect their interaction with the bacterial cell. More sophisticated mechanisms may be involved, and further experiments are required to confirm whether this reduced effect on bacterial cell growth occurs over longer time periods. If the decrease is related to the physical barrier or coating provided by the SRHA, it could happen that after longer exposure times the microorganisms could degrade the coating and directly interact with the particle again.

4.4.4 Toxicity of latex nanoparticles

Latex nanoparticles (Section 2.4) were used as a negative control. Latex NPs were found to have a small but significant negative effect on bacterial growth after 24 h, at pH 6 and 7.5 when SRHA were not present; indicating some limited intrinsic toxicity of the nanoparticle even when made of non-toxic materials. Determining the reasons of such toxicity was above the scope of this work, and therefore it has not been investigated nor will be discussed. However, for future studies latex NPs should not be used as size-specific negative controls since they showed some effect on bacterial biomass at certain pH values. Most likely this is caused by an intrinsic size based toxicity, as the starting materials have a low toxicity. Instead bulk Ag particles (>100 nm) may be an appropriate treatment for investigating particle effects.

The mechanism of toxicity of Ag NPs at pH 9 was not investigated. However, the observed bactericidal effect of Ag NPs at this pH suggests the importance of appropriate guidelines for the handling and disposal of Ag NPs to prevent their release to the environment and any impact to microbial communities. These results have proven that Ag NPs are toxic under certain environmental

conditions, and that the toxicity is mainly caused by the Ag particle and not due to its soluble fraction. SRHA show a protective effect after a short exposure (up to 24 h), but neither the bactericidal mechanism of the particle nor the protective mechanism from the SRHA have not been investigated in this work.

The expected high release of Ag NPs in the environment from Ag containing products is expected to be of ca. 30 tonnes per annum (Mueller & Nowack 2008). Ag NPs will end up in the environment and may affect the performance or effectiveness of natural bacterial communities of microorganisms (i.e. sewage sludge bacterial community or nutrient cycling bacteria in the soil). Since bacteria prevail as biofilms the following chapters investigate the interaction and effects of Ag NPs to laboratory grown single species biofilm (Chapter 5) as well as to a natural marine biofilm community (Chapter 6).

5 Results and Discussion 3: Silver Nanoparticles in Biofilms

Results from Chapters 5 have been published at Environmental Science and Technology (Appendix 2).

5.1 Summary

The effect of Ag NPs to biofilm growth and cell viability, as well as their interaction with the bacteria was investigated in laboratory grown *Pseudomonas putida* biofilms (Section 2.7.4) at pH 6 and 7.5. The effects of fulvic substances (10 mg l^{-1} SRFA Section 2.3) were also examined. Biofilms were grown for 3 days in flow cells (Section 2.7.4.1; 25 ºC and flow rate of 0.1 ml min^{-1}) before being exposed to different concentrations of Ag NPs (0, 20, 200 and 2000 ppb; Section 2.7.1.3) for 24 h at the same temperature and flow rate. Variations in biovolume to surface area (BVSA), cellular viability, metal uptake in biofilms and metal concentrations along the biofilm reactor were measured. The results suggest that pH and presence/absence of SRFA did not affect significantly the growth of control (Ag NPs unexposed) biofilms. However SRFA had an effect on the Ag NPs and on their interaction with bacterial cells.

Biofilms exposed to Ag NPs suspensions at pH 6 showed the highest susceptibility to Ag NPs, with concentrations as low as 20 ppb decreasing their biovolume to surface area (BVSA) (ANOVA, $p< 0.05$). At pH 7.5 a minimum concentration of 200 ppb was required to see a similar thinning effect (ANOVA, $p < 0.05$). Surprisingly, the decrease on biovolume was not concentration dependent. A larger amount of Ag NPs did not lead to increased thinning of attached biofilm cells. This could be the result of a particle 'saturation' in the biofilm as well as a thinning mechanism based on the friction and consequent detachment of cells due to the flow

of aggregates of 100-300 nm over biofilms of cells 10 times larger. Also, the viability of cells in the biofilm was not significantly different among pH values and conditions tested. However the higher pH is closer to optimal growth conditions and perhaps the biofilms were better able to remove uptake NPs or prevent uptake.

5.2 Interaction of Ag NPs with *P. putida* cells

Biofilms were grown for 3-d in flow though cells (Section 2.7.4.2) at pH 6 or pH 7.5 before being exposed for 24 h to different concentration of Ag NPs ranging from 20-2000 ppb or no Ag NPs (control) with and without SRFA (Section 2.7.1.3). When biofilms were exposed to Ag NP suspensions without any SRFA, the Ag NPs could not be visualised or detected in the biofilm either by TEM or EDX mapping (Fig 5.1, Section 2.9.1). However, when SRFA were mixed with the NP solution before exposure to biofilms (Section 2.7.4.3) aggregates were detected within the biofilm at both pH values (Fig 5.1), and appeared to be more abundant as the concentration of particles increased, but again only in the presence of SRFA; in their absence no Ag NPs could be imaged. In Figure 5.1, three representative TEM micrographs from a biofilm exposed to Ag NPs without (B), and with (C) SRFA illustrate the effect SRFA had on retaining Ag NPs within the biofilm matrix. The aggregates observed were relatively large (~ 0.5 μm in total), and strongly interacted with the bacterial cell surface (Fig 5.1-C, and Fig 5.2). Indeed, intimate interactions with SRFA and EPS were apparent, such as apparent invagination of the cell wall and membrane (Fig 5.2). The presence of nanoparticles was confirmed by elemental mapping analysis using the X- ray energy dispersive spectrometer (EDS) in the TEM (Fig. 5.3) (Section 2.9.1). Dark dots resembling Ag NPs were seen in the cytoplasm

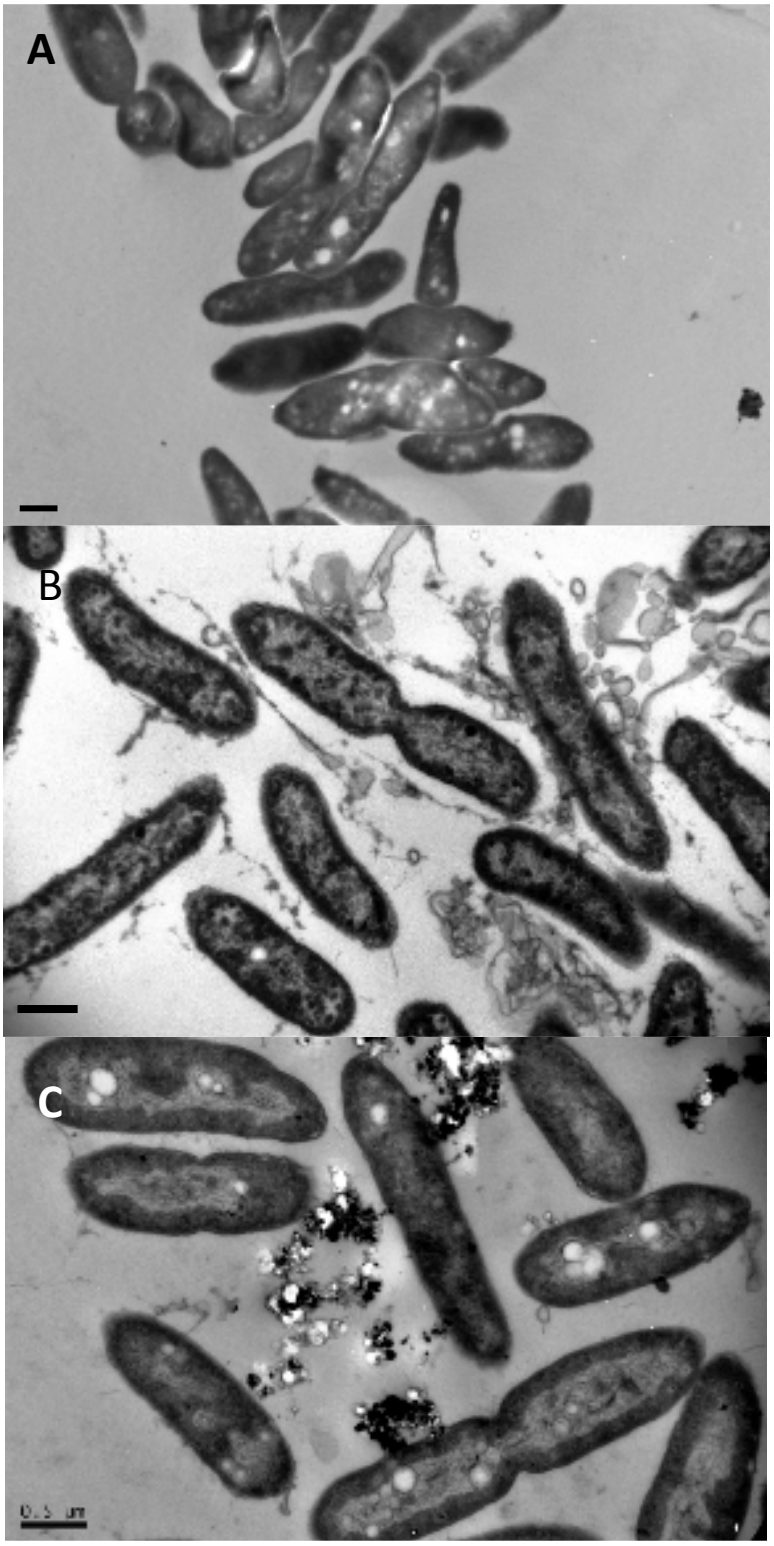

Figure 5.1 TEM micrographs of a 4-d old *P.putida* biofilm at pH 7.5 A) not exposed to Ag NPs; B) exposed to 2000 ppb Ag NPs, and C) exposed to 2000 ppb Ag NPs with 10 mg l^{-1} SRFA. A central region of lower lectron density is noticeable in these biofilms in contact with Ag NPs. Bar represents 500 nm.

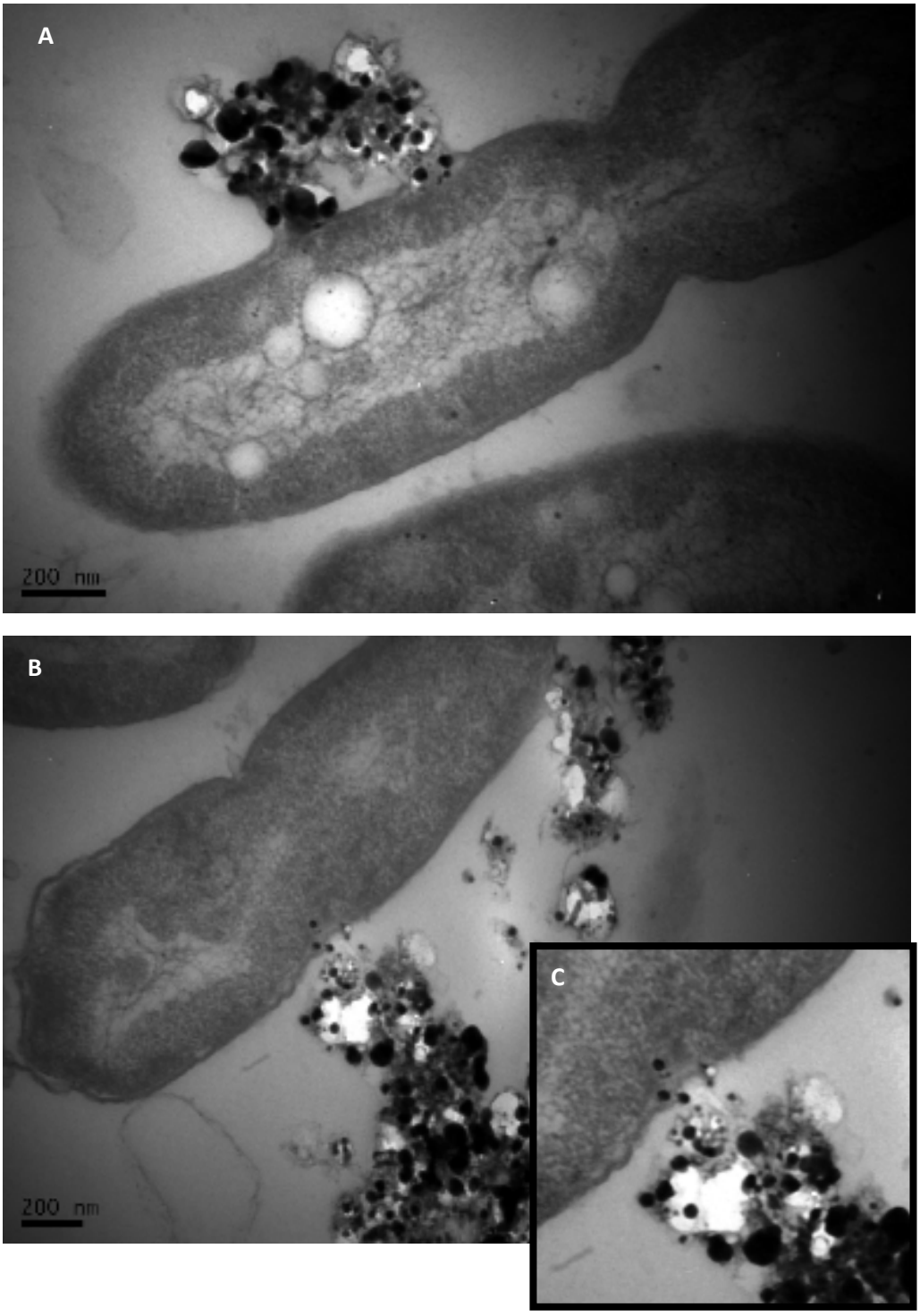

Figure 5.2 TEM micrographs of A) *P.putida* biofilm cell interacting with aggregates of Ag NPs at pH 7.5 with 10 mg l^{-1} SRFA; and B) potential uptake of Ag NPs by the cell. C) is a close up of the uptake/interaction from B. Bar represents 200 nm.

in most samples. In the majority of these cases, analysis by EDX confirmed that the particles were precipitates from the stains used during the TEM sample preparation

(Figure 5.4; Section 2.9.1.1). In some occasions their metal composition was found to be Ag (Fig. 5.3). In a small number of images NPs were detected which had penetrated the cell wall (Fig 5.2), but could not be detected in the cytoplasm. When Ag NPs interacted with bacterial cells (Fig. 5.1 and Fig. 5.2) the cells were found to have regions of considerably lower electron density compared to the controls.

5.3 Effect of Ag NPs to *P. putida* biofilm biovolume to surface area

Figure 5.5 and Figure 5.6 show the effect on the biovolume to surface area (BVSA), of different concentration of Ag NPs, and presence/absence of SRFA to *P. putida* biofilms at pH 6 and 7.5, respectively. The pH and presence/absence of SRFA did not have a significant effect on the BVSA of the control biofilms (not exposed to Ag NPs, Table 5.1).

Effects of Ag NPs were noticeable at concentrations as low as 20 ppb at pH 6, and 200 ppb at pH 7.5, without SRFA (Figure 5.5-A and Fig. 5.6-B, ANOVA $p < 0.05$). This bactericidal effect was determined by the decrease on BVSA of ca. 8 % for all these concentrations. However, regardless of the pH value, when the solution of Ag NPs was mixed with 10 mg l^{-1} of SRFA (Section 2.7.4.3), the toxicity of Ag NPs was mitigated as seen by the unchanged biovolume to surface area (BVSA) compared to the control, at increasing concentrations of exposure (Fig 5.5-B and Fig. 5.6-B; ANOVA, $p<0.05$).

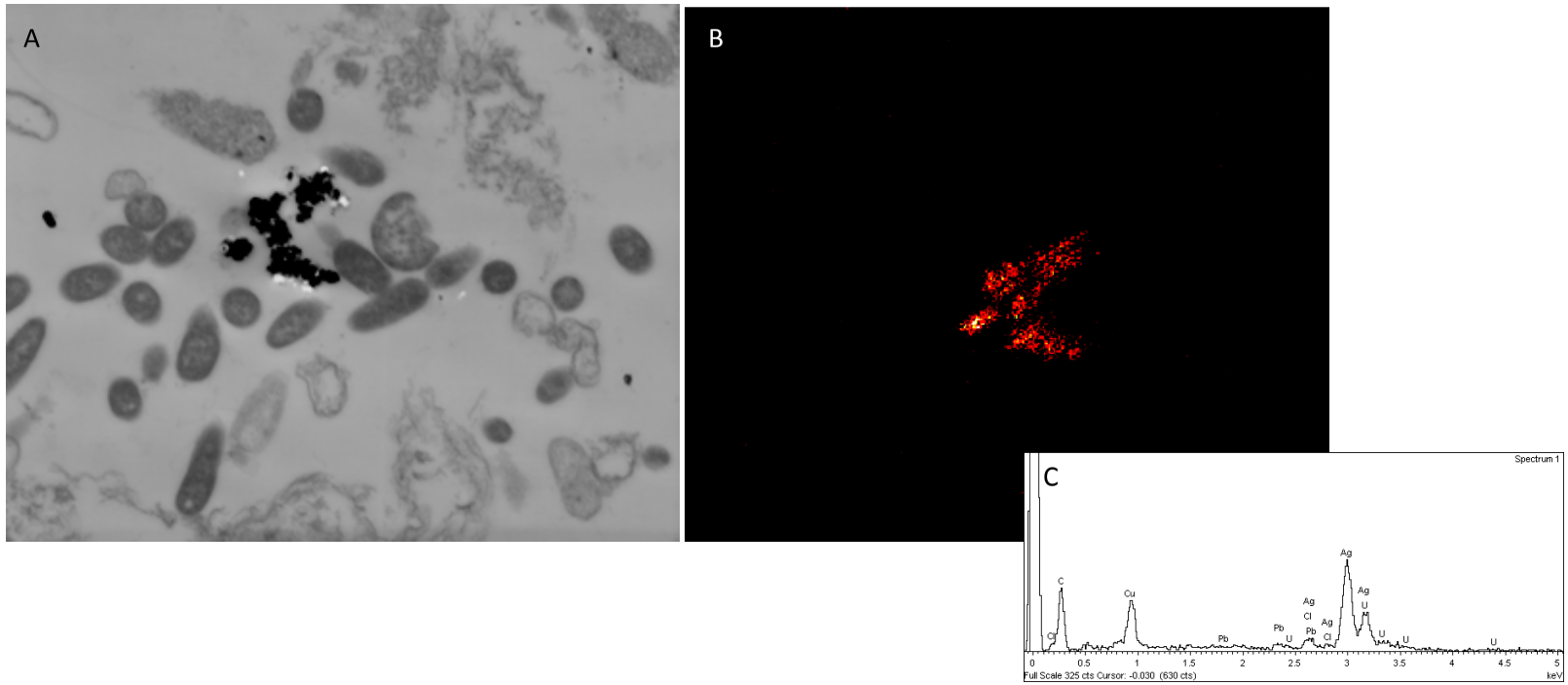

Figure 5.3 A) TEM micrograph of a *P. putida* biofilm at pH 6 with SRFA and 200 ppb Ag NPs; and B) EDX mapping of Ag in the biofilm A. C) EDX spectrum of B.

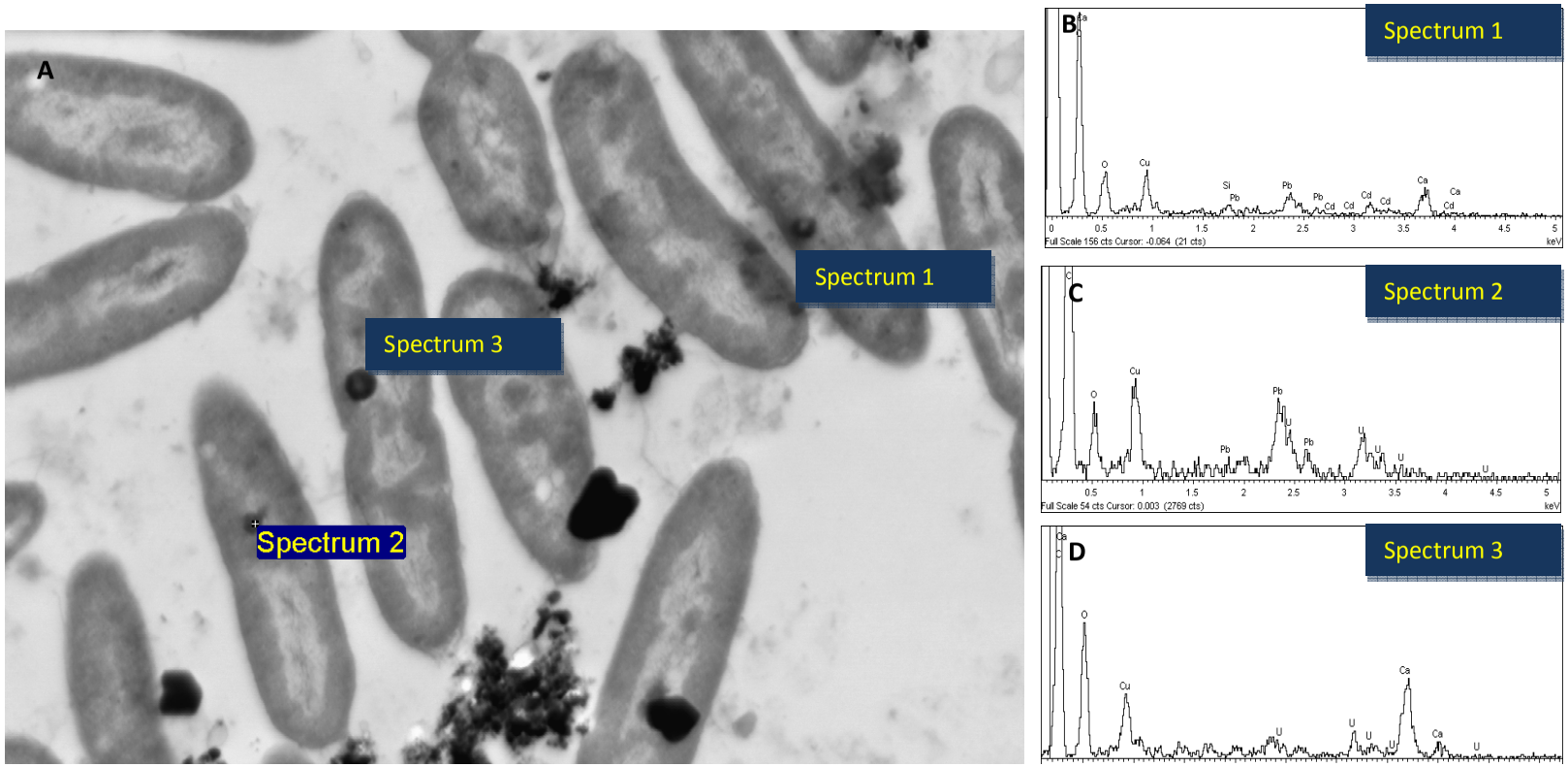

Figure 5.4 A) TEM micrograph of *P. putida* biofilm at pH 6 with 2000 ppb Ag NPs; and B-D) EDX spectra of selected potential nanoparticles within the cells.

Table 5.1 Biovolume ($\mu m^3\ \mu m^{-2}$) of 4-d old biofilm not exposed to Ag NPs (CONTROLS) grown in MDM at pH values of 6 and 7.5 with and without 10 mg l^{-1} SRFA.

	SRFA (mg l^{-1})			
	0	10	0	10
pH	6		7.5	
Biovolume ($\mu m^3\ \mu m^{-2}$)	1.01 ± 0.012	1.02 ± 0.07	1.01 ± 0.02	0.99 ± 0.05

Biofilms are subjected to a turnover of cells that provokes a constant cell detachment during growth and establishment (O'Toole et al. 2000, Busscher and van der Mei 2000). Fig. 5.7 and 5.8 show the amount of bacterial cells that sloughed off with exposure to different concentrations of Ag NPs (Section 2.7.4.5.1 & Section 2.7.4.5.2) at pH 6 and 7.5, respectively. The effect of the Ag NPs on the biofilm varied over time of exposure, pH, concentration and presence of HS. The highest effect, defined by a larger number of cells being detached, was seen during initial exposure to NPs (0-4 h) and was concentration dependent when HS were not present in the media.

5.4 Ag NP uptake by biofilms

The Ag uptake by biofilms was quantified as described in Section 2.8. Figures 5.5 and 5.6, and Table 5.2 show the uptake of Ag NPs by biofilms under different conditions (Section 2.7.4.2). The mass of Ag NPs biofilms were exposed to over 24 h was of 2.28, 22.8 and 228 µg for the 20, 200 and 2000 ppb solutions calculated by:

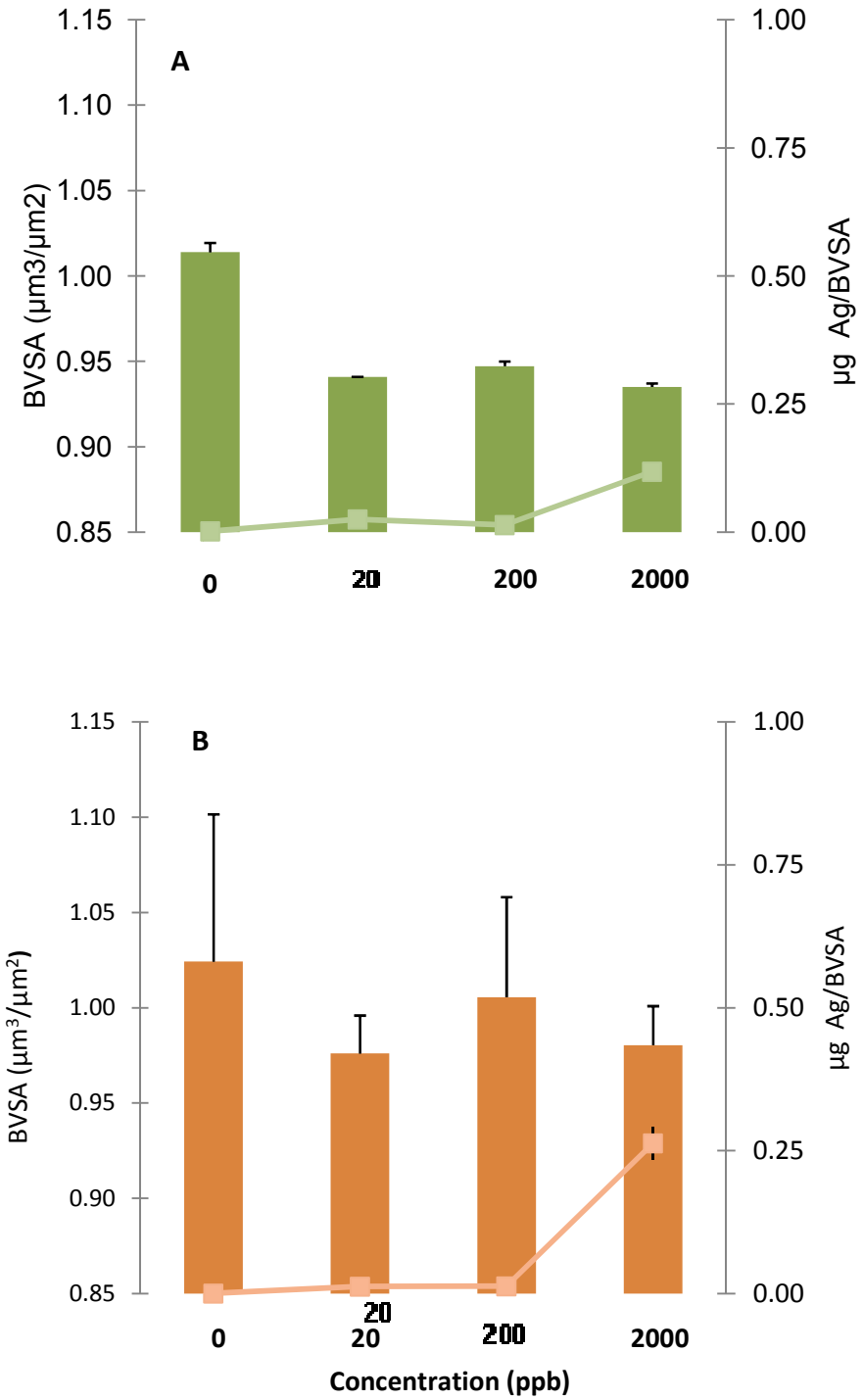

Figure 5.5 Changes on biovolume per surface area (BVSA, solid bars) for *P. putida* biofilms grown at pH 6 for 4-d in MDM and exposed for the last 24 h to different concentrations of Ag NPs, or no Ag NPs, without (A) and with (B) 10 mg l^{-1} SRFA. The total Ag NPs uptake (µg) by the biofilms is represented by the solid line. Error bars represent 1 standard deviation. Dots ( ) represent treatments in which Ag NPs had a significant effect on BV compared to the control (ANOVA, $p<0.05$).

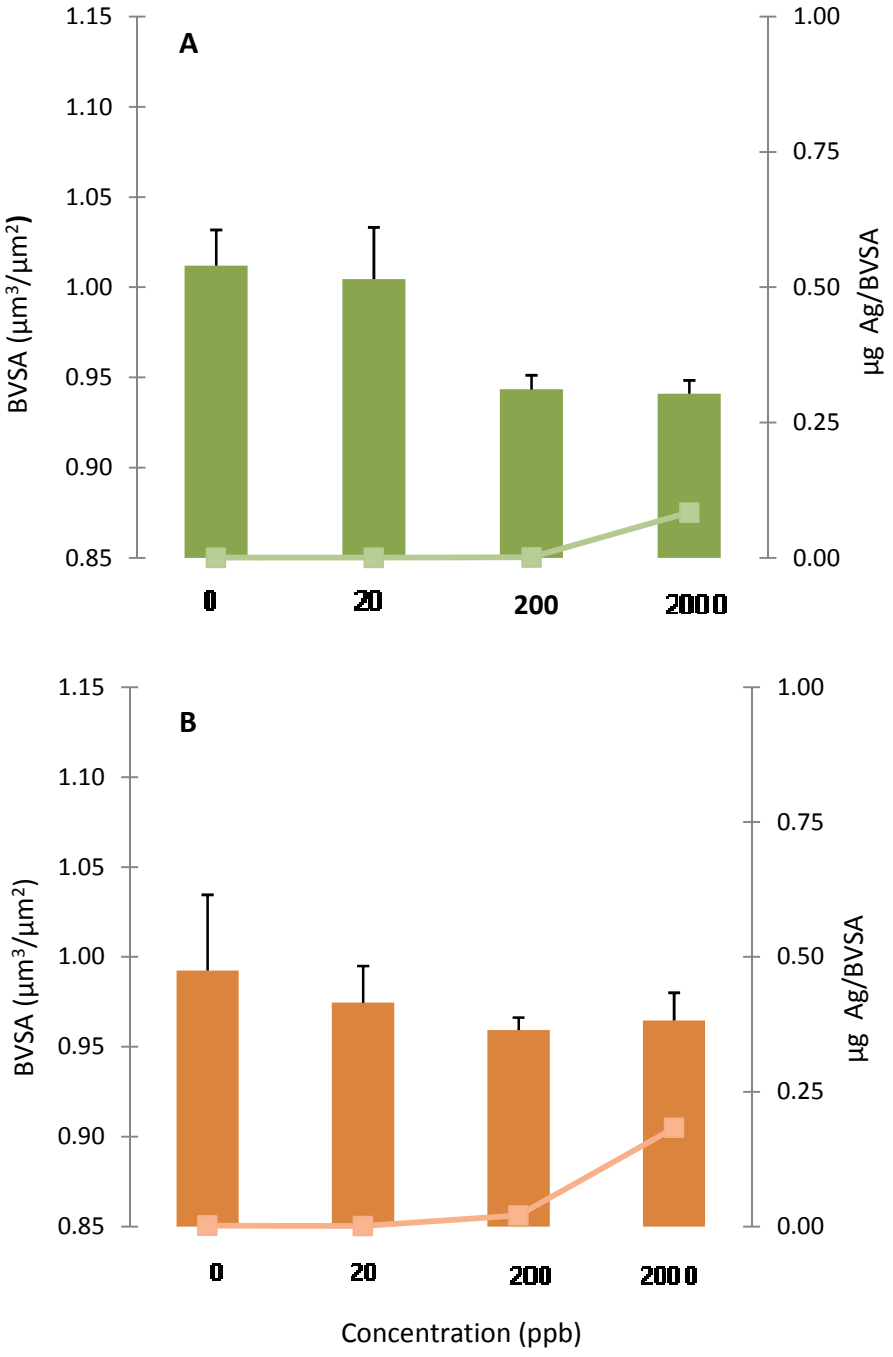

Figure 5.6 Changes on biovolume per surface area (BVSA, solid bars) for *P. putida* biofilms grown at pH 7.5 for 4-d in MDM and exposed for the last 24 h to different concentrations of Ag NPs, or no Ag NPs without (A) and with (B) 10 mg l^{-1} SRFA. The total Ag NPs uptake (µg) by the biofilm is represented by the solid line. Error bars represent 1 standard deviation. Dots ( ) represent treatments in which Ag NPs had a significant effect on BV, compared to the control (ANOVA, $p<0.05$).

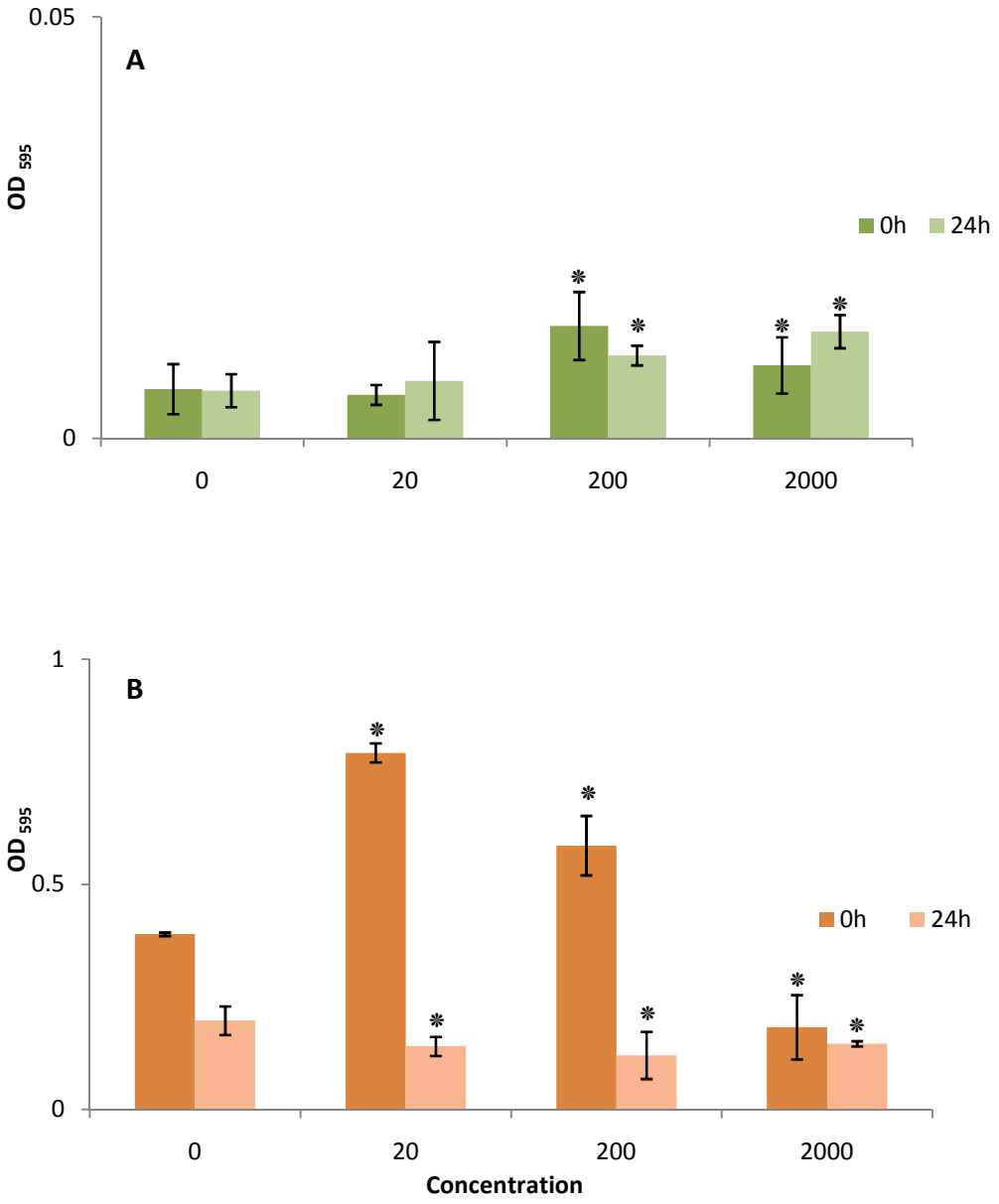

Figure 5.7 Amounts of bacterial cells from biofilm of biofilm (OD_{595}) grown at pH 6 without (A) and with SRFA (B) slough off due to Ag NPs after initial exposure (0-4 h, '0h'), and from 8-24 h ('24h'). Dots (*) represent treatments in which Ag NPs had a significant effect on the amount of BVSA detaching compared to the control (ANOVA, $p<0.05$).

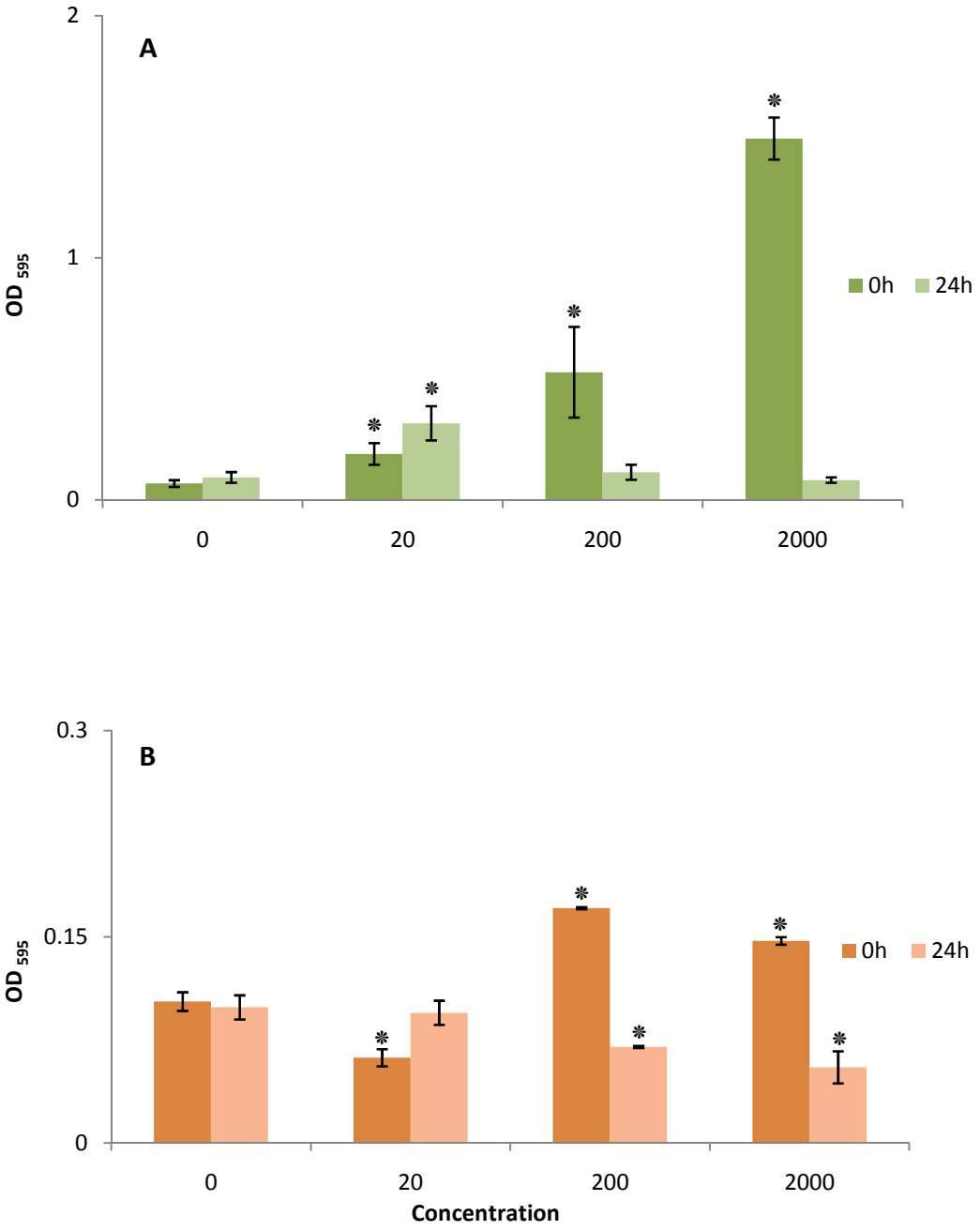

Figure 5.8 Amounts of bacterial cells from biofilm (OD $_{595}$) grown at pH 7.5 without (A) and with SRFA (B) sloughed off due to Ag NPs after initial exposure (0-4 h, '0h'), and from 8-24 h ('24h'). Dots (*) represent treatments in which Ag NPs had a significant effect on the amount of BV detaching compared to the control (ANOVA, $p<0.05$).

- Flow rate (0.1 ml min^{-1}) * Exposure time (24 h) = 144 ml of Ag NP solution exposed to each biofilm.
    - 20 ppb = 2 µg l^{-1} * 0.144 = 2.88 µg
    - 200 ppb = 20 µg l^{-1} * 0.144 = 28.8 µg
    - 2000 ppb = 20 µg l^{-1} * 0.144 = 288 µg

The effect of pH and presence or absence of SRFA on biofilm uptake of Ag NPs was more noticeable at the highest concentration of 2000 ppb. SRFA increased the uptake of Ag NPs by biofilms at both pH values (23.17 ± 2.55 and 15.88 ± 1.09 µg at pH 6 and pH 7.5 respectively). Without SRHA the uptake decreased by more than 50 %, and for both conditions it was consistently higher at pH 6. The higher uptake of Ag NPs when SRFA are present corroborates the TEM images obtained (Fig. 5.1) which show an increase in the number of particles and aggregates interacting with the bacterial cells when Ag NPs are previously mixed with HS.

Table 5.2 Uptake of Ag (µg, mean ± standard deviation) by the biofilm grown in the flow cell reactor. Number in parenthesis represents the mass (µg) biofilms were exposed to over 24 h.

Treatment	Ag NPs (ppb) and total (µg) Ag NPs exposed over 24h		
	20 ***(2.28 µg)***	**200** ***(22.8 µg)***	**2000** ***(228 µg)***
pH 6	2.12 ± 0.2	1.21 ± 0.28	9.92 ± 1.29
pH 6 SRFA	1.1 ± 0.15	1.17 ± 0.62	23.17 ± 2.55
pH 7.5	0.05 ± 0.008	0.09 ± 0.02	7.09 ± 0.65
pH 7.5 SRFA	0.12 ± 0.05	1.78 ± 0.32	15.88 ± 1.09

5.5 Cell viability in biofilms

The cellular viability of biofilms after exposure for 24 h to different concentrations of Ag NPs was measured using a LIVE/DEAD® *Bac*Light™ Bacterial Viability Kit coupled to CSLM (Section 2.9.2.2); viable cells are stained green whereas dead ones are red (Fig 5.9). The results are summarised in Table 5.3, and quantified as the change (%) in the proportion of dead cells in the Ag NPs exposed biofilms compared to the control (not exposed to Ag NPs).

Table 5.3. Change on the percentage of dead cells from biofilms exposed to Ag NPs in comparison with the number of dead cells present in unexposed biofilms (percentage ± 1 standard deviation). Negative numbers (-) indicate a decrease on the number of dead cells from biofilms not exposed to Ag NPs, while positive numbers (+) indicate an increase.

	Ag NP Concentration		
	20	*200*	*2000*
pH 6	1.1 ± 0.29	0.87 ± 0.45	-4.99 ± 3.97
pH 6 HS	-0.16 ± 0.66	-2.1 ± 1.09	1.07 ± 0.51
pH 7.5	-0.43 ± 1.4	1.43 ± 0.17	1.86 ± 0.37
pH 7.5 HS	2.36 ± 1.52	0.92 ± 0.35	1.31 ± 0.71

Although changes on BVSA were apparent among treatments as seen in Fig. 5.5 and 5.6, the cellular viability from the biofilms after exposure did not vary significantly with pH and the presence/absence of SRFA. Cellular viability did not decrease with increasing Ag NP concentration, indicating lack of toxicity of NPs to bacterial cells. Fig 5.9 shows a representative CSLM image of a control biofilm and a biofilm exposed to 2000 ppb Ag NPs. The images show qualitatively that the proportion of dead cells (red) to live cells (green) does not change significantly. Fig. 5.10 shows a CSLM scan composite of 17 images from scans of a control biofilm. The image

shows the architecture of a 4-d old biofilm grown in a flow though cell, with the biofilm cells in the lower layers being more compacted than the upper layers.

5.6 Physico-chemical properties of Ag NPs in the biofilm reactor

Size, shape and charge are factors that highly influence the internalisation and intracellular transport of particles by cells (Gratton *et al.* 2008). Figure 5.11 shows Ag NPs at pH 7.5 in MDM (A), Ag NPs in MDM with 10 mg l^{-1} SRHA (B), and Ag NPs within the biofilm (C). Humic substances and extracellular polysaccharides create a film surrounding the particles (Fig 5.11 B and C), which can confer stability to the particles in suspension and also may increase disaggregation (Baalousha *et al.* 2008) (See Ch. 3) due to the changes on charge and ultimately on dispersion. Due to the large amounts of polysaccharides produced by *P. putida* Ag NPs are surrounded by a relatively thick layer of *ca*. 80 nm (Fig 5.11 C); in comparison to the thinner layer (of a few nm) result of the absorption of 10 mg $l^{-1}$of SRFA to the particle (Fig. 5.11B).

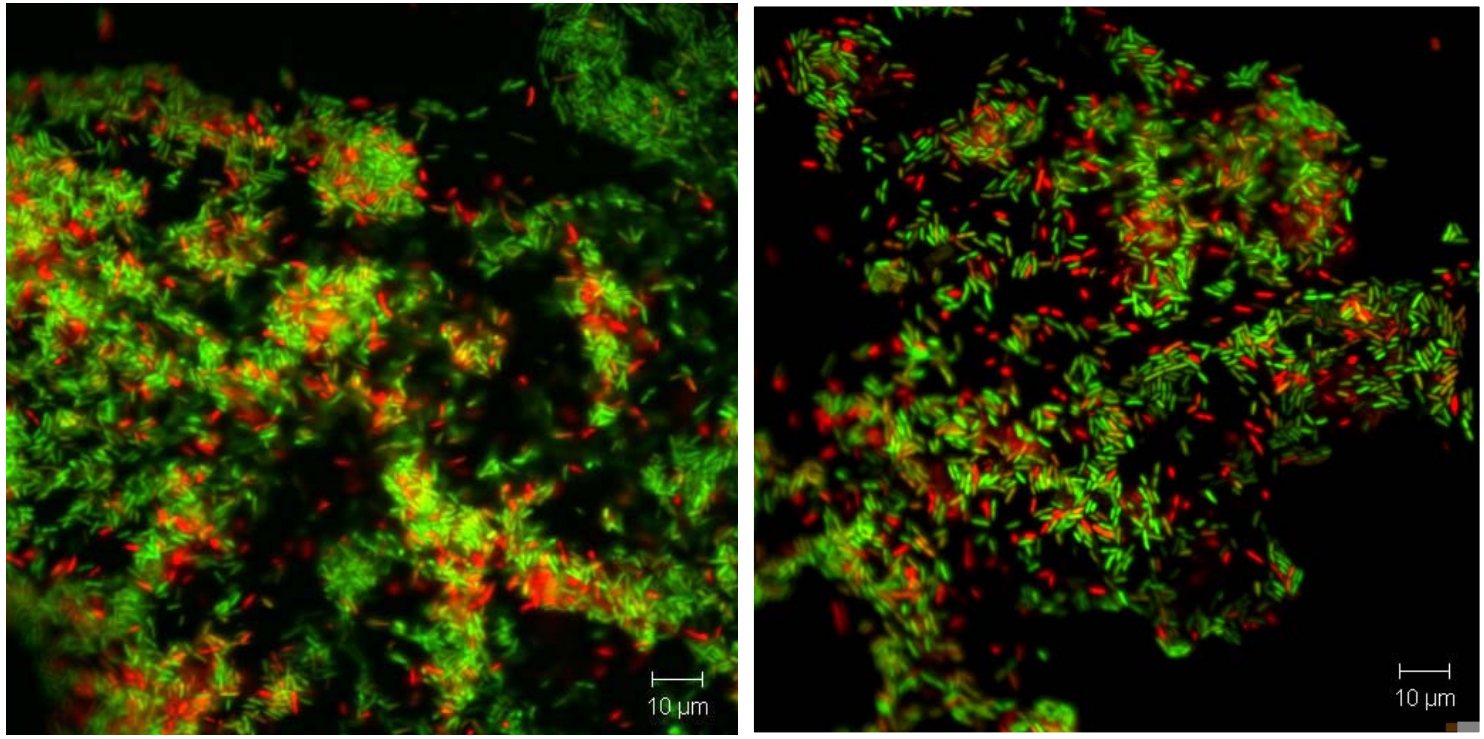

Figure 5.9 Selected confocal scanning laser images (Section 3.9.2) of A) *P.putida* biofilm at pH 7.5 and B) *P. putida* biofilm at pH 7.5 and 2000 ppb Ag NPs stained with LiveDead Baclight bacterial viability kit. Green cells represent live cells, and red cells are dead cells.

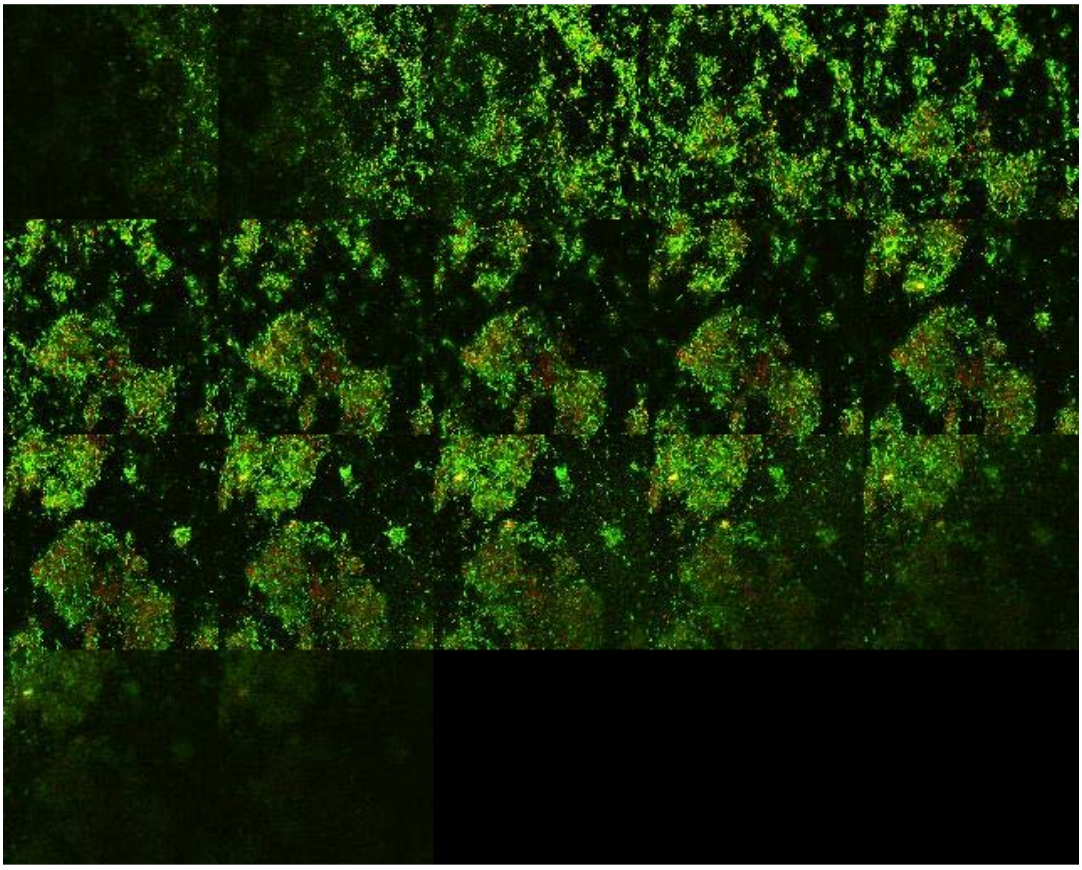

Figure 5.10. Examples of confocal scanning laser composite (17 slices, Section 3.9.2) of *P. putida* biofilm at pH 6 not exposed to Ag NPs. Green and red cells represent live and dead cells respectively. Upper left to bottom right: basal biofilm layer to uppermost layer.

Without HS or polysaccharides the nanoparticles form denser and more compact aggregates (Fig 5.11 A). Thus disaggregation is less likely (See Chapter 3).

Figure 5.12 shows the electrophoretic mobility of the particles at pH 7.5 before and after being in contact with the biofilms without (A) and with (B) 10 mg l^{-1} SRFA (Section 2.6.2.3 & Section 2.7.4.5). After exposure to the biofilms the readings obtained for particle stability were independent of the initial concentration of Ag NPs present. However, it is more likely the readings correspond to the surface charge of the bacterial cells than to the particles in solution, due to the large amounts of biofilm cells slough off.

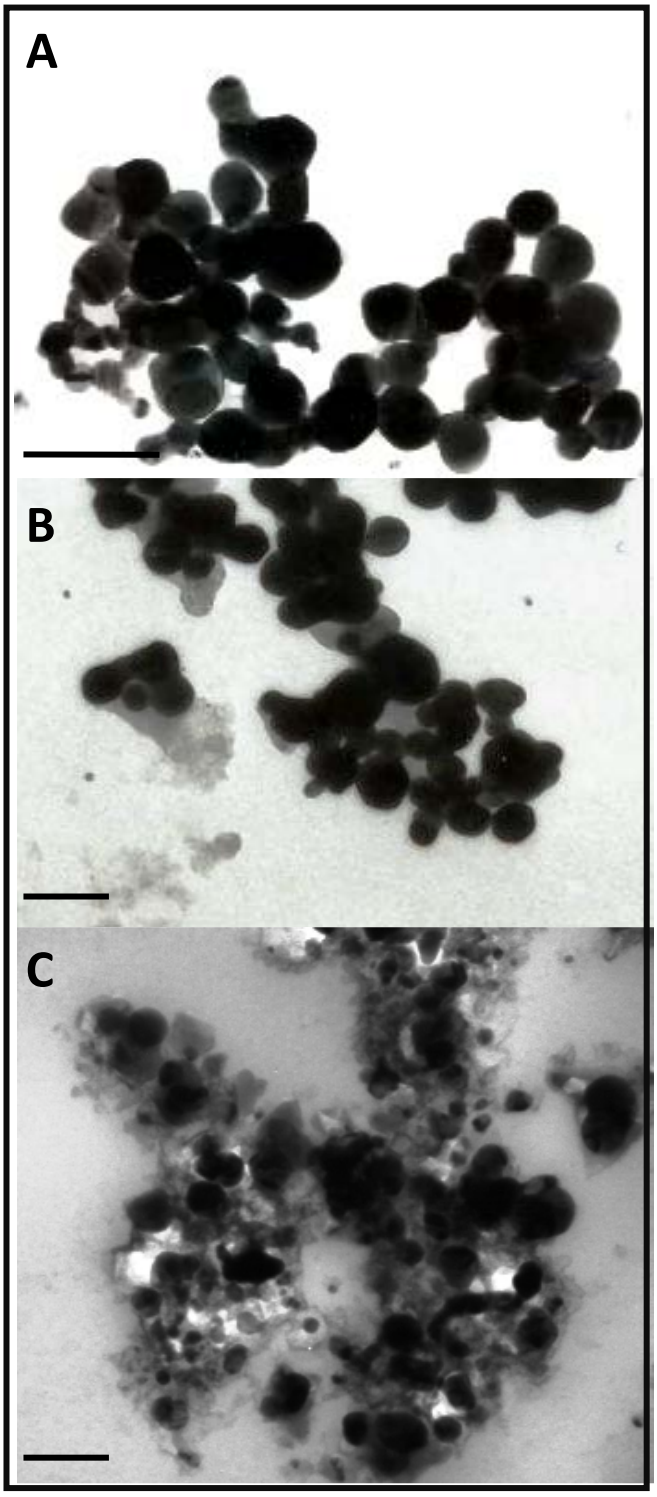

Figure 5.11. TEM micrographs of A) Ag NPs in MDM at pH 7.5 B) Ag NPs in MDM at pH 7.5 with 10 mg l-1 SRHA and C) Ag NPs with SRFA within the extracellular polysaccharide matrix created by *P. putida* biofilms. Bar represents 100 nm.

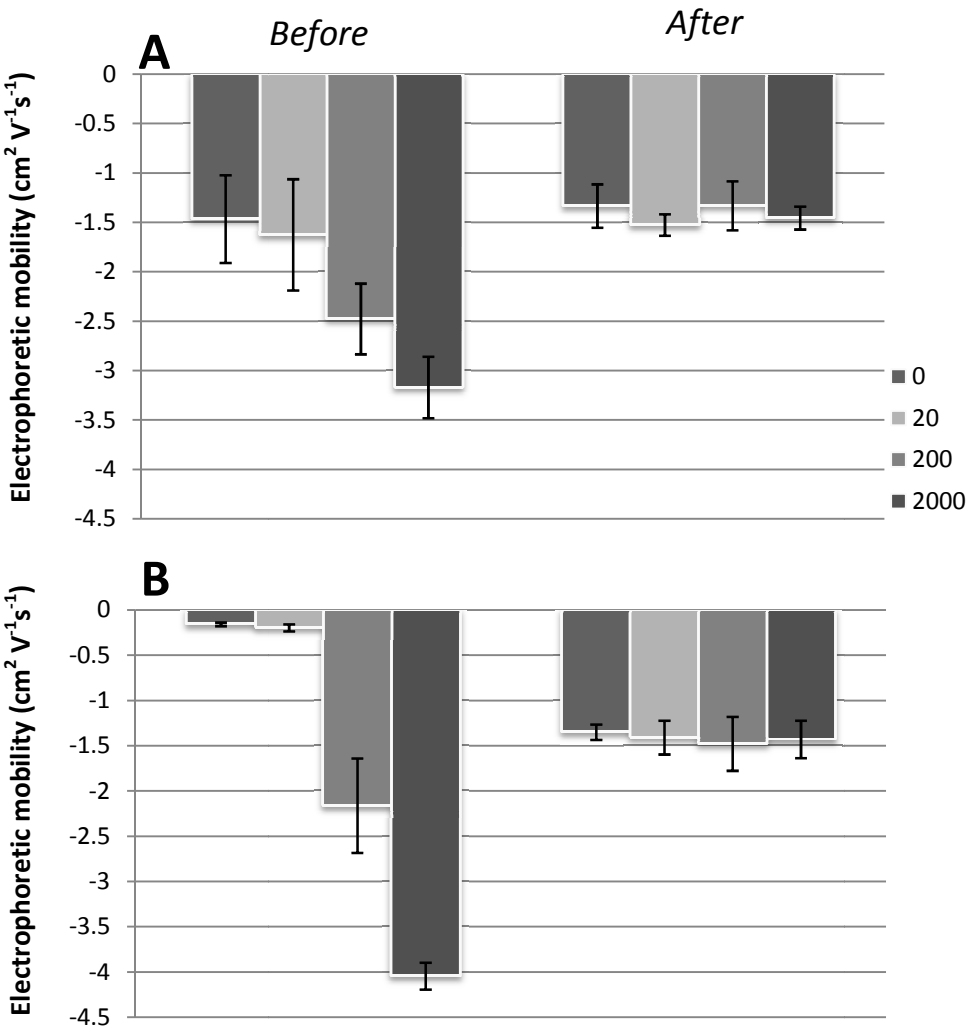

Figure 5.12 Electrophoretic mobility of different concentrations of Ag NPs in MDM (20-2000 ppb and MDM without Ag NPs; pH 7.5) before being in contact with *P.putida* biofilms ("Before") and after having passed over the 3-d old *P. putida* biofilm ("After"). A) represents suspensions without 10 mg l^{-1} SRFA, and B) with 10 mg l^{-1} SRFA. (N=3)

Figures 5.13, 5.14 and 5.15 describe the distribution of Ag NPs within the flow cell reactor for suspensions with initial concentrations of 20, 200 and 2000 ppb, respectively. Ag NPs were recovered at different points along the reactor: before entering and being in contact with the biofilm grown within the flow cells (*i.e.* the initial concentration; in graphs represented as (1)), and when exiting the flow cell after contact with the biofilm; in graphs represented as (2). The concentration of Ag NPs remaining in suspension after filtration at point 2 was also measured, in graphs

represented as (3) (Section 2.7.4.5.1.2). The latter results would give an estimate of the amount of free Ag NPs and small aggregates which would pass through the 0.22 μm pore size filter, assuming dissolved Ag to be negligible (See Fig. 2.5 and Section 2.7.4.5.1.4).

Overall, the pattern of behaviour observed for Ag NPs varied with pH and presence of SRFA, but it was the same for all concentrations of exposure at a particular pH value. At pH 6, Ag NPs aggregate and precipitate faster than under any other condition. Thus their recovery after exposure to the biofilm (2), and after filtration (3) was the lowest, with less than a 10 % being recovered. Between sampling point 2 and 3 the total Ag recovered does not change significantly (Fig. 5.13, 5.14 and 5.15). With SRFA, more nanoparticles are recovered after biofilm exposure (2), being 30-50 % at pH 6, and more variable but 50 % or higher at pH 7.5, potentially indicating a higher stability of the NPs in suspension. Generally, with increasing concentration of Ag NP, a lower % of the NPs was recovered after having been in contact with the biofilm, indicating that the tendency for aggregation and destabilisation of NPs increases with increasing concentration in suspension. At pH 6 the amount of bacterial cells sloughing off from the biofilm is minimal (Fig 5.7 A), thus few Ag NPs bound to detached cells and exudates are retained by filtration. This also suggests that most Ag NPs recovered after exposure to biofilms are as free-Ag NP. At pH 7.5 Ag NPs ca. 30 % of the Ag NPs are recovered after exposure to biofilms (2; Fig 5.13-5.15). At this pH value, NPs are more stable and remain in suspension longer than at pH 6.

After filtration, the amount of Ag NPs recovered under all pH values and conditions is < 20 %.

Filtrate solutions (only from those treatments without SRFA) were ultrafiltered (Section 2.7.4.5.1.4) to estimate changes in particle solubility. At both pH values and all concentrations the amounts were below the limits of detection (< 0.22 ppb) and could not be quantified with AAS (Section 2.8), indicating that solubility (< 2 % in MDM, Section 3.8.1) remained low.

5.7 Discussion

5.7.1 Interaction of Ag NPs with bacterial cells

The physico-chemical characterisation of NMs in the media used for exposure assays must be defined in order to understand the fate and behaviour of NMs and to identify the type of interaction and toxicity to bacteria. In general NMs tend to aggregate in aqueous media (Chapter 3); therefore they are susceptible to precipitation in a short time. This precipitation makes it difficult to quantify the actual dose of nanoparticles organisms are exposed to in the assay (Klaine *et al.* 2008). The toxicity of nanoparticles has been attributed to their large surface area per volume ratio, size distribution, chemical composition (purity, crystal structure, electronic properties, etc.), surface structure (surface reactivity, surface groups, inorganic or organic coatings, etc.), solubility, shape, as well as aggregation (Nel *et al.* 2006). The same properties that influence their toxicity are also the most

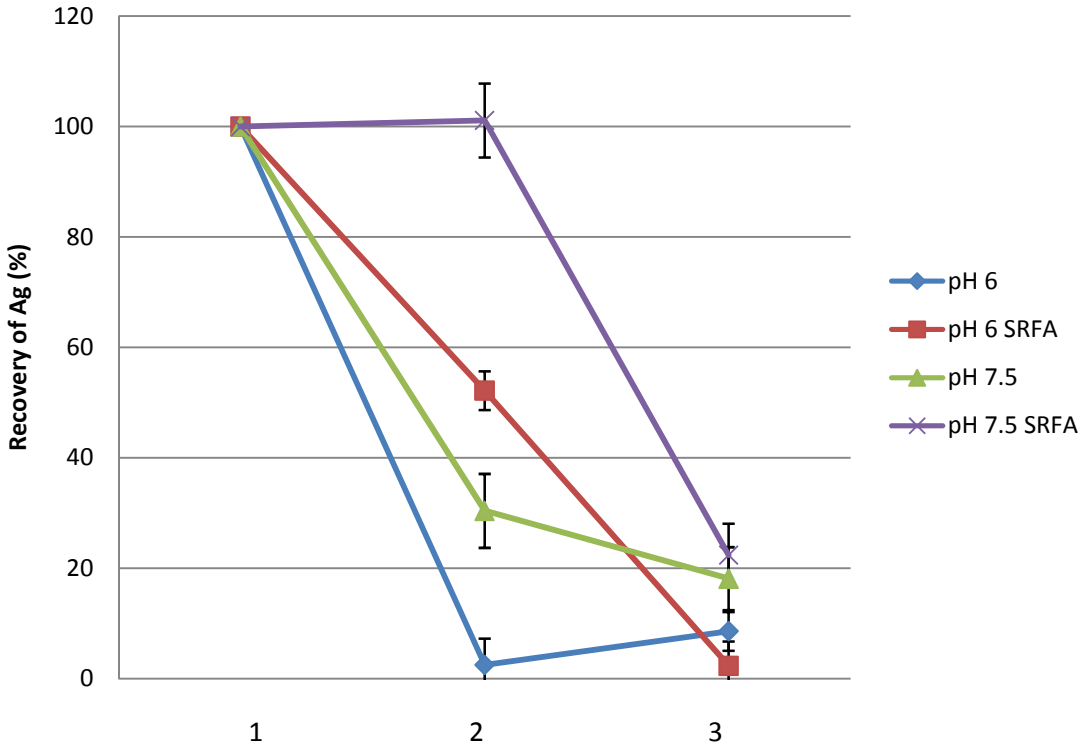

Figure 5.13 Recovery (%) of Ag NPs at different points in the flow cell reactor of a 20 ppb solution of Ag NPs at different pH values with and without 10 mg l^{-1}SRFA. 1) refers to initial concentration of AgNPs (%); 2) refers to the concentration of Ag NPs recovered (%) after exposure to the biofilm grown within the flow cell, estimating the amount of Ag NPs flowing through and not being taken up by the biofilm; and 3) refers to the Ag NPs recovered (%) after filtration resulting with an estimate of the amount of free-Ag NPs (which would pass through the 0.22 µm pore size filter).

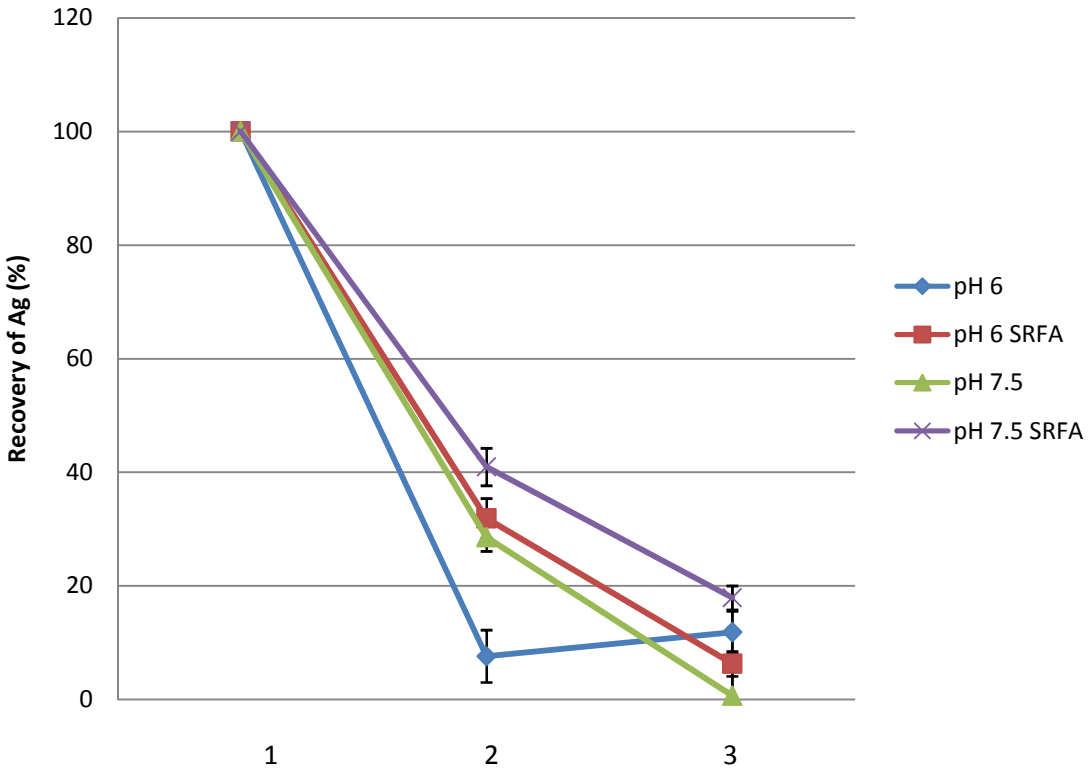

Figure 5.14 Recovery (%) of Ag NPs at different points in the flow cell reactor of a 200 ppb solution of Ag NPs at different pH values with and without 10 mg l^{-1}SRFA. 1) refers to initial concentration of Ag NPs (%); 2) refers to the concentration of Ag NPs recovered (%) after exposure to the biofilm grown within the flow cell, estimating the amount of Ag NPs flowing through and not being taken up by the biofilm; and 3) refers to the Ag NPs recovered (%) after filtration resulting with an estimate of the amount of free-Ag NPs (which would pass through the 0.22 µm pore size filter).

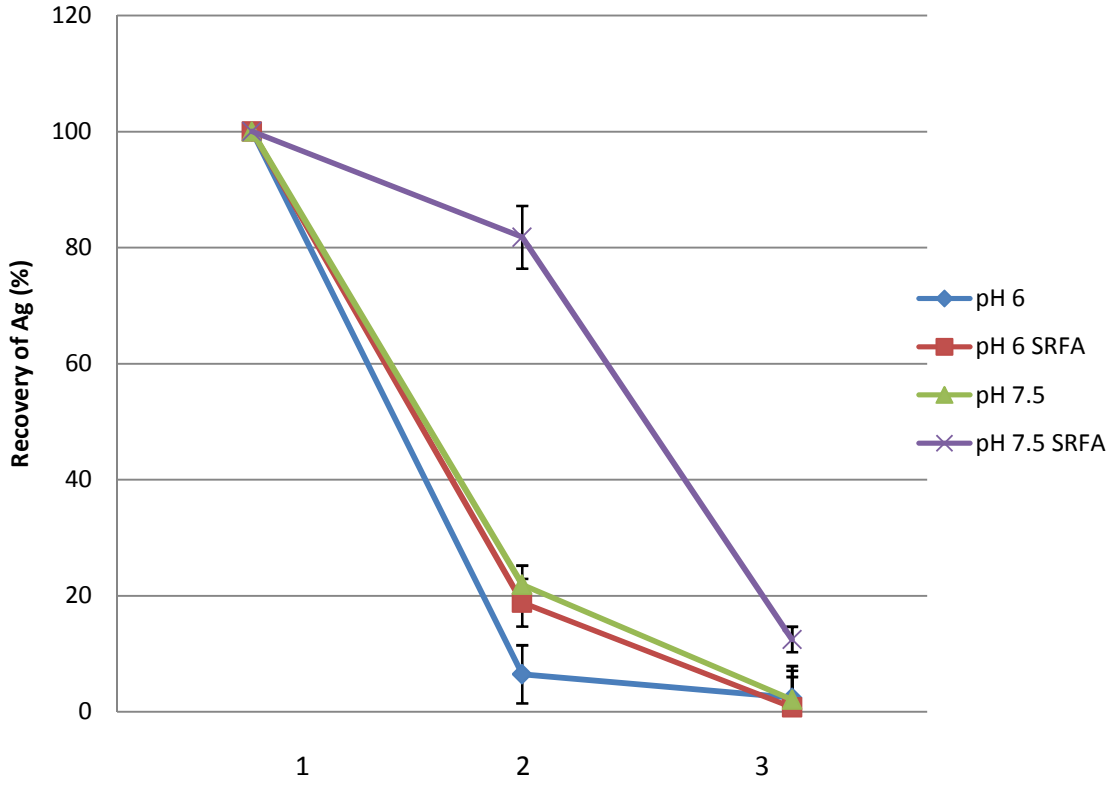

Figure 5.15 Recovery (%) of Ag NPs at different points in the flow cell reactor of a 2000 ppb solution of Ag NPs at different pH values with and without 10 mg l^{-1}SRFA. 1) refers to initial concentration of AgNPs (%); 2) refers to the concentration of Ag NPs recovered (%) after exposure to the biofilm grown within the flow cell, estimating the amount of Ag NPs flowing through and not being taken up by the biofilm; and 3) refers to the Ag NPs recovered (%) after filtration resulting with an estimate of the amount of free-Ag NPs (which would pass through the 0.22 µm pore size filter).

important properties governing their stability and dispersion in aquatic environments (Navarro *et al.* 2008). In theory, the more stable the NM suspensions are, the higher the likelihood of interacting with planktonic organisms. The physico-chemical properties of NMs in the media used for this assay (MDM, Section 2.2.2), with and without humic substances (SRFA, Section 2.3) were analysed and have been discussed in chapter 3. In this chapter the effect of the polysaccharides produced by bacteria, will also be taken into consideration due to their relevance for NM stability (Buffle *et al.* 1998).

The results of this study confirm that Ag NPs interact with *P. putida* cell membrane (Fig. 5.1 and Fig 5.2). Bacterial cells did not interact with a particular size

fraction only; Ag NPs aggregates were detected at both pH values tested, only with SRFA present (Fig 5.1, Fig 5.2 and Fig 5.3). SRFA affected the physico-chemical properties of the particle, but also is used as a source of carbon to *P. putida* cells (Chapter 4). Hence, *P. putida* cells may be interacting with the humic substances coating the NPs, and ultimately with the Ag NPs within the HS matrix. There is not much information in the literature relating uptake of NMs and effects of HS, nevertheless a study done by Roberts et al. (Roberts *et al.* 2007) has showed an increased ingestion of CNTs by Daphnia when these were coated with lipids, a good source of carbon for this organisms. We measured relatively short term effects (4 day maximum). Nevertheless, in those treatments containing SRFA increasing exposure concentrations resulted in an increase in the number of interactions and NPs aggregates associated with the biofilms. It is also important to consider that all biofilm samples visualized by TEM were from biofilm slices of ~ 80 nm thickness (Section 2.9.1). Therefore, if the larger Ag NP aggregates that formed without SRFA interact mostly with the uppermost biofilm layer, of only a few nanometer thicknesses, sample manipulation could have resulted in the lack of detection of NPs in treatments without SRFA.

In this study the mode of interaction of the particles with the cell was not investigated. For instance, it is uncertain if NPs were disaggregated in the media and aggregated once in contact with the cell membrane. Initially NPs formed small aggregates in suspension, and some fully dispersed NPs were detected with HS present (Chapter 3); however it is uncertain if the cell interacts with the NP directly or if biofilms are indirectly sequestering the NPs within the matrix by directly interacting with the SRFA coating the particle. A few NPs were found in the inner part of the cell membrane as seen in Fig 5.2 B and C. The EPS matrix of the biofilm

is negatively charged, and the pH influences the diffusion of charged surfaces and particles (Willaert *et al.* 2004). Since Ag NPs are also negatively charged at pH 6 and 7.5 (Section 4.7), by electrostatic forces they could be repelled by the EPS matrix and not easily interact with the biofilm. In addition, the size of the voids (empty spaces between bacterial cells) connecting microcolonies is quite small, and their volume deceases with biofilm maturation (Venugopalan *et al.* 2005). Hence, aggregates of Ag NPs of several hundred nanometers (Section 4.7) may be impeded, becoming less bioavailable to bottom layers of the biofilm, and could also explain the reason Ag NPs could not be visualized by TEM in certain treatments. Although Ag NPs were only detected in treatments containing SRFA, such interaction did not translate into an increased sloughing of biofilm into the medium (as seen in Fig. 5.5 and 5.6). Nevertheless NPs were accumulating in the biofilms with and without HS (Section 5.3, metal analysis) which could lead to bigger long term effects.

The external wall and membranes of gram negative bacteria play a crucial role in controlling entrance of NPs into the cell (Xu *et al.* 2004). The transport mechanism of microbial cells differs substantially to those in mammalian cells. For example, common uptake mechanisms for particles in eukaryotic cells such as endocytosis and pinocytosis, are not present in prokaryote cells (Madigan *et al.* 1997; Xu *et al.* 2004). In the case of prokaryotic cells, the external membrane is composed of lipopolysaccharides, and contains specific proteins called porins, which act as channels for the entry and exiting of hydrophilic substances of low molecular weight. The largest porins allow entry of substances of 5,000 Dalton (Madigan *et al.* 1997), and their size should prevent entrance of larger particulates such as NPs into the cell (Choi & Hu 2008a). Nevertheless, the size of membrane pores are highly difficult to determine with current techniques (using fluorescent dyes and protein

crystallization) and real time kinetic information and transport in living cells are hard to quantify. So, many questions regarding membrane transport in living cells are still unanswered. For instance Xu et al. (Xu *et al.* 2004) detected individual Ag NPs of up to 80 nm inside *P. aeruginosa* cells, and accumulating in the cytoplasm. When chloramphenicol was used, membrane permeability increased and a larger number of Ag NPs accumulated inside the cell and aggregated, but cell disruption could not be detected and neither could particles > 80 nm. It has also been suggested that the interactions of cells with NPs could lead to the formation of new pores, which might be larger than usual and thus increase the internalization of the NPs through the cell membrane (Navarro *et al.* 2008a). In our case, TEM images show invagination after Ag NP contact.

Several studies have investigated the interactions of Ag NPs with planktonic bacteria and agar bacterial colonies. Sondi and Salopek-Sondi (2004) used electron microscopy analysis to evaluate the surface morphology of planktonic cells treated with Ag NPs; and found treated cells showing the formation of 'pits' in their cell membranes. Furthermore, quantitative metal analysis and TEM imaging determined Ag NPs were being accumulated onto the membrane, with some of them successfully penetrated into the cells. Xu *et al.* (2004) investigated the uptake of Ag NPs in cell suspensions of *P. aeruginosa* by dark-field microscopy and TEM. Ag NPs with sizes up to 80 nm were detected being transported though the inner and outer cellular membranes. Ag NPs also accumulated in the cytoplasmic space and a few underneath the cellular membrane. In 2005, Morones *et al.* studied the interaction of Ag NPs of 1-10 nm with planktonic *E. coli* using scanning transmission electron microscopy. Results revealed that the majority of the Ag NPs were localized on the membranes of treated cells, but were also able to penetrate

inside the cells. The authors of this study also investigated the selective interaction of particle facets with bacterial surfaces, concluding that the high-atom-density {111} facets of Ag NPs were the most reactive and also interacted the most with the bacterial surfaces. Pal *et al.* (2007) also studied by the interaction and toxicity of differently shaped Ag NPs with the gram negative bacterium *E. coli.* The interactions were visualised by energy-filtered TEM, and showed that triangular Ag NPs (with a higher {111} facet density) were more toxic that round Ag NPs. Hence, both authors defined the existence of a shape-dependent interaction among NPs and bacterial cell membranes. The shapes of the nanoparticles used for this study were not homogenous and both round particles and truncated triangular particles were observed by TEM (Fig 3.3 and Fig 5.11). XRD results (Section 3.2) also did show a high {111} facet density from the particles (Section 3.2; Fig 3.1).

A phenomenon also observed in biofilms after exposure to Ag NPs is the lower electron density area within the bacterial cells exposed to 200-2000 ppb, at both pH values tested (Fig 5.1 and Fig 5.2). This observation has previously been described by Morones et al (2005) when *E.coli* cells were being exposed to 100 ppm Ag nitrate solution, but to my knowledge has never been observed with exposure to Ag NPs. This low electron density area is the result of conglomerated DNA as a mechanism of defence by the bacteria when sensing noxious compounds (Morones *et al.* 2005, Feng *et al.* 2000). The solubility of Ag NPs at the pH values 6-9 and concentrations tested is less than 2% (or ranging from 50-175 nM (6-18 ppb, respectively), Ch 3 Section 3.8.1). Taking into consideration the results of planktonic studies (see Chapter 4) only concentrations as low as 200 ppb of Ag nitrate showed a bactericidal effect. Concentrations of 6-18 ppb Ag^{+} are too low (just above permissible drinking water levels, Ch 2, Section 2.7.1.3) to affect the cells in this

study and produce this lower electron density region. Therefore, this indicates that although a low number of NPs are being taken up, there is also a potentially NP mediated effect disrupting cytoplasmatic functions when in contact cell membranes. However, cell viabilities compare to the control treatments were not significantly different, indicating that cells remain viable, at least for a certain period of time, after interacting with NPs.

Ag NPs are potential environmental stressors and because of their size they may be likely to interact with the uppermost layer of bacteria in biofilms what could explain the amount of cells being detached from the biofilms (Section 5.3). This initial high concentration of biofilm cells detaching could be a defence mechanism to protect the established biofilm population. Cells bound to NPs may detach from the biofilm to remove the noxious particle from the surrounding environment protecting the biofilm. However, this was not investigated and further studies should be undertaken to understand the effects of NPs biofilm structure and composition. Recovery of the nanoparticles at this stage is strongly related to the amounts of biofilm cells being detached from the biofilms during NP exposure (Fig 5.7 and 5.8). The larger the volume of cells detached, the more Ag will bind to active sites of polysaccharides and exudates and get retained by in the filter. Thus, less free-Ag is to be expected as higher volumes of biofilm cells being shed. During initial exposure to Ag NPs biofilms are subjected to stronger thinning effects, thus as bacterial cells detach, the biofilm also gets thinner, which corroborates the fact that at later exposure times the amount of bacterial cells shed decreases as increasing concentration, a phenomenon observed particularly at pH 7.5 (Fig 5.8 A and B).

Studies done on algae and bacteria forming biofilms have shown how under stress by metal pollution, organisms secrete a higher amount of EPS that acts not

only as a physical barrier but also help to detoxify. EPS contain high amounts of negatively charged functional groups (i.e. carboxyl, phosphates) that act as metal binding sites (Sutherland 1999). Nevertheless, detachment is still one of the least understood phenomena in biofilms, and a few suggested key factors include secretion of matrix degrading enzymes (Allison *et al.* 1998), microbial generated gas bubbles (Ohashi & Harada 1994), nutrient levels (Hunt *et al.* 2004) and growth, fluid shear stress (Picioreanu *et al.* 2001), quorum sensing (Allison *et al.* 1998) and activation of bacteriophages (Webb *et al.* 2003).

5.7.2 Toxicity of Ag NPs and uptake by biofilms

The results of this chapter indicate that although there is an interaction of Ag NPs by those biofilms exposed to Ag NPs and SRFA (Fig 5.1 and Fig 5.2), as well as a higher uptake of Ag of ca. 50 % in comparison to biofilms exposed to Ag NPs without SRFA; the effect on biofilm biovolume is lower when HS are present (Fig 5.5 B and Fig 5.6 B). Hence, the physico-chemical properties of the particles are highly relevant to ecotoxicological behaviour, as is exposure concentration. Although Ag NPs were not detected in association with the cells by TEM at pH 6 and pH 7.5 without SRFA the effect of Ag NPs is significant by the observed decrease on the biofilm BVSA of these treatments. Surprisingly, the decrease in BVSA observed in Fig 5.5 A and 5.6 A is independent of the exposure concentration *i.e.* a higher amount of Ag NPs does not lead to an enhanced degree of toxicity. This could be the result of a particle either a saturation state in the biofilm (a solution of 20 ppb contains 600,000,000 particles, while a solution of 2000 ppb has 100 times this value (Chapter 3; Section 3.4; Table 3.1)); or a thinning mechanism based on the friction and consequent detachment of cells due to the flow of aggregates of 200-300

nm over biofilms of cells 8 to 10 times larger. The viability of the biofilm was not significantly different among pH values and conditions tested (Table 5.2), suggesting the observed thinning effect is caused by detachment of bacterial cells by friction or by cells detaching to removed noxious particles from the biofilm, and not by chemical inhibition of growth.

The overall pattern in Fig. 5.7 and Fig 5.8 indicate that biofilms were more susceptible to thinning by Ag NP as soon as the NPs contacted the biofilm, as seen by the increased numbers of bacterial cells being detached from the biofilms at exposure time from 0-4 h in comparison to the number of cells detached from 8-24 h.

The amounts of Ag NPs biofilms were exposed to vary for each treatment due to differences among particle stabilities (Chapter 3; Section 3.7), and hence different precipitation rates for the Ag NPs with different pH and conditions tested. The low Ag NP stability at pH 6 (Ch 3, Section 3.7.1) translated to a high precipitation and, thus low recovery after exposure to biofilms (Fig 5.13, Fig 5.14 and Fig 5.15), whilst the presence of HS at both pH values increased significantly the recovery of Ag NPs after exposure to biofilm, and also increased metal uptake by biofilms (Fig. 5.5, Fig 5.6 and Fig. 5.7). Polysaccharides (EPS) produced by the pseudomonad can also enhance stability and disaggregation under certain conditions, as well as decrease it in others, and could explain the reason why more than 90 % of the Ag was not being taken up by the biofilm, and exit the system in aggregates larger than 220 nm, as estimated from Fig 5.13, Fig 5.14 and Fig.5.15 (sampling point 3).

To date, there is not an extensive literature on the toxicity of nanomaterials to prokaryotes, in comparison to eukaryotic organisms. Nevertheless, Ag NPs are one of the best studied nanoparticles due to their antimicrobial action. The mode of

action of Ag NPs is still not well understood (Sharma et al 2008), however the antimicrobial activity of Ag NPs has often been attributed to the release of Ag ions, independently of the high reactivity and size of the particle (Lok *et al.* 2006; Lok *et al.* 2007; Tian *et al.* 2007). It is well known that silver ions interact with thiol groups inactivating respiratory enzymes and proteins; they disrupt DNA replication and affect the structure and permeability of the cell membrane (Slawson *et al.* 1992a; Feng *et al.* 2000; Silver 2003). Silver ions are produced from Ag NPs when oxygen is present, but not in reducing conditions (Henglein 1998). In order to investigate the mechanism of toxicity of Ag NPs, Lok *et al*. (2007) compared the toxicity of reduced Ag NPs with a partially oxidised Ag NPs. The results show *E. coli* bacteria colony formation was not affected by treatment of reduced nano-Ag, but cells treated with oxidized nano-Ag showed marked decreases in colony formation. The results indicated that the antibacterial activities of nano-Ag are critically dependent on surface oxidation; thus the toxicity was interpreted based on the levels of chemisorbed Ag^{+} ions released. Also, the smaller the particles the larger the surface area to mass ratio, hence the higher the relative concentrations of chemisorbed Ag^{+}. Franklin *et al.* (2007) investigated the effects of ZnO to freshwater microalgae and concluded that particles were very soluble and the release of Zn^{2+} was responsible for the toxicity observed. Navarro *et al*. (2008) investigated and compared the effects of Ag NPs and Ag nitrate. Ag NPs were very insoluble (<1%), and initially toxicity was thought to be mediated by the particle. Nevertheless the authors detected a higher release of Ag ions from Ag NPs in the presence of algae which could be the source of toxicity to algae (Navarro *et al.* 2008). However, in our study, increased dissolution by the cells as other authors suggest was not detected but it could be that any dissolved Ag is rapidly taken up by the bacteria. Choi *et al* (2008) also

investigated and compared the toxicity of Ag and Ag NPs to a nitrifying community of microorganism and found species-specific differences in toxicity. For instance Ag NPs were very toxic to autotrophic organisms, whereas silver ions were more toxic to heterotrophic (Choi *et al.* 2008). Tian *et al*. (2007) using proteomic and biochemical studies demonstrated that exposure of *E.coli* cells to Ag NPs at the nM levels affected the proton motive force and killed the cells within minutes. The observed toxicity was very similar to the toxicity of Ag ions in solution, and as Lok *et al.* (2007) they also suggested that Ag NPs antimicrobial activity was via Ag^{+} release. However, Pal *et al.* (2007) investigated the interaction and toxicity of differently shaped Ag NPs with the gram negative bacterium *E. coli.* Although the cell-Ag NP interaction seemed to be similar among nanoparticles with distinctly different shapes, the inhibition results differ. Inhibition can be explained in terms of the percent active facets present in nanoparticles of different shapes, and the higher the percentage of the facet {111} the more toxic Ag NPs .

In the natural environment, the majority of bacteria exist as biofilms (Teitzel 2003). Biofilms are embedded in a large matrix of extracellular polymeric substances (EPS), in comparison to the planktonic cells. EPS confer many advantages to bacteria but especially increases protection to toxins (Wingender *et al.* 1999). Exposure of 3-d old biofilms to Ag NPs by means of a slow but constant flow (0.1 ml min^{-1} for 24 h) did not affect the viability of the biofilm and there was no increase in toxicity with increasing Ag NP concentrations. The decrease in BVSA observed seems to be the consequence of a mechanical mechanism causing bacterial cell detachment and not physico-chemical mode of action inhibiting biofilm growth.

6 Results and Discussion 4: The effects of Ag NPs to a natural marine biofilms

6.1 Summary

This study aimed to evaluate the environmental impact of Ag NPs on a natural marine biofilms. Ag NPs were characterised by aggregate size (Section 3.7), stability (Section 3.8.2), and solubility (Section 3.9.2) in artificial seawater at the same pH, temperature and TOC content as in the natural seawater (Section 2.7.5.3). Biofilms were grown for 3 days (D3) in the west marina of Singapore (Section 2.7.5.3) before being transported into the laboratory and exposed to different concentrations of Ag NPs (20, 200 and 2000 ppb, Section 2.7.1.3) or left untreated for 24 h (4-day old biofilm). The impact of Ag NP exposure on biofilm biovolume to surface area (BVSA) was evaluated using two different techniques: the crystal violet assay (Section 2.7.2.1.2) and by bacterial extrapolysaccharide staining coupled to confocal scanning laser microscopy (Section 2.7.2.1.3). The results from the EPS staining showed that Ag NPs were toxic at concentrations as low as 200 ppb (ANOVA, $p<0.05$), causing a decrease in biovolume to surface area (BVSA) of ~30 and 40 %, at 200 and 2000 ppb respectively, and compared to the untreated biofilms. The results from the crystal violet assay showed that only 2000 ppb were significantly toxic (ANOVA, $p<0.05$) to the biofilm. However, despite the discrepancy between techniques, the pattern of toxicity of Ag NPs was the same in both (Fig 6.1 and Fig 6.2). TRFLP analysis (Section 2.7.5.10) was used to quantify and determine the potential shifts of species and relative abundance of taxa in the 4-day old (4D) treated biofilms with 2000 ppb Ag NPs and 4D untreated biofilms.

Overall, the results show that Ag NPs not only caused a decrease in BVSA of the treated biofilm, but also impeded the succession of the natural community. The mechanism by which Ag NPs affected succession was not investigated. Planktonic bacteria, known to be more susceptible to toxicants than biofilms (Hentzer *et al.* 2001; Surdeau *et al.* 2006), could have been more affected by Ag NPs, affecting dispersal and preventing their settling and colonization. Presence of Ag NPs on the substrate may also have prevented the successful settling of bacteria.

6.2 Toxicity of Ag NPs to biofilms

Natural marine biofilms were grown for 3 days (3D) in Singapore harbour (Section 2.7.5.2) and used as: 3D controls (biofilms grown in the sea for 3 days not exposed to Ag NPs), 4D-0 (biofilms grown in the sea for 3D and taken into the laboratory where they were grown in natural seawater for further 24h not exposed to Ag NPs), and 4D-(20-2000) (biofilms grown in the sea for 3D and taken into the laboratory where they were grown in natural seawater for further 24h and exposed to 20, 200 or 2000 ppb Ag NPs). The effect of different concentrations of Ag NPs to biofilms (Section 2.7.1.3) is summarised in Figures 6.1 and 6.2 using crystal violet assay (Section 2.7.2.1.2) and EPS staining coupled to CSLM (Section 2.7.2.1.3), respectively. Both techniques, crystal violet and EPS staining, were used to quantify the changes in volume per surface area. However, natural biofilms produce a large natural spatial patchiness which can lead to a large variation on growth. Patchiness is a phenomenon encountered in natural biofilms due to microorganisms growth, recruitment and grazing (Stafford & Davies 2005; Hutchinson *et al.* 2006). This spatial variation in growth together with the large number of treatments and

replicates, and the large substrate area used for growing individual samples (glass microscope slides) suggested that two different approaches to quantifying bacterial BVSA should be taken into consideration. EPS-CSLM is the more accurate of the two techniques, is non-invasive and yields to three-dimensional images of colonised surfaces with high optical quality and resolution in the sub-µm scale (Bressel *et al.* 2003). However, the limitation of this technique is that the area that was analysed per scan was of 10,000 μm^2, a small area if we consider that each microscope slide used as substrate was 20 million times larger. Therefore, although EPS-CSLM is a precise technique which is able to provide accurate BVSA quantifications, the results may not be representative of the overall biofilm, due to the low surface area analysed with this technique and the large number of replicates and treatments analysed. The crystal violet assay is also used for the quantification of adherent bacteria, and it is a good technique for comparing total BVSA across treatments (Vieira *et al.* 1993). This assay is not as accurate as the EPS-CSLM technique since it is based on absorbance readings of total dye bound to cell membranes and small variations in BVSA (μm^3range) are hard to detect. In addition, this technique is time consuming given the calibration curves required for each pH value investigated which are needed to obtain total biomass values. However, this assay is quick and easy to perform and provides representative information. This assay is especially useful when sample sizes are large.

Figure 6.1 shows the results obtained with the crystal violet assay. Exposure for 24 h to a concentration of 2000 ppb of Ag NPs (D4-2000) was the only treatment causing a significant effect on biofilm BVSA. Biofilm BVSA decreased by ca. 25 % (ANOVA, $p<0.05$) compared to the control day 4 (D4-0), not exposed to Ag NPs. The total BVSA at d4-200 was not significantly different from the control D3,

indicating that this concentration of Ag NPs could be acting in a bacteriostatic manner. However, a bacteriostatic concentration value is not easy to determine for complex communities of organisms as found here, as discussed further on in this chapter.

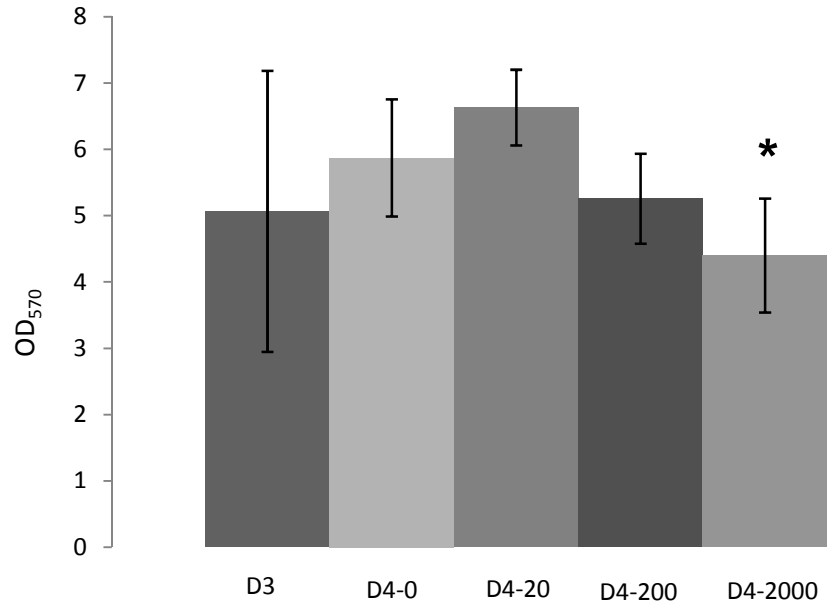

Figure 6.1 Effects of different concentrations of Ag NPs to natural marine biofilms, quantified using the crystal violet assay (n=5). * represents concentrations that were significantly different from the control d4-0 (ANOVA, $p<0.05$). Error bars represent 1 standard deviation. D3=biofilms grown for 3 days in the sea; D4-0 biofilms grown for 3 days in the sea, taken into the laboratory and grown for further 24 h in natural sweater; D4-20 biofilms grown for 3 days in the sea and taken to the laboratory and grown for further 24 h exposed to 20 ppb Ag NPs; D4-200 biofilms grown for 3 days in the sea and taken to the laboratory and grown for further 24 h exposed to 200 ppb Ag NPs; D4-2000 biofilms grown for 3 days in the sea and taken to the laboratory and grown for further 24 h exposed to 2000 ppb Ag NPs;

Figure 6.2 summarises the changes on bacterial BVSA obtained by EPS staining with lectin Concanavalin A and imaged by CSLM (Section 2.9.2.1) of control and treated biofilms. With this technique exposures to the concentrations of 200 (D4-200) and 2000 ppb (D4-2000) resulted in a significant decrease in the

biofilm BVSA (ca. 30 and 41 %, respectively ANOVA, $p<0.05$) compared to the control D4-0. An overall similar pattern to crystal violet results on the effects of Ag NPs to BVSA is observed.

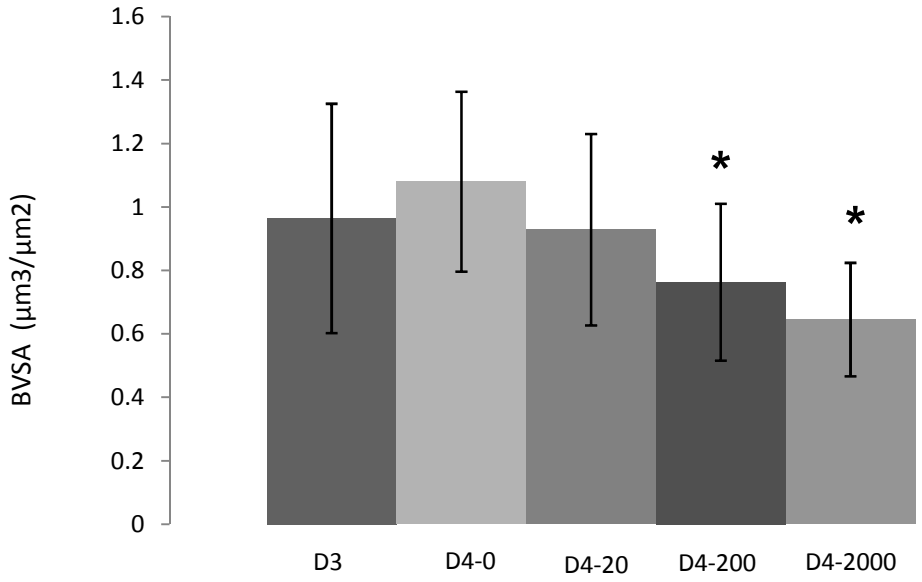

Figure 6.2 Effects of different concentrations of Ag NPs to natural marine biofilms, quantified using the EPS staining coupled to CSLM(n=30). * represents concentrations that were significantly different from the control d4 (ANOVA, p<0.05). Error bars represent 1 standard deviation. . D3=biofilms grown for 3 days in the sea; D4-0 biofilms grown for 3 days in the sea, taken into the laboratory and grown for further 24 h in natural sweater; D4-20 biofilms grown for 3 days in the sea and taken to the laboratory and grown for further 24 h exposed to 20 ppb Ag NPs; D4-200 biofilms grown for 3 days in the sea and taken to the laboratory and grown for further 24 h exposed to 200 ppb Ag NPs; D4-2000 biofilms grown for 3 days in the sea and taken to the laboratory and grown for further 24 h exposed to 2000 ppb Ag NPs;

Biofilms were only grown for three days in the field before being taken into the laboratory. The reason for this short immersion time is that the seawater in the harbour contained large quantities of debris, organic matter and after 3 days marine macroinvertebrates started to settle on the microscope slides, which would impede proper microscopy analysis. This short growth period led to a maximum thickness of the biofilms analysed of ca. 3 µm to 7 µm, depending on the treatment (Ag NP

exposure), as determined by CSLM (Section 2.9.2.1) and ISA-2 software analysis (Section 2.9.2.3; Figure 6.3). In addition to the overall biofilm BVSA decreasing after exposure to concentrations of 200 and 2000 ppb, the maximum and minimum biofilm thickness were also affected by Ag NPs. At higher doses, biofilms tended to be thinner, when considering either the minimum and maximum biofilm thickness (Fig 6.3). This strongly suggests that exposure to Ag NPs created an overall thinning effect of the natural biofilm community, and the resultant decrease in BVSA was not the result of a patchy growth of the biofilm as a result of Ag NP exposure.

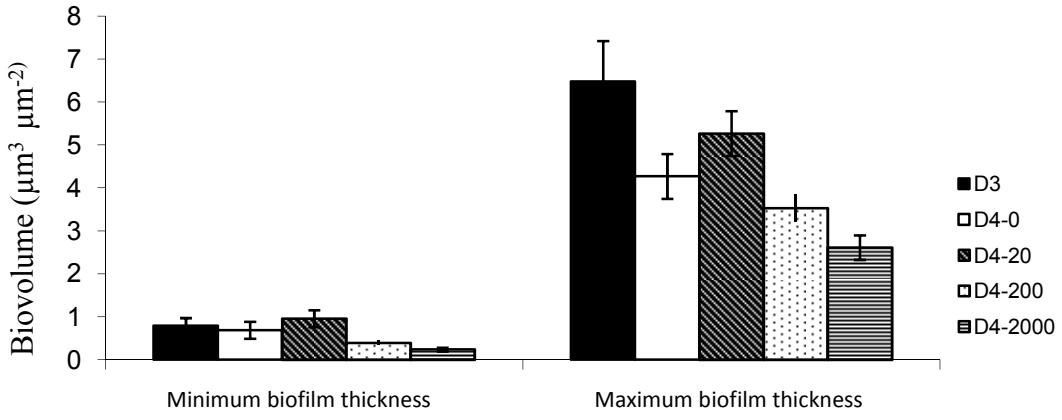

Figure 6.3 Maximum biofilm thicknesses of biofilms stained with lectin Concanavalin A and analysed with CSLM and ISA-2 software analysis. Bars represent 1 standard deviation.

Figure 6.4 shows selected CSLM images representing the proportional decrease on BVSA across treatments. Analysis of the controls D3 and D4-0 show how D4-0 increase by ca. 12 % on BVSA after 24h, indicating its successful growth and development in laboratory conditions.

The effects of a higher dose (2000 ppb) of Ag NPs to the community structure of this marine biofilm were studied and are discussed in Section 6. 4

6.3 Uptake of Ag NPs by biofilms

Total concentration of Ag uptake by biofilms as well as the concentration in seawater was quantified by AAS (Section 2.8). Over 24 hours, concentrations of total Ag (NP + dissolved; but primarily as NP, as only 1 % dissolution, see chapter 3) in control containers (seawater + Ag NP only) changed by 15-25 % (Table 6.1), indicating a loss over the time period used for the biofilm exposure, due to unavoidable aggregation and sedimentation and, possibly, to sorption to container walls. Thus the actual exposure doses were reduced by this factor over the 24 hours of experiment and the nominal values of 20, 200 and 2000 ppb were overestimates of actual dose. The Ag remaining in seawater after the 24h exposure to biofilms was also quantified (Section 2.8). 40-70% of Ag NP (depending on the initial concentration) stayed in suspension (Table 6.1). The total Ag NPs uptake was accurately determined by AAS (Section 2.8, Figure 6.5)

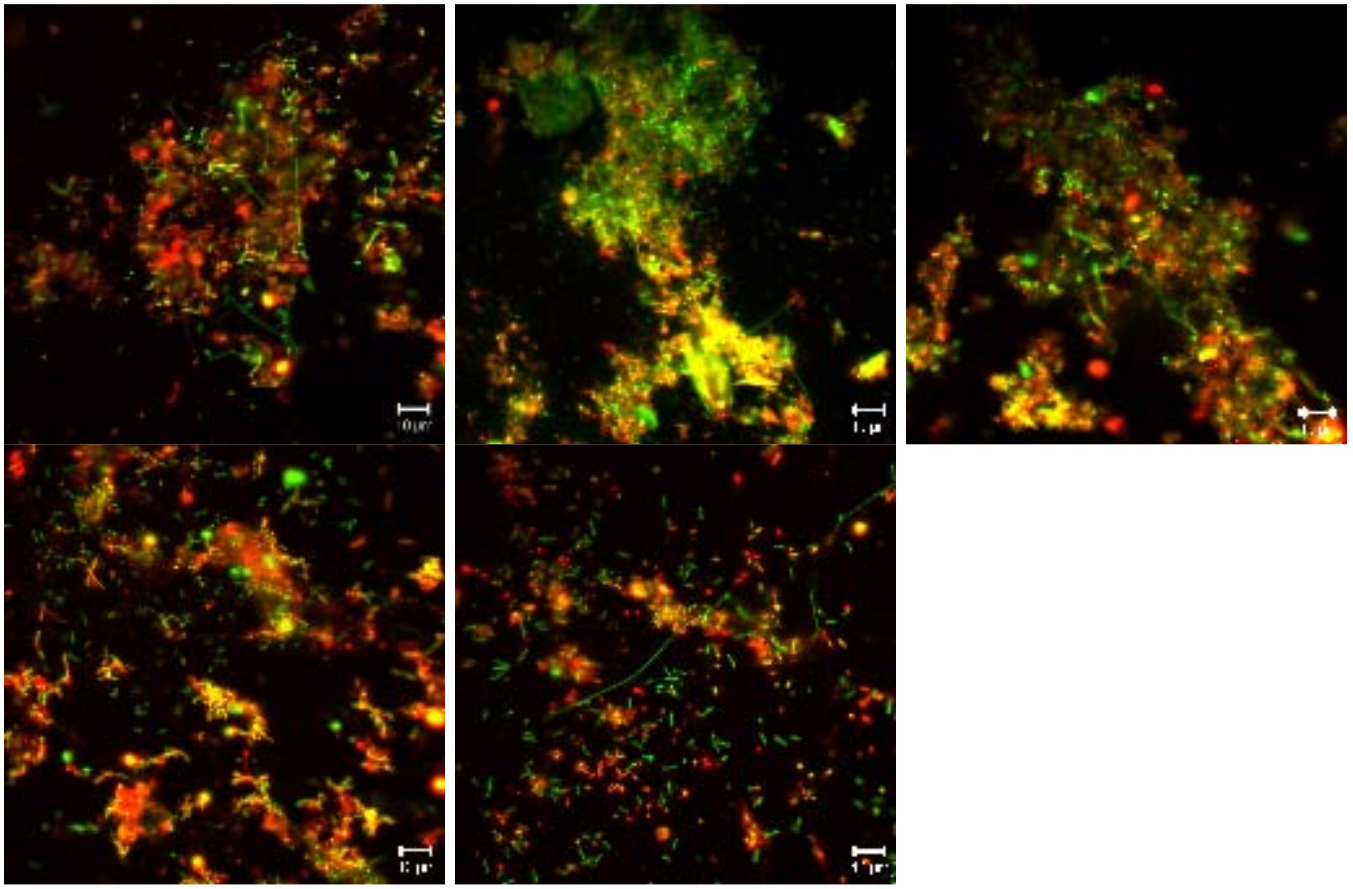

Figure 6.4. CSLM images of biofilms treated with different concentrations of Ag NPs. A) D3-0ppb; B) D4 0ppb; C) D4-20ppb; D) D4-200 ppb and E) D4-2000ppb. Bar represents 10 µm.

Table 6.1. Amount of Ag loss (%) over 24 h in treatment containers (without biofilms). Amount of Ag remaining (%) in seawater after a 24 h exposure with 3-d old biofilms.

Concentration (ppb)	*% Ag loss*	*% Ag remaining*
20	15.08 ± 3.18	45.2 ± 9.8
200	16.65 ± 5.15	53 ±15.75
2000	24.96 ± 9.38	69.10 ± 3.13

Figure 6.5 shows the uptake of Ag by biovolume of biofilm. The amount of Ag taken up per unit BVSA, by biofilms exposed to 20 ppb was 1.65±0.36 µg Ag cm^{-3}, exposed to 200 ppb was 18.32 ± 1.2 µg Ag cm^{-3} and almost 10 times higher for biofilms exposed to 2000 ppb, being 203.86 ± 31.26 µg Ag cm^{-3}. The uptake was linear: the Ag concentration in the BVSA increasd by 10-fold as the concentration of Ag NPs in suspension increased 10-fold.

Although biofilms were grown in a harbour with a high volume of industrial activities in the area the background levels of Ag in seawater were always below the limits of detection of the AAS (< 0.222 ppb).

6.4 Effect of Ag NPs on the biofilm community structure

Data in this section were analysed by Dr. Rui Zhang, University of Singapore

Terminal restriction fragment length polymorphisms (TRFLPs), a cultivation-independent DNA fingerprinting method mainly based on 16s rRNA gene sequence,

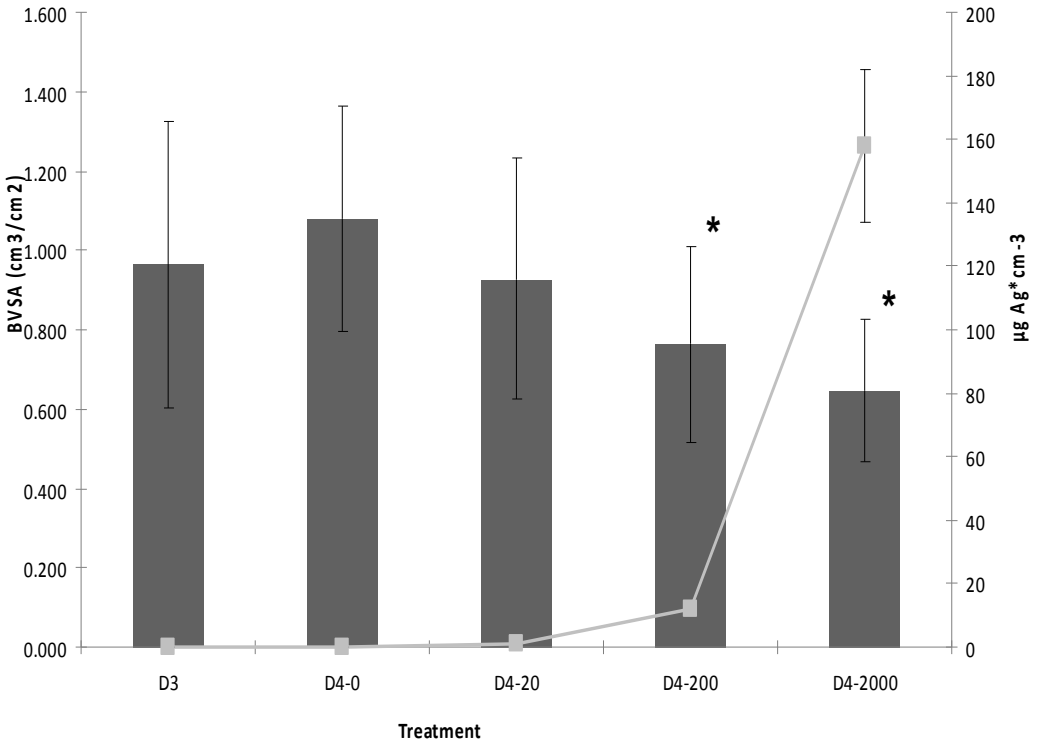

Figure 6.5 Amount of Ag NPs taken up per unit of biovolume (µg Ag cm^{-3}) from biofilm exposure for 24 h to different concentrations of Ag NPs (0-2000 ppb). Solid bars represent biovolume per surface area (BVSA); lines represent µg Ag cm^{-3} uptake per unit biovolume Error bars represent 1 standard deviation. * represent treatments significantly different from D4-0.

is a useful technique for estimating the complexity of natural bacterial communities (Liu *et al.* 1997), since only a minor fraction of natural occurring bacteria can be cultured and studied in the laboratory (Amann *et al.* 1995). TRFLPs method is used for the identification of different genotypes in communities (Zhang *et al.* 2008); it has been shown to be a rapid, convenient and highly reproducible method in microbial ecology (Kitts 2001; Zhang *et al.* 2008) and has already been used for the

comparison of bacterial communities in soils (Mrkonjic Fuka *et al.* 2009), bioreactors (Whang *et al.* 2008; Falk *et al.* 2009) and waters (Dillon *et al.* 2009). TRFLP results combined with phylogenetic studies (clone library analysis) allows a more detailed and more complete understanding of the effects of Ag NP to biofilm development and succession with a possible taxonomic assignment to terminal restriction fragment (T-RFs) and their relative abundance. Generally, T-RF patterns are generated by amplifying DNA fragments from bacterial assemblage using PCR with fluorescently labelled primers, and digesting the fragments with specific restriction enzymes (Zhang *et al.* 2008). The resulting DNA fragments or "DNA fingerprints" produced by specific restriction enzymes are used to assess the diversity and dynamics of microbial communities (Section 2.7.5.11).

In this study terminal restriction fragment (T-RF) patterns were generated by amplifying DNA fragments (Section 2.7.5.6) from the marine biofilms D3, D4-0 and D4-2000 using PCR with fluorescently labelled primers (Section 2.7.5.7). The amplified DNA was initially digested with three different restriction enzymes: *Rsa* I, *Hha* I and *Alu* I. These enzymes were chosen since their documented library is good and allows potential genotype identification of organisms based on their TR-F pattern obtained (Section 2.7.5.10). Fig. 6.6, Fig. 6.7 and Fig.6.7 represents the different type of taxa (number of TR-Fs or peaks) and abundance (TR-F/peak area) obtained by digesting the PCR product with *Rsa* I, *Hha* I and *Alu* I, respectively. The results show how the restriction enzyme *Rsa* I was not able to digest a large proportion of the PCR product (observed by detecting a very large T-RF peak at

about 920 base pairs (bp), instead of detecting a range of peaks of different base pairs, each peak representing a different taxa (Fig 6.6)). With the restriction enzyme *Hha* I the digestion showed very few T-RFs or peaks, which were mostly distributed near the detection limit of the CEQ machine (of ca. 50-60 bp, Fig 6.7; Section 2.7.5.11). Only *Alu* I digestion produced good T-RF patterns with more T-RFs and an even distribution, and therefore this profile was selected for cluster analysis.

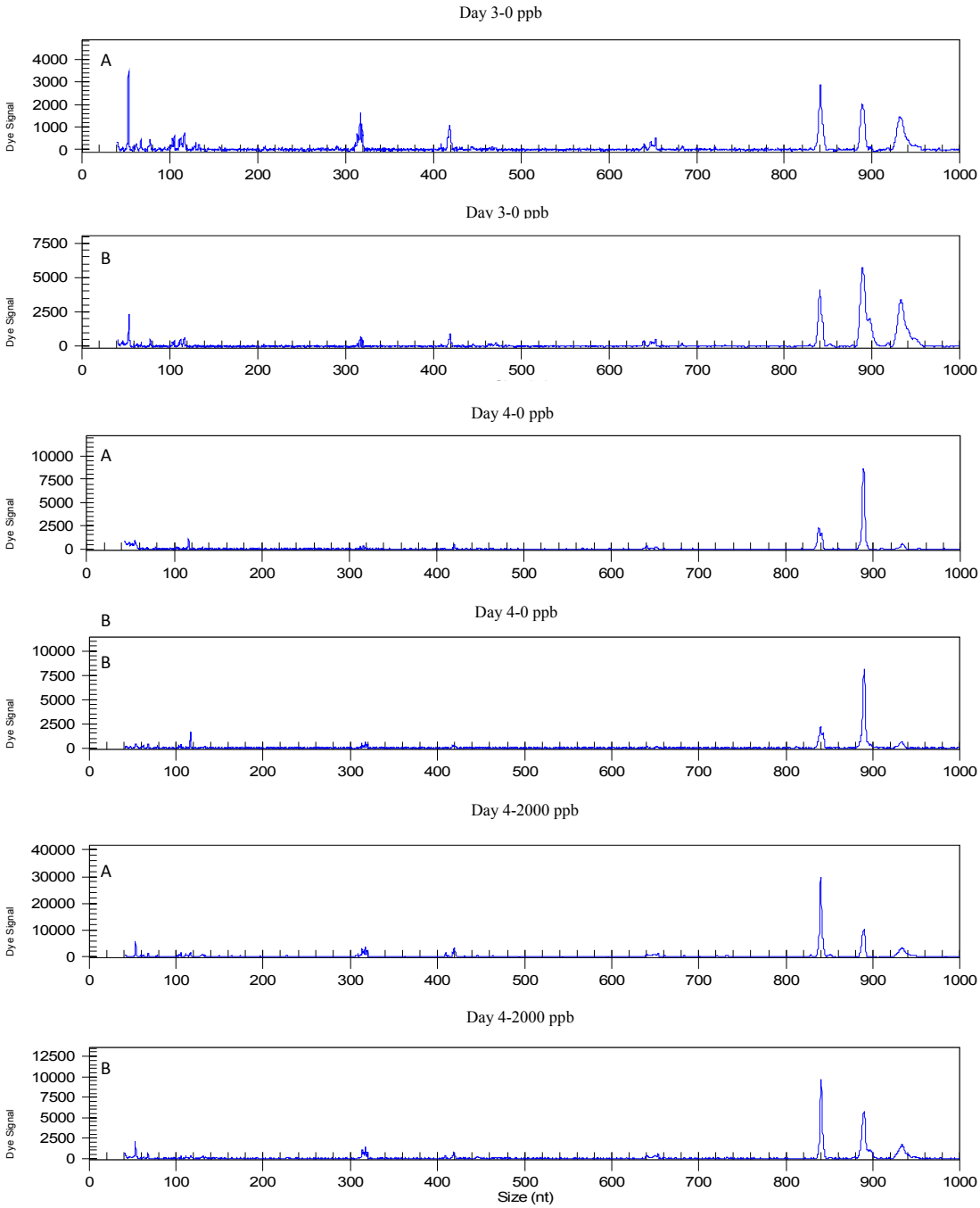

Figure 6.6 Terminal restriction fragment (T-RF) patterns generated with Rsa I restriction enzyme from the marine biofilm at D3,D4-0 and D4-2000 using PCR with fluorescently labelled primers. Labels A and B are replicates from the same treatment.

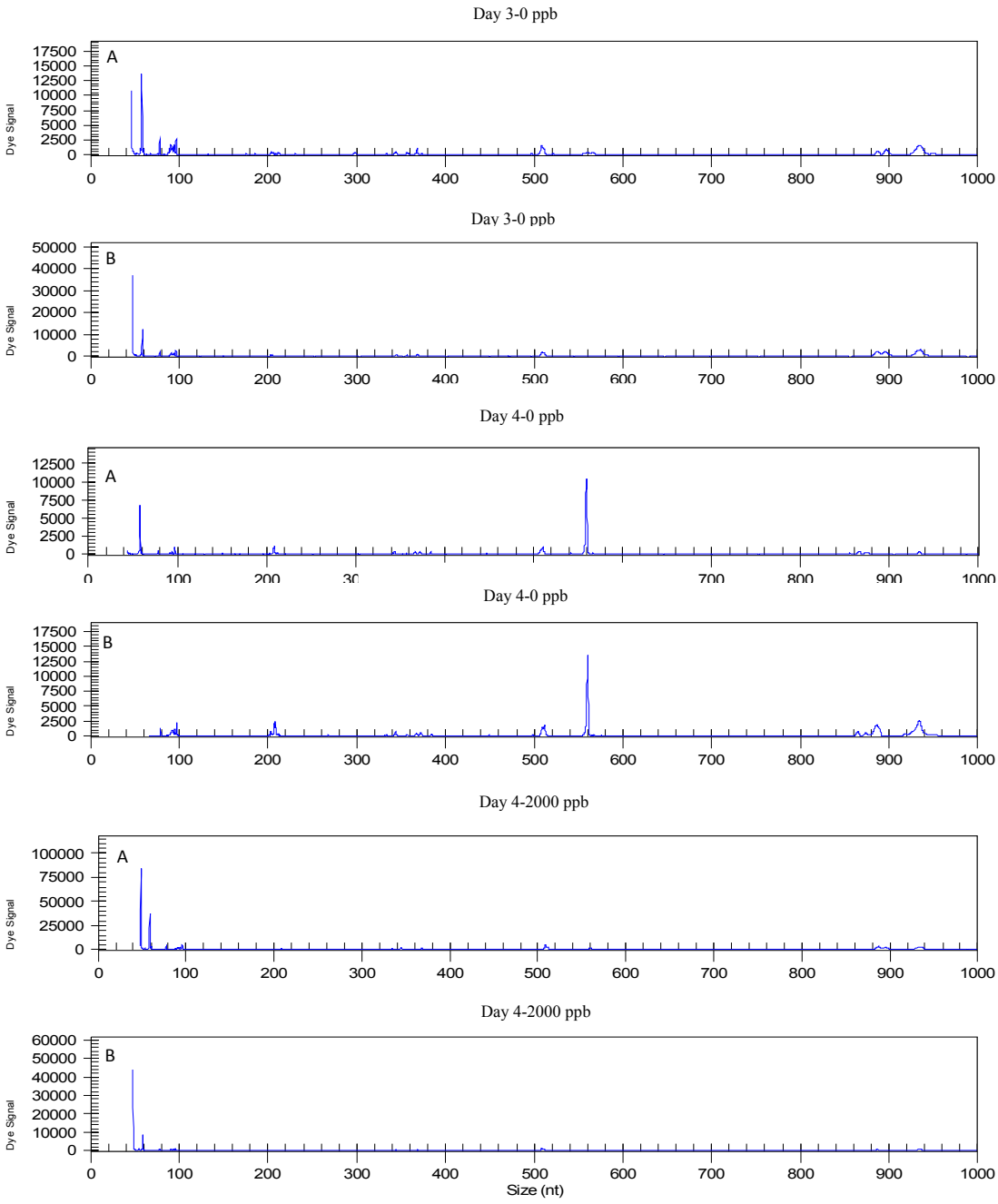

Figure 6.7 Terminal restriction fragment (T-RF) patterns generated with Hha I restriction enzyme from the marine biofilm at D3,D4-0 and D4-2000 using PCR with fluorescently labelled primers. Labels A and B are replicates from the same treatment

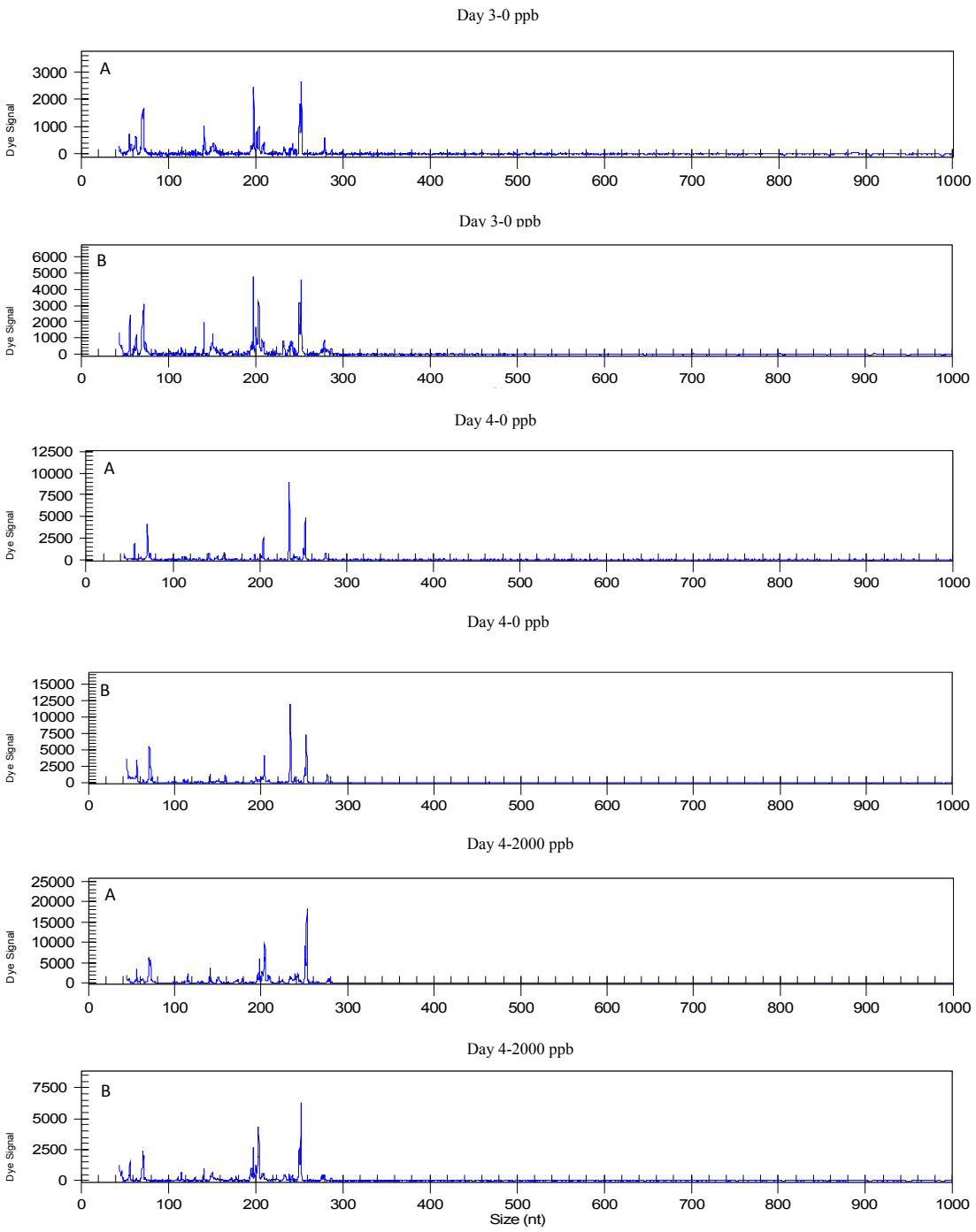

Figure 6.8 Terminal restriction fragment (T-RF) patterns generated with Alu I restriction enzyme from the marine biofilm at D3, D4-0 and D4-2000 using PCR with fluorescently labelled primers. Labels A and B are replicates from the same treatment

A cluster analysis (or analysis that partitions the data into groups and subgroups indicating the relationship among the resultant groups) was performed for all three biofilms and the results are shown in Figure 6.9. A cluster analysis/phylogenetic relationship among both clone libraries (D4-0 and D4-2000) was obtained (based on the grouping by "presence/absence" of taxa in the community), and confirmed the similarity among replicates (showed by clustering together, Fig. 6.9). After a 24 h incubation with Ag NP, the bacterial community structures of the exposed biofilm (D4-2000) showed similar T-RFLP pattern to that of the control biofilm at day 3 (D3). However, relatively different bacterial community structures were observed for control biofilm at day 4 (D4-0). The latter biofilm was a 3D old biofilm brought into the laboratory and allowed to develop for further 24 h in freshly sampled seawater under laboratory conditions and not exposed to Ag NPs (Section 2.7.5.3). The results indicated that, at the general community structure level, Ag NP treatment might "stop" the development or succession of biofilms, since the 4-day old biofilm exposed to Ag NPs and the 3-day old biofilm showed a similar community structure and both differed from the 4-day old unexposed biofilm.

Figure 6.9. Typical T-RFLP profiles (right panel) and cluster analysis (left panel) showing the dynamics of bacterial community structures of biofilm with different Ag treatment. Common T-RFs were indicated outside of profiles, while specific T-RFs were labeled in the according profile(s). Day 3: control biofilms at day 3; Day 4-Ag: 4 day old biofilm exposed for 24 h to 2000 ppb Ag NPs; Day 4-C: control biofilm at day 4.

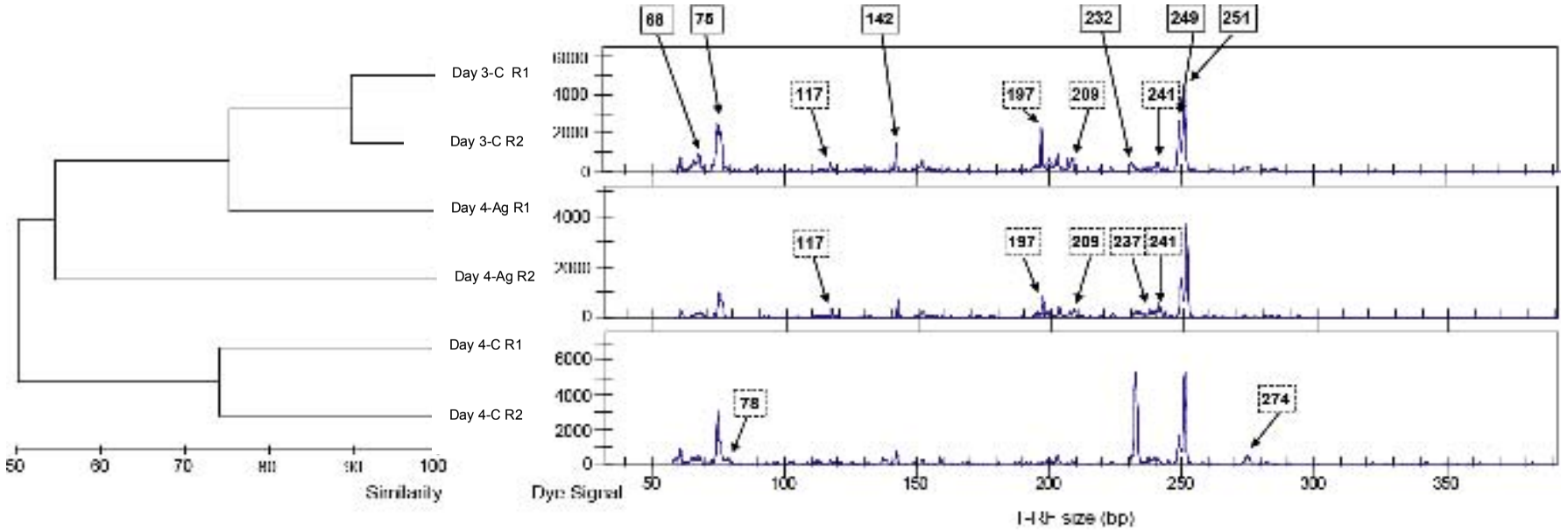

Two clone libraries from D4-0 and D4-2000 were created with the aim of determining and comparing changes in species richness between both treatments. A total of 70 clones were selected from both treatments and a total of 55 operational taxonomic units (OTUs) for Ag NP treated biofilm and 57 OTUs for the 4D control biofilm were obtained (Table 6.2). α-, γ-Proteobacteria and Flavobacteria were the most abundant phylogenetic groups in both clone libraries, and their abundance did not vary significantly among treatments. However, γ-Protecobacteria slightly decreased in abundance and species richness when Ag NPs were present. On the other hand, Cyanobacteria OTUs and clones showed a clear increase in number of species in biofilms incubated with Ag NPs (Table 6.2).

Table 6.3 shows possible taxonomic groups to T-RFs and their relative abundance (%). The major T-RFs were possibly produced by α-/ γ-Proteobacteria or Flavobacteria (T-RF 75 bp) and α-Proteobacteria (T-RF 251 bp). In terms of relative abundance γ-Proteobacteria was highly suppressed when Ag NPs were present (T-RF 232 bp), in contrast to of Cyanobacteria, which increased in relative abundance in the Ag NP treated biofilms (T-RF 197 bp).

Table 6.2 . Phylogenetic composition of clone libraries generated from samples with Ag treatment and control after four days incubation.

	Control		Ag	
Class	OTU	clone	OTU	clone
Alphaproteobacteria	23	35	25	34
Gammaproteobacteria	14	17	11	13
Flavobacteria	9	9	9	9
Cyanobacteria	2	2	6	7
Sphingobacteria	3	3	2	2
Actinobacteria	2	2	2	2
Deltaproteobacteria	1	1	1	1
Planctomycetacia	1	1	0	0
Lentisphaerae	0	0	1	1
Total	55	70	57	69

Table 6.3. Presence and possible phylogenetic assignment, revealed T-RFLP analysis of clone library, of T-RFs. The relative abundance (mean ± SD) were showed for present T-RFs. NA: not available.

	Day 3	Day 4		Phylogenetic assignment	
T-RF	Control	Control	Ag	Class	
68	6.14 ± 1.07%	2.48 ± 1.15%	1.39 ± 0.35%	α-proteobacteria	Uncultured bacterium
75	20.96 ± 0.64%	16.13 ± 0.61%	12.72 ± 1.88	γ-proteobacteria	Alteromonas sp., Thalassomonas sp., Oceanospirillum sp., Uncultured bacterium
				Flavobacteria	Uncultured bacterium
				Actinobacteria	Uncultured bacterium
78		1.30 ± 0.10%		NA	
117	1.03 ± 0.04%		1.32 ± 0.27%	α-proteobacteria	Uncultured bacterium
142	3.28 ± 0.08%	1.64 ± 0.12%	2.09 ± 0.90%	α-proteobacteria	Erythrobacter sp.
				Lentisphaerae	Lentisphaera sp.
197	5.31 ± 0.17%		2.34 ± 1.24%	Cyanobacteria	Bacillariophyta sp. Chloroplast
209	2.46 ± 0.34%		1.30 ± 0.05%	α-proteobacteria	Oceanicaulis sp., Uncultured bacterium
232	2.04 ± 0.97%	24.03 ± 0.17%	2.03 ± 1.03%	γ-proteobacteria	Alteromonas sp., Oleiphilus sp., Uncultured bacterium
237			1.78 ± 0.58%	Actinobacteria	Acidimicrobium sp., Uncultured bacterium
				Flavobacteria	Algibacter sp., Uncultured bacterium
				γ-proteobacteria	Alkalilimnicola sp.
				Sphingobacteria	Uncultured bacterium
241	1.90 ± 0.48%		3.05 ± 0.51%	Flavobacteria	Uncultured bacterium
249	8.41 ± 1.10%	6.18 ± 0.26%	7.08 ± 0.27%	α-proteobacteria	Jannaschia sp., Paracoccus sp., Roseovarius sp., Silicibacter sp., Uncultured bacterium
251	16.73 ± 1.60%	18.73 ± 0.61%	21.64 ± 0.68%	α-proteobacteria	Jannaschia sp., Silicibacter sp., Uncultured bacterium
				γ-proteobacteria	Vibrio sp.
274		1.38 ± 0.07%		NA	

6.5 Discussion

6.5.1 Ag NPs effect to marine biofilms

The crystal violet assay is a reliable and simple method for quantifying changes on growth and for sample sizes as large as the ones used for this experiment. This technique has been applied to quantify bacterial BVSA since the mid-1980s (Bonnekoh *et al.* 1989), works well and has been verified in a number of studies (Arnold 2007; Jagani *et al.* 2009; Van Essche *et al.* 2009). Although calibration curves were not produced which quantified the volume of BVSA per unit of substrate it was an appropriate technique for determining changes of BVSA across Ag NP treatments. CSLM results yield large standard deviation bars (Fig 6.2) indicating a larger number of replicates are required because of regional differences on the substrate.

Results show that exposure to Ag NPs caused a detrimental effect on young natural bacterial communities in marine biofilms. Concentrations of 200-2000 ppb produced a decrease in the biofilm thickness compared to the control biofilm. In addition, exposure to a concentration of 2000 ppb also affected the species composition after a short exposure time of 24 h (Fig. 6.10 & Fig. 6.11). Although the 4D-20 biofilm did not show any variation in growth compared to 3D the data collected are not sufficient to determine whether 20 ppb causes a bacteriostatic effect, altering the composition of the microbial population. Ag NPs could be suppressing the growth of certain organisms in the mixed marine biofilm

community, allowing other organisms to benefit from the reduced growth of those potential competitors and partially or totally displace them. This could lead to equal amounts of BVSA but a very different composition and abundance of species. Bacteriostatic concentrations should be determined individually for each taxon to understand the development the community may experience.

The uptake of Ag NPs was significant in all treatments, increasing by *ca.* 10-fold as the concentration increased 10-fold. Thus, this indicates that Ag NPs or dissolved Ag product derived from the Ag NPs remained bioavailable to the microorganism community with increasing concentration. However, neither the uptake mechanism nor interaction among cells and NPs were determined in this work, since behaviour and toxicity of Ag NPs to marine aquatic systems and to natural communities of marine microorganisms are difficult to investigate due to the complexity of Ag speciation in the marine environment (Erickson *et al.* 1998; Bury *et al.* 1999; Bielmyer *et al.* 2007).

6.5.2 Ag uptake by biofilms

The Ag uptake by biofilms was quantified by AAS (Fig. 6.3), and showed Ag was taken up by microorganisms. Ag NPs were soluble at a fraction of 1% only (salinity of 30 ‰, 25 °C, Chapter 3). However, the total Ag taken up by the biofilms ranged from 5-40 % (Table 6.1; depending on the initial concentration), concluding that regardless of the higher bioavailability of the chloro-complexes produced as a result of solubilised Ag (< 1%), a high percentage of Ag NPs were also taken up by the biofilm (4-39%). Nevertheless, the potential enhanced dissolution of Ag NPs

when microorganisms were present was not quantified, and could have increased the concentration of ionic silver in solution (Navarro *et al*. 2008).

This solubility of Ag NPs (ca. 1 %) in culture medium has also been determined by Navarro *et al.* (2008), who investigated the toxicity of Ag NPs on the algae *Chlamydomonas reinhardtii.* Overall, the literature describing toxicity of various NMs to microorganisms is still very limited although silver NPs, along with fullerenes and titanium dioxide are among the best studied NMs with respect to microbial toxicity (Handy *et al.* 2008; Klaine *et al.* 2008). The toxicity mechanism of Ag NPs has been investigated in bacterial cells in culture media, and has been mostly attributed to formation of ionic Ag and oxidative damage by the formation of ROS (Choi & Hu 2008a; Hwang *et al.* 2008; Schrand *et al.* 2008; Sharma *et al.* 2009). Small particle size uptake (< 5 nm) and pitting of cell membranes has also been reported by many authors (Morones *et al.* 2005; Pal *et al.* 2007; Hwang *et al.* 2008).

6.5.3. Ag NPs effect to community structure

Terminal restriction fragment length polymorphism (T-RFLP) results (which allows analysis of complex bacterial communities) combined with phylogenetic studies (clone library analysis) allow a more detailed and more complete understanding of the effects of Ag NP to biofilm development and succession with a possible taxonomic assignment to T-RFs, and their relative abundance. T-RFLPs analysis was applied to day 4 marine biofilm with/without Ag NP-treatment, as well as to day 3 control (before Ag NP incubation). T-RFLP patterns and subsequent

cluster analysis showed similar bacterial community structure among replicates, which confirm the reproducibility of the experimental setup. Digestion with three different enzymes (*Alu* I, *Hha* I and *Rsa* I) revealed similar clustering among treatments (Figure 6.9). After 24 h incubation with 2000 ppb Ag NPs (day 4-2000), bacterial community structures of the Ag NP-exposed biofilm showed a similar T-RFLP pattern, and hence a similar community structure, to that of the 3-day control biofilm (day 3-0). However, different bacterial community structures were observed for 4-day control biofilm (not exposed to Ag NP; (day4-0)). Close observation of T-RFs showed that, six major peaks (T-RFs of 68, 75, 142, 232, 249, and 251bp) appeared in all samples, while other four peaks (T-RFs of 117, 197, 209 and 241bp) were present only in 3-day control biofilm and 2000 ppb Ag NP-exposed biofilm (day 4-2000). One and two unique peaks were observed in day 4-2000 and day 4-0 biofilms, respectively (Figure 6.9).

Two clone libraries from day 4-0 and day 4-2000 were also constructed to determine and compare changes on bacterial communities among both treatments. A total of about 70 clones were selected from each treatment and a total of 55 operational taxonomic units (OTUs), based on 97% similarity of bacterial 16S rRNA gene sequence, for the Ag NP treated biofilm and 57 OTUs for the day 4-0 biofilm were obtained (Table 6.2). Most of the major T-RFs could be matched to clones by both *in silico* digestion and the true T-RFLP analysis (Figure 6.3). Common peaks which appeared in all three sets of samples included α- and γ-*Proteobacteria*, *Flavobacteria*, *Actinobacteria* or *Lentisphaerae*. Compared to clone library analysis,

similar trends of increasing *Cyanobacteria* (T-RF of 197 bp) in Ag NPs-treated samples were indicated based on T-RFLP pattern after phylogenetic assignment of T-RFs. Furthermore, a γ-*Proteobacteria* (*Alteromonas*-like) T-RF （232bp, Table 2 and Figure 4) bloom was revealed in day 4 control biofilms by T-RFLP analysis. However, our attempts to identify unique T-RFs in Ag NPs treated and untreated samples were unsuccessful due to both matching of peaks to multi-clones and no matching of peaks (Table 6.3).

The results on T-RFLP and subsequent cluster and phylogenetic analysis showed that exposure to Ag NPs significantly affected the community structure of marine biofilms. Nevertheless, all treated biofilms showed the presence of major bacterial groups (γ-*Proteobacteria*, *Flavobacteria*, *α-Proteobacteria* and *Cyanobacteria*) suggesting that even at the highest concentrations studied the major taxonomic groups are not displaced. However, the variations in T-RF peak areas indicate that Ag NPs do affect the relative abundance of major bacterial groups in the Ag NP exposed biofilms. This observation suggests that exposure to Ag NPs stopped normal biofilm development and succession in these samples. In addition two unique peaks appeared in the control at day 4, suggesting that the presence of Ag NPs prevents settlement or colonization of new bacterial groups onto the biofilm, and that biofilm succession is significantly modified by the presence of the NPs. In the Ag NP exposed biofilms, one small novel peak (T-RF of 237 bp) appeared, but could not be identified; whether the bacterium producing this peak was a Ag-resistant or Ag-favourable organism need further investigation.

The impact of Ag NPs have been previously investigated in well established sediment and soil microbial communities (Bradford *et al.* 2009), and sludge plant nitrifying bacterial assemblages (Choi *et al.* 2008; Choi & Hu 2008b; Choi *et al.* 2009). Whereas a size dependent inhibition on growth was responsible for a ca. 90 % decrease on growth on a natural nitrifying community (Choi *et al.* 2008; Choi & Hu 2008b); little or no perturbations were detected after a 30 day exposure to Ag NPs on the genetic assemblages of soil communities. Most likely the reduced toxicity is due the increased organic and solid phase material in sediments, which has been shown to reduce short term toxicity (Choi *et al.* 2009; Gao *et al.* 2009). In this study a rapid turnover of species and succession was seen in the untreated samples (day 3 to day 4 control biofilms) as it is expected (Ohashi & Harada 1994; Busscher *et al.* 2000). Yet, Ag NP treatment affected this succession and had significant effects on bacterial species distributions, with potential longer term effects on community structure and function. Impeded succession could be due to a toxic effect on potential planktonic colonisers or accumulation of Ag NPs on the biofilm affecting settling and cell attachment with consequent proliferation.

Overall, microbial communities are often resilient to perturbations (Nannipieri *et al.* 2003), and microorganisms that tolerate certain environmental stress (i.e toxicants, drastic pH changes, etc) may appear with time . This could be the case in our present study, in which Ag-resistant microorganisms might have been selected and would proliferate if the community remained exposed to the metal. A

slight enrichment of a bacterial group after 24 h could lead to a larger scale shift after a chronic exposure.

7 Conclusions & future work

The present study was designed to investigate the physico-chemical changes of Ag NPs in aqueous suspension under different environmental parameters, and their effect on bacterial cells; with particular focus of how changes of relevant environmental conditions, such as pH and the presence of organic matter, can modify Ag NP uptake, cellular interactions, and the ultimate fate and behaviour in water systems.

Currently, several researchers have investigated the effects of Ag NPs to laboratory grown bacteria, however comprehensive studies on biofilms and the implication of different environmental parameters on the uptake and interaction of Ag NPs are lacking.

Preliminary experiments demonstrated that the model organisms chosen: *Pseudomonas fluorescens* and *Pseudomonas putida,* grown as planktonic cells and as biofilms respectively, were suitable for investigating the biological effects and interactions of Ag NPs at pH 6, 7.5 and 9 as well as with the presence of humic or fulvic substances. Pseudomonas growth showed comparable growth curves at pH values of 6, 7.5 and 9, with slightly different lag phases and biomass concentrations at the stationary phase. The biomass concentration in MDM increased when SRHA were present, indicating that these bacteria can use HS as a carbon source.

The compromise between using a culture media with appropriate buffering capacity, and a media that due to the high concentrations of salts would increase the aggregation and precipitation rates of Ag NPs, was attained using MDM. Previous studies looking at the toxicity of nanotubes have also used MDM as bacterial media due to the benefits of its lower phosphate content reducing NP precipitation (Lyon *et*

al. 2005; Lyon *et al.* 2006; Lyon *et al.* 2008c). The changes in the pH of the MDM during incubations were monitored and were found to be minimal, confirming that MDM is a suitable medium for planktonic 24 h exposure assays of Ag NPs.

The development of this work has also helped to design an appropriate flow though cell reactor for investigating the effects of Ag NPs to laboratory grown biofilms. The designed flow through cell system is adequate for allowing the independent sampling of biofilms, as well as the media containing Ag NPs before and after exposure to biofilms, with direct implications for the understanding of NP behaviour before and after contact with biofilms.

The initial part of this research was laboratory based, so that variations on environmental factors that affect Ag NP behaviour could be controlled. A field experiment was also performed to establish weather Ag NPs are likely to affect natural bacterial assemblages in a more complex water system than the artificial media used in the laboratory.

The initial aim of this project was to determine if the behaviour of Ag NPs in different aqueous suspensions would differ with varying environmental parameters such as pH and presence of organic matter. In order to address this matter, the following hypotheses were tested:

Ho: If Ag NPs behaviour does not vary with changes of pH values of 6, 7.5 and 9, and presence or absence of 10 mg l^{-1} humic substances, then no variations on aggregate formation, residence time in suspension and solubility will be observed across conditions.

H1: If Ag NPs behaviour does vary with changes of pH values of 6, 7.5 and 9, and presence or absence of 10 mg l^{-1} humic substances, then variations on aggregate formation, residence time in suspension and solubility will be observed across conditions

This work has shown that Ag NPs tend to form aggregates of a few hundred

nanometers once suspended in both, MDM and seawater, and aggregate formation and residence time of the nanoparticle in suspension were affected by pH and presence of humic substances. Thus, the hypothesis *Ho* was rejected. Solubility of Ag NPs in both media and the consequent formation of Ag ions were minimal under all conditions and always < 2%. Formation of Ag ions can play a major role on Ag NP toxicity as previously determined by other authors (Navarro et al. 2008, Lok et al. 2007), and for the purpose of this work it was necessary to differentiate between the toxicity exerted by the nanoparticle itself (surface, charge and/or shape) from the toxicity of the soluble fraction of the particle (due to release of Ag ions). In MDM, a low ionic strength solution (I=0.05M), the major component affecting Ag NPs stabilisation and variations in the resident time in suspension changing Ag NP stability, size of aggregates, and charge was the presence of humic substances in the medium. Humic substances absorbed on the Ag NP surface, as shown previously for other NPs (Baalousha *et al.* Submitted) and for colloids (Lead *et al.* 2005), consequently affected forces of attraction and repulsion between NPs. However, in seawater, a much higher ionic strength solution (I=0.7M), HS aggregated as a result of the high $CaCl_2$ concentrations (Wilkinson 2005; Chen & Elimelech 2007) and their effects on the change Ag NP behaviour and fate were not significant.

A second aim of this research was to investigate if the toxicity of Ag NPs to *Pseudomonas fluorescens* planktonic bacteria would be affected by variations on the pH of the exposure media, as well as by the presence of organic matter. In order to address this matter the following hypotheses were tested:

Ho: If the toxicity of Ag NPs to planktonic Pseudomonas fluorescens does not vary with changes of pH values of 6, 7.5 and 9, and presence or absence of 10 mg l^{-1} humic substances, then no variations on the population density of the exposed bacteria will be observed across conditions.

H1: If the toxicity of Ag NPs to planktonic Pseudomonas fluorescens does vary with changes of pH values of 6, 7.5 and 9, and presence or absence of 10 mg l^{-1} humic substances, then variations on the population density of the exposed bacteria will be observed across conditions.

Ag NPs were toxic only at the highest concentration tested and at pH 9 without SRHA. Thus, the hypothesis *Ho* was rejected. Under these conditions, the soluble fraction of the Ag NPs was only ~ 2% (43.3 ± 0.06 ppb), and was considerably lower than the concentration of Ag ions required to cause similar decrease in bacterial cell density (of > 200 ppb Ag NO_3). Therefore the observed toxic effect of the Ag NPs was not only caused by the dissolved Ag^+ from the Ag NPs. The cause of toxicity was related to the NP itself and its interactions with the bacteria. TEM results suggest that Ag NPs tend to disaggregate with SRHA, and give a high concentration of very small NPs. Initially, and considering pervious research that suggests that NP toxicity relates to the size and individuality of NPs in suspension (Sondi & Salopek-Sondi 2004; Morones *et al.* 2005; Pal *et al.* 2007; Choi *et al.* 2008), a higher increase in toxicity from the Ag NPs was expected with SRHA. Although the presence of SRHA decreased the size of the Ag NPs aggregates, leading not only to smaller aggregates but also to single NPs, they also decreased their toxicity. Most likely, toxicity was mitigated due to the sorption of SRHA onto the NP surface and consequent changes in surface properties of the particle. The HS may simply be providing a physical barrier between the cell and NP. In addition, the change on the surface charge of the Ag NPs once coated will also affect their interaction with the bacterial cell. More sophisticated mechanisms may be involved, and further experiments are required to confirm whether this reduced effect on bacterial cell growth occurs over longer time periods. If the decrease is related to the physical barrier or coating provided by the SRHA, it could happen that after longer

exposure times the microorganisms could degrade the coating and directly interact with the Ag NP again.

Planktonic bacterial cells are ubiquitous in natural systems and are the vectors for colonization of new niches by existing biofilms. The results of this work suggest that in freshwater and under natural conditions (circumneutral pH values and concentrations of organic matter of ca. 10 mg L^{-1}) Ag NPs toxicity is negligible to planktonic *P. fluorescens,* and is more likely due to HS coating the NP and changing their properties. In freshwater systems of low organic matter content, the toxicity exerted by the NP increases due to the lack of the protective effect of HS coating the NP. Ag NPs stability in suspension also increases with the presence of organic matter, increasing dispensability of the NPs and lowering aggregation rates.

Preliminary results showed the stability of the Ag NPs in aqueous suspension was low, and their ultimate fate was likely to be a benthic system. Hence, benthic ecosystems, such as biofilm communities, might be more appropriate models than planktonic organisms for predicting fate of Ag NPs when entering natural waters. Thus, in order to investigate the implications of Ag NPs on biofilms, the effects of different environmental conditions on the interaction and uptake of Ag NPs by *Pseudomonas putida* biofilm were studied, and the following hypotheses were addressed:

Ho: If the effects of Ag NPs to biofilm Pseudomonas putida do not vary with changes of pH values of 6 and 7.5, and presence or absence of 10 mg l^{-1} fulvic substances, then no effect on the biofilm biovolume, cellular viability and silver uptake of the exposed bacteria will be observed across conditions.

H1: If the effects of Ag NPs to biofilm Pseudomonas putida do not vary with changes of pH values of 6 and 7.5, and presence or absence of 10 mg l^{-1} fulvic substances, then an effect on the biofilm biovolume, cellular viability and silver uptake of the exposed bacteria will be observed across conditions.

The results of this study confirm that Ag NPs interact and are taken up by *P. putida* cells. The degree of Ag NP-cell interaction as well as uptake was dependent on the pH and of the presence of SRFA in the media. Thus, the hypothesis *Ho* was rejected. Indeed, Ag NPs were detected in biofilm cell membranes at both pH values tested, but only with SRFA present. Also, at both pH values, with SRFA a higher uptake of ca. 50 % was quantified in comparison to biofilms exposed to Ag NPs without SRFA. However, although biouptake was higher when SRFA were present, the effects of exposure of high concentrations of Ag NPs to biofilm biovolume were only significant without SRFA. Hence, the physico-chemical properties of the particles are highly relevant to ecotoxicological behaviour, as is exposure concentration. This could be explained since SRFA not only affect the physico-chemical properties of the particle, but also is used as a source of carbon to *P. putida* cells. Consequently, *P. putida* cells may be increasing the Ag NP uptake since they are initially interacting with the humic substances coating the NPs. Longer exposure times may have shown different results, if ultimately *P.putida* cells would use up the SRFA coating and interact with the Ag NPs within the matrix.

The significant decrease in biovolume to surface area observed at pH 6 and 7.5 without SRFA was independent of the exposure concentration; *i.e.* a higher amount of Ag NPs did not lead to an enhanced degree of toxicity. This could be the result of either a particle a saturation state in the biofilm (a solution of 20 ppb contains 600,000,000 particles, while a solution of 2000 ppb has 100 times this value); or a thinning mechanism based on the friction and consequent detachment of cells due to the flow of aggregates of 200-300 nm over biofilms of cells 8 to 10 times larger. The viability of the biofilm was not significantly different among pH values

and conditions tested, suggesting the observed thinning effect is caused by detachment of bacterial cells by friction or by cells detaching to remove noxious particles from the biofilm, and not by a chemical inhibition of growth.

Ag NPs are potential environmental stressors and because of their size they may be likely to interact with the uppermost layer of bacteria in biofilms. This could explain the high amount of cells being detached from the biofilms. This initial high concentration of biofilm cell detachment could be a defence mechanism to protect the established biofilm population. However, this was not investigated and further studies should be undertaken to understand the effects of NPs biofilm structure and composition.

A phenomenon also observed in biofilms after exposure to Ag NPs is the lower electron density area within the bacterial cells at both pH values tested. This observation has previously been described by Morones *et al.* (2005) when *E.coli* cells were being exposed to Ag nitrate solution, but to my knowledge has never been observed with exposure to Ag NPs. This low electron density area is the result of conglomerated DNA which is a mechanism of defence by the bacteria when sensing noxious compounds (Morones *et al.* 2005, Feng *et al.* 2000). This indicates that although a low number of NPs are being taken up, there is also a potentially NP mediated effect disrupting cytoplasmatic functions when in contact with cell membranes.

The mode of interaction of the particles with the cell was not investigated in this work. For instance, it is uncertain if NPs were disaggregated in the media and aggregated once in contact with the cell membrane. Initially NPs formed small aggregates in suspension, and some fully dispersed NPs were detected with HS present; however it is uncertain if the cell interacts with the NP directly or if biofilms

are indirectly sequestering the NPs within the matrix by directly interacting with the SRFA coating the particle.

The last aim of this research was to investigate the potential effects of Ag NPs when released into natural waters. In order to address this question the effects Ag NPs may have on a natural bacterial biofilm community the following hypotheses were formulated:

Ho: If exposure of Ag NPs does not affect marine biofilms, then a change on biofilm biovolume and variations on the species composition of the community will not be observed.

H1: If exposure of Ag NPs does affect marine biofilms, then a change on biofilm biovolume and variations on the species composition of the community will be observed.

Results show that marine biofilms were able to uptake Ag NPs from the surrounding seawater, and exposure to Ag NPs caused a detrimental effect, decreasing biofilm biovolume and affecting species succession after a short exposure time of 24 h. Thus, the hypothesis *Ho* was rejected. The uptake of Ag NPs was significant in all treatments, increasing by *ca*. 10-fold as the concentration increased 10-fold. Therefore, this indicates that Ag NPs or a dissolved Ag product derived from the Ag NPs remains bioavailable to the microorganism community with increasing concentration. However, neither the uptake mechanism nor interaction among cells and NPs were determined in this work, since behaviour and toxicity of Ag NPs to marine aquatic systems and to natural communities of marine microorganisms is difficult to investigate due to the complexity of Ag speciation in the marine environment (Erickson *et al.* 1998; Bury *et al.* 1999; Bielmyer *et al.* 2007). The results on T-RFLP and subsequent cluster and phylogenetic analysis showed that exposure to Ag NPs significantly affected the community structure of

marine biofilms. Nevertheless, all treated biofilms showed the presence of major bacterial groups (γ-*Proteobacteria*, *Flavobacteria*, *α-Proteobacteria* and *Cyanobacteria*) suggesting that even at the highest concentrations studied the major taxonomic groups are not displaced. However, the variations in T-RF peak areas indicate that Ag NPs do affect the relative abundance of major bacterial groups in the Ag NP exposed biofilms. A rapid turnover of species and succession was seen in the untreated samples as is expected for young bacterial communities (Ohashi & Harada 1994; Busscher *et al.* 2000). Yet, Ag NP treatment affected this succession and had significant effects on bacterial species distributions, with potential longer term effects on community structure and function. Impeded succession could be due to a toxic effect on potential planktonic colonisers or accumulation of Ag NPs on the biofilm affecting settling and cell attachment with consequent proliferation.

Biofilms have shown to be a very good model for investigating Ag NP behaviour and their effects. Natural aquatic bacterial communities are complex systems with vital roles in nutrient cycling and in food webs. Investigating the effects of Ag NPs to these communities under different environmental conditions brings a more realistic approach of the long term effects Ag NPs can have in the environment.

The outcomes of these investigations have shown the role environmental parameters such as pH and presence of humic substances have on the behaviour, fate of Ag NPs in aqueous suspensions, and ultimately to planktonic and biofilm bacterial cells. The results of this work suggest that in order to assess toxicity of NMs in the environment a detailed understanding on the physico-chemical changes of NMs under relevant environmental conditions is needed.

Recommendations for future work

Future work investigating the toxicity and fate of NMs to organisms and to the environment should use well defined NMs, and ideally their physico-chemical changes should be monitored over the time of exposure.

Off-the-shelf samples are not recommended for this type of studies since parameters such as the size of the aggregates vary systematically, affecting behaviour and possibly the consequent interactions with microorganisms.

It is also important to refine and standardise protocols for NP dispersion in different aqueous solutions. A defined sample handling and preparation is crucial for cross-lab unbiased results. Future work on toxicity should take into consideration factors that could enhance particle toxicity (i.e. sonication vs. stirring, use of surfactants, etc.).

Future research investigating the effects and uptake of Ag NPs by bacterial cells are required, and a special focus on the mechanisms of biouptake is needed to understand the mode of action of Ag NPs to prokaryotic organisms. Investigating the toxicity mechanisms of Ag NPs could benefit from segregating particles based on narrower size distributions and shapes, since these two parameters have been suggested by researchers to affect toxicity. Investigating sublethal effects of Ag NPs could also facilitate defining their mode of action to bacteria.

The results of this thesis also indicate that longer term studies and exposures are needed to define the long term effects of the use of NMs. The Ag NP exposures in this work were of only 24h. When Ag NPs were mixed with humic substances

prior exposure biofilms increased their uptake possibly due to the use of the humic substances coating the Ag NPs as a food source. This coating also mitigated short term toxicity. Yet, if longer term studies were conducted, and after biofilm cells would have utilised the humic substance coating of the Ag NP, an increased toxicity might have been observed.

References

Adams L.K., Lyon D.Y. & Alvarez P.J.J. (2006). Comparative eco-toxicity of nanoscale TiO2, SiO2, and ZnO water suspensions. *Water Research*, 40, 3527-3532.

Ahamed M., Karns M., Goodson M., Rowe J., Hussain S.M., Schlager J.J. & Hong Y. (2008). DNA damage response to different surface chemistry of silver nanoparticles in mammalian cells. *Toxicology and Applied Pharmacology*, 233, 404-410.

Ahmad A., Mukherjee P., Senapati S., Mandal D., Khan M.I., Kumar R. & Sastry M. (2003). Extracellular biosynthesis of silver nanoparticles using the fungus Fusarium oxysporum. *Colloids and Surfaces B: Biointerfaces*, 28, 313.

Aitken R.J., Chaudhry M.Q., Boxall A.B.A. & Hull M. (2006). Manufacture and use of nanomaterials: current status in the UK and global trends. *Occupational Medicine-Oxford*, 56, 300-306.

Ajayan P.M. & Zhou O.Z. (2001). Applications of carbon nanotubes. In: *Carbon Nanotubes: Synthesis, Structure, Properties and Applications.* Springer, pp. 391-421.

Alarcon-Waess O. & Mendez-Alcaraz J.M. (2008). Electrophoretic mobility of colloidal particles in dilute suspensions. In: *Recent Developments in Physical Chemistry: Third Mexican Meeting on Mathematical and Experimental Physics. AIP Mexico City* (Mexico), pp. 83-94.

Allison D.G., Ruiz B., SanJose C., Jaspe A. & Gilbert P. (1998). Extracellular products as mediators of the formation and detachment of Pseudomonas fluorescens biofilms. *FEMS Microbiol. Lett.*, 167, 179-184.

Amann R.I., Ludwig W. & Schleifer K.H. (1995). Phylogenetic Identification and in-Situ Detection of Individual Microbial-Cells without Cultivation. *Microbiological Reviews*, 59, 143-169.

Amos M.D. & Willis J.B. (1966). Use of high-temperature pre-mixed flames in atomic absorption spectroscopy. *Spectrochimica Acta*, 22, 1325-&.

Arcoleo V. & Liveri V.T. (1996). AFM investigation of gold nanoparticles synthesized in water/AOT/n-heptane microemulsions. *Chemical Physics Letters*, 258, 223-227.

Arnold J.W. (2007). Colorimetric assay for biofilms in wet processing conditions. In: *2nd International Conference on Environmental, Industrial and Applied Microbiology*. Springer Heidelberg Seville, SPAIN, pp. 1475-1480.

AshaRani P.V., Mun G.L.K., Hande M.P. & Valiyaveettil S. (2009). Cytotoxicity and Genotoxicity of Silver Nanoparticles in Human Cells. *Acs Nano*, 3, 279-290.

ASTM I. (2006). Terminology for nanotechnology.

Atlas R. (1993). *Handbook of Microbiological Media*. CRC, Boca raton, Forida.

Azároff L.V., R. R.K., Kato N., Weiss R.J., Wilson A.J.C. & Young R.A. (1974). *X-ray diffraction*. McGraw-Hill.

Baalousha M., Alexa N.-A., Cieslak E., Manciulea A. & Lead J.R. (Submitted). Transport mechanisms of carbon nanotubes in the natural aquatic environment. *Environ. Sci. Technol.*

Baalousha M. & Lead J.R. (2007). Size fractionation and characterization of natural aquatic colloids and nanoparticles. *Sci. Total Environ.*, 386, 93-102.

Baalousha M., Manciulea A., Cumberland S., Kendall K. & Lead J.R. (2008). Aggregation and surface properties of iron oxide nanoparticles: Influence of pH and natural organic matter. *Environmental Toxicology and Chemistry*, 27, 1875–1882

Balan L., Malval J.P., Schneider R. & Burget D. (2007). Silver nanoparticles: New synthesis, characterization and photophysical properties. *Materials Chemistry and Physics*, 104, 417-421.

Barnett B.P., Arepally A., Karmarkar P.V., Qian D., Gilson W.D., Walczak P., Howland V., Lawler L., Lauzon C., Stuber M., Kraitchman D.L. & Bulte J.W.M. (2007). Magnetic resonance-guided, real-time targeted delivery and imaging of magnetocapsules immunoprotecting pancreatic islet cells. *Nature Medicine*, 13, 986-991.

Bauer B.J., Becker M.L., Bajpai V., Fagan J.A., Hobbie E.K., Migler K., Guttman C.M. & Blair W.R. (2007). Measurement of single-wall nanotube dispersion by size exclusion chromatography. *Journal of Physical Chemistry C*, 111, 17914-17918.

Baun A., Hartmann N.B., Grieger K. & Kusk K.O. (2008). Ecotoxicity of engineered nanoparticles to aquatic invertebrates: a brief review and recommendations for future toxicity testing. *Ecotoxicology*, 17, 387-395.

Benn T.M. & Westerhoff P. (2008). Nanoparticle silver released into water from commercially available sock fabrics. *Environmental Science & Technology*, 42, 4133-4139.

Beveridge T.J., Makin S.A., Kadurugamuwa J.L. & Li Z. (1997). Interactions between biofilms and the environment. *FEMS Microbiology Reviews*, 20, 291-303.

Beyenal H., Donovan C., Lewandowski Z. & Harkin G. (2004). Three-dimensional biofilm structure quantification. *Journal of Microbiological Methods*, 59, 395-413.

Bhattacharjee S., Ko C.H. & Elimelech M. (1998). DLVO interaction between rough surfaces. *Langmuir*, 14, 3365-3375.

Bianchini A., Playle R.C., Wood C.M. & Walsh P.J. (2005). Mechanism of acute silver toxicity in marine invertebrates. *Aquat. Toxicol.*, 72, 67-82.

Bianchini A. & Wood C.M. (2008). Does sulfide or water hardness protect against chronic silver toxicity in Daphnia magna? A critical assessment of the acute-to-chronic toxicity ratio for silver. *Ecotox. Environ. Safe.*, 71, 32-40.

Bielmyer G.K., Brix K.V. & Grosell A. (2008). Is Cl- protection against silver toxicity due to chemical speciation? *Aquat. Toxicol.*, 87, 81-87.

Bielmyer G.K., Grosell M., Paquin P.R., Mathews R., Wu K.B., Santore R.C. & Brix K.V. (2007). Validation study of the acute biotic ligand model for silver. *Environ. Toxicol. Chem.*, 26, 2241-2246.

Birla S.S., Tiwari V.V., Gade A.K., Ingle A.P., Yadav A.P. & Rai M.K. (2009). Fabrication of silver nanoparticles by Phoma glomerata and its combined effect against Escherichia coli, Pseudomonas aeruginosa and Staphylococcus aureus. *Letters in Applied Microbiology*, 48, 173-179.

Bitton G. (2002). *Encyclopedia of environmental microbiology*. John Willey and Sons, Inc edn. University of Florida, Gainsville, Florida.

Blaise C., Gagné F., Férard J.F. & Eullaffroy P. (2008). Ecotoxicity of selected nano-materials to aquatic organisms. *Environmental toxicology*, 23, 591-598.

Blaser S.A., Scheringer M., MacLeod M. & Hungerbühler K. (2008). Estimation of cumulative aquatic exposure and risk due to silver: Contribution of nano-functionalized plastics and textiles. *Sci. Total Environ.*, 390, 396-409.

Boccaccini A.R., Karapappas P., Marijuan J.M. & Kaya C. (2004). TiO2 coatings on silicon carbide and carbon fibre substrates by electrophoretic deposition. *Journal of Materials Science*, 39, 851-859.

Bonnekoh B., Wevers A., Jugert F., Merk H. & Mahrle G. (1989). Colorimstric growth assay for epidermal-cell culture by their crystal violet binding-capacity. *Arch. Dermatol. Res.*, 281, 487-490.

Bootz A., Vogel V., Schubert D. & Kreuter J. (2004). Comparison of scanning electron microscopy, dynamic light scattering and analytical ultracentrifugation for the sizing of poly(butyl cyanoacrylate) nanoparticles. *European Journal of Pharmaceutics and Biopharmaceutics*, 57, 369-375.

Bouby M., Geckeis H. & Geyer F.W. (2008). Application of asymmetric flow field-flow fractionation (AsFlFFF) coupled to inductively coupled plasma mass spectrometry (ICPMS) to the quantitative characterization of natural colloids and synthetic nanoparticles. *Anal. Bioanal. Chem.*, 392, 1447-1457.

Bouldin J.L., Ingle T.M., Sengupta A., Alexander R., Hannigan R.E. & Buchanan R.A. (2008). Aqueous toxicity and food chain transfer of quantum Dots (TM) in freshwater algae and Ceriodaphnia dubia. *Environmental Toxicology and Chemistry*, 27, 1958-1963.

Boulos L., Prevost M., Barbeau B., Coallier J. & Desjardins R. (1999). LIVE/DEAD (R) BacLight (TM): application of a new rapid staining method for direct enumeration of viable and total bacteria in drinking water. *Journal of Microbiological Methods*, 37, 77-86.

Boxall A., Chaudhry Q., Jones A., Jefferson B. & Watts C. (2008). Current and future predicted environmental exposure to engineered nanoparticles. In. Report to Defra.

Boxall A.B., Tiede K. & Chaudhry Q. (2007). Engineered nanomaterials in soils and water: How do they behave and could they pose a risk to human health? *Nanomedicine*, 2, 919-927.

Boyle E.A., Edmond J.M. & Sholkovitz E.R. (1977). Mechanism of Iron Removal in Estuaries. *Geochim. Cosmochim. Acta*, 41, 1313-1324.

Bradford A., Handy R.D., Readman J.W., Atfield A. & Muhling M. (2009). Impact of Silver Nanoparticle Contamination on the Genetic Diversity of Natural Bacterial Assemblages in Estuarine Sediments. *Environmental Science & Technology*, 43, 4530-4536.

Bragg P.D. & Rainnie D.J. (1974). Effect of silver ions on respiratory chain of Escherichia coli C*anadian Journal of Microbiology*, 20, 883-889.

Brant J., Lecoanet H. & Wiesner M.R. (2005). Aggregation and deposition characteristics of fullerene nanoparticles in aqueous systems. *Journal of Nanoparticle Research*, 7, 545-553.

Bressel A., Schultze J.W., Khan W., Wolfaardt G.M., Rohns H.-P., Irmscher R. & Schoning M.J. (2003). High resolution gravimetric, optical and electrochemical investigations of microbial biofilm formation in aqueous systems. *Electrochimica Acta Electrochemistry in Molecular and Microscopic Dimensions*, 48, 3363-3372.

Browne P., Rice O., Miller S.H., Burke J., Dowling D.N., Morrissey J.P. & O'Gara F. (2009). Superior inorganic phosphate solubilization is linked to phylogeny within the Pseudomonas fluorescens complex. *Applied Soil Ecology*, 43, 131-138.

Brunner T.J., Wick P., Manser P., Spohn P., Grass R.N., Limbach L.K., Bruinink A. & Stark W.J. (2006). In vitro cytotoxicity of oxide nanoparticles: Comparison to asbestos, silica, and the effect of particle solubility. *Environmental Science & Technology*, 40, 4374-4381.

Buffle J., Wilkinson K.J., Stoll S., Filella M. & Zhang J.W. (1998). A generalized description of aquatic colloidal interactions: The three-colloidal component approach. *Environmental Science & Technology*, 32, 2887-2899.

Bury N.R., Galvez F. & Wood C.M. (1999). Effects of chloride, calcium, and dissolved organic carbon on silver toxicity: comparison betweeen rainbow trout and fathead minnows. *Environ. Toxicol. Chem.*, 18, 56-62.

Busscher H.J., van der Mei H.C. & . (2000). Initial adhesion events: mechanisms an implications. In: *Community Structure and Co-operation in Biofilms* (ed. D.G. Allison PG, H.M. Lappin-Scott, and M. Wilson). Soc. Gen. Microbiol. Symp. Ser. Cambridge University Press Cambridge pp. 25-36.

Cannas C., Casu M., Lai A., Musinu A. & Piccaluga G. (1999). XRD, TEM and Si-29 MAS NMR study of sol-gel ZnO-SiO2 nanocomposites. *Journal of Materials Chemistry*, 9, 1765-1769.

Capek I. (2004). Preparation of metal nanoparticles in water-in-oil (w/o) microemulsions. *Advances in Colloid and Interface Science*, 110, 49-74.
Chakraborty S., Sahoo B., Teraoka I. & Gross R.A. (2003). Starch nanoparticles and their derivatives dispersed in DMSO and water as studied by dynamic light scattering. *Abstracts of Papers of the American Chemical Society*, 226, 306-PMSE.
Chau J.L.H., Hsu M.-K., Hsieh C.-C. & Kao C.-C. (2005). Microwave plasma synthesis of silver nanopowders. *Materials Letters*, 59, 905.
Chen C.S. (2008). Remote control of living cells. *Nat. Nanotechnol.*, 3, 13-14.
Chen K.L. & Elimelech M. (2007). Influence of humic acid on the aggregation kinetics of fullerene (C-60) nanoparticles in monovalent and divalent electrolyte solutions. *Journal of Colloid and Interface Science*, 309, 126-134.
Chen K.L. & Elimelech M. (2008). Interaction of Fullerene (C-60) Nanoparticles with Humic Acid and Alginate Coated Silica Surfaces: Measurements, Mechanisms, and Environmental Implications. *Environmental Science & Technology*, 42, 7607-7614.
Chen Z.J., Wang W., Cai Q., Chen X., Wu Z.H., Li R.P., Che C.Q. & Pan W. (2008). SAXS and XRD studies on the microstructure of TiO2 nanoparticles. *Acta Physica Sinica*, 57, 5793-5799.
Cheng J.P., Flahaut E. & Cheng S.H. (2007). Effect of carbon nanotubes on developing zebrafish (Danio rerio) embryos. *Environmental Toxicology and Chemistry*, 26, 708-716.
Cho K.H., Park J.E., Osaka T. & Park S.G. (2005). The study of antimicrobial activity and preservative effects of nanosilver ingredient. *Electrochimica Acta*, 51, 956-960.
Choi O., Cleuenger T.E., Deng B.L., Surampalli R.Y., Ross L. & Hu Z.Q. (2009). Role of sulfide and ligand strength in controlling nanosilver toxicity. *Water Research*, 43, 1879-1886.
Choi O., Deng K.K., Kim N.J., Ross L., Surampalli R.Y. & Hu Z.Q. (2008). The inhibitory effects of silver nanoparticles, silver ions, and silver chloride colloids on microbial growth. *Water Research*, 42, 3066-3074.
Choi O. & Hu Z. (2008a). Size Dependent and Reactive Oxygen Species Related Nanosilver Toxicity to Nitrifying Bacteria. *Environ. Sci. Technol.*, 42, 4583-4588.
Choi O. & Hu Z.Q. (2008b). Size dependent and reactive oxygen species related nanosilver toxicity to nitrifying bacteria. *Environmental Science & Technology*, 42, 4583-4588.
Chou W.L., Yu D.G. & Yang M.C. (2005). The preparation and characterization of silver-loading cellulose acetate hollow fiber membrane for water treatment. *Polymers for Advanced Technologies*, 16, 600-607.
Christensen B.B., Sternberg C., Andersen J.B., Palmer R.J., Toftgaard Nielsen A., Givskov M., Molin S. & Ron J.D. (1999). Molecular tools for study of biofilm physiology. *Methods in Enzymology*, Volume 310, 20-42.
Christian P., Von der Kammer F., Baalousha M. & Hofmann T. (2008). Nanoparticles: structure, properties, preparation and behaviour in environmental media. *Ecotoxicology*, 17, 326-343.
Clarke K.R. & Warwick R.M. (1994). *Change in Marine Communities: An Approach to Statistical Analysis and Interpretation.* , Plymouth, U.K.
Cornfield A.H. (1977). Effects of addition of 12 metals on carbon-dioxide release during incubation of an acid sandy soil. *Geoderma*, 19, 199-203.
Cowan C.E., Jenne E.A. & Crecelius E.A. (1993). Silver speciation in seawater: the importance of sulfide and organic complexation. *Proceedings of the First International Conference on Transport, Fate, and Effects of Silver in the Environment, University of Wisconsin-Madison*, 15-18.
Dang H.Y. & Lovell C.R. (2000). Bacterial primary colonization and early succession on surfaces in marine waters as determined by amplified rRNA gene restriction

analysis and sequence analysis of 16S rRNA genes. *Applied and Environmental Microbiology*, 66, 467-475.
Davey M.E. & O'Toole G.A. (2000). Microbial Biofilms: from Ecology to Molecular Genetics. *Microbiology and molecular biology reviews*, Vol. 64, No. 4, 847–867.
Davies D.G. (2000.). Physiological Events in Bioflim Formation. In: *Community Structure and Cooperation in Biofilms*. Society for General Microbiology. Symposium 59. Cambridge University Press, pp. 37-52.
Decho A. (1999). Chemical Communication Within Micorbial Biofilms: Chemotaxis and Quorum Sensing in Bacterial Cells. In: *Microbial Extracellular Polymeric Substances. Characterization, Structure and Function* (eds. Wingender J, Neu TR & Flemming H-C). Springer, pp. 155-165.
Delaquis P.J., Caldwell D.E., Lawrence J.R. & McCurdy A.R. (1989). Detachment of Pseudomonas-Fluorescens from Biofilms on Glass Surfaces in Response to Nutrient Stress. *Microbial Ecology*, 18, 199-210.
Denko C.W. & Anderson A.K. (1944). Studies on the toxicity of gold compounds in rats. *Journal of Laboratory and Clinical Medicine*, 29, 1168-1176.
Derfus A.M., Chan W.C.W. & Bhatia S.N. (2004). Probing the Cytotoxicity of Semiconductor Quantum Dots. In, pp. 11-18.
Derjaguin B. & Sidorenkov G. (1941). Thermoosmosis at ordinary temperatures and its analogy with the thermomechanical effect in helium II. *Comptes Rendus De L Academie Des Sciences De L Urss*, 32, 622-626.
Diegoli S., Manciulea A.L., Begum S., Jones I.P., Lead J.R. & Preece J.A. (2008). Interaction between manufactured gold nanoparticles and naturally occurring organic macromolecules. *Sci. Total Environ.*, 402, 51-61.
Dillon J.G., Miller S., Bebout B., Hullar M., Pinel N. & Stahl D.A. (2009). Spatial and temporal variability in a stratified hypersaline microbial mat community. *Fems Microbiology Ecology*, 68, 46-58.
Domingos R.F., Tufenkji N. & Wilkinson K.J. (2009). Aggregation of Titanium Dioxide Nanoparticles: Role of a Fulvic Acid. *Environmental Science & Technology*, 43, 1282-1286.
Duguet E., Vasseur S., Mornet S. & Devoisselle J.M. (2006). Magnetic nanoparticles and their applications in medicine. *Nanomedicine*, 1, 157-168.
Dunne W.M., Jr. (2002). Bacterial Adhesion: Seen Any Good Biofilms Lately? *Clin. Microbiol. Rev.*, 15, 155-166.
Dunphy Guzman K.A., Taylor M.R. & Banfield J.F. (2006). Environmental Risks of Nanotechnology: National Nanotechnology Initiative Funding, 2000-2004. *Environ. Sci. Technol.*, 40, 1401-1407.
Duran N., Marcato P., Alves O., De Souza G. & Esposito E. (2005). Mechanistic aspects of biosynthesis of silver nanoparticles by several Fusarium oxysporum strains. *Journal of Nanobiotechnology*, 3, 8.
Duran N., Marcato P.D., De Souza G.I.H., Alves O.L. & Esposito E. (2007). Antibacterial effect of silver nanoparticles produced by fungal process on textile fabrics and their effluent treatment. *Journal of Biomedical Nanotechnology*, 3, 203-208.
Duval J.F.L., Wilkinson K.J., Van Leeuwen H.P. & Buffle J. (2005). Humic substances are soft and permeable: Evidence from their electrophoretic mobilities. *Environmental Science & Technology*, 39, 6435-6445.
Efrima S. & Bronk B.V. (1998). Silver colloids impregnating or coating bacteria. *Journal of Physical Chemistry B*, 102, 5947-5950.
Ehlers L.J. (2000). Gene Transfer in Biofilms. In: *Community Structure and Cooperation in Biofilms* (ed. D.G Allison PG, H.M Lappin-Scott, and M. Wilson). Society for General Microbiology. Symposium 59. Cambridge University Press, pp. 215-256.

Elechiguerra J., Burt J., Morones J., Camacho-Bragado A., Gao X., Lara H. & Yacaman M. (2005). Interaction of silver nanoparticles with HIV-1. *Journal of Nanobiotechnology*, 3, 6.

Engineering R.S.a.R.A.o. (2004). Nanoscience and nanotechnologies: opportunities and uncertainties. RS policy document. In: (ed. Engineering RSaRAo).

Erickson R.J., Brooke L.T., Kahl M.D., Vende Venter F., Harting S.L., Markee T.P. & Spehar R.L. (1998). Effects of laboratory test conditions on the toxicity of silver to aquatic organisms. *Environmental Toxicology and Chemistry*, 17, 572-578.

Eslami A., Nasseri S., Yadollahi B., Mesdaghinia A., Vaezi F., Nabizadeh R. & Nazmara S. (2008). Photocatalytic degradation of methyl tert-butyl ether (MTBE) in contaminated water by ZnO nanoparticies. *Journal of Chemical Technology and Biotechnology*, 83, 1447-1453.

Falk M.W., Song K.G., Matiasek M.G. & Wueytz S. (2009). Microbial community dynamics in replicate membrane bioreactors - Natural reproducible fluctuations. *Water Research*, 43, 842-852.

Farre M., Gajda-Schrantz K., Kantiani L. & Barcelo D. (2009). Ecotoxicity and analysis of nanomaterials in the aquatic environment. *Anal. Bioanal. Chem.*, 393, 81-95.

Feder B. (2006). Technology's future: A look at the dark side. In: *The New York Times*.

Feder B. (May 17 2006). Technology's future: A look at the dark side. In: *The New York Times*.

Federici G., Shaw B.J. & Handy R.D. (2007). Toxicity of titanium dioxide nanoparticles to rainbow trout (Oncorhynchus mykiss): Gill injury, oxidative stress, and other physiological effects. *Aquat. Toxicol.*, 84, 415-430.

Fein J.B., Daughney C.J., Yee N. & Davis T.A. (1997). A chemical equilibrium model for metal adsorption onto bacterial surfaces. *Geochim. Cosmochim. Acta*, 61, 3319.

Feng Q.L., Wu J., Chen G.Q., Cui F.Z., Kim T.N. & Kim J.O. (2000). A mechanistic study of the antibacterial effect of silver ions on Escherichia coli and Staphylococcus aureus. *Journal of Biomedical Materials Research*, 52, 662-668.

Ferguson E.A. & Hogstrand C. (1998). Acute silver toxicity to seawater-acclimated rainbow trout: Influence of salinity on toxicity and silver speciation. *Environmental Toxicology and Chemistry*, 17, 589-593.

Ferin J., Oberdorster G., Penney D.P., Soderholm S.C., Gelein R. & Piper H.C. (1990). Increased pulmonary toxicity of ultrafine particles. 1. Particle clearance, translocation, morphology. *Journal of Aerosol Science*, 21, 381-384.

Ferris F.G., S. SCHULTZE, T. C. WITTEN, W. S. FYFE & BEVERIDGE2* T.J. (1989). Metal Interactions with Microbial Biofilms in Acidic and Neutral pH Environments. *Applied and Environmental Microbiology*, 1249-1257.

Filella M., Zhang J.W., Newman M.E. & Buffle J. (1997). Analytical applications of photon correlation spectroscopy for size distribution measurements of natural colloidal suspensions: Capabilities and limitations. *Colloids and Surfaces a-Physicochemical and Engineering Aspects*, 120, 27-46.

Flemming H.C., Wingender J., Griebe T. & Mayer C. (2000). Physico-chemcial properties of biofilms. In: *Biofilms: recent advances in their study and control* (ed. Evans LV). Harwood academic publishers Amsterdam, pp. 19-35.

Flury M. & Qiu H.X. (2008). Modeling colloid-facilitated contaminant transport in the vadose zone. *Vadose Zone Journal*, 7, 682-697.

Fortner J.D., Lyon D.Y., Sayes C.M., Boyd A.M., Falkner J.C., Hotze E.M., Alemany L.B., Tao Y.J., Guo W., Ausman K.D., Colvin V.L. & Hughes J.B. (2005a). C_{60} in Water: Nanocrystal Formation and Microbial Response. *Environ. Sci. Technol.*, 39, 4307-4316.

Fortner J.D., Lyon D.Y., Sayes C.M., Boyd A.M., Falkner J.C., Hotze E.M., Alemany L.B., Tao Y.J., Guo W., Ausman K.D., Colvin V.L. & Hughes J.B. (2005b). C-60 in water: Nanocrystal formation and microbial response. *Environmental Science & Technology*, 39, 4307-4316.

Franklin N.M., Rogers N.J., Apte S.C., Batley G.E., Gadd G.E. & Casey P.S. (2007). Comparative toxicity of nanoparticulate ZnO, bulk ZnO, and ZnCl2 to a freshwater microalga (Pseudokirchneriella subcapitata): The importance of particle solubility. *Environmental Science & Technology*, 41, 8484-8490.

Frattini A., Pellegri N., Nicastro D. & Sanctis O.d. (2005). Effect of amine groups in the synthesis of Ag nanoparticles using aminosilanes. *Materials Chemistry and Physics*, 94, 148-152.

French R.A., Jacobson A.R., Kim B., Isley S.L., Penn R.L. & Baveye P.C. (2009). Influence of Ionic Strength, pH, and Cation Valence on Aggregation Kinetics of Titanium Dioxide Nanoparticles. *Environmental Science & Technology*, 43, 1354-1359.

Funfer E., Kronast B. & Kunze H.J. (1963). Experimental results on light scattering by theta-pinch plasma using a ruby laser. *Physics Letters*, 5, 125-127.

Funnell-Harris D.L., Pedersen J.F. & Marx D.B. (2008). Effect of sorghum seedlings, and previous crop, on soil fluorescent Pseudomonas spp. *Plant Soil,* 311, 173-187.

Gagne F., Auclair J., Turcotte P., Fournier M., Gagnon C., Sauve S. & Blaise C. (2008). Ecotoxicity of CdTe quantum dots to freshwater mussels: Impacts on immune system, oxidative stress and genotoxicity. *Aquat. Toxicol.*, 86, 333-340.

Galvez F. & Wood C.M. (1997). The relative importance of water hardness and chloride levels in modifying the acute toxicity of silver to rainbow trout (Onchorynchus mykiss. *Environmental Toxicology and Chemistry*, 16, 2363-2368.

Gao J., Youn S., Hovsepyan A., Llaneza V.L., Wang Y., Bitton G. & Bonzongo J.C.J. (2009). Dispersion and Toxicity of Selected Manufactured Nanomaterials in Natural River Water Samples: Effects of Water Chemical Composition. *Environmental Science & Technology*, 43, 3322-3328.

Ge C.C., Lao F., Li W., Li Y.F., Chen C.Y., Qiu Y., Mao X.Y., Li B., Chai Z.F. & Zhao Y.L. (2008). Quantitative Analysis of Metal Impurities in Carbon Nanotubes: Efficacy of Different Pretreatment Protocols for ICPMS Spectroscopy. *Analytical Chemistry*, 80, 9426-9434.

Geys J., Nemmar A., Verbeken E., Smolders E., Ratoi M., Hoylaerts M.F., Nemery B. & Hoet P.H.M. (2008). Acute Toxicity and Prothrombotic Effects of Quantum Dots: Impact of Surface Charge. *Environmental Health Perspectives*, 116, 1607-1613.

Giasuddin A.B.M., Kanel S.R. & Choi H. (2007). Adsorption of humic acid onto nanoscale zerovalent iron and its effect on arsenic removal. *Environmental Science & Technology*, 41, 2022-2027.

Global Industry Analysts I. (ed.) (2008). Nanotechnology: a global strategic industry report. Global Industry Analysts, Inc, San Jose, CA.

Glover C.N., Playle R.C. & Wood C.M. (2005). Heterogeneity of natural organic matter amelioration of silver toxicity to Daphnia magna: Effect of source and equilibration time. *Environmental Toxicology and Chemistry*, 24, 2934-2940.

Gratton S.E.A., Ropp P.A., Pohlhaus P.D., Luft J.C., Madden V.J., Napier M.E. & DeSimone J.M. (2008). The effect of particle design on cellular internalization pathways *PNAS*, 105, 11613-11618

Griffitt R.J., Hyndman K., Denslow N.D. & Barber D.S. (2009). Comparison of Molecular and Histological Changes in Zebrafish Gills Exposed to Metallic Nanoparticles. *Toxicological Sciences*, 107, 404-415.

Griffitt R.J., Luo J., Gao J., Bonzongo J.C. & Barber D.S. (2008). Effects of particle composition and species on toxicity of metallic nanomaterials in aquatic organisms. *Environmental Toxicology and Chemistry*, 27, 1972-1978.

Griffitt R.J., Weil R., Hyndman K.A., Denslow N.D., Powers K., Taylor D. & Barber D.S. (2007). Exposure to Copper Nanoparticles Causes Gill Injury and Acute Lethality in Zebrafish (Danio rerio). In, pp. 8178-8186.

Grosell M., De Boeck G., Johannsson O. & Wood C.M. (1999). The effects of silver on intestinal ion and acid-base regulation in the marine teleost fish, Papophrys vetulus. *Comparative Biochemistry and Physiology C-Toxicology & Pharmacology*, 124, 259-270.

Gu Y.L., Xie H., Gao J.X., Liu D.X., Williams C.T., Murphy C.J. & Ploehn H.J. (2005). AFM characterization of dendrimer-stabilized platinum nanoparticles. *Langmuir*, 21, 3122-3131.

Gunnars A., Blomqvist S., Johansson P. & Andersson C. (2002). Formation of Fe(III) oxyhydroxide colloids in freshwater and brackish seawater, with incorporation of phosphate and calcium. *Geochim. Cosmochim. Acta*, 66, 745-758.

Gupta A., Matsui K., Lo J.F. & Silver S. (1999). Molecular basis for resistance to silver cations in Salmonella. *Nature Medicine*, 5, 183-188.

Gupta A. & Silver S. (1998). Molecular genetics - Silver as a biocide: Will resistance become a problem? *Nature Biotechnology*, 16, 888-888.

Gupta A.K. & Gupta M. (2005). Synthesis and surface engineering of iron oxide nanoparticles for biomedical applications. *Biomaterials*, 26, 3995-4021.

Guzman K.A.D., Finnegan M.P. & Banfield J.F. (2006). Influence of surface potential on aggregation and transport of titania nanoparticles. *Environmental Science & Technology*, 40, 7688-7693.

Handy R.D., von der Kammer F., Lead J.R., Hassellov M., Owen R. & Crane M. (2008). The ecotoxicology and chemistry of manufactured nanoparticles. *Ecotoxicology*, 17, 287-314.

Hardman R. (2006). A toxicologic review of quantum dots: Toxicity depends on physicochemical and environmental factors. *Environmental Health Perspectives*, 114, 165-172.

Harhaji L., Isakovic A., Vucicevic L., Janjetovic K., Misirkic M., Markovic Z., Todorovic-Markovie B., Nikolic N., Vranjes-Djuric S., Nikolic Z. & Trajkovic V. (2008). Modulation of tumor necrosis factor-mediated cell death by fullerenes. *Pharmaceutical Research*, 25, 1365-1376.

Hattori T. & Fujino T. (2006). Enhancing effect on photocatalitic activity of TiO2/Pt/Al2O3 and TiO2/Sn/Al2O3 films on anodically oxidized aluminum. *Materials Transactions*, 47, 868-873.

Henglein A. (1998). Colloidal Silver Nanoparticles: Photochemical Preparation and Interaction with O2, CCl4, and Some Metal Ions. *Chem. Mater.*, 10, 444-450.

Henriques M., Azeredo J. & Oliveira R. (2006). Candida albicans and Candida dubliniensis: comparison of biofilm formation in terms of biomass and activity. *British journal of biomedical science,* 63,5-11.

Hentzer M., Teitzel G.M., Balzer G.J., Heydorn A., Molin S., Givskov M. & Parsek M.R. (2001). Alginate Overproduction Affects Pseudomonas aeruginosa Biofilm Structure and Function, *J. Bacteriol.*, 183, 5395-5401.

Hermant M.C., Klumperman B., Kyrylyuk A.V., van der Schoot P. & Koning C.E. (2009). Lowering the percolation threshold of single-walled carbon nanotubes using polystyrene/poly(3,4-ethylenedioxythiophene): poly(styrene sulfonate) blends. *Soft Matter*, 5, 878-885.

Hernandez-Sierra J.F., Ruiz F., Pena D.C.C., Martinez-Gutierrez F., Martinez A.E., Guillen A.d.J.P., Tapia-Perez H. & Castanon G.M. (2008). The antimicrobial sensitivity of Streptococcus mutans to nanoparticles of silver, zinc oxide, and gold. *Nanomedicine*, 4, 237-40.

Herrera M., Carrion P., Baca P., Liebana J. & Castillo A. (2001). In vitro antibacterial activity of glass-ionomer cements. *Microbios*, 104, 141-148.

Herrin R.T., Andren A.W., Shafer M.M. & Armstrong D.E. (2001). Determination of silver speciation in natural waters. 2. Binding strength of silver ligands in surface freshwaters. *Environmental Science & Technology*, 35, 1959-1966.

Hogstrand C., Ferguson E.A., Galvez F., Shaw J.R., Webb N.A. & Wood C.M. (1999). Physiology of acute silver toxicity in the starry flounder (Platichthys stellatus) in seawater. *Journal of Comparative Physiology B-Biochemical Systemic and Environmental Physiology*, 169, 461-473.

Hogstrand C. & Wood C.M. (1998). Toward a better understanding of the bioavailability, physiology and toxicity of silver in fish: Implications for water quality criteria. *Environmental Toxicology and Chemistry*, 17, 547-561.

Holt K.B. & Bard A.J. (2005). Interaction of silver(I) ions with the respiratory chain of Escherichia coli: An electrochemical and scanning electrochemical microscopy study of the antimicrobial mechanism of micromolar Ag. *Biochemistry*, 44, 13214-13223.

Honeyman B.D. & Mackay D.M. (1993). THE ROLE OF COLLOIDS IN THE TRANSPORT OF CONTAMINANTS AT THE ROCKY-MOUNTAIN ARSENAL, DENVER, CO. *Abstracts of Papers of the American Chemical Society*, 205, 86-NUCL.

Hoshino A., Fujioka K., Oku T., Suga M., Sasaki Y.F., Ohta T., Yasuhara M., Suzuki K. & Yamamoto K. (2004). Physicochemical properties and cellular toxicity of nanocrystal quantum dots depend on their surface modification. *Nano Letters*, 4, 2163-2169.

Hozumi A., Inagaki M. & Shirahata N. (2006). Vapor phase formation of a well-ordered aldehyde-terminated self-assembled monolayer on a SiO2 surface and formation of silver film on the surface based on the silver mirror reaction. *Surface Science*, 600, 4044-4047.

Hsu H.L., Jehng H.M., Sung Y., Wang L.C. & Yang S.R. (2008). The synthesis, characterization of oxidized multi-walled carbon nanotubes, and application to surface acoustic wave quartz crystal gas sensor. *Materials Chemistry and Physics*, 109, 148-155.

Hu X.L., Liu J.F., Mayer P. & Jiang G. (2008). Impacts of some environmentally relevant parameters on the sorption of polycyclic aromatic hydrocarbons to aqueous suspensions of fullerene. *Environmental Toxicology and Chemistry*, 27, 1868-1874.

Huang H.-C., Huang G.-L., Chen H.-L. & Lee Y.-D. (2006). Immobilization of TiO2 nanoparticles on Fe-filled carbon nanocapsules for photocatalytic applications. *Thin Solid Films*, 515, 1033-1037.

Huang Q., Shi X., Pinto R.A., Petersen E.J. & Weber W.J. (2008). Tunable Synthesis and Immobilization of Zero-Valent Iron Nanoparticles for Environmental Applications. *Environmental Science & Technology*, 42, 8884-8889.

Hunt S.M., Werner E.M., Huang B.C., Hamilton M.A. & Stewart P.S. (2004). Hypothesis for the role of nutrient starvation in biofilm detachment. *Applied and Environmental Microbiology*, 70, 7418-7425.

Hutchinson N., Nagarkarl S., Aitchison J. & Williams G. (2006). Microspatial variation in marine biofilm abundance on intertidal rock surfaces. *Aquatic microbial ecology*, 42, 187-197.

Hwang E.T., Lee J.H., Chae Y.J., Kim Y.S., Kim B.C., Sang B.-I. & Gu M.B. (2008). Analysis of the Toxic Mode of Action of Silver Nanoparticles Using Stress-Specific Bioluminescent Bacteria. *Small*, 4, 746-750.

Hwang M.G., Katayama H. & Ohgaki S. (2007). Inactivation of Legionella pneumophila and Pseudomonas aeruginosa: Evaluation of the bactericidal ability of silver cations. *Water Research*, 41, 4097-4104.

Hyung H., Fortner J.D., Hughes J.B. & Kim J.H. (2007). Natural organic matter stabilizes carbon nanotubes in the aqueous phase. *Environmental Science & Technology*, 41, 179-184.

Ibrahim Z., Ahmad W.A. & Baba A.B. (2001). Bioaccumulation of Silver and the Isolation of Metal-Binding Protein from P. diminuta. *Brazilian Archives of Biology and Technology*, 44, 223-225.

Isaeva E.I., Gorbunova V.V., Sirotinkin N.V., Shchukarev A.V. & Boitsova T.B. (2006). Photochemical formation of silver nanoparticles in elastomer films. *Russian Journal of General Chemistry*, 76, 687-693.

Ishikawa Y., Katoh Y. & Ohshima H. (2005). Colloidal stability of aqueous polymeric dispersions: Effect of pH and salt concentration. *Colloid Surf. B-Biointerfaces*, 42, 53-58.

Ito T., Sun L., Bevan M.A. & Crooks R.M. (2004). Comparison of nanoparticle size and electrophoretic mobility measurements using a carbon-nanotube-based coulter counter, dynamic light scattering, transmission electron microscopy, and phase analysis light scattering. *Langmuir*, 20, 6940-6945.

Ivanova E.P., Gorshkova N.M., Sawabe T., Hayashi K., Kalinovskaya N.I., Lysenko A.M., Zhukova N.V., Nicolau D.V., Kuznetsova T.A., Mikhailov V.V. & Christen R. (2002). Pseudomonas extremorientalis sp. nov.,isolated from a drinking water reservoir. *International Journal of Systematic and Evolutionary Microbiology*, 52, 2113-2120.

Jagani S., Chelikani R. & Kim D.S. (2009). Effects of phenol and natural phenolic compounds on biofilm formation by Pseudomonas aeruginosa. *Biofouling*, 25, 321-324.

Jain P. & Pradeep T. (2005). Potential of silver nanoparticle-coated polyurethane foam as an antibacterial water filter. *Biotechnology and Bioengineering*, 90, 59-63.

Janes N. & Playle R.C. (1995). Modelling silver-binding to gills of rainbow trout (Onchorhyncus mykiss). *Environmental Toxicology and Chemistry*, 14, 1847-1858.

Jeevananda T., Siddaramaiah, Kim N.H., Heo S.B. & Lee J.H. (2008). Synthesis and characterization of polyaniline-multiwalled carbon nanotube nanocomposites in the presence of sodium dodecyl sulfate. *Polymers for Advanced Technologies*, 19, 1754-1762.

Ji J.H., Jung J.H., Kim S.S., Yoon J.U., Park J.D., Choi B.S., Chung Y.H., Kwon I.H., Jeong J., Han B.S., Shin J.H., Sung J.H., Song K.S. & Yu I.J. (2007). Twenty-eight-day inhalation toxicity study of silver nanoparticles in Sprague-Dawley rats. *Inhalation Toxicology*, 19, 857-871.

Jiang J.K., Oberdorster G. & Biswas P. (2009). Characterization of size, surface charge, and agglomeration state of nanoparticle dispersions for toxicological studies. *Journal of Nanoparticle Research*, 11, 77-89.

Jou M.J. (2008). Pathophysiological and pharmacological implications of mitochondria-targeted reactive oxygen species generation in astrocytes. *Advanced Drug Delivery Reviews*, 60, 1512-1526.

Ju-Nam Y. & Lead J.R. (2008). Manufactured nanoparticles: An overview of their chemistry, interactions and potential environmental implications. *Sci. Total Environ.*, 400, 396-414.

Ju W.G., Zhang X.H. & Wu S.K. (2005). Wet chemical synthesis of Ag nanowires array at room temperature. *Chemistry Letters*, 34, 510-511.

Kachynski A.V., Kuzmin A.N., Nyk M., Roy I. & Prasad P.N. (2008). Zinc oxide nanocrystals for nonresonant nonlinear optical microscopy in biology and medicine. *Journal of Physical Chemistry C*, 112, 10721-10724.

Karl D. (1986). Determination of in situ biomass, viability, metabolism and growth. In: *Bacteria in Nature. Methods and Special Applications in Bacterial Ecology*. Plenum Press New York:.

Kaschl A., Romheld V. & Chen Y. (2002). Cadmium Binding by Fractions of Dissolved Organic Matter and Humic Substances from Municipal Solid Waste Compost. *J Environ Qual*, 31, 1885-1892.

Khan J.A., Pillai B., Das T.K., Singh Y. & Maiti S. (2007). Molecular effects of uptake of gold nanoparticles in HeLa cells. *Chembiochem*, 8, 1237-1240.

Kim J.S., Kuk E., Yu K.N., Kim J.H., Park S.J., Lee H.J., Kim S.H., Park Y.K., Park Y.H., Hwang C.Y., Kim Y.K., Lee Y.S., Jeong D.H. & Cho M.H. (2007). Antimicrobial effects of silver nanoparticles. *Nanomedicine-Nanotechnology Biology and Medicine*, 3, 95-101.

Kitts C.L. (2001). Terminal restriction fragment patterns: a tool for comparing microbial communities and assessing community dynamics. *Curr Issues Intest Microbiol*, 2, 17-25.

Klaine S.J., Alvarez P.J.J., Batley G.E., Fernandes T.F., Handy R.D., Lyon D.Y., Mahendra S., McLaughlin M.J. & Lead J.R. (2008). Nanomaterials in the environment: Behavior, fate, bioavailability, and effects. *Environmental Toxicology and Chemistry*, 27, 1825-1851.

Klaus T., Joerger R., Olsson E. & Granqvist C.G. (1999). Silver-based crystalline nanoparticles, microbially fabricated. *Proceedings of the National Academy of Sciences of the United States of America*, 96, 13611-13614.

Kocberber Kilic N. & Donmez G. (2008). Environmental conditions affecting exopolysaccharide production by Pseudomonas aeruginosa, Micrococcus sp., and Ochrobactrum sp. *Journal of hazardous materials*, 154, 1019-1024.

Kola H., Laglera L.M., Parthasarathy N. & Wilkinson K.J. (2004). Cadmium Adsorption by Chlamydomonas reinhardtii and its Interaction with the Cell Wall Proteins. In: *Environ. Chem.*, pp. 172-179

Korber D.R., Lawrence J.R. & Caldwell D.E. (1994). Effect of Motility on Surface Colonization and Reproductive Success of Pseudomonas-Fluorescens in Dual-Dilution Continuous-Culture and Batch Culture Systems. *Applied and Environmental Microbiology*, 60, 1421-1429.

Kvitek L., Panacek A., Soukupova J., Kolar M., Vecerova R., Prucek R., Holecova M. & Zboril R. (2008). Effect of surfactants and polymers on stability and antibacterial activity of silver nanoparticles (NPs). *Journal of Physical Chemistry C*, 112, 5825-5834.

Kvitek L., Vanickova M., Panacek A., Soukupova J., Dittrich M., Valentova E., Prucek R., Bancirova M., Milde D. & Zboril R. (2009). Initial Study on the Toxicity of Silver Nanoparticles (NPs) against Paramecium caudatum. *Journal of Physical Chemistry C*, 113, 4296-4300.

Laiho R., Vlasenko L.S. & Vlasenko M.P. (2008). Optical detection of magnetic resonance and electron paramagnetic resonance study of the oxygen vacancy and lead donors in ZnO. *Journal of Applied Physics*, 103.

Landsdown A.B.G. & Williams A. (2007). Bacterial resistance to silver in wound care and medical devices. *J Wound Care*, 16, 15-9.

Langley S. & Beveridge T.J. (1999). Effect of O-Side-Chain-Lipopolysaccharide Chemistry on Metal Binding. *Appl. Environ. Microbiol.*, 65, 489-498.

Lattner D., Flemming H.-C. & Mayer C. (2003). 13C-NMR study of the interaction of bacterial alginate with bivalent cations. *International Journal of Biological Macromolecules*, 33, 81-88.

Lead J.R., Balnois E., Hosse M., Menghetti R. & Wilkinson K.J. (1999). Characterization of Norwegian natural organic matter: Size, diffusion coefficients, and electrophoretic mobilities. *Environment International*, 25, 245-258.

Lead J.R., Muirhead D. & Gibson C.T. (2005). Characterization of freshwater natural aquatic colloids by atomic force microscopy (AFM). *Environ. Sci. Technol.*, 39, 6930-6936.

Lead J.R. & Wilkinson K.J. (2006a). Aquatic colloids and nanoparticles: current knowledge and future trends. *Environ. Chem.*, 3, 159-171.

Lead J.R. & Wilkinson K.J. (2006b). Aquatic colloids and nanoparticles: Current knowledge and future trends. *Environ. Chem.*, 3, 159-171.

Lee C., Kim J.Y., Il Lee W., Nelson K.L., Yoon J. & Sedlak D.L. (2008a). Bactericidal effect of zero-valent iron nanoparticles on Escherichia coli. *Environmental Science & Technology*, 42, 4927-4933.

Lee C.G., Kim G.H., Lee W.J., Kim S.H., Kjm Y.J., Smith C. & Kim I. (2008b). Synthesis of high-purity silver colloids using a thermal decomposition method. *Metals and Materials International*, 14, 189-192.

Lee S.H., Reeves J.M., Wilson J.C., Hunton D.E., Viggiano A.A., Miller T.M., Ballenthin J.O. & Lait L.R. (2003). Particle formation by ion nucleation in the upper troposphere and lower stratosphere. *Science*, 301, 1886-1889.

Lekas D. (2005). Analysis of nanotechnology from an industrial ecology perspective. Part II: Substance flow analysis of carbon nanotubes. In: *Project on Emerging Nanotechnologies Report*. Woodrow Wilson International Centre for Scholars Washington, DC.

Li D., Lyon D.Y., Li Q. & Alvarez P.J.J. (2008a). Effect of soil sorption and aquatic natural organic matter on the antibacterial activity of a fullerene water suspension *Environ Toxicology and Chemistry*, 27, 1888–1894.

Li J.J., Zou L., Hartono D., Ong C.N., Bay B.H. & Yung L.Y.L. (2008b). Gold nanoparticles induce oxidative damage in lung fibroblasts in vitro. *Advanced Materials*, 20, 138-+.

Li Q.L., Mahendra S., Lyon D.Y., Brunet L., Liga M.V., Li D. & Alvarez P.J.J. (2008c). Antimicrobial nanomaterials for water disinfection and microbial control: Potential applications and implications. *Water Research*, 42, 4591-4602.

Liu A.H., Watanabe T., Honma I., Wang J. & Zhou H.S. (2006). Effect of solution pH and ionic strength on the stability of poly(acrylic acid)-encapsulated multiwalled carbon nanotubes aqueous dispersion and its application for NADH sensor. *Biosens. Bioelectron.*, 22, 694-699.

Liu W.T., Marsh T.L., Cheng H. & Forney L.J. (1997). Characterization of microbial diversity by determining terminal restriction fragment length polymorphisms of genes encoding 16S rRNA. *Appl. Environ. Microbiol.*, 63, 4516-4522.

Lok C., Ho C., Chen R., He Q., Yu W., Sun H., Tam P., Chiu J. & Che C. (2006). Proteomic analysis of the mode of antibacterial action of silver nanoparticles. *Journal of Proteome research* 5, 916-624.

Lok C.N., Ho C.M., Chen R., He Q.Y., Yu W.Y., Sun H., Tam P.K.H., Chiu J.F. & Che C.M. (2007). Silver nanoparticles: partial oxidation and antibacterial activities. *Journal of Biological Inorganic Chemistry*, 12, 527-534.

Long T.C., Saleh N., Tilton R.D., Lowry G.V. & Veronesi B. (2006). Titanium Dioxide (P25) Produces Reactive Oxygen Species in Immortalized Brain Microglia (BV2): Implications for Nanoparticle Neurotoxicity. *Environ. Sci. Technol.*, 40, 4346-4352.

Loree T.R. & Radziemski L.J. (1981). Laser induce breakdown spectroscopy- A technique for atomic detection and molecular identification. *Proceedings of the Society of Photo-Optical Instrumentation Engineers*, 288, 241-244.

Lovell C.R. & Piceno Y. (1994). Purification of DNA from estuarine sediments. *Journal of Microbiological Methods* 20, 161-174.

Lovern S.B. & Klaper R. (2006). Daphnia magna mortality when exposed to titanium dioxide and fullerene (C-60) nanoparticles. *Environmental Toxicology and Chemistry*, 25, 1132-1137.

Lovern S.B., Strickler J.R. & Klaper R. (2007). Behavioral and physiological changes in Daphnia magna when exposed to nanoparticle suspensions (titanium dioxide, nano-C-60, and C(60)HxC(70)Hx). *Environmental Science & Technology*, 41, 4465-4470.

Lovric J., Bazzi H.S., Cuie Y., Fortin G.R.A., Winnik F.M. & Maysinger D. (2005). Differences in subcellular distribution and toxicity of green and red emitting CdTe quantum dots. *J. Mol. Med.*, 83, 377-385.

Lu Z.S., Li C.M., Bao H.F., Qiao Y., Toh Y.H. & Yang X. (2008). Mechanism of antimicrobial activity of CdTe quantum dots. *Langmuir*, 24, 5445-5452.

Lucente-Schultz R.M., Moore V.C., Leonard A.D., Price B.K., Kosynkin D.V., Lu M., Partha R., Conyers J.L. & Tour J.M. (2009). Antioxidant single-walled carbon nanotubes. *J Am Chem Soc*, 131, 3934-41.

Luoma S.N. (2008). Silver nanotechnologies and the environment: old problems and new challenges? In. Woodrow Wilson International Center for Scholars or The PEW Charitable Trusts Washington DC, p. 72.

Luoma S.N., Ho Y.B. & Bryan G.W. (1995). Fate, bioavailability and toxicity of silver in estuarine environments. *Marine Pollution Bulletin*, 31, 44-54.

Lyon D.Y., Adams L.K., Falkner J.C. & Alvarez P.J.J. (2006). Antibacterial Activity of Fullerene Water Suspensions: Effects of Preparation Method and Particle Size. *Environ. Sci. Technol.*, 40, 4360-4366.

Lyon D.Y. & Alvarez P.J.J. (2008). Fullerene Water Suspension (nC(60)) Exerts Antibacterial Effects via ROS-Independent Protein Oxidation. *Environmental Science & Technology*, 42, 8127-8132.

Lyon D.Y., Brown D., Sundstrom E.R. & Alvarez P.J.J. (2008a). Assessing the antibiofouling potential of a fullerene-coated surface. *International Biodeterioration & Biodegradation*, 62, 475-478.

Lyon D.Y., Brown D.A. & Alvarez P.J.J. (2008b). Implications and potential applications of bactericidal fullerene water suspensions: effect of nC(60) concentration, exposure conditions and shelf life. *Water Science and Technology*, 57, 1533-1538.

Lyon D.Y., Brunet L., Hinkal G.W., Wiesner M.R. & Alvarez P.J.J. (2008c). Antibacterial activity of fullerene water suspensions (nC(60)) is not due to ROS-mediated damage. *Nano Letters*, 8, 1539-1543.

Lyon D.Y., Fortner J.D., Sayes C.M., Colvin V.L. & Hughes J.B. (2005). Bacterial cells association and antimicrobial activity of a C60 water suspension. *Environmental Toxicology and Chemistry*, 24, 2757-2762.

Madden A.S., Hochella J.M.F. & Luxton T.P. (2006). Insights for size-dependent reactivity of hematite nanomineral surfaces through Cu2+ sorption. *Geochim. Cosmochim. Acta*, 70, 4095-4104.

Madden A.S. & Hochella M.F. (2005). A test of geochemical reactivity as a function of mineral size: Manganese oxidation promoted by hematite nanoparticles. *Geochim. Cosmochim. Acta*, 69, 389-398.

Madigan M.T., Martinko J.M. & Parker J. (1997). *Brock Biology of Microorganisms*. 8 edn. Prentice Hall Iberia, Madrid.

Mallin M.P. & Murphy C.J. (2002). Solution-phase synthesis of sub-10 nm Au-Ag alloy nanoparticles. *Nano Letters*, 2, 1235-1237.

Mao Z., Wang B., Ma L., Gao C. & Shen J. (2007). The influence of polycaprolactone coating on the internalization and cytotoxicity of gold nanoparticles. *Nanomedicine: Nanotechnology, Biology and Medicine*, 3, 215-223.

Marsh P.D. & Bowden G.H.W. (2000). Microbial Community Interactions in Biofilms. In: *Community Structure and Cooperation in Biofilms* (ed. D.G Allison PG, H.M Lappin-Scott, and M. Wilson). Society for General Microbiology. Symposium 59. Cambridge University Press., pp. 167-198.

Maynard A.D., Aitken R.J., Butz T., Colvin V., Donaldson K., Oberdorster G., Philbert M.A., Ryan J., Seaton A., Stone V., Tinkle S.S., Tran L., Walker N.J. & Warheit D.B. (2006). Safe handling of nanotechnology. *Nature*, 444, 267.

McWilliams A. (2006). BCC report highlights. Nanotechnology: arealistic market assessment. URL http://www.bccresearch.com/report/NAN031B.html.

Medarova Z., Pham W., Farrar C., Petkova V. & Moore A. (2007). In vivo imaging of siRNA delivery and silencing in tumors. *Nature Medicine*, 13, 372-377.

Miller L.A. & Bruland K.W. (1995). Organic speciation of solver in marine waters. *Environmental Science & Technology*, 29, 2616-2621.

Misirkic M.S., Todorovic-Markovic B.M., Vucicevic L.M., Janjetovic K.D., Jokanovic V.R., Dramicanin M.D., Markovic Z.M. & Trajkovic V.S. (2009). The protection of cells from nitric oxide-mediated apoptotic death by mechanochemically synthesized fullerene (C(60)) nanoparticles. *Biomaterials*, 30, 2319-28.

Mittelman M.W. G.G.G. (1985). Cooper-binding characterisitcs of exopolymemrs from a freshwater sediment bacterium. *Applied and Environmental Microbiology*, 49, 846-851.

Monirith I., Ueno D., Takahashi S., Nakata H., Sudaryanto A., Subramanian A., Karuppiah S., Ismail A., Muchtar M., Zheng J.S., Richardson B.J., Prudente M., Hue N.D., Tana T.S., Tkalin A.V. & Tanabe S. (2003). Asia-Pacific mussel watch: monitoring contamination of persistent organochlorine compounds in coastal waters of Asian countries. *Marine Pollution Bulletin*, 46, 281-300.

Moore M.N. (2006). Do nanoparticles present ecotoxicological risks for the health of the aquatic environment? *Environment International*, 32, 967-976.

Morgan I.J., Henry R.P. & Wood C.M. (1997). The mechanism of acute silver nitrate toxicity in freshwater rainbow trout (Oncorhynchus mykiss) is inhibition of gill Na+ and Cl-1 transport. *Aquat. Toxicol.*, 38, 145-163.

Morones J.R., Elechiguerra J.L., Camacho A., Holt K., Kouri J.B., Ramírez J.T. & Yacaman M.J. (2005). The bactericidal effect of silver nanoparticles. *Nanotechnology,* 16, 2346-2353

Mrkonjic Fuka M., Engel M., Hagn A., Munch J.C., Sommer M. & Schloter M. (2009). Changes of Diversity Pattern of Proteolytic Bacteria over Time and Space in an Agricultural Soil. *Microb Ecol*, 57, 391-401.

Mueller N.C. & Nowack B. (2008). Exposure Modeling of Engineered Nanoparticles in the Environment. *Environmental Science & Technology*, 42, 4447-4453.

Murray P.T. & Shin E. (2008). Formation of silver nanoparticles by through thin film ablation. *Materials Letters*, 62, 4336-4338.

Mylon S.E., Chen K.L. & Elimelech M. (2004). Influence of natural organic matter and ionic composition on the kinetics and structure of hematite colloid aggregation: Implications to iron depletion in estuaries. *Langmuir*, 20, 9000-9006.

Nannipieri P., Ascher J., Ceccherini M.T., Landi L., Pietramellara G. & Renella G. (2003). Microbial diversity and soil functions. *European Journal of Soil Science*, 54, 655-670.

Nanotechnologies P.o.E. (2009). Consumer Products Inventory

Navarro E., Baun A., Behra R., Hartmann N.B., Filser J., Miao A.J., Quigg A., Santschi P.H. & Sigg L. (2008a). Environmental behavior and ecotoxicity of engineered nanoparticles to algae, plants, and fungi. *Ecotoxicology*, 17, 372-386.

Navarro E., Piccapietra F., Wagner B., Marconi F., Kaegi R., Odzak N., Sigg L. & Behra R. (2008b). Toxicity of Silver Nanoparticles to Chlamydomonas reinhardtii. *Environmental Science & Technology*, 42, 8959-8964.

Neal A.L. (2008). What can be inferred from bacterium-nanoparticle interactions about the potential consequences of environmental exposure to nanoparticles? *Ecotoxicology*, 17, 362-371.

Nel A., Xia T., Madler L. & Li N. (2006). Toxic Potential of Materials at the Nanolevel. *Science*, 311, 622-627.

Neu T.R. & Lawrence J.R. (1997). Development and structure of microbial biofilms in river water studied by confocal laser scanning microscopy. *FEMS Microbiology Ecology*, 24, 11-25.

Neu T.R. & Lawrence J.R. (1999). Lectin-binding analysis in biofilm systems. In: *Biofilms*, pp. 145-152.

Nichols J.W., Brown S., Wood C.M., Walsh P.J. & Playle R.C. (2006). Influence of salinity and organic matter on silver accumulation in Gulf toadfish (Opsanus beta). *Aquat. Toxicol.*, 78, 253.

Nieboer E. & Richardson D.H.S. (1980). The replacement of non-descriptive heavy metals by a biologically and chemically significant classification of metal-ions. *Environmental Pollution Series B-Chemical and Physical*, 1, 3-26.

Niemeyer C. (2001). Nanoparticles, proteins, and nucleic acids:biotechnology meets materials science. *Angew Chem Int Ed*, 40, 4128-58.

Nowack B. (2009). Is anything out there? What life cycle perspectives of nano-products can tell us about nanoparticles in the environment. *Nano Today*, 4, 11-12.

Nowack B. & Bucheli T.D. (2007). Occurrence, behavior and effects of nanoparticles in the environment. *Environmental Pollution*, 150, 5-22.

Nyberg L., Turco R.F. & Nies L. (2008). Assessing the impact of nanomaterials on anaerobic microbial communities. *Environmental Science & Technology*, 42, 1938-1943.

O'Toole G.A. & Kolter R. (1998). Initiation of biofilm formation in Pseudomonas fluorescens WCS365 proceeds via multiple, convergent signalling pathways: a genetic analysis. In, pp. 449-461.

Oberdorster G. (2001). Pulmonary effects of inhaled ultrafine particles. *International Archives of Occupational and Environmental Health*, 74, 1-8.

Oberdorster G., Ferin J., Finkelstein G., Wade P. & Corson N. (1990). Increased pulmonary toxicity of ultrafine particles. 2. Lung lavage studies. *Journal of Aerosol Science*, 21, 384-387.

Oberdorster G., Ferin J. & Lehnert B.E. (1992). Correlation between particle size, in vivo particle persistence, and lung injury. In: *Workshop on Biopersistence of Respirable Synthetic Fibers and Minerals*. Natl Inst Environ Health Sci Lyon, France, pp. 173-179.

Oberdorster G., Gelein R.M., Ferin J. & Weiss B. (1995). Association of particulate air pollution and acute mortality-Involvement of ultrafine particles. *Inhalation Toxicology*, 7, 111-124.

Ogura K. & Uchida H. (1987). Electrocatalytic reduction of CO2 to methanol.8.Photoassisted electrolysis and electrochemical photocell with N-TiO2 anode. *Journal of Electroanalytical Chemistry*, 220, 333-337.

Ohashi A. & Harada H. (1994). Characterisation of detachment mode of biofilm developed in an attached growth reactor. *Water Science and Technology*, 30, 35-45.

Orlic I. & Tang S.M. (1998). Elemental depth profiles in marine sediments of Singapore coastal waters. In: *8th International Conference on PIXE and its Analytical Applications*. Elsevier Science Bv Lund, Sweden, pp. 291-297.

Padmavathy N. & Vijayaraghavan R. (2008). Enhanced bioactivity of ZnO nanoparticles-an antimicrobial study. *Science and Technology of Advanced Materials*, 9.

Pal S., Tak Y.K. & Song J.M. (2007). Does the antibacterial activity of silver nanoparticles depend on the shape of the nanoparticle? A study of the gram-negative bacterium Escherichia coli. *Applied and Environmental Microbiology*, 73, 1712-1720.

Palgrave R.G. & Parkin I.P. (2006). Aerosol assisted chemical vapor deposition using nanoparticle precursors: A route to nanocomposite thin films. *Journal of the American Chemical Society*, 128, 1587-1597.

Pan B. & Xing B.S. (2008). Adsorption Mechanisms of Organic Chemicals on Carbon Nanotubes. *Environmental Science & Technology*, 42, 9005-9013.

Pan Y., Neuss S., Leifert A., Fischler M., Wen F., Simon U., Schmid G., Brandau W. & Jahnen-Dechent W. (2007). Size-dependent cytotoxicity of gold nanoparticles. *Small*, 3, 1941-1949.

Pang C.M., Hong P.Y., Guo H.L. & Liu W.T. (2005). Biofilm formation characteristics of bacterial isolates retrieved from a reverse osmosis membrane. *Environmental Science & Technology*, 39, 7541-7550.

Pang C.M. & Liu W.T. (2007). Community Structure Analysis of Reverse Osmosis Membrane Biofilms and the Significance of Rhizobiales Bacteria in Biofouling. *Environ. Sci. Technol.*, 41, 4728-4734.

Paquin P.R., Gorsuch J.W., Apte S., Batley G.E., Bowles K.C., Campbell P.G.C., Delos C.G., Di Toro D.M., Dwyer R.L., Galvez F., Gensemer R.W., Goss G.G., Hogstrand C., Janssen C.R., McGeer J.C., Naddy R.B., Playle R.C., Santore R.C., Schneider U., Stubblefield W.A., Wood C.M. & Wu K.B. (2002). The biotic ligand model: a historical overview. *Comparative Biochemistry and Physiology C-Toxicology & Pharmacology*, 133, 3-35.

Patra H.K., Banerjee S., Chaudhuri U., Lahiri P. & Dasgupta A.K. (2007). Cell selective response to gold nanoparticles. *Nanomedicine-Nanotechnology Biology and Medicine*, 3, 111-119.

Percival S.L., Walker J.T. & Hunter P.R. (2000). *Microbiological aspects of biofilms and drinking water*. 1 edn. CRC Press, Boca Raton, Florida.

Persson Y., Shchukarev A., Oberg L. & Tysklind M. (2008). Dioxins, chlorophenols and other chlorinated organic pollutants in colloidal and water fractions of groundwater from a contaminated sawmill site. *Environ. Sci. Pollut. Res.*, 15, 463-471.

Petersen F.C., Tao L. & Scheie A.A. (2005). DNA binding-uptake system: a link between cell-to-cell communication and biofilm formation. *Journal of Bacteriology*, 187, 4392-4400.

Pettibone J.M., Cwiertny D.M., Scherer M. & Grassian V.H. (2008). Adsorption of organic acids on TiO2 nanoparticles: Effects of pH, nanoparticle size, and nanoparticle aggregation. *Langmuir*, 24, 6659-6667.

Picioreanu C., Loosdrecht M.C.M.v. & Heijnen J.J. (2001). Two-dimensional model of biofilm detachment caused by internal stress from liquid flow. *Biotechnology & Bioengineering*, 72, 205-218.

Pierce J.R. & Adams P.J. (2007). Efficiency of cloud condensation nuclei formation from ultrafine particles. *Atmos. Chem. Phys.*, 7, 1367-1379.

Plaza C., Brunetti G., Senesi N. & Polo A. (2006). Molecular and Quantitative Analysis of Metal Ion Binding to Humic Acids from Sewage Sludge and Sludge-Amended Soils by Fluorescence Spectroscopy. *Environ. Sci. Technol.*, 40, 917-923.

Poland C.A., Duffin R., Kinloch I., Maynard A., Wallace W.A.H., Seaton A., Stone V., Brown S., Macnee W. & Donaldson K. (2008). Carbon nanotubes introduced into the abdominal cavity of mice show asbestos-like pathogenicity in a pilot study. *Nat Nanotechnol*, 3, 423-8.

Powell M., Griffin M. & StephanieTai (2008). Bottom-Up Risk Regulation? How Nanotechnology Risk Knowledge Gaps Challenge Federal and State Environmental Agencies. *Environmental Management*, 42, 426-443.

Raffi M., Hussain F., Bhatti T.M., Akhter J.I., Hameed A. & Hasan M.M. (2008). Antibacterial characterization of silver nanoparticles against E. coli ATCC-15224. *Journal of Materials Science & Technology*, 24, 192-196.

Rastogi R., Kaushal R., Tripathi S.K., Sharma A.L., Kaur I. & Bharadwaj L.M. (2008). Comparative study of carbon nanotube dispersion using surfactants. *Journal of Colloid and Interface Science*, 328, 421-428.

Ratte H.T. (1999). Bioaccumulation and toxicity of silver compound: a review. *Environ. Toxicol. Chem.*, 18, 89-108.

RCEP (2008). Novel Materials in the Environment: The Case of Nanotechnology. In: (ed. Pollution RCoE).

Reinfelder J.R. & Chang S.I. (1999). Speciation and microalgal bioavailability of inorganic silver. *Environmental Science & Technology*, 33, 1860-1863.

Richmonds C. & Sankaran R.M. (2008). Plasma-liquid electrochemistry: Rapid synthesis of colloidal metal nanoparticles by microplasma reduction of aqueous cations. *Appl. Phys. Lett.*, 93, 3.

Rivas A., Bodis M., Bruce J., Anderson K., Klein R., Gonzalez R., Quimby F., Batt C. & Lein D. (2001). Molecular epidemiologic features and antimicrobial susceptibility profiles of various ribotypes of Pseudomonas aeruginosa isolated from humans and ruminants. *American journal of veterinary research* 62, 864-870.

Roberts A.P., Mount A.S., Seda B., Souther J., Qiao R., Lin S., Ke P.C., Rao A.M. & Klaine S.J. (2007). In vivo Biomodification of Lipid-Coated Carbon Nanotubes by Daphnia magna. *Environ. Sci. Technol.*, 41, 3025-3029.

Roe D., Karandikar B., Bonn-Savage N., Gibbins B. & Roullet J.-B. (2008). Antimicrobial surface functionalization of plastic catheters by silver nanoparticles. *Journal of Antimicrobial Chemotherapy*, 61, 869-876.

Ros T.D., Spalluto G. & Prato M. (2001). Biological Applications of Fullerene Derivatives: A Brief Overview. *Croatia chemica acta*, 74 743-755.

RS/RAE (2004). Nanosciences and Nanotechnologies: Opportunities and Uncertainties. In: (ed. Engineering TRSTRAo).

Salkar R.A., Jeevanandam P., Aruna S.T., Koltypin Y. & Gedanken A. (1999). The sonochemical preparation of amorphous silver nanoparticles. *Journal of Materials Chemistry*, 9, 1333-1335.

Samonin V.V., Nikonova V.Y. & Podvyaznikov M.L. (2008). The sorption properties of active carbons modified with fullerenes with respect to copper, silver, and lead cations in aqueous solutions. *Russ. J. Phys. Chem. A*, 82, 1371-1375.

Sanudo-Willhelmy S. & Flegal R. (1992). Anthropogenic silver in the southern California Bight: a new tracer of sewage in coastal waters. *Environ. Sci. Technol.*, 26, 2147-2151.

SCENIHR (2005). Opinion on the appropriateness of existing methodologies to assess the potential risks associated with engineered and adventitious products of nanotechnologies. . In: *Scientific Committee on Emerging and Newly Identified Health Risks*. European Commission SCENIHR/002/05.

Schierz A. & Zanker H. (2009). Aqueous suspensions of carbon nanotubes: surface oxidation, colloidal stability and uranium sorption. *Environ Pollut*, 157, 1088-94.

Schrand A.M., Braydich-Stolle L.K., Schlager J.J., Dai L. & Hussain S.M. (2008). Can silver nanoparticles be useful as potential biological labels? *Nanotechnology*, 19, 235104.

Schreurs W.J. & Rosenberg H. (1982). Effect of silver ions on transport and retention of phosphate by Escherichia coli. In, pp. 7-13.

Sealy C. (2008). Carbon nanotubes could be as harmful as asbestos. *Materials Today*, 11, 10-10.
Sengul H., Theis T.L. & Ghosh S. (2008). Toward sustainable nanoproducts: An overview of nanomanufacturing methods. *J. Ind. Ecol.*, 12, 329-359.
Shahverdi A.R., Fakhimi A. & Shahverdi H.R. (2007). Synthesis and effect of silver nanoparticles on the antibacterial activity of different antibiotics agains Staphylococcus aureus and Escherichia coli. *Nanomedicine: Nanotechnology, Biology and Medicine*, 3, 68-171.
Sharma V.K., Yngard R.A. & Lin Y. (2009). Silver nanoparticles: Green synthesis and their antimicrobial activities. *Advances in Colloid and Interface Science*, 145, 83-96.
Shi J.P., Evans D.E., Khan A.A. & Harrison R.M. (2001). Sources and concentration of nanoparticles (< 10 nm diameter) in the urban atmosphere. *Atmospheric Environment*, 35, 1193-1202.
Shinohara N., Matsumoto T., Gamo M., Miyauchi A., Endo S., Yonezawa Y. & Nakanishi J. (2009). Is Lipid Peroxidation Induced by the Aqueous Suspension of Fullerene C-60 Nanoparticles in the Brains of Cyprinus carpio? *Environmental Science & Technology*, 43, 948-953.
Shrivastava S., Bera T., A.Roy, G.Singh, Ramachandrarao P. & Dash D. (2007). Characterization of enhanced antibacterial effects of novel silver nanoparticles. *J Nanotechnology*, 18, 225103-225112.
Shukla R., Bansal V., Chaudhary M., Basu A., Bhonde R.R. & Sastry M. (2005). Biocompatibility of gold nanoparticles and their endocytotic fate inside the cellular compartment: A microscopic overview. *Langmuir*, 21, 10644-10654.
Sikora F. & Stevenson F. (1988). Silver complexation by humic substances:conditional stability constant and nature of reactive sites. *Geoderma*, 42.
Silby M.W., Cerdeno-Tarraga A.M., Vernikos G.S., Giddens S.R., Jackson R.W., Preston G.M., Zhang X.X., Moon C.D., Gehrig S.M., Godfrey S.A.C., Knight C.G., Malone J.G., Robinson Z., Spiers A.J., Harris S., Challis G.L., Yaxley A.M., Harris D., Seeger K., Murphy L., Rutter S., Squares R., Quail M.A., Saunders E., Mavromatis K., Brettin T.S., Bentley S.D., Hothersall J., Stephens E., Thomas C.M., Parkhill J., Levy S.B., Rainey P.B. & Thomson N.R. (2009). Genomic and genetic analyses of diversity and plant interactions of Pseudomonas fluorescens. *Genome Biology*, 10.
Silver S. (2003). Bacterial silver resistance: molecular biology and uses and misuses of silver compounds. *Fems Microbiology Reviews*, 27, 341-353.
Silver S., Phung L.T. & Silver G. (2005). Silver as biocides in burn and wound dressings and bacterial resistance to silver compounds. In: *Annual Meeting of the Society-for-Industrial-Microbiology* Chicago, IL, pp. 627-634.
Simon-Deckers A., Brun E., Gouget B., Carriere M. & Sicard-Roselli C. (2008). Impact of gold nanoparticles combined to X-Ray irradiation on bacteria. *Gold Bulletin*, 41, 187-194.
Simonet B. & Valcárcel M. (2009). Monitoring nanoparticles in the environment. *Anal. Bioanal. Chem.*, 393, 17-21.
Singh G. & Song L.F. (2007). Experimental correlations of pH and ionic strength effects on the colloidal fouling potential of silica nanoparticles in crossflow ultrafiltration. *J. Membr. Sci.*, 303, 112-118.
Slaveykova V.I. & Wilkinson K.J. (2005). Predicting the Bioavailability of Metals and Metal Complexes: Critical Review of the Biotic Ligand Model. In: *Environ. Chem.*, pp. 9-24
Slawson R.M., Trevors J.T. & Lee H. (1992a). Silver Accumulation and Resistance in Pseudomonas-Stutzeri. *Archives of Microbiology*, 158, 398-404.
Slawson R.M., Vandyke M.I., Lee H. & Trevors J.T. (1992b). Germanium and Silver Resistance, Accumulation, and Toxicity in Microorganisms. *Plasmid*, 27, 72-79.

Sondi I. & Salopek-Sondi B. (2004). Silver nanoparticles as antimicrobial agent: a case study on E-coli as a model for Gram-negative bacteria. *Journal of Colloid and Interface Science*, 275, 177-182.

Spencer C.G., Campbell P.M., Buschang P.H., Cai J. & Honeyman A.L. (2009). Antimicrobial Effects of Zinc Oxide in an Orthodontic Bonding Agent. *Angle Orthodontist*, 79, 317-322.

Spohn P., Hirsch C., Hasler F., Bruinink A., Krug H.F. & Wick P. (2009). C60 fullerene: a powerful antioxidant or a damaging agent? The importance of an in-depth material characterization prior to toxicity assays. *Environ Pollut*, 157, 1134-9.

Stafford R. & Davies M.S. (2005). Spatial patchiness of epilithic biofilm caused by refuge-inhabiting high shore gastropods. *Hydrobiologia*, 545, 279-287.

Stolpe B. & Hassellov M. (2007). Changes in size distribution of fresh water nanoscale colloidal matter and associated elements on mixing with seawater. *Geochim. Cosmochim. Acta*, 71, 3292-3301.

Stoodley K.S., 1,2D. G. Davies,2 and J.W. Costerton1 (2002). Biofilms as complex differentiated communities. *Annu. Rev. Microbiol.*, 56, 187–209.

Sun L., Singh A.K., Vig K., Pillai S.R. & Singh S.R. (2008). Silver nanoparticles inhibit replication of Respiratory Syncytial Virus. *Journal of Biomedical Nanotechnology*, 4, 149-158.

Sun L., Zhang Z., Wang S., Zhang J., Li H., Ren L., Weng J. & Zhang Q. (2009). Effect of pH on the Interaction of Gold Nanoparticles with DNA and Application in the Detection of Human p53 Gene Mutation. *Nanoscale Research Letters*, 4, 216-220.

Sung J.H., Ji J.H., Yoon J.U., Kim D.S., Song M.Y., Jeong J., Han B.S., Han J.H., Chung Y.H., Kim J., Kim T.S., Chang H.K., Lee E.J., Lee J.H. & Yu I.J. (2008). Lung function changes in Sprague-Dawley rats after prolonged inhalation exposure to silver nanoparticles. *Inhalation Toxicology*, 20, 567-574.

Surdeau N., Laurent-Maquin D., Bouthors S. & Gelle M.P. (2006). Sensitivity of bacterial biofilms and planktonic cells to a new antimicrobial agent, Oxsil(R) 320N. *Journal of Hospital Infection*, In Press, Corrected Proof.

Sutherland I. (1999). Biofilms exopolysaccharides. In: *Microbial Extracellular Polymeric Substances* (ed. Wingender J NT, Fleming HC). Springer Berlin, pp. 73-92.

Suzuki H., Toyooka T. & Ibuki Y. (2007). Simple and Easy Method to Evaluate Uptake Potential of Nanoparticles in Mammalian Cells Using a Flow Cytometric Light Scatter Analysis. *Environ. Sci. Technol.*, 41, 3018-3024.

Swanson R., Ney J. & Smith P.K. (1947). Influence of bal on the acute toxicity of gold salts in mice. *Federation Proceedings*, 6, 375-376.

Tan H., Li S.P. & Fan W.Y. (2006). Core-shell and hollow nanocrystal formation via small molecule surface photodissociation; Ag@Ag2Se as an example. *Journal of Physical Chemistry B*, 110, 15812-15816.

Teitzel G. (2003). Heavy metal resistance of biofilm and planktonic Pseudomonas aeruginosa. *Appl Environ Microbiol*, 69, 2313-2320.

Terada A., Yuasa A., Tsuneda S., Hirata A., Katakai A. & Tamada M. (2005). Elucidation of dominant effect on initial bacterial adhesion onto polymer surfaces prepared by radiation-induced graft polymerization. *Colloids and Surfaces B: Biointerfaces*, 43, 99.

Throback I.N., Johansson M., Rosenquist M., Pell M., Hansson M. & Hallin S. (2007). Silver (Ag+) reduces denitrification and induces enrichment of novel nirK genotypes in soil. *FEMS Microbiol. Lett.*, 270, 189-194.

Thurman E.M. (1985). *Organic Geochemistry of Natural Waters*, Boston.

Tian J., Wong K., Ho C., Lok C., Yu W., Che C., JF J.C. & Tam P. (2007). Topical delivery of silver nanoparticles promotes wound healing. *Chem Med Chem*, 2, 129–136.

Tiede K., Hassellov M., Breitbarth E., Chaudhry Q. & Boxall A.B.A. (2009). Considerations for environmental fate and ecotoxicity testing to support environmental risk assessments for engineered nanoparticles. *J Chromatogr A*, 1216, 503-9.

Tikhomirov A.A., Andrievsky G.V. & Nedzvetsky V.S. (2008). Disorders in the Cytoskeleton of Astroglia and Neurons in the Rat Brain Induced by Long-Lasting Exposure to Ethanol and Correction of These Shifts by Hydrated Fullerene C-60. *Neurophysiology*, 40, 279-287.

Tipping E. & Higgins D.C. (1982). The effects of adsorbed humic substances on the colloid stability of hematite particles. *Colloids and Surfaces*, 5, 85-92.

Trevors J.T. (1987). Silver resistance and accumulation in bacteria. *Enzyme and Microbial Technology*, 9, 331.

Tronczynski J. (1992). Interactions between dissolved organic matter and organic contaminants. *Analusis*, 20, M54-M56.

Tsezos M., Remoudaki E. & Angelatou V. (1997). Biosorption sites of selected metals using electron microscopy. *Comparative Biochemistry and Physiology Part A: Physiology*, 118, 481-487.

Tsuang Y.H., Sun J.S., Huang Y.C., Lu C.H., Chang W.H.S. & Wang C.C. (2008). Studies of photokilling of bacteria using titanium dioxide nanoparticles. *Artificial Organs*, 32, 167-174.

Tsuji T., Okazaki Y. & Tsuji M. (2008). Photo-induced morphological conversions of silver nanoparticles prepared using laser ablation in water - Enhanced morphological conversions using halogen etching. *Journal of Photochemistry and Photobiology a-Chemistry*, 194, 247-253.

Tuncel S.G., Yenisoy-Karakas S. & Dogangun A. (2004). Determination of metal concentrations in lichen samples by inductively coupled plasma atomic emission spectroscopy technique after applying different digestion procedures. *Talanta*, 63, 273-277.

USEPA (1987). Toxic Chemical Release Reporting; Community Right-to-Know Act. *52 FR 21152*.

van de Mortel M. & Halverson L.J. (2004). Cell envelope components contributing to biofilm growth and survival of Pseudomonas putida in low-water-content habitats. *Molecular Microbiology*, 52, 735-750.

Van Essche M., Quirynen M., Sliepen I., Van Eldere J. & Teughels W. (2009). Bdellovibrio bacteriovorus Attacks Aggregatibacter actinomycetemcomitans. *J. Dent. Res.*, 88, 182-186.

van Hoogmoed C.G., van der Kuijl-Booij M., van der Mei H.C. & Busscher H.J. (2000). Inhibition of Streptococcus mutans NS Adhesion to Glass with and without a Salivary Conditioning Film by Biosurfactant- Releasing Streptococcus mitis Strains. *Appl. Environ. Microbiol.*, 66, 659-663.

Van Wees S.C.M., Van der Ent S. & Pieterse C.M.J. (2008). Plant immune responses triggered by beneficial microbes. *Current Opinion in Plant Biology*, 11, 443-448.

Vanderkooij D. (1977). Occurrence of Pseudomonas-Spp in Surface-Water and in Tap Water as Determined on Citrate Media. *Antonie Van Leeuwenhoek Journal of Microbiology*, 43, 187-197.

Vanderkooij D., Visser A. & Oranje J.P. (1982). Multiplication of Fluorescent Pseudomonads at Low Substrate Concentrations in Tap Water. *Antonie Van Leeuwenhoek Journal of Microbiology*, 48, 229-243.

Vanitha S.C., Niranjana S.R., Mortensen C.N. & Umesha S. (2009). Bacterial wilt of tomato in Karnataka and its management by Pseudomonas fluorescens. *Biocontrol*, 54, 685-695.

Vargas W.E., Amador A. & Niklasson G.A. (2006). Diffuse reflectance of TiO2 pigmented paints: Spectral dependence of the average pathlength parameter and the forward scattering ratio. *Optics Communications*, 261, 71-78.

Veiseh O., Sun C., Gunn J., Kohler N., Gabikian P., Lee D., Bhattarai N., Ellenbogen R., Sze R., Hallahan A., Olson J. & Zhang M.Q. (2005). Optical and MRI multifunctional nanoprobe for targeting gliomas. *Nano Letters*, 5, 1003-1008.

Venugopalan V.P., Kuehn M., Hausner M., Springael D., Wilderer P.A. & Wuertz S. (2005). Architecture of a Nascent Sphingomonas sp. Biofilm under Varied Hydrodynamic Conditions. *Applied and Environmental Microbiology,*71, 2677-2686.

Verwey E.J.W. & Overbeek J.T.G. (1948). *Theory of teh Stability of Lyophobic Colloids*. Elsevier, Amserdam.

Vieira M.J., Oliveira R., Melo L., Pinheiro M.M. & Martins V. (1993). Effect of metallic ions on the adhesion of biofilms formed by Pseudomonas fluorescens. *Colloids and Surfaces B: Biointerfaces*, 1, 119-124.

Viudez A.J., Madueno R., Pineda T. & Blazquez M. (2006). Stabilization of gold nanoparticles by 6-mercaptopurine monolayers. Effects of the solvent properties. *Journal of Physical Chemistry B*, 110, 17840-17847.

Wang J.X., Chen C.Y., Li B., Yu H.W., Zhao Y.L., Sun J., Li Y.F., Xing G.M., Yuan H., Tang J., Chen Z., Meng H., Gao Y.X., Ye C., Chai Z.F., Zhu C.F., Ma B.C., Fang X.H. & Wan L.J. (2006). Antioxidative function and biodistribution of [Gd@C-82(OH)(22)](n) nanoparticles in tumor-bearing mice. *Biochemical Pharmacology*, 71, 872-881.

Wang Y., Duncan K.L., Wachsman E.D. & Ebrahimi F. (2007). Effects of Reduction Treatment on Fracture Properties of Cerium Oxide. *Journal of the American Ceramic Society*, 90, 3908-3914.

Ward T.J., Boeri R.L., Hogstrand C., Kramer J.R., Lussier S.M., Stubblefield W.A., Wyskiel D.C. & Gorsuch J.W. (2006). Influence of salintiy and organic carbon on the chronic toxicity of silver to mysids (Americamysis bahia) and silversides (Menidia beryllina). *Environmental Toxicology and Chemistry*, 25, 1809-1816.

Warheit D.B., Brock W.J., Lee K.P., Webb T.R. & Reed K.L. (2005). Comparative pulmonary toxicity inhalation and instillation studies with different TiO2 particle formulations: Impact of surface treatments on particle toxicity. *Toxicological Sciences*, 88, 514-524.

Warheit D.B., Webb T.R., Reed K.L., Frerichs S. & Sayes C.M. (2007). Pulmonary toxicity study in rats with three forms of ultrafine-TiO2 particles: Differential responses related to surface properties. *Toxicology*, 230, 90-104.

Webb J.S., Thompson L.S., James S., Charlton T., Tolker-Nielsen T., Koch B., Givskov M. & Kjelleberg S. (2003). Cell death in Pseudomonas aeruginosa biofilm development. *Journal of Bacteriology*, 185, 4585-4592.

Webb N.A. & Wood C.M. (2000). Bioaccumulation and distribution of silver in four marine teleosts and two marine elasmobranchs: influence of exposure duration, concentration, and salinity. *Aquat. Toxicol.*, 49, 111-129.

Wen L.S., Santschi P.H., Gill G.A., Paternostro C.L. & Lehman R.D. (1997). Colloidal and Particulate Silver in River and Estuarine Waters of Texas. *Environ. Sci. Technol.*, 31, 723-731.

Whang L.M., Yang Y.F., Huang S.J. & Cheng S.S. (2008). Microbial ecology and performance of nitrifying bacteria in an aerobic membrane bioreactor treating thin-film transistor liquid crystal display wastewater. *Water Science and Technology*, 58, 2365-2371.

Wigginton N.S., Haus K.L. & Hochella M.F. (2007). Aquatic environmental nanoparticles. *Journal of Environmental Monitoring*, 9, 1306-1316.

Wildeson J., Smith A., Gong X.B., Davis H.T. & Scriven L.E. (2008). Understanding and improvement of TiO2 efficiency in waterborne paints through latex design. *Jct Coatingstech*, 5, 32-39.

Wilkinson K.J.a.A.R. (2005). Contrasting roles of natural organic matter on colloidal stabilization and flocculation in freshwaters. In: *Flocculation in natural and engineered environmental systems*. CRC Press, pp. 143-170.

Willaert R., Baron G.V. & Nedovic V. (2004). Diffusive Mass Transfer in Immobilised Cell Systems. In: *Fundamentals of Cell Immobilisation Biotechnology* (eds. Nedovic V & Willaert R). Kluwer Academic Publisher, p. 550.

Wilson S.R. (2000). The Fullerene Handbook. In: (ed. Ruoff KKaR). Wiley New York, pp. 437-465.

Wingender J., Neu T.R. & H.-C.Flemming (1999). *Microbial Extracellular Polymeric Substances: Characterization, Structure and Function*. 1st edn. Springer.

Wolfaardt G.M., J.R.Lawrence & Korber D.R. (1999). Function of EPS. In: *Microbial Extracellular Polymeric Substances. Characterization, Structure and Function* (ed. J. Wingender TRN, and H.-C. Flemming). Springer, pp. 171-195.

Wood C.M., Grosell M., Hogstrand C. & Hansen H. (2002). Kinetics of radiolabelled silver uptake and depuration in the gills of rainbow trout (Oncorhynchus mykiss) and European eel (Anguilla anguilla): the influence of silver speciation. *Aquat. Toxicol.*, 56, 197-213.

Wood C.M., Hogstrand C., Galvez F. & Munger R.S. (1996). The physiology of waterborne silver toxicity in freshwater rainbow trout (Oncorhynchus mykiss) 1. The effects of ionic Ag+. *Aquat. Toxicol.*, 35, 93.

Wood C.M., McDonald M.D., Walker P., Grosell M., Barimo J.F., Playle R.C. & Walsh P.J. (2004). Bioavailability of silver and its relationship to ionoregulation and silver speciation across a range of salinities in the gulf toadfish (Opsanus beta). *Aquat. Toxicol.*, 70, 137-157.

Wood C.M., Playle R.C. & Hogstrand C. (1999). Physiology and modelling mechanisms of silver uptake and toxicity in fish. *Environmental Toxicology and Chemistry*, 18, 71-83.

WoodrowWilson (2009). Consumer Products InventoryIn: *Project on Emerging Nanotechnologies, A project of the Woodrow Wilson International Center for Scholars.*

Woodward D.H. (1963). HE-NE laser as source for light scattering measurements. *Applied Optics*, 2, 1205-1207.

Xu X., Brownlow W., Kyriacou S., Wan Q. & Viola J. (2004). Real-time probing of membrane transport in living microbial cells using single nanoparticle optics and living cell imaging. *Biochemistry*43 10400-10413

Yang G.W. & Li H.L. (2008). Sonochemical synthesis of highly monodispersed and size controllable Ag nanoparticles in ethanol solution. *Materials Letters*, 62, 2193-2195.

Yang H., Liu C., Yang D.F., Zhang H.S. & Xi Z.G. (2009). Comparative study of cytotoxicity, oxidative stress and genotoxicity induced by four typical nanomaterials: the role of particle size, shape and composition. *Journal of Applied Toxicology*, 29, 69-78.

Yang Y. & Gao M.Y. (2005). Preparation of Fluorescent SiO2 Particles with Single CdTe Nanocrystal Cores by the Reverse Microemulsion Method. *Advanced Materials*, 17, 2354-2357.

Yang Y., Jing L., Yu X., Yan D. & Gao (2007). Coating Aqueous Quantum Dots with Silica via Reverse Microemulsion Method: Toward Size-Controllable and Robust Fluorescent Nanoparticles. *Chemistry of Materials*, 19, 4123-4128.

Yao H.C. & Yao Y.F.Y. (1984). Ceria in automotive exhaust catalyst. 1. oxygen storage. *J. Catal.*, 86, 254-265.

Yoon K.Y., Byeon J.H., Park C.W. & Hwang J. (2008). Antimicrobial Effect of Silver Particles on Bacterial Contamination of Activated Carbon Fibers. In, pp. 1251-1255.
Zar J. (1999). *Biostatistical Analysis*. 4th edn. Prentice Hall, New Jersey.
Zeiri L., Bronk B.V., Shabtai Y., Czege J. & Efrima S. (2002). Silver metal induced surface enhanced Raman of bacteria. *Colloids and Surfaces a-Physicochemical and Engineering Aspects*, 208, 357-362.
Zhang R., Thiyagarajan V. & Qian P.Y. (2008). Evaluation of terminal-restriction fragment length polymorphism analysis in contrasting marine environments. *Fems Microbiology Ecology*, 65, 169-178.
Zhang W.-w., Hu Y.-h., Wang H.-l. & Sun L. (2009a). Identification and characterization of a virulence-associated protease from a pathogenic Pseudomonas fluorescens strain. *Vet Microbiol*, 139, 183-8.
Zhang W.-x. (2003). Nanoscale Iron Particles for Environmental Remediation: An Overview. *Journal of Nanoparticle Research*, 5, 323-332.
Zhang W., Qiao X. & Chen J. Synthesis of nanosilver colloidal particles in water/oil microemulsion. *Colloids and Surfaces A: Physicochemical and Engineering Aspects*, In Press, Corrected Proof.
Zhang Y.Z., Wu L.H., Liu Y.P., Xie E.Q., Yan D. & Chen J.T. (2009b). Preparation of ZnO Nanospheres and Their Applications in Dye-Sensitized Solar Cells. *Chinese Physics Letters*, 26.
Zhou B., Nichols J., Playle R.C. & Wood C.M. (2005). An in vitro biotic ligand model (BLM) for silver binding to cultured gill epithelia of freshwater rainbow trout (Oncorhynchus mykiss). *Toxicology and Applied Pharmacology*, 202, 25.
Zhu S.Q., Oberdorster E. & Haasch M.L. (2005). Toxicity of an engineered nanoparticle (fullerene, C-60) in two aquatic species, Daphnia and fathead minnow. In: *13th International Symposium on Pollutant Responses in Marine Organisms (PRIMO 13)*. Elsevier Sci Ltd Alessandria, ITALY, pp. S5-S9.
Zhu S.Q., Oberdorster E. & Haasch M.L. (2006). Toxicity of an engineered nanoparticle (fullerene, C-60) in two aquatic species, Daphnia and fathead minnow. *Marine Environmental Research*, 62, S5-S9.

APENDIX 1

1.1 Minimal Davis Media

- 0.7 g l^{-1} K_2HPO_4
- 0.2 g $l^{-1}$$KH_2HPO_4$
- 1 g $(NH_4)_2SO_4$
- 0.5 g l^{-1} Sodium citrate
- 0.1 g $l^{-1}$$MgSO_4$
- 1 g l^{-1} glucose

Ionic strength of this solution is 0.055M

(Filter sterilize glucose and add it after autoclaving)

The pH of this solution is about 7.25

1.2 Artificial Seawater (30 ‰)

- 21.19 g l^{-1} NaCl
- 0.57 g l^{-1} KCl
- 1.17 g l^{-1} $CaCl_2*2H_2O$
- 3.99 g l^{-1} $MgCl_2*6H2O$
- 5.39 g l^{-1} $MgSO_4*7H_2O$
- 0.15 g l^{-1} $NaHCO_3$

The pH of this solution if about 8.3

Ionic strength of this solution is 0.6M

APENDIX 2

Publications within peer-review journals arising from the studies reported herein.

1. Fabrega J., Fawcett S.R, Renshaw J.C & Lead J.R. 2009. Silver nanoparticles impact on bacterial growth: effect of pH, concentration and organic matter. Accepted for publication in *Environmental Science and Technology*.

2. Fabrega J., Renshaw J.C & Lead J.R. Interactions of silver nanoparticles with *Pseudomonas putida* biofilms. Submitted to *Environmental Science and Technology*.